The effects of different types of dietary fats in the liver

Sim, Pei Ying

Awarding institution:
King's College London

THE EFFECTS OF DIFFERENT TYPES OF DIETARY FATS IN THE LIVER

A THESIS SUBMITTED IN PART FULFILMENT FOR THE DEGREE OF DOCTOR OF PHILOSOPHY IN THE KING'S COLLEGE LONDON

BY

PEI YING SIM

DIABETES & NUTRITIONAL SCIENCES DIVISION

THE SCHOOL OF MEDICINE, KING'S COLLEGE LONDON

2011

ABSTRACT

The role of dietary fat in the causation of fatty liver and its progression to non-alcoholic steatohepatitis (NASH) is reviewed. A series of experiments to induce fatty liver were conducted in mice. The effects of high fat vs high carbohydrate, eicosapentaenoic acid (EPA) vs docosahexaenoic acid (DHA) and altered palmitic rich triacylglycerol structure were studied. Increasing the proportion of energy from fat, promoted adipose tissue fat accumulation and only slightly increased liver fat, but did not exacerbate hepatic damage compared to a high carbohydrate intake. Both types of hypercaloric diet resulted in the accumulation predominantly of palmitic and oleic acid in the liver. DHA decreased hepatic fat accumulation and tended to decrease liver damage but like EPA reduced hepatic cholesteryl oleate accumulation. Triacylglycerols with a high proportion of palmitic acid in the *sn*-2 position (lard and randomized palm olein) increased hepatic cholesteryl oleate compared with palm olein where the palmitic acid is mainly in the *sn*-1 and *sn*-3 position. Triacylglycerol from native palm olein vs randomized palm oil also resulted in greater accumulation of long-chain n-3 polyunsaturated fatty acids in all lipid fractions. These finding indicate that triacylglycerol structure influences the fate of fatty acids in the liver. Proteins separated by 2-D differential-in gel-electrophoreis (DIGE) and identified by high resolution LC-MS/MS showed significant differences in expression between hypercaloric vs eucaloric control groups: isoform 1 of epoxide hydrolase 2, catalase, ATP synthase subunit-alpha mitochondrial, ornithine carbamoyltransferase-mitochondrial (OTC), regucalcin and carbonic anhydrase 3. There were no differences in protein expression between high fat and high carbohydrate hypercaloric diets or between EPA and DHA. High carbohydrate/low fat hypercaloric diet down-regulated miR-199a-5p, miR-200b, miR-324-3p, miR-21*, miR-31* and miR-451 by -66%, -76%, -37%, -33%, -57% and -9%, respectively compared to controls. Overfeeding with high fat hypercaloric diet down-regulated miR-199a-5p, miR-200b, miR-324-3p, miR-21*, miR-31*, miR-345-3p and miR-466f by -86%, -86%, -51%, -76%, -76%, -72% and -62%, respectively compared to control. The expressions of miR-21* and miR-466f were lower following the high fat compared to the high carbohydrate/low fat diet. Perturbations in protein profiles may reflect the changes in liver profiles seen with dietary intervention. The findings reported in this thesis indicate that excessive calories intake is more important in generating fatty liver than whether the energy is derived from fat or carbohydrate. The findings are discussed in the context of how to prevent and treat fatty liver disease.

DEDICATION

TO MY PARENTS FOR THEIR ENDLESS SUPPORT

ACKNOWLEDGEMENTS

First and foremost, I would like to express my deepest gratitude to both my supervisors Professor Thomas Sanders and Professor Victor Preedy for their valuable time, effort and help throughout the whole study. Without their guidance and support this study would have never been accomplished and I am truly grateful to have them as my supervisors. Thank you ever so much for your patience and encouragement.

I would also like to extend my gratitude to my colleagues in the department, especially Aseel Al-Saleh, Sarah Cottin, Sowmya Bharani, Stephanie Cheung Hoi Man, Androulla Filippou and Virginia Govoni for their endless moral support in times of need and for creating a positive environment in the work place. Besides that, the technical support from Robert Gray, Rosie Calokatsia, Tracey Dew, Joaquim Pombo, and Patrick Cox is very much appreciated.

From the Genomics centre of King's College London, I would like to thank Dr. Estibaliz Aldekoa-Otalora, Dr. Matthew Arno, Dr. Josef Rasinger and Yuen Fei Wong for their expertise, time and help in proteomics and miRNA related work. In addition, I would like to thank Professor Bernard Portmann and Dr. Alberto Quaglia for their help given to me in liver histology.

Last but not least, I would like to thank my beloved parents for their continual support and motivation in guiding me through the hard times and ensuring that my experience in writing this thesis was as pleasant as possible. I would also like to thank my sister, Pei Lin and brothers, Biing Huei and Biing Tyan for comforting me with kind words. Without my family, this would not have been at all possible and I'm thankful for all the unconditional love and care.

Other friends who I have missed out on this one page of acknowledgement, you know who you are and I truly appreciate all your effort and time for creating a wonderful PhD experience for me.

Knowingly, I am glad that I have completed this thesis and in years to come, I hope the best for the people I've met along the way and may we stay in touch. Thank you all for believing in me.

Contents

List of Figures

Chapter 1

Chapter 2

Chapter 3

Chapter 4

Chapter 5

Chapter 6

Chapter 7

Chapter 8

List of Tables

Chapter 2

Chapter 3

Chapter 4

Chapter 5

Chapter 6

Chapter 7

Chapter 8

List of abbreviations

16:0	Palmitic acid
16:1	Palmitoleic acid
18:0	Stearic acid
18:1n-7	Vaccenic acid
18:1n-9	Oleic acid
18:2n-6	Linoleic acid
18:3n-3	Linolenic acid
20:3n-6; DGLA	Dihomo-gamma linolenic acid;
20:4n-6; AA	Arachidonic acid
20:5n-3; EPA	Eicosapentaenoic acid;
22:4n-6	Adrenic acid
22:5n-3, DPA	Docosapentaenoic acid
22:5n-6	Osbond acid
22:6n-3; DHA	Docosahexaenoic acid;
2D	2 Dimensional
ACAT	Acyl-CoA: cholesterol acyltransferase
ACOD	Acyl-coenzyme A oxidase
ACS	Acyl-coenzyme A synthetase
AGCC	Affymetrix GeneChip Command Console
ALP	Alkaline phosphatase
ALT	Alanine aminotransferase
AMP	Aminomethylpropanol
ANOVA	Analysis of variance
AP-1	Activating protein-1
Apo	Apolipoprotein
APS	Ammonium persulfate solution
AST	Aspartate aminotransferase
ATP	Adenosine triphosphate
ATP5a1	ATP synthase subunit alpha
BH4	Tetrahydropterin
BPB	Bromophenol blue
BSA	Bovine serum albumin
Btg2	B-cell translocation gene 2
CAR3	Carbonic anhydrase 3
CAT	Catalase
CCK	Cholecystokinin
CCl_4	Carbon tetrachloride
cDNA	Complementary DNA
CE	Cholesterol esters
CI	Confidence interval
CM	Condensed milk
CO	Corn oil

CoA	Coenzyme A
COL	Collagen
CPT	Carnitine palmitoyltransferase
CR	Chylomicron remnants
Ct	Cycle threshold
Cyp	Cytochrome
DGAT	Diacylglycerol acyltransferase
DIA	Differential In-Gel Analyses
DIGE	Differential In-Gel Electrophoresis
DMF	dimethylformamide
DNA	Deoxyribonucleic acid
DTT	Dithiothrietol
EMP1	Epithelial membrane protein1
EPHX2	Epoxide hydrolase 2
ErbB	Epidermal growth factor receptor
ESCC	Oesophageal squamous cell carcinoma
ETFb	Electron transfer flavoprotein subunit beta
FA	Fatty acids
FADH	Flavin adenine dinucleotide
FAS	Fatty acid synthetase
FGFR	Fibroblast growth factor receptor type 1
GLC	Gas liquid chromatography
GSTO1	Glutathione S-transferase omega-1
GSTP1	Glutathione S-transferase P1
GSTPA3	Glutathione S-transferase A3
H&E	Hematoxylin and eosin
HCC	Hepatocellular carcinoma cells
HCl	Hydrochloric acid
HDL	High density lipoprotein
HF	High fat
HFDHA	High fat docosahexaenoic acid
HFEPA	High fat eicosapentaenoic acid
HFL	High fat lard
HOSO	High oleic sunflower oil
HSL	Hormone sensitive lipase
IDL	Intermediate density lipoprotein
IEF	Isoelectric focusing
IL	Interleukin
IOTF	International Obesity Task Force
IPG	Immobilized pH gradient
IPG	Immobilized pH gradient
IPO	Interesterified palm oil
IR	Internal reference
IU	International unit

K_2CO_3	Potassium carbonate
KO	Knockout
KSR2	Kinase suppressor of ras 2
LCFA	Long chain fatty acids
LCM	Light condensed milk
LC-MS/MS	Liquid chromatography-tandem mass spectrometry
LCP	Long chain polyunsaturated fatty acids
LCT	Long chain triacylglycerol
LDL	Low density lipoprotein
LF	Low fat
LFR	Low fat reference
LMW	Low molecular weight
LPL	Lipoprotein lipase
LPS	Lipopolysaccharides
LXR	Liver X-Receptor
MAG	Monoacylglycerols
MAPK	Mitogen-activated protein kinase
MCD	Methionine choline deficient
Mcl-1	Myeloid cell leukemia-1
MCT	Medium chain triacylglycerol
MDH1	Malate dehydrogenase
MEHA	3-methyl-N-ethyl-N-ß-hydroxyethyl-aniline
miRNA	micro RNA
MUFA	Monounsaturated fatty acids
MW	Molecular weight
NADH	Nicotinamide adenine dinucleotide
NADPH	Nicotinamide adenine dinucleotide phosphate
NAFLD	Non-alcoholic fatty liver disease
NaOH	Sodium hydroxide
NASH	Non-alcoholic steatohepatitis
NEFA	Non-esterified fatty acids
NF-kappaB	Nuclear factor kappa beta
NFKB1	Nuclear factor kappa-B subunit 1
NHANES	National Health and Nutrition Examination Surveys
NRF	Nuclear respiratory factor
OCT	Optimal cutting temperature
OPO	Oleic:Palmitic:Oleic acid
OTC	Ornithine carbamoyltransferase
OTC	Ornithine carbamoyltransferase
PAP	Phosphatidic acid phosphatase
PBS	Phosphate buffered saline
PBS	Phosphate buffered saline
PEPCK	Phosphoenol-pyruvate carboxykinase
PFA	Paraformaldehyde

pI	Isoelectric point
PKC	Protein kinase C
PL	Phopholipids
PNPP	Para-nitrophenyl phosphate
PO	Palm oil
PPAR	Peroxisome proliferator-activated receptor gamma
PPi	Pyrophosphoric acid
PTEN	Phosphatase and tensin
PUFA	Polyunsaturated fatty acids
QC	Quality control
QDPR	Quinoid dihydropteridine reductase
qPCR	Quantitative polymerase chain reaction
RGN	Regucalcin
RGS4	Regulator of G-protein signalling 4
RIN	RNA integrity number
RISC	RNA-induced silencing complex
RNA	Ribonucleic acid
ROS	Reactive oxygen species
RT	Reverse transcriptase
SD	Standard deviation
SDS	Sodiumdodecylsulphate
SEM	Standard error mean
SFA	Saturated fatty acids
SL-DG	Structured lipids-diacylglycerol
Sno	Small nucleolar
SOCS	Suppressor of cytokine signaling
SPE	Solid phase extraction
SPR	Sepiapterin reductase
SREBP-1c	Sterol-regulatory element binding protein-1c
Stat3	Signal transducer and activator of transcription 3
TAG	Triacylglycerols
TCA	Tricarboxylic acid
TEMED	Tetramethylethylenediamine
TLC	Thin layer chromatography
TNF	Tumour necrosis factor
VLDL	Very low density lipoprotein
w/v	weight by volume
w/w	weight by weight

Chapter 1:

The effect of the level and type of dietary fat in non-alcoholic steatohepatitis (NASH)

1.0 Introduction

Non-alcoholic steatohepatitis (NASH) has emerged as a major cause of liver failure and liver cancer and is linked to the increased prevalence of obesity and insulin resistance (Marchesini et al, 1999; Farrell & Larter 2006; Qureshi & Abrams 2007; Cong et al, 2008; Pascale et al, 2010; Leavens & Birnbaum 2011; Wree et al, 2011). According to the European Association for the Study of Liver Disease (EASL), there is a need for non-invasive diagnosis of NASH in order to reduce the risk of developing fibrosis in patients (Ratziu et al, 2010). One of the aims of this research presented in the thesis was to identify novel biomarkers for NASH. However, few studies have examined the effect of varying fat composition on NASH. This thesis therefore investigates the hypothesis that the type and level of fat consumed influences the development of NASH. It is first, however, necessary to describe the relationship between non-alcoholic fatty liver disease (NAFLD), NASH and the related pathologies.

1.1 Spectrum of NAFLD in relation to NASH

NAFLD refers to the accumulation of fats in the liver exceeding 5% to 10% by weight (Neuschwander-Tetri & Caldwell 2003). NASH is the term used to describe the accumulation of fats in the liver and this is commonly associated with signs of inflammation (Neuschwander-Tetri & Caldwell 2003, Harmon et al, 2011). Most of the fat is present as triacylglycerols (TAG) within hepatocytes. Although fatty liver may be a benign state it can under some circumstances progress to NASH and then cirrhosis which is characterised by inflammation, oxidative stress and scarring (Angulo 2002). The multiple factors that lead to this progression are uncertain, but involve the production of pro-inflammatory cytokines, activation of stellate cells, dysregulation of lipolysis and lipogenesis (Postic & Girard 2008) and oxidative changes possibly influenced by the type of fat (Larter & Farrell 2006; Stanton et al, 2011).

1.1.1 Definition of NASH

In 1980, the term NASH was first coined to describe the biopsy results of obese patients with fatty liver in the absence of a history of alcohol misuse, which in some cases led to cirrhosis (Ludwig et al, 1980). NASH appears to be commonly associated with obesity, hyperlipidemia, and insulin resistance, which include diabetes and

metabolic syndrome (Marchesini et al, 2001; Neuschwander-Tetri and Caldwell 2003; Abdelmalek & Diehl 2007).

Steatosis increases the vulnerability of the liver to NASH involving environmental and genetic factors that ultimately leads to end-stage liver cirrhosis (Leite et al, 2009). In summary, NASH is defined as a type of cryptogenic liver disease accompanied by the accumulation of triacylglycerols (TAGs) with signs of hepatic inflammation excluding the influence of viral hepatitis, autoimmune, toxicities and alcohol consumption of more than 20 g/day for men and more than 10 g/day for women (Moore 2010).

In 1998, the 2-hit hypothesis to explain the progression of non-alcoholic fatty liver disease was proposed by Day and James (***Figure 1.1***). This hypothesis stated that insulin resistance and hepatic fatty acid oxidation causes NAFLD and the progression from steatosis in the presence of inflammation leads to fibrogenesis (Day & James 1998). However, the complexity of defining NASH was reviewed by Charlton (2007) and proposed NAFLD is likely to be more complex than the 2-hit phenomenon and therefore suggested at least a 3-hit phenomenon.

Undoubtedly, the mechanisms underlying NASH are awaiting clarification due to the complications in defining the progression of steatosis to NASH.

Figures 1. 1: The progressive development of NASH

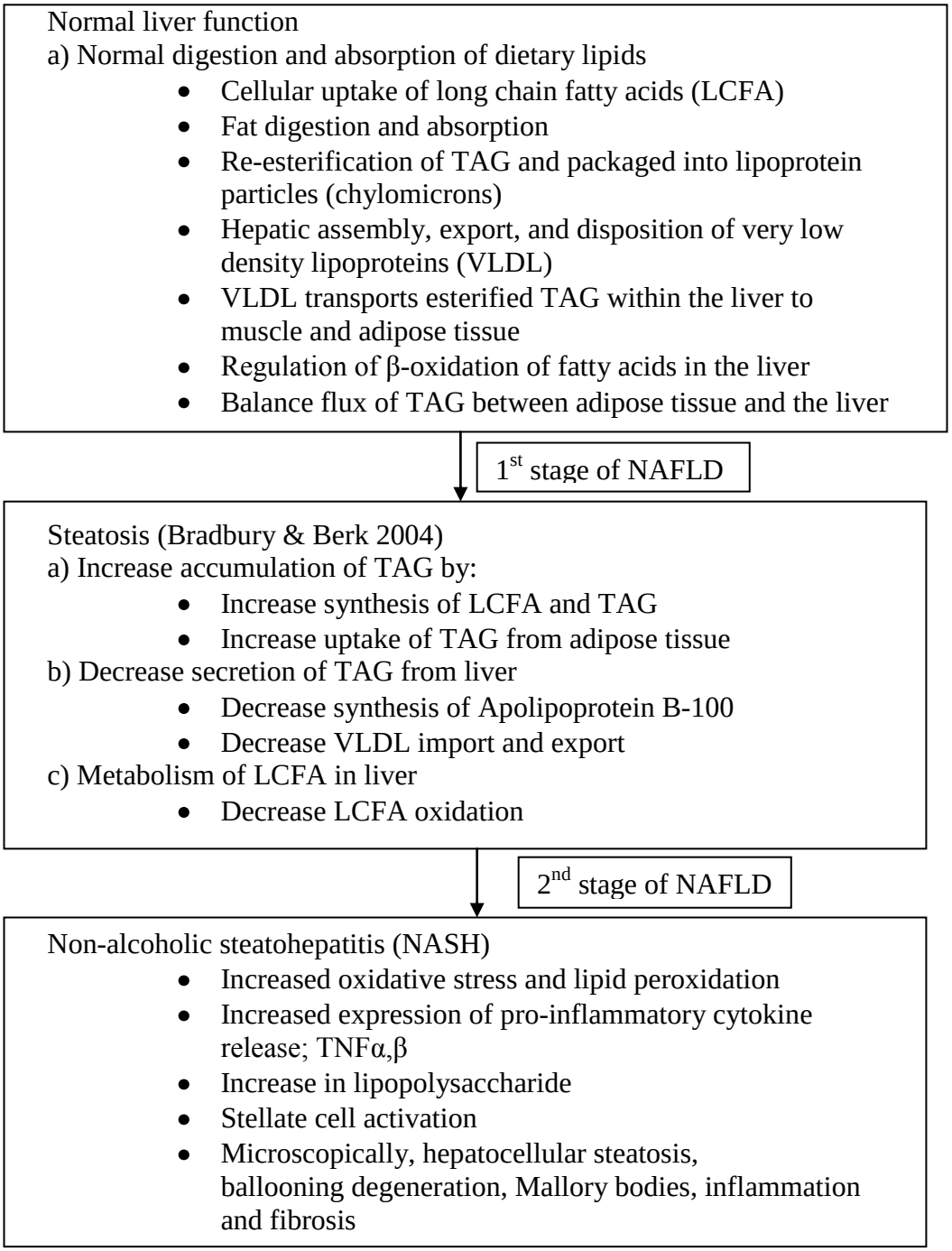

Source: Day & James (1998) and Bradbury & Berk (2004)

1.2 The prevalence of NASH as a new epidemic of NAFLD

In the United States, 30 % of the adult population suffers from liver steatosis which is defined when TAG content is more than 5.5% normal TAG content (Angulo 2007). The prevalence is estimated to be one third of NAFLD cases which parallels the frequency of obesity (Caldwell et al, 2004; Gholam et al, 2007; Moore 2010), insulin

resistance (Seppala-Lindroos et al, 2002) and metabolic syndrome (Marchesini & Marzocchi 2007; Moore 2010).

Similarly in animal models, mainly rodents, experimental studies showed an association of obesity, insulin resistance and metabolic syndrome with hepatic steatosis (Coleman 1982; den Boer et al, 2004; Nanji 2004; Larter & Yeh 2008; Gaemers et al, 2011). In humans, steatohepatitis and the development of fibrosis predispose to cirrhosis and have a survival of 7 to 10 years (Farrell and Larter 2006).

1.2.1 Prevalence of NASH in different age groups

In 2004, the International Obesity Task Force (IOTF) reported there was a prevalence of 22 million overweight children followed by 20 million overweight children younger than 5 years of age in the European Union. A National Health and Nutrition Examination Survey (NHANES) study from 1999 to 2004 associated the elevated levels of circulating alanine aminotransferase (ALT) with increased waist circumference and insulin resistance in adolescents aged 12 to 19 years (Fernandez et al, 2004). The elevated ALT levels increased according to age (Fraser et al, 2007). However, there are still complications in standardizing the measurements of children between age 5 and 14 years due to rapid growth in height and weight. Therefore, clinical trials are required to develop different cut-off points for ALT levels as a benchmark for assessing children before diagnosing for NASH.

As for adults, the prevalence of NAFLD in the UK was mainly found in the middle-aged (≥ 50 to < 60) and the elderly (≥ 60) (Frith et al, 2009). Although ALT levels have been used as a biomarker to identify patients with hepatocyte damage for the past 55 years (Karmen et al, 1955), it has been reported that normal ALT levels do not indicate the absence of NAFLD (Mofrad et al, 2003). Therefore further work needs to be carried out to identify biomarkers for NAFLD more accurately.

Aging-related studies in animals showed increased prevalence of liver diseases in old mice aged 24-36 months (Ito et al 2007; Gregg et al, 2012). Old age in mice showed increased hepatic sinusoid which led to impairment in clearance of chylomicron remnant and disruption of microcirculation (Warren et al, 2005; Le Couteur et al, 2008). The thickening of the endothelium and increased hepatic sinusoid also known as pseudocapillatication is common in aged liver (Le Couteur et al, 2008) and may have implications for NAFLD as shown in a human study by Kagansky et al, (2004).

1.2.2 Prevalence of NASH by gender

The prevalence of NAFLD in female adults is commonly found to be higher than in males due to different metabolic behaviour such as higher visceral fat, TAG and LDL-cholesterol levels in women (Fernandes et al, 2010; Fracanzani et al, 2011).

Animal studies on gene expression related to lipid metabolism in response to high fat diets have highlighted important gender differences after 6 months of high-fat feeding. Male rats had higher hepatic peroxisome proliferator-activated receptor–alpha (PPAR-α) and carnitine palmitoyltransferase-1 (CPT-1) expression compared to female rats indicating higher lipid oxidation and higher hepatic TAG (Priego et al, 2008). In contrast, female rats gained more weight with higher adiposity index and increased gene expression related to energy influx in adipose tissue (Rodriguez et al, 2004). Therefore female rats have a higher capacity for fat storage in adipose tissue and fat oxidation in muscles whereas males have a higher risk of hepatic fat accumulation.

1.2.3 Prevalence of NASH by race and ethnicity

Different racial and ethnic group studies show different susceptibility towards visceral adiposity, hepatic fat accumulation and insulin resistance. The prevalence of NASH is dependent on ethnicity whereby the frequency of NASH is highest in Hispanics, followed by whites and blacks (Browning et al 2004). In the Asia-Pacific region, NASH is highest in the Indian population compared with the Chinese and Malays (Chitturi et al, 2007; Amarapurkar et al, 2007). Chow et al (2007) showed that 73% Singaporeans Chinese non-diabetic patients with histological proven NASH went on to develop fibrosis.

These ethnic and racial variations may reflect differences in environmental and genetic susceptibility towards visceral adiposity, hepatic fat accumulation and fatty acids regulation (Weston et al, 2005). Therefore the differentiation between steatosis and NASH should take into account the ethnic and racial background towards NAFLD, which is spreading epidemically throughout the world.

1.3 Metabolic pathways leading to lipid accumulation

Although the exact biochemical pathway of NASH is still unclear, there is strong evidence showing that the infiltration and accumulation of TAG increases the risk of lipid peroxidation in the liver leading to inflammation. The potential pathways of dietary fat contributing to NASH include the following:

i) High fat dietary intake to the liver through chylomicrons.

ii) Suppression of mitochondrial beta-oxidation in the liver.

iii) High influx of non-esterified fatty acids (NEFA) from adipose tissue to the liver (also known as lipolysis).

iv) Fatty acids made within the liver through *de novo* lipogenesis.

v) Low secretion rate of very low-density lipoprotein (VLDL) from the liver.

Figures 1. 2: Flow chart of the fatty acid regulatory system

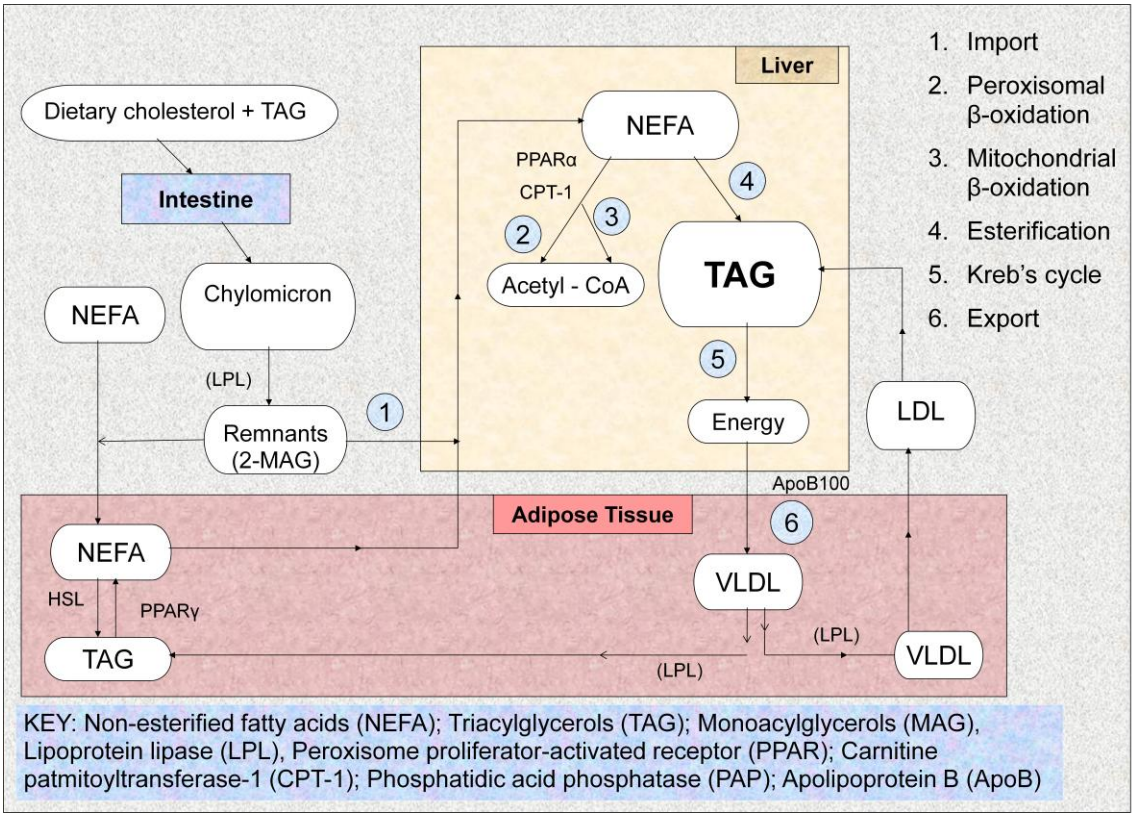

Adapted from various sources including Hussain et al, (2000) and Dallinga-Thie et al, (2010)

Plasma lipids are transported in 2 forms namely NEFA and TAG (***Figure 1.2***). NEFA is derived from adipocytes and transported with plasma albumin whereas TAG

and cholesteryl esters are transported in the core of plasma lipoproteins. Dietary fat is secreted and transported by chylomicrons to the liver for storage. Dietary cholesterol is transported to the liver by chylomicron remnants. TAG is then released from the liver in the form of VLDL for utilisation or storage in extrahepatic tissues. In the conversion of VLDL to LDL, these lipoproteins are packed with cholesteryl esters (Spector 1984). The occurrence of NASH due to the accumulation of fats in the liver may be affected by the types and composition of fatty acids ingested.

1.3.1 Delivery of dietary fat to the liver through chylomicrons

Chylomicrons are fat transporters (mainly TAGs) from the intestine to the liver and adipose tissue (Hussain et al, 2000). Ingested fats travel down the oesophagus to the duodenum, stimulating secretion of cholecystokinin (CCK) causing the gall bladder to contract and release bile into the duodenum (Glatzle et al, 2003). The bile emulsifies and breaks down fats allowing fats to be absorbed by the enterocytes, epithelial cells of intestine. Fats and cholesterols are then packaged into chylomicrons in the enterocytes. A chylomicron is a single monolayer of phospholipids and cholesterol that contains mainly TAGs with an integral protein apolipoprotein B-48 which is important for chylomicron synthesis. The absence or defect in apolipoprotein B-48 will cause disruption in formation of chylomicrons and fats will either accumulate in the intestine or be secreted in faeces (Lo et al, 2008). Chylomicrons are then released from the basolateral site of enterocytes to lacteals and travel to the lymphatic system and end up in the thoracic duct, then the circulatory system to the blood stream, obtaining 2 new integral proteins (apolipoprotein C and E). From the blood vessels, chylomicron travels to either the liver or adipose tissue.

In the liver, hepatocytes have LDL receptors which bind to apolipoprotein E. When bound to the LDL receptors, TAG in the chylomicrons will be taken up by the liver. In the adipose tissue, adipocytes express enzyme lipoprotein lipases (LPL) which bind to apolipoprotein C. When bound to LPL, TAG will be cleaved to glycerol and individual fatty acids and absorbed by the adipocytes therefore decreasing the levels of TAG in chylomicrons. When TAGs within the chylomicron are reduced to 20%, apolipoprotein C will be detached forming chylomicron remnants (Cooper et al, 1997). Chylomicron remnants (CR) then travel to the liver and binds to the CR receptors to absorb the remaining TAG. The hepatic uptake of TAG from the CR is dependent on the type of dietary fats as shown in a study by Lambert et al, (2000). Saturated

chylomicrons are metabolized slower compared with polyunsaturated ones (Green et al, 1984).

1.3.2 Suppression of beta-oxidation in the liver

The process of beta-oxidation occurs in the mitochondria or peroxisomes (van Roermund et al, 1998) and serves to break down fatty acids in the form of acyl-CoA to generate acetyl-CoA which then enters the Kreb cycle to generate ATP as an energy source. The rate of oxidation decreases with increasing fatty acid chain length (Leyton et al., 1987). Long chain fatty acids (LCFA) are actively transported from the cytoplasm into mitochondria by carnitine palmitoyl transferase -1 (CPT-1) for beta-oxidation to take place. In the mitochondria, LCFA are broken down in 4 steps; dehydration, hydration, oxidation and thiolysis. The result of one cycle is formation of one acetyl-CoA and the release of 2 carbons from the end of the fatty acid chain. This cycle continues to shorten the fatty acid through oxidation until the entire chain of fatty acid is converted to acetyl CoA. The fate of acetyl-CoA transported to the Krebs cycle (citric acid cycle) is oxidation to CO_2 and H_2O which increases the formation of $FADH_2$ and $NADH + H^+$ (energy carriers). These carriers transfer energy, and oxidation takes place in the mitochondrial electron transport system to generate ATP. Besides that, acetyl-CoA can also be transported to the liver for the production of ketone bodies. High fat diets can increase total peroxisomal beta-oxidation by 1.4 to 2.4 fold in rat liver (Neat et al, 1980).

Suppression of mitochondrial beta-oxidation regulated by CPT-1 is associated with hepatic fat accumulation (Serviddio et al, 2011). The effects of mitochondrial beta-oxidation are commonly studied in methionine choline deficient (MCD) mice. These mouse models show higher rates of oxidative phosphorylation and low efficiency of cytochrome oxidase activity. In rats, provision of MCD deficient diets result in decreased mitochondrial ATP synthesis that may cause steatosis and oxidative stress reflecting the features of NASH (Romestaing et al, 2008). Mitochondrial dysfunction was also associated with the over production of reactive oxygen species in hepatocytes causing NASH (Sato 2007).

Mutations in mitochondrial DNA are found to cause fat accumulation and cellular stress in myocytes due to the activation of Jun N-terminal kinase (Lu & Archer 2007). In the hepatocytes, the disrupted flow of electrons causes the increase formation of ROS and peroxynitrite generated by ROS during lipid peroxidation. Therefore, liver

lesions caused by mitochondrial oxidative stress due to lipid peroxidation products may also result in NASH.

1.3.3 High influx of NEFA to the liver

The main source of NEFA in the liver is from the adipose tissue. Hydrolysis of TAG produces glycerol and NEFA. NEFA release from adipocytes is regulated by hormone sensitive lipase (HSL) activated by glucagon and epinephrine but inhibited by insulin (Emanuele et al, 2004). The muscle and liver are the major target tissues of NEFA bound to albumin (Larter et al, 2008). In the liver, NEFA is passively absorbed by hepatocytes bound to fatty acid binding protein followed by the activation process of NEFA converting into CoA derivatives for energy production in the mitochondria with CPT as the carrier (Nosadini et al, 1984).

A metabolic labelling study using hyperlipidemic mice showed that the increased TAG synthesis rate contributing to excessive TAG stores in the liver was due to esterification of fatty acids (Donnelly et al, 2004). Furthermore, the quantification of hepatic TAG in NAFLD patients who were obese with fasting hypertriglyceridemia and hyperinsulinemia demonstrated that 59% of TAG was derived from NEFA, 26% from *de novo* lipogenesis and 15% from the diet (Donnelly et al, 2005). These quantitative metabolic labelling studies affirmed that the accumulation of hepatic TAG is mainly contributed by NEFA. The influx of NEFA to the liver leads to TAG synthesis in the liver.

C57BL/6J mice have an average TAG content determined by genetic factors influencing the hepatic fatty acid synthesis rates and TAG secretion compared to other strains such as BALB/c and SWR/J mice (Lin et al, 2005). Additionally, BALB/c mice presented the highest increase in fasting plasma NEFA and hepatic TAG concentrations followed by C57BL/6J and least in SWR/J mice. Findings from the aforementioned study concluded that the accumulation of hepatic TAG is strain-dependent (Lin et al, 2005).

The rates of oxidation of fatty acids are dependent on chain length and degree of unsaturation. Short and medium chain saturated fatty acids are oxidised rapidly. Of the major fatty acids, oleic acid is oxidised more rapidly than palmitic acid. Rates of TAG secretion by the liver can be according to type of fatty acid (Kohout et al, 1971). Kohout et al, (1971) concluded that maximal rates of TAG secretion will only occur when the metabolic pool for NEFA reaches an appropriate concentration with oleic acid being the

most suitable substrate for TAG secretion followed by palmitic and linoleic acid. These findings are consistent with more recent *in vitro*, studies with HepG2 cells showing that oleic acid is a potent stimulator of VLDL secretion.

In humans, TAG is secreted as VLDL containing apolipoprotein B-100 rather than apolipoprotein B-48 in rodents (Brown et al, 1997). Despite the differences, the fractional rates of TAG turnover are similar in both mice and rats. However, humans may retain a larger proportion of TAG within the cell compared to rodents which have a higher rate of VLDL-TAG secretion (Salter et al, 1998). Long-chain *n-3* polyunsaturated fatty acids decrease TAG synthesis from the liver and decreases VLDL-TAG secretion from the liver but it is uncertain whether these fatty acids reduce fat accumulation in the liver in overfeeding models.

1.3.4 Low VLDL-TAG secretion rate

VLDL is produced by the liver to transport fats from the liver to adipose and other tissues. VLDL carries TAG and CE with apolipoprotein B-100 (in man) or apolipoprotein B-48 in rodents as the integral protein (Chen et al, 2008). Similar to the chylomicrons, VLDL travels into the blood vessels and obtains 2 new peripheral proteins (apolipoprotein C and E) from HDL. Apolipoprotein C then binds to the lipoprotein lipase (LPL) and cleaves TAG into glycerol and free fatty acids. When the TAG levels in VLDL decrease to 50%, apolipoprotein C unbinds and travels back to the liver (Qin et al, 2011). The increased production of TAG and decreased secretion of TAG exported as VLDL could be related to the mechanisms involved in TAG accumulation which influences NAFLD (Goldberg & Ginsberg 2006).

Obese NAFLD subjects showed higher VLDL-TAG secretion but no difference in VLDL-apolipoprotein B-100 secretion rates when compared to subjects with normal hepatic TAG content (Fabbrini et al, 2008); ie they secreted VLDL particles that were enriched in TAG. The increase in VLDL-TAG is caused by the high influx of NEFA derived from lipolysis but the increased VLDL-TAG secretion is insufficient to normalize hepatic TAG content in NAFLD (Fabbrini et al, 2008). The increased rates of lipolysis and hepatic VLDL-TAG secretion may contribute to hypertriglyceridemia and may exacerbate insulin resistance which in turn would promote NAFLD (Seppala-Lindroos et al, 2002).

The alterations in VLDL-TAG metabolism in adipose tissue and liver in NAFLD remains controversial due to other factors influencing hepatic lipoprotein metabolism such as gender and adiposity (Mittendorfer et al, 2003).

1.4 The effects of different types of fats in the liver

The different type of fatty acids in the liver may be a more important factor affecting the pathogenesis and progression of non-alcoholic fatty liver disease (NAFLD) compared to the quantity of fat (Barboriak et al, 1957). Dietary fats were reported to inhibit the release of fatty acid synthesised *de novo* from the liver to the plasma which led to the accumulation of fatty acids in the liver. In contrast, a fat-free diet showed significant increase in SFA and MUFA but not PUFA in both the liver and plasma (Nelson et al, 1987).

Alterations in hepatic fatty acid composition and content may be important in the pathogenesis of NASH. For example: obese mice have significantly higher linoleic acid (18:2n-6) in liver phospholipids (PL), cholesterol esters (CE) and triacylglycerols (TAG) (Emanuele et al, 2004) compared to the controls. Phosphatidylcholine is the most common PL in the diet and is absorbed by the intestine, which then appears in plasma lipoproteins and blood (Noga & Vance 2003; Wu & Cohen 2005). EPA and DHA may replace arachidonic acid (AA) in membrane phospholipids in liver and these changes are accompanied by alterations in cytochrome P450 enzymes (Arnold et al, 2010). Other PL such phosphatidylethanolamine, phosphatidylserine and phosphatidylinositol are ingested in small amounts (Koba et al, 1994; Jacobs et al, 2010). Dihomo-gamma-linolenic acid (DGLA; 20:3n-6) increases in PL with weight gain ($P<0.001$). However, PL arachidonic acid (AA; 20:4n-6) does not show significant differences with obesity status (Phinney et al, 1994). Cholesterol esters are less polar compared with free-cholesterol and contains high proportion of PUFA mainly of phosphatidylcholine.

1.4.1 Effects of high fat hypercaloric feeding in the liver

The recommendations by World Health Organization (2003) consists of 15 - 30% of total fat whereby <10% is derived from saturated fats, 5 - 8 % from n-6 polyunsaturated fats (PUFA) and 1 – 2% from n-3 PUFA. Animal studies have generally used nutritional models based on high-fat diets providing 40% to 70% energy

from fat to induce obesity, hyperglycemia, insulin resistance and progression of NASH that may lead to fibrosis (Nishikawa et al, 2007; Satyanarayana et al, 2011; Yimin et al, 2011).

One well-established high-fat diet protocol designed for animal studies is the Lieber-DeCarli feeding regimen whereby the controls are fed 35% fat, 47% carbohydrate, 18% protein. However, in this liquid diet model it is to be noted that most of the energy is derived from carbohydrate. The regimen is an overfeeding model rather than a high fat diet. In an experiment, when rats were fed *ad libitum* with 71% energy fat, 11% energy carbohydrate and 18% energy protein for 3 weeks there was a 2-fold increase in panlobular steatosis when compared to controls fed the standard diet (Lieber et al, 2004). Furthermore, the rats developed abnormal mitochondria with degenerating cristae, mononuclear inflammation with increased hepatic TNF-α and Cyp2e1 mRNA, significant hepatic oxidant damage indicated by increased levels of 4-hydroxynonenal and increased hepatic concentrations of collagen type 1 and 1α procollagen mRNA (Lieber et al, 2004). As expected in controls there were less steatosis, inflammation, oxidative stress and lower plasma insulin concentrations. However, this high fat diet did not increase body weight or alter ALT activities in the serum (Lieber et al, 2004).

Intragastric overfeeding of mice with 85% fat for 9 weeks, increased body weight by 71% caused by the accumulation of visceral fat and led to hyperglycemia, hyperinsulinemia, hyperleptinemia, glucose intolerance and insulin resistance (Deng et al, 2005). Forty-six percent of these mice developed NASH with increased plasma ALT by 5-6 fold and neutrophil infiltration in liver. Similarly, in human NASH, there is sinusoidal and pericellular fibrosis. The excess build-up of white adipose tissue developed higher TNF-α and leptin, reduced adiponectin mRNA expression, increased expression of lipogenic transcription factors (SREBP-1c, PPARγ and LXRα) and reduced the expression of lipolytic nuclear transcription factor, PPARα (Deng et al, 2005).

A study by Li et al (2005) administered a high fat diet (59% energy) to C57BL-6 mice for 13 weeks. This aforementioned study resulted in decreased hepatic natural killer T (NKT) cells with sensitization of the liver to low-dose lipopolysaccharides (LPS) (Li et al, 2005). This study showed decreased hepatic natural killer T (NKT) cells with sensitization of the liver to low-dose lipopolysaccharides (LPS) (Li et al, 2005). The decreased levels of NKT cells decreased the expression of anti-inflammatory cytokines (Th-2) and increased expression of pro-inflammatory cytokines (Th-1) in the

liver of mice fed the 59% fat diet. ALT activities were also elevated following stimulation by LPS. However, levels of inflammation or fibrosis after high-fat feeding were not reported (Li et al, 2005).

Similarly, based on a 'two hit' approach by Ito et al (2006), C57BL-6 mice fed with a 60 % fat with tetracycline diet resulted in increased serum ALT activities with development of hepatic inflammation. In addition, a 60 % by weight lard diet was used to trigger the 2nd hit and cause steatohepatitis in fa/fa rats. Consequently, these rats developed oxidative stress induced NASH due to increase NADPH oxidase activity, lipid peroxidation and protein carbonyl formation followed by a significant reduction in serum adiponectin caused by the reduced activation of PPARα-mediated liver fatty acid pathway (Carmiel-Haggai et al, 2005). The test diet, however, was nutritionally imbalanced.

1.4.2 Effects of polyunsaturated fatty acids (PUFA) on lipid metabolism

There are two families of polyunsaturated fatty acids derived from linoleic and α-linolenic acid that give rise to the *n-6* and *n-3* series respectively by alternating desaturation and chain elongation. Linoleic acid is an essential nutrient with a wide variety of functions and many of its effects are mediated via arachidonic acid. The essentiality of α-linolenic acid hinges on its conversion to docosahexaenoic acid, which has an important physiological role in the retina and the brain. These polyunsaturated fatty acids have effects on cell signalling and gene expression which includes inflammatory signalling and lipid metabolism. The long-chain derivatives of α-linolenic acid, eicosapentaenoic acid and docosahexaenoic acid which are found in marine lipids have been shown to possess a variety of physiological effects that are different from their parent fatty acids. In particular, they have anti-inflammatory effects and stimulate fatty acid oxidation and decrease triglyceride synthesis in the liver.

In n-6 PUFA family, arachidonic acid (AA) is the predominant long chain metabolite and it regulates cellular functions through conversion to prostaglandins, lipooxygenase and cyclooxygenase products (Schmitz & Ecker 2008). AA can be replaced by EPA but its eicosanoid metabolites are generally inactive. Linoleic acid, itself has a role in cholesteryl ester transport and is the preferred substrate for lecithin cholesteryl acyl transferase. Mice supplemented with n-6 PUFA also show increased expression of leptin gene transcripts in epididymal fats but do not change in mice fed n-3 PUFA.

Studies have reported that hepatic transcription genes related to fat metabolism are directly correlated to the different types of dietary fats delivered to the liver (Radonjic et al, 2009; Yang et al, 2010; Do et al, 2011). EPA and DHA are ligands for PPAR-α, which is transcription factor regulating fat oxidation and hepatic TAG synthesis.

There are reports that n-3 PUFA may have a favourable effect in animals with NASH. Therefore, supplementing diets with n-3 PUFA such as EPA and DHA, may prevent or reverse NASH either by (i) inhibition of lipogenesis due to a decrease in mature sterol–regulatory element-binding proteins (SREBPs) or (ii) stimulation of fatty acid oxidation via peroxisome proliferator-activator receptor (PPAR) alpha (Hirako et al, 2010).

In a 12-month study, Tanaka et al, (2008) reported that NASH patients supplemented with 2700 mg/d of purified EPA resulted in enhanced ALT activities, and increased serum free fatty acids and plasma soluble tumour necrosis factor (TNF) receptor 1 and 2 levels. Although there was no change in either body weight, insulin and adiponectin concentrations, there was a significant decrease in oxidative stress in the liver. The liver biopsy showed a decrease in hepatic fibrosis, hepatocyte ballooning and lobular inflammation. Other studies have reported inhibition of linolenic acid conversion pathways (desaturation and elongation) in response to increasing dietary EPA and DHA intake (Emken et al., 1999; Vermunt et al., 2000). Conversion of EPA to DHA involves Δ5 and Δ6-desaturation chain elongation, desaturation and limited peroxisomal beta-oxidation (Sprecher 2000).

However, the effects of EPA and DHA as individual fatty acids remains unclear and further supplementation studies are required to investigate the optimal amount of n-3 PUFA necessary for inducing positive biological effects.

1.4.3 Effects of EPA in the liver

EPA was shown to reduce fatty droplets in hepatic cells, decrease liver weights, lower plasma levels of total cholesterol, free total cholesterol, phospholipids and triacylglycerols (Nemoto et al, 2009). EPA may have a greater serum TAG reducing agent compare to DHA (Gotoh et al, 2009) but the evidence is not consistent and the totality of evidence indicates that both EPA and DHA are equipotent. A 1000 mg dosage of eicosapentaenoic acid (EPA) per day per kg body weight was shown to decrease serum TAG by 45% after 10 days while there was no significant differences in

serum cholesterol when compared to mice fed palmitic acid and controls (Demoz et al, 1992). EPA was also found to reduce levels of hepatic lipid peroxides while no change was observed in palmitic acid fed mice in comparison to the controls (Demoz et al, 1992). Therefore, it was suggested that EPA may be able to prevent non-alcoholic steatohepatitis.

Mice fed a high fat diet for 6 weeks followed by an EPA diet for 5 weeks showed reduced insulin resistance, reduced adipose inflammation, lipogenesis and markers of fatty acid oxidation (Kalupahana et al, 2010). In addition, 16 weeks of feeding saturated fats followed by supplementation with 98% of purified EPA for 12 weeks in PPAR-null mice was shown to result in amelioration of steatosis through inhibition of sterol-responsive element-binding protein-1 (SREBP-1) in the absence of PPAR-alpha. Furthermore, fatty acid uptake was suppressed and hydrolysis of intrahepatic TAG was enhanced in the presence of EPA, independent of PPAR-alpha. Therefore, the aforementioned effects of EPA in the absence of PPAR-alpha activation demonstrates the potent function of EPA in decreasing lipid peroxides and ameliorating steatosis by reducing hepatic oxidative stress (Tanaka et al, 2010).

A followed-up study by Sugiyama et al, (2008) showed the increased composition of hepatic TAG and monounsaturated fatty acids (MUFA) in mice a fed high fat and high sucrose diet (HFHSD) for 2 weeks was altered when EPA was administered to mice. In the presence of EPA, hepatic TAG content was significantly suppressed and MUFA composition of palmitoleic acid (C16:1) and oleic acid (C18:1) was lowered. Besides that, n-3 PUFA such as EPA and DHA were increased in liver (Kajikawa et al, 2009).

Although EPA is used clinically used to treat hypertriglyceridemia, there is a lack of evidence to demonstrate that it has beneficial effect in patients with NASH.

1.4.4 Effects of DHA in the liver

In the liver, DHA may exert its anti-inflammatory effects by inhibiting cytokines and eicosanoid metabolism (Gonzalez-Periz et al, 2006; Beharry et al, 2007). DHA but not EPA was reported to reduce insulin resistance through an increase in circulating adiponectin (Vemuri et al, 2007). DHA on its own is highly susceptible to lipid peroxidation due to its volatile chemical structure with six double bonds. Peroxidation of DHA causes cell membrane degeneration (Song et al, 2000).

Dietary DHA was shown to be mainly incorporated into phosphatidylethanolamine and phosphatidylcholine of the liver and adipose tissue after 4 days of feeding mice with a DHA rich diet which resulted in an improved profile of adipokines (Lefils et al, 2010). Recently, Sun et al, (2011) reported that DHA increased the expression of lipogenesis and lipolysis genes in adipose tissue, whereas in the liver lipogenesis genes were decreased and lipolysis genes were increased by DHA. Therefore, this study concluded that DHA could reduce body fat mass by regulating lipogenesis and lipolysis genes (Sun et al, 2011).

The reduction of hepatic TAG content in DHA fed mice was shown to be related to the suppression of hepatic enzymes related to TAG synthesis (Kim et al, 2008). Also, mice administered with DHA for 4 weeks show reduced fatty acid synthase (FAS) and malic enzyme activity (Gotoh et al, 2009). Besides that, the serum adiponectin concentrations were raised due to the suppression of TAG synthesis (Gotoh et al, 2009).

1.4.5 Effects of TAG structure in dietary fats in the liver

The differential positional distribution of TAG in fatty acids affect lipid metabolism (Christensen et al, 1998; Sundram et al, 2007). It has been suggested that animal fats such as lard which are high in saturated fatty acids (SFA) exacerbates fatty liver disease (Sanders et al 2011). Lard consists of a high proportion of SFA in the sn-2 position of TAG whereas vegetable fats such as palm oil contain the SFA in the sn-1 and sn-3 position. Kayden et al, (1967) demonstrated that SFA in the sn-2 position of TAG are well absorbed in rodents whereas randomized lard is less well absorbed. Fatty acids in the sn-2 position are retained in that position upon absorption and TAG synthesis in the intestine retains the same fatty acid as in the sn-2 monoacylglycerol (Small 1991).

Lieber et al, (2008) demonstrated that medium-chain TAG (MCT) which consists mainly of C8-C10 saturated fatty acids is not toxic in the liver in the absence of long chain TAG (LCT). Indeed, MCT are used in the dietary management of liver disorders. LCT emulsions (derived from soybean oil) cause slow clearance from the bloodstream and reticuloendothelial system (Seidner et al, 1989). MCT, however, do not result in chylomicron formation and are transported to the liver in the hepatic portal vein and rapidly oxidized by the liver. The total replacement of dietary LCT with MCT is beneficial whereas partial replacement becomes toxic unless dietary restrictions take place. Partial replacement increases TNF-alpha and its mRNA but does not promote

hepatic fat accumulation. However, when 70% fat is fully replaced with MCT, steatosis does not develop and hepatic TNF-alpha decreases. Similar results are obtained when all MCT are replaced with carbohydrates (Lieber et al, 2008).

Fatty acids distribution in the liver may depend of the type of fatty acids in the *sn*-2 position of TAG (Robins et al, 1991; Schmid et al, 1997). A TAG with unsaturated fat in sn-2 position may lead to different effects on hepatic lipids and distribution of fatty acids when compared to saturated fats in the sn-2 position.

1.5 Liver proteomes of mice fed either low fat or high fat hypercaloric diets

The term proteomics was coined in 1994 by Marc Wilkins and the proteome is defined as a complement of proteins expressed in a cell (Wasinger et al, 1995). Proteins are important in the development of cells and tissues and regulate their function. Proteomics, using 2 dimensional – differential in gel electrophoresis (2D-DIGE) have been carried out to investigate changes in protein expression in response to the various types of dietary fat. For example, dietary fat intakes have been shown to modify mitochondrial proteomes in the liver such as superoxide dismutase 2 (Lee et al, 2008) and alter proteins in various pathways such as nitric oxide metabolism (Eccleston et al, 2011), cellular adaptation (de Roos et al, 2009), and methionine metabolism (DiBello et al, 2010). The proteomics approach of these aforementioned studies using 2D-DIGE did not investigate the effects of different types of hypercaloric diets on the liver. In the study for this thesis we investigate how various dietary fats cause changes in the liver proteome.

1.5.1 Protein expression in mouse liver associated with high fat hypercaloric feeding

Liver PPAR-α and PPAR-γ play major roles in the pathogenesis of NASH by affecting hepatic lipogenesis and fatty acid oxidation (Issemann & Green 1990). Although in humans, hepatic PPAR-alpha is less abundant compared to rodents, human PPAR-alphas appear to have similar functional characteristics to rodents (Holden & Tugwood 1999). Studies in mice with defective peroxisomal fatty acid β-oxidation showed increased hepatic PPAR-α, cytochrome (Cyp) P450, Cyp 4a10, Cyp 4a14 expression and elevated hydrogen peroxide (H_2O_2) at 4 to 5 months of age (Infante et al,

2002). This is followed by a drastic increase in fatty acid (FA) oxidation particularly long chain fatty acids. By 15 months of age, mice with defective peroxisomal fatty acid β-oxidation develope adenomas and carcinomas. In contrast, the activation of PPAR-α is known to regulate fatty acid metabolism by increasing lipolysis and clearance of chylomicron remnants (Sugden et al, 2002). PPAR- α also stimulates the conversion of fatty acid to acyl-CoA derivatives, inducing beta-oxidation, reducing TAG synthesis and decreasing VLDL production (Schoonjans et al, 1996). Recently, a study showed that hepatic steatosis was ameliorated by EPA, independent of PPAR-α by inhibiting sterol-responsive element-binding protein-1c (SREBP-1c) (Tanaka et al, 2010). The effects of n-3 polyunsaturated fatty acids in the liver will be discussed in the next sub-chapter.

PPAR-γ is a nuclear receptor involved in glucose and lipid homeostasis. Its down-regulation protects mice from hepatic steatosis induced by a high fat hypercaloric diet. The down-regulation of PPAR-γ cascades to the down-regulation of genes related to lipogenesis (SCD-1 and SREBP-1c) and β-oxidation such as PPAR- α (Moran-Salvador et al, 2011). Other studies, although not directly looking at the effects of high fat hypercaloric diets, showed that there was a reduction in lipogenesis in mice fed high fat diets due to the down-regulation of SREBP-1c. This leads to a decreased fat accumulation in the liver (Sheng et al, 2011; Murase et al, 2011). SREBPs are transcription factors that regulate lipid homeostasis by activating enzymes required for endogenous non-esterified fatty acids, triacylglycerols, cholesterol and phospholipids synthesis (Eberle et al, 2004).

Aside from the high fat diet, a methionine-choline deficient (MCD) diet is commonly administered to mice in order to investigate the underlying mechanisms of NASH (Rinella et al, 2008; Lee et al, 2011). MCD diets potentially exacerbate fatty liver but do not cause insulin resistance in mice fed high fat (45% calories) diets when compared to mice fed 10% calories of low fat diet (Raubenheimer et al, 2006). MCD diets incorporated with a high carbohydrate or sugar content may induce NASH rapidly in mice models (Pickens et al, 2010). In addition, MCD diets inhibit diacylglycerol acyltransferase-2 (DGAT-2) hence resulting in the development of hepatic steatosis, necroinflammation, and fibrosis in mice (Yamaguchi et al, 2008). Interestingly, a reduction in hepatic expression of tumour necrosis factor-alpha (TNF-α), elevates adiponectin and improves insulin sensitivity, does not attenuate steatosis but leads to the development of NASH (Yamaguchi et al 2007). The aforementioned study concluded

that, TNF- α, adiponectin in adipose tissue and insulin sensitivity may not be appropriate biomarkers for NASH (Yamaguchi et al 2007).

TNF- α converting enzyme (TACE) was shown to be significantly expressed in livers of mice overfed a high fat diet (Ono et al, 2003). Palmitic acid, lipolysaccharide, high glucose, and high insulin were reported to be responsible for the raised TACE activity. The over-expression of TACE resulted in the impairment of insulin-dependent phosphorylation of AKT and glycogen synthase kinase 3 (GSK3) in mouse hepatocytes (Fiorentino et al, 2010). The up-regulation of Akt in sterol regulatory element binding proteins-1c (SREBP-1c) knock-out mice is associated with hypertriglyceridemia, hepatic triglyceride accumulation and hypoglycaemia (Ono et al, 2003).

Previous studies on the effects of hypercaloric diets on mice liver have confirmed that the genetic models of NASH commonly develop hepatocellular adenomas and carcinomas unexpectedly (Lieber et al, 2008; Sheng et al, 2011). However, these models do not present a distinctive phase between steatosis and NASH. On the other hand, genetically modified animals may be preferred in investigating the mechanisms involved in the development of carcinomas in the liver rather than the progression of NASH from steatosis.

For the studies in this thesis, the effects of different types of diets on the protein profiles of the liver will be investigated.

1.5.2 The effects different types of dietary fats on protein expression in mice liver

The different types of dietary fats mainly saturated and polyunsaturated fats as described in ***Chapter 1.4*** may directly be associated with the differential expression of proteins in mouse liver.

Chronic high fat diets (70% energy as fat, 11% carbohydrate and 18% protein) administered to mice for 16 weeks have previously demonstrated to cause steatosis, altered nitric oxide metabolism and modified proteomes in liver mitochondria. The liver mitochondrial proteins involved were ATP synthase and pyruvate and malate dehydrogenase (Eccleston et al, 2011). Another high fat model, consisting of 45% of energy from fat with palm oil as the main source of the fat, was shown to cause alterations in hepatic one-carbon metabolism. In simple terms, the hepatic one-carbon metabolism involves the coupling of high levels of choline and low levels of methionine (Rubio-Aliaga et al, 2011).

The effect of fish oil on lowering the levels of hepatic enzymes related to steatosis such as epoxide hydrolase (Mavrommatis et al, 2010) has been used extensively. Long n-3 polyunsaturated fats in fish oils, mainly EPA and DHA, may have beneficial effects on the liver by suppressing TAG synthesis and up-regulating protective mechanism that decrease oxidative stress. However, high intakes of fish oil have well documented adverse effects and promote steatitis and the effects of EPA and DHA may differ when fed separately. Furthermore, many studies have failed to ensure that diets containing additional EPA and DHA are matched with an increased intake of vitamin E.

One study showed that fish oil but not pure DHA significantly lowered hepatic epoxide hydrolase levels in male apolipoprotein E knockout mice when compared to mice fed high-oleic sunflower oil (Mavrommatis et al, 2010). It was suggested that EPA rather than DHA is responsible for the lowering expoxide hydrolase observed with fish oil feeding. On the other hand, DHA was found to be more efficient in enhancing lipoprotein metabolism and reducing oxidative stress in comparison with EPA (Mavrommatis et al, 2010).

Mice fed a high-fat fish oil diet for 3 weeks presented significant increases in peroxisomal beta-oxidation and catalase activity in both liver and myocardium (De Craemer et al, 1994). Further investigations were carried out whereby 2% (w/w) of DHA administered to healthy mice showed slight but significant increases in catalase activity of myocardium after 3 weeks, but no change in the liver. In addition, there were no changes in the peroxisomes of the myocardium and liver indicating that DHA dosage used in the aforementioned study did not disrupt fatty acid metabolism in the liver (De Craemer et al, 1996).

On the other hand, the administration of EPA has shown to be involved beneficially, in the development of insulin resistance and lowering of adipokine production, which stimulates AMP-activated protein kinase (Lorente-Cebrian et al, 2009). Mice fed on a high fat diet (45% energy from fat) for 6 weeks, followed by a high EPA diet (45% energy from fat; 36 g/kg EPA) resulted in improvement of insulin resistance and lower plasma adiponectin. Furthermore, proteomic work in the aforementioned study reported an increase in markers of fatty acid oxidation and reduction in lipogenesis (Kalupahana et al, 2010). One key lipogenic enzyme, namely glycerol-3-phosphate dehydrogenase was reduced (Kalupahana et al, 2010).

In relation to proteomics of n-3 fatty acid composition in the liver, Demoz et al, (1992) showed that hepatic acyl-CoA oxidase and catalase activities increased by 50% and 30%, respectively, in EPA administered mice. EPA was shown to reduce levels of hepatic lipid peroxides while no change was observed in palmitic acid fed mice in comparison to the controls (Demoz et al, 1992). To this date, although fish oil is known for its protective effects against high fat-induced fatty liver and inflammation, the biological mechanisms of EPA and DHA as individual source of fatty acid are still being elucidated. For this thesis, the protein changes in the liver caused by the effects of hypercaloric diets are investigated, followed by the dietary effects of supplemental EPA and DHA, as individual fatty acids.

1.6 MicroRNA (miRNA) expression in fatty liver of mice

MicroRNAs (miRNAs) are single stranded non-coding RNAs comprising of 19 - 25 nucleotides and play an important role in the regulation of gene expression by binding to complementary site of target messenger RNA causing either transcript degradation or translational repression (Wiklund et al, 2010). Transcript degradation occurs when miRNA is a perfect match with its target gene causing the transcripts to cleave whereas translational repression happens when there are imperfect matches throughout the transcripts causing it to bind at the 3'UTR (untranslated region) of target messenger RNAs (mRNAs). To this date, the miRNA Registry contains 5071 miRNA loci expressing 5922 mature miRNA from 58 species *(http://microrna.sanger.ac.uk/;* Griffiths-Jones 2008).

It has been estimated that 30% of mammalian genes are regulated by miRNAs and a single miRNA can inhibit translation of more than 200 different mRNAs at one time by binding to the 3'UTR of target mRNAs (Bartel 2004). As a result, the inhibition of protein synthesis and destabilization of mRNA may be an important mechanism for causing disease. For example, the down-regulation of the liver-specific miRNA-122 results in reduced rates of cholesterol synthesis and enhanced hepatic fatty acid metabolism in a diet-induced mouse model of obesity (Esau et al, 2006).

The possibility of using miRNAs in understanding complicated diseases and its biological processes have received wide interest among researchers. It has been proposed that there is a need to further develop therapeutic uses of miRNAs as potential diagnostic and biomarker tools in disease (Bala et al, 2009).

1.6.1 Biogenesis of miRNA

The biogenesis of miRNA involves enzymatic processes in the following order (***Figure 1.3***):

- miRNA transcribed by polymerase II to primary transcripts.
- Dorsha and Pasha process primary miRNA to pre-miRNA by cleaving at the stem loop.
- Pre-miRNA is transported from nucleus to cytoplasm by Exportin-5.
- Cleavage of pre-miRNA to miRNA duplexes by Dicer.
- The duplexes are unwinded into a single strand and incorporated into the RICS to bind to3'UTR or target mRNA.
- The target mRNA is then translationally repressed or cleaved depending on the degree of homology.

Figures 1. 3: Biogenesis of miRNA

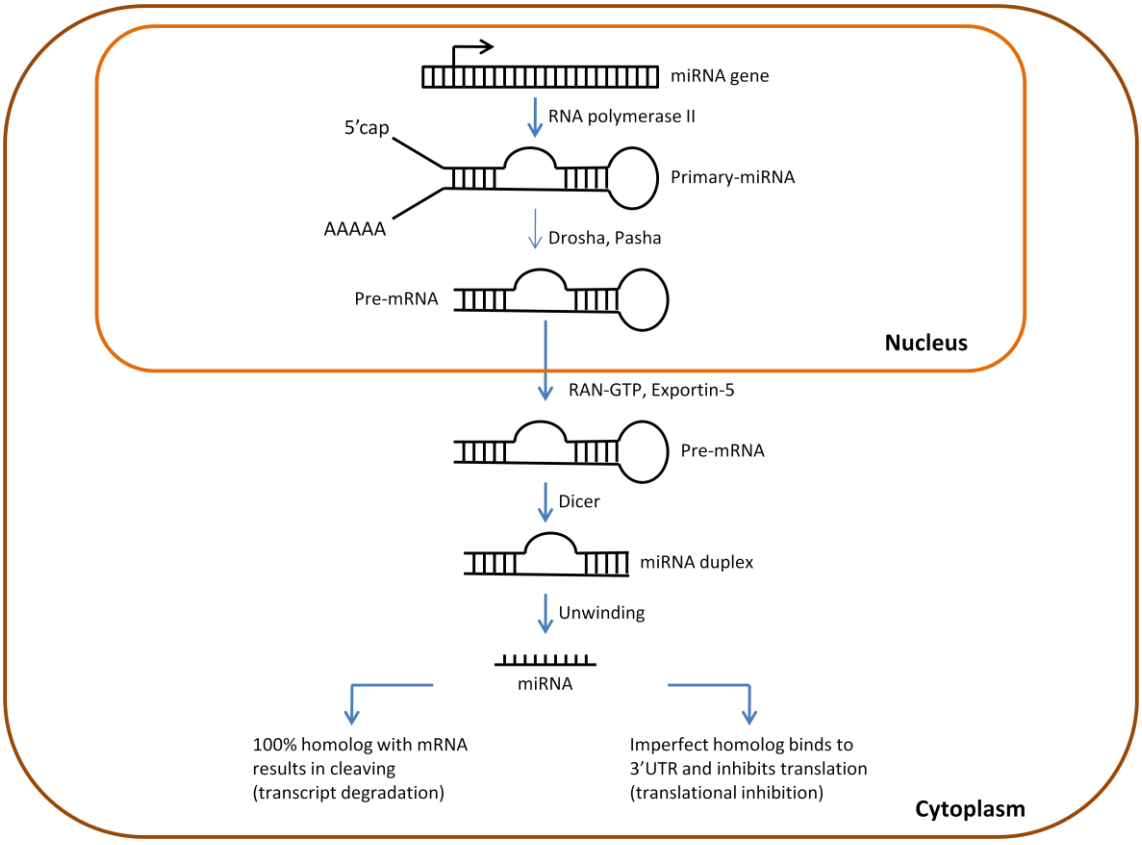

Source: Adapted from (Kim et al, 2009)

It has been suggested that miRNAs in humans reside in intron of either coding or non-coding transcription units (Rodriguez et al, 2004). Primary-miRNAs (pri-miRNA; 50-80 nucleotides) are products of independent genes which are transcribed by

RNA polymerase II (Morlando et al, 2008). The nuclear microprocessor protein complex containing Drosha and Pahsa cleaves pri-miRNAs into precursor-miRNAs (pre-miRNAs; 50-70 nucleotides). Drosha promotes intron degradation before splicing, which may influence maturation of mRNAs. Pre-miRNAs are then transported actively into the cytoplasm by RAN-GTP-dependent factor exportin-5. In the cytoplasm, Dicers cleave pre-miRNAs into duplexes consisting of 20 – 24 nucleotide mature miRNAs (Tijsterman & Plasterk 2004). The duplexes are located into the RNA-induced silencing complex (RISC) containing argonaute, which determines the functional strand before localizing the single stranded miRNA in the cytoplasm (Rand et al., 2005). Each pre-miRNA produces a single mature miRNA. As a result, post-transcriptional gene repression takes place either by transcript degradation or translational inhibitions depending on the complementarities of target mRNA to the miRNA. Other detailed aspects of miRNA metabolism and control can be found in selective reviews, for example Kim et al, (2009).

1.6.2 Implications of miRNA in gene regulation

The developmental timing in *Caenorhabditis elegans* led to the first miRNAs being discovered, namely lin-4 and let-7. Both these miRNAs were found to repress translation of their respective targets, namely lin-14 and lin-41 genes (Ambros 2004). Since then, advanced understanding of the mechanisms of miRNA in developmental processes such as differentiation and apoptosis have been investigated (Alvarez-Garcia & Miska 2005; Cheng et al, 2005). Studies on animal viruses have used miRNA for RNA silencing by targeting mRNAs for gene regulation (Pfeffer et al, 2004). This has led to a growing interest in miRNA in relation to cancer research. For example, down-regulation of miR-15 and -16 leads to chronic lymphatic leukaemia (Calin et al, 2002) and up-regulation of miR-221, -222 and -146 leads to the development of tumours (He et al, 2005). Undeniably, there is an increasing interest in the emerging role of miRNA either in gene regulation, as potential biomarkers or in therapeutics. In this study for the thesis, there is a focus on the miRNAs in the liver which alter in response to different types of hypercaloric diets.

1.6.3 MiRNA expression and pathways involved in hepatic steatosis

The understanding of miRNA in the underlying mechanisms and pathways of hepatic metabolism is rather limited and thus unclear. Recent studies have shown that

miR-122 is the most abundant miRNA (Young et al, 2010; Li et al, 2011) followed by miR-192 and miR-199a/b (Hou et al, 2011). These account for 52%, 16.9% and 4.9% of total liver miRNAs, respectively (Hou et al, 2011). More interestingly Cheung et al, (2008) reported that miR-122 was 63% down-regulated in livers of NASH patients and affected the expression levels of mRNAs encoding SREBP-1c.

In a normal mouse, the inhibition of miR-122 was found to reduce plasma cholesterol levels, increase hepatic fatty acid-oxidation and decrease hepatic fatty acid concentration (Esau et al, 2006).

There are some well-established cancer studies on miR-199 and miR-200 families (Yeligar et al, 2009; Murakami et al, 2011). For example, these show that the up-regulation of miR-199 attenuate hypoxia-inducible factor-1alpha (HIF-1 alpha) and endothelin-1 (ET-1) expression directly (Yeligar et al, 2009). Administration of anti-miR-199 showed reversed effects (Yeligar et al, 2009). HIF-1 and ET-1 are related to hypoxia and hepatic microcirculation, respectively, which may cause liver inflammation and cirrhosis. The miR-200 family is down-regulated in liver metastases and primary tumours by relieving inhibition of mesenchymal transcription factor Zeb1 that then suppresses E-cadherin (Olson et al, 2009). It is known that tumours that progress from adenomas to invasive carcinoma are characterized by loss of E-cadherin (Perl et al, 1998).

The up-regulation of miR-21 leads to significant changes in the miR-21 targets such as phosphatase and tensin homolog (PTEN) (Zhu et al, 2010). The up-regulation of miR-21 is dependent on the up-regulation of the AP-1 and ErbB/Stat3 pathway that plays an important role in liver carcinogenesis (Zhu et al, 2010). Another study on miR-21 showed its up-regulation was responsible for the reduced expression of hepatic PTEN in the early stages of hepatocarcinogenesis in C57BL/6J mice fed choline-deficient diet (Wang et al 2009). Additionally, the expression of miR-21 was significantly decreased in liver of rats fed fructose-enriched diets but showed no change in liver of rats fed a combined high fat and high fructose diets (Alisi et al, 2011).

Several studies have shown miRNAs are strongly associated with liver cancer (Calin et al, 2004; Braconi et al, 2011) and the differentiation state of hepatocellular carcinoma cells (Wong et al, 2008; Liu et al, 2011). Therefore, a miRNA profile in relation to NASH may be generated in order to understand the pathogenesis of these conditions. For this thesis, we will be investigating the effects of hypercaloric diets, which may lead to the development of NASH. However, the limitations in miRNA

profiling and validation towards understanding the mechanisms on how dietary fats affects the liver is mainly due to the lack of biological data linking specific miRNA expression to respective mRNA targets. Current software such as MiRanda and TargetScan are available for finding list of targets regulated by miRNAs but requires further validation (Ioshikhes et al, 2007).

1.7 Aims and hypotheses of the thesis

The aim of this project was to investigate the effects of varying the level and type of fat on the development of fatty liver in mice and to ascertain the extent of changes in the liver using biochemical and histological indices of liver damage. Proteomic and microRNA (miRNA) studies were conducted to identify changes in protein expression and molecular regulation in order to look for potential markers of liver damage and/or to identify points of regulatory control.

The hypotheses of this project are:

1. Different types of hypercaloric high fat diets cause alteration in lipid accumulation in the liver and exacerbate NASH.
2. Dietary n-3 PUFA such as EPA and DHA play a protective role by regulating synthesis and oxidation of fatty acids and alters the pattern of fat accumulation in the liver.
3. Palmitic acid in the sn-2 position may be more detrimental to liver lipid metabolism than it is in the sn-1 and sn-3 position.
4. Proteomics using 2-dimensional differential ingel electrophoresis can determine proteins that change in response to high fat diets and n-3 polyunsaturated fatty acids.
5. Hypercaloric feeding of mice with either low or high fat diets result in the changes in miRNA expression.

Chapter 2:
Materials and methods

2.1 Materials

2.1.1 Apparatus: List of suppliers

a) Diet preparation

- Electric blender for 1 kg of feed - Kenwood
- Electric blender for 10 kg of feed - The Hobart, MFG. Co. Ltd
- Weighing scale - Oertling
- Freeze dryer - LSL Secfroid
- Bomb calorimeter - Gallenkamp
- Soxhlet extractor - Sigma
- Markham steam distillation apparatus – Sigma

b) Animal work

- Raised bottom wired cages – Tecniplast
- Utemp1284 mouse cages - Tecniplast
- Wood chips bedding – Aspen-wood chips, B and K Ltd
- Paper roll
- Bench-top centrifuge (Microlite Microfuge) - Thermo Electron Corporation
- Light microscope (Microphot FX) – Nikon

c) Lipidomics

- Oxygen cylindrical tank – BOC
- Gas chromatography 6890 series – Agilent technologies
- Water bath tank – Grant Instruments (Cambridge) Ltd
- Centrifudge GS-6R – Beckman
- Concentrator SF50 for Teflon tubes – Genelac
- Concentrator 5301 for 2 ml tubes – Eppendorf
- Vacmaster – Tecsis

d) Proteomics

- Tissue lyser with adapter sets (TissueLyser II) – Qiagen
- Plate-reader Synergy HT - Biotek
- IPGphor machine, chamber, manifold, white electrode pads, electrodes, cups – GE Healthcare
- EttanDaltTwelve tank
- EttanDaltScanner
- 96-well microplates (flat bottom) - Starlabs

e) Genomics

- Nanodrop ND-1000 spectrophotometer – Thermo Scientific
- 7900 HT Fast RT-PCR System – Applied Biosystems

- Agilent 2100 bioanalyzer RNA 6000 NanoChip - Agilent Technologies
- Affymetrix Hybridization Oven 640
- Affymetrix Fluidics Station 450
- GeneChip Scanner 3000 7G
- Biomek FX Liquid handling robot - Beckman Coultier
- Centrifudge with plate holders – Major Laboratory Supplier (MLS)
- PTC-225 Peltier Thermal Cycler – Bio Rad
- Microcentrifudge - MLS

2.1.2 Lab consumables: List of suppliers

a) Diet preparation

- Hexagonal 45 ml jam jars - Euro-bottles
- Cotton threads, crucibles for bomb calorimeter - Gallenkamp
- Extraction thimbles, Cotton wool for Soxhlet extractor -
- Nitrogen-free paper, anti-bumping granules for Kjeldahl method

b) Animal work

- 1 litre polypropylene bottles - Nalgene
- Syringes (1 ml), needles (25 g x 16 mm) - Plastipak
- StarTags Laser Sheets (3.5 x 1.25 cm) - Starlabs
- Cryogenic tubes - Starlabs
- Cryogenic boxes - Starlabs
- Microcentrifudge tubes (0.5, 1.5 and 2.0 ml) - Starlabs

c) Lipidomics

- Aminopropyl cartridges (Strata C18-E) - Sigma
- Teflon lined screw-capped tube – Pyrex
- 2 ml screw top vials with blue silicone/PTFE screw caps – Chromacol Ltd
- Weighing scale Precisa 125A – PAT COSHH Limited

d) Genomics

- 1.5 ml microcentrifudge tubes – Starlab
- ABI Prism 96-Well Optical Reaction plate with barcode (code 128) – Applied Biosystems
- ABI Prism 384-Well Clear Optical Reaction Plate with barcode (code 128) – Applied Biosystems
- ABI Prism Optical Adhesive Covers – Applied Biosystems

e) Proteomics

- Microcentrifuge tubes (2 ml, 0.5 ml; Protein LoBind) - Eppendorf
- Test-tubes (15 ml, 50 ml) - Greiner
- Grinding balls, 5 mm stainless steel - VWR International
- pH indicator paper sticks – Fisher Scientific

- Lint free tissue – Fisher Scientific
- 96 well digester plates (ProGest Blue Microtiter Plates) – Genomics solutions
- Immobiline DryStrip gels 3-11NL (24cm) – GE Healthcare
- IPG buffer 3-11 NL, Pharmalytes pH 3-10 – GE Healthcare
- CyDye DIGE Fluor kit (5 nmol / dye) of Cy2, Cy3, Cy5 – GE Healthcare
- Paper electrode pads – GE Healthcare
- Loading cups – GE Healthcare
- Paraffin oil; DryStrip cover fluid – GE Healthcare
- 2-D Quant Kit - GE Healthcare
- 2-D Clean-up kit - GE Healthcare
- Pierce 660 protein assay kit - Thermo Scientific
- Parafilm – VWR International
- Pre-cast gels - GE Healthcare

2.1.3 Chemicals: List of suppliers

a) Animal work

- Ethanol ACS grade - Sigma
- Formalin – Sigma
- Isofluorane (IsoFlo) - Abott Laboratories Ltd
- Phosphate buffered saline (PBS) – Oxoid

b) Diet preparation

- Concentrated sulphuric acid – Fisher Scientific
- 30% hydrogen peroxide - Sigma
- Boric acid - Sigma
- Sodium carbonate - Sigma
- Ammonium sulphate - Sigma
- Kjeltabs CTC catalyst tablets (contains potassium sulphate to raise boiling point, copper and titanium as catalysts) - Sigma
- Methyl orange indicator - Sigma

2.1.4 Buffers and reagents

a) Serum analyses

- Glucose reagent - Siemens Healthcare Diagnostics Ltd
- Alkaline phosphatase (ALP) reagent - Siemens Healthcare Diagnostics Ltd
- Aspartate transaminase (AST) reagent - Siemens Healthcare Diagnostics Ltd
- Alanine transaminase (ALT) reagent - Siemens Healthcare Diagnostics Ltd
- NEFA assay kit - WAKO Chemicals
- Cholesterol reagents - Siemens Medical Solutions Diagnostics Ltd
- Triacylglycerol reagents - Siemens Medical Solutions Diagnostics Ltd

b) Genomics

- TRIzol Reagent – Invitrogen

- Ambion RNA nuclease free water – Qiagen
- Reverse transcription kits
- TaqMan MicroRNA Reverse transcription kit - Applied Biosystems
- PCR Master Mixes
- TaqMan Universal PCR Master Mix II, No UNG – Applied Biosystems
- TaqMan 2x Universal PCR Master Mix - Applied Biosystems

c) Proteomics

- Bromophenol blue - PlusOne
- 7 M Urea - PlusOne
- 2 M Thiourea - PlusOne
- 4 % CHAPS - PlusOne
- 30 mM Tris - PlusOne
- MilliQ water
- Lysine; Mw 182.6 - Sigma
- DIGE Destreak Rehydration solution
- 0.5 % (v/v) Pharmalyte pH 3-10
- Acrylamide, bis solution - PlusOne
- Mixed bed ion exchanger - Amberlite
- Sodiumdodecylsulphate (SDS) - PlusOne
- Glycine - PlusOne
- Agarose – PlusOne
- 30 % Glycerol - PlusOne
- Dithiothrietol (DTT) - PlusOne
- Iodoacetamide - PlusOne
- 2% v/v IPG buffer - Pharmalyte
- SDS Gel buffer Tris-Cl pH 8.8 (4x conc)
- Hydrochlolric acid – Fisher Scientific
- Ammonium persulfate solution (APS) - PlusOne
- Acrylamide, Bis solution - PlusOne
- N,N,N,N-Tetramethylethylenediamine (TEMED; 100%) - PlusOne
- Glycerol - PlusOne
- Reference markers - IR markers
- Bind silane – PlusOne
- Deep Purple stain – GE Heatlhcare
- 15% Ethanol – Fisher Scientific
- 10% Glacial acetic acid – Fisher Scientific
- 1% Citric acid – Fisher Scientific
- 6.2% Boric acid – Fisher Scientific
- Sodium hydroxide – Fisher Scientific

2.1.5 Animal experiments

C57BL/6J male mice were obtained from Charles River, UK, Manston Road, Margate, CT9 4LT, Kent, England.

a) Diets

- Mineral mix (AIN-93-G-MX) - MP Biomedicals
- Vitamin mix (AIN-93-VX) - MP Biomedicals
- Light condensed milk - Nestle
- Sucrose - BDH Chemicals
- Cellulose - BDH Chemicals
- Casein - BDH Chemicals
- Cornstarch - BDH Chemicals
- L- Methionine - BDH Chemicals
- Choline hydrogen tartrate - Merck
- Lard - Sainsbury
- DHA 500 TG SR, SF06340 - Incromega
- EPA 500 TG SR, SF05244 - Incromega
- Corn oil – Mazola

2.2 Methodologies

2.2.1 Preparation of the semi-synthetic solid food

Diets were prepared by mixing the dry components for an hour with an electric blender followed by another 30 minutes when different types of fats were added to the dry mixture. 100 ml of water was added to every 200 g of diets and mixed for 15 minutes to get a malleable dough consistency. The dough was shaped into 6 cm^3 blocks and arranged individually on a tray lined with aluminium foil. The nutrient compositions of the diets incorporated with different types of fats are represented in ***Table 2.1*** and ***2.3***. The diets were prepared separately in batches of 10 kg, differentiated by shapes and stored in a -40°C freezer for 12 hours. Finally, the frozen diets were transferred to a freeze dryer for 3 days for lyophilisation. The freeze-dried pellets were stored in a 4°C cold room until needed.

The energy content of diets was quantified using a bomb calorimeter by measuring the heat of chemical reactions. The fat and protein content of the diets were determined using the Soxhlet extraction and Kjeldahl method, respectively. The energy composition of the diets is presented in ***Table 2.2***.

2.2.2 Preparation of the fat-free condensed milk incorporated with fats

Different types of fats were added to the fat-free condensed milk (*Light* condensed milk Carnation, Nestle, UK) to make up the fat to carbohydrate ratio relatively similar to the pellets. Condensed milk (CM) in the low fat and high fat hypercaloric groups were incorporated with 1% and 8% fats respectively. Energy compositions of the CM incorporated with fats are presented in ***Table 2.4***. All mice groups abbreviated with LF, HF, HFDHA, HFEPA, HOSO, PO, IPO and LARD were fed on light condensed milk incorporated with 8% test fat except for LFR group (see ***Table 2.5*** for detailed description of the groups).

Table 2. 1: The nutrient composition of mice pelleted diets containing either 2% corn oil (co), 18% palm oil (po), 15% palm oil with 3% docosahexaenoic acid (dha) or 15% palm oil with 3% eicosapentaenoic acid (epa) presented in grams and kilocalories

Ingredients	2% corn oil		18% palm oil		15% palm oil + 3%DHA		15% palm oil + 3%EPA	
	gram	kcal	gram	kcal	gram	kcal	gram	kcal
Casein	19.8	79.2	19.8	79.2	19.8	79.2	19.8	79.2
L-Methionine	0.2	0.8	0.2	0.8	0.2	0.8	0.2	0.8
Cornstarch	58.0	208.8	42.0	151.2	42.0	151.2	42.0	151.2
Sucrose (Icing Sugar)	10.0	37.5	10.0	37.5	10.0	37.5	10.0	37.5
Solka-floc (Cellulose)	5.3	0.0	5.3	0.0	5.3	0.0	5.3	0.0
MineralMix (AIN93G)	3.5	3.1	3.5	3.1	3.5	3.1	3.5	3.1
VitaminMix AIN93VX	1.0	3.9	1.0	3.9	1.0	3.9	1.0	3.9
Choline Bititrate	0.2	0.0	0.2	0.0	0.2	0.0	0.2	0.0
Corn oil	2.0	18.0	0.0	0.0	0.0	0.0	0.0	0.0
Palm oil	0.0	0.0	18.0	162.0	15.0	135.0	15.0	135.0
DHA	0.0	0.0	0.0	0.0	3.0	27.0	0.0	0.0
EPA	0.0	0.0	0.0	0.0	0.0	0.0	3.0	27.0
Total	100.0	351.3	100.0	437.7	100.0	437.7	100.0	437.7

Energy composition from protein, carbohydrate and fat of the pelleted diets determined by Kjeldahl, bomb calorimeter and Soxhlet method, respectively can be referred to Table 2.2.

Table 2. 2: Energy composition from protein, carbohydrate and fat diets determined by Kjeldahl, bomb calorimeter and Soxhlet method respectively.

		Low fat pellets	High fat hypercaloric pellets
Protein	**(g/100 g)**	20.0 (22.8)	20.0 (18.3)
Carbohydrate	**(g/100 g)**	78.0 (83.3)	62.0 (44.7)
Fat	**(g/100 g)**	2.0 (5.1)	18.0 (37.0)
Energy	**(kcal/100 g)**	351.3	437.7

Values in parentheses represent the % energy. Energy contents are calculated using Atwater factors of 4 kcal/g for protein, 3.75 kcal/g for carbohydrates and 9 kcal/g for fat.

Table 2. 3: The nutrient composition of mice pelleted diets containing either 18% high oleic sunflower oil (HOSO), 18% palm oil (PO), 18% interesterified palm oil (IPO) or 18% lard presented in grams and kilocalories

	18% HOSO		**18% PO**		**18% IPO**		**18% lard**	
	gram	***kcal***	***gram***	***kcal***	***gram***	***kcal***	***gram***	***kcal***
Casein	19.8	79.2	19.8	79.2	19.8	79.2	19.8	79.2
L-Methionine	0.2	0.8	0.2	0.8	0.2	0.8	0.2	0.8
Cornstarch	42.0	151.2	42.0	151.2	42	151.2	42	151.2
Sucrose (Icing Sugar)	10.0	37.5	10.0	37.5	10.0	37.5	10.0	37.5
Solka-floc(Cellulose)	5.3	0.0	5.3	0.0	5.3	0.0	5.3	0.0
Mineral Mix (AIN 93G)	3.5	3.1	3.5	3.1	3.5	3.1	3.5	3.1
Vitamin Mix (AIN 93VX)	1.0	3.9	1.0	3.9	1.0	3.9	1.0	3.9
Choline bititrate	0.2	0.0	0.2	0.0	0.2	0.0	0.2	0.0
Sunflower oil	18	162	0.0	0.0	0.0	0.0	0.0	0.0
Palm oil	0.0	0.0	18	162	0.0	0.0	0.0	0.0
Interesterified palm oil	0.0	0.0	0.0	0.0	18	162	0.0	0.0
Lard	0.0	0.0	0.0	0.0	0.0	0.0	18	162
TOTAL	100	437.7	100	437.7	100	437.7	100	437.7

Energy composition from protein, carbohydrate and fat of the pelleted diets determined by Kjeldahl, bomb calorimeter and Soxhlet method, respectively can be referred to Table 2.2.

Table 2. 4: Energy composition of light condensed milk (CM) incorporated with 1% and 8% of fats in low fat and high fat hypercaloric groups respectively

		Light condensed milk (LCM)	**Low fat LCM**	**High fat hypercaloric LCM**
Protein	**(g/100 g)**	9.3 (3.4)	9.3 (13.8)	9.3 (10.9)
Carbohydrate	**(g/100 g)**	59.5 (21.5)	59.5 (82.9)	59.5 (65.2)
Fat	**(g/100 g)**	0.2 (0.07)	1.0 (3.3)	8.0 (21.1)
Energy	**(kcal/100 g)**	277.0	284.2	342.0

Values in parentheses represent the % energy. Energy contents are calculated using Atwater factors of 4 kcal/g for protein, 3.75 kcal/g for carbohydrate and 9 kcal/g for fat. Light condensed milk was used in both the condensed milk incorporated with fats for all diets in Chapter 4, 5, 6, 7, 8, 9, 10 and 11

2.2.3 Measurement of energy composition in diets with bomb calorimeter

a) *Principle* (Miller & Payne 1959)

The gross energy content of the diets was calculated using the ballistic bomb colorimeter by measuring the amount of heat released when the samples were completely oxidised during combustion. The change of conductivity in the thermocouple attached to the bomb calorimeter is proportional to the amount of heat released with an assumption of no heat loss. The change in conductivity was determined by the deflection on the galvanometer. Sucrose was used to calibrate the galvanometer. The availability of energy to the body depends on the amount of energy lost in feaces and urine which was assumed to be 5%. Therefore, digestible energy content was calculated by multiplying gross energy by 0.95 and metabolisable energy was calculated by subtracting 0.075 x N% (kcal/g) of the diet.

b) *Methods*

Firstly, the calorimeter was bombed with no samples in the crucible to obtain a blank value. Approximately 1 g of sucrose was weighed in a crucible and 3 strands of cotton thread were embedded in the sample and looped to the firing wire. The bomb body was fitted and thermocouple inserted at the top. A pressure of constant 25 atm of oxygen was released gradually to the bomb calorimeter without developing excessive pressure. The galvanometer was zeroed and the firing button was pressed. The pressure gauge and galvanometer readings increased in 5 seconds after firing and the reading on the galvanometer was noted after 35 seconds when the peak reading was attained. Then the gas pressure was released and the bomb body was removed and cooled under running water in preparation for the next sample. The factor of sucrose standards was calculated using the formula,

$$\text{Factor} = 3.94 / (\text{Deflection} - \text{Blank value}) / \text{weight}$$

After cooling the bomb body under running water, the body was wiped thoroughly. The steps were repeated for the samples in duplicates ensuring that the diets were of low bulk density and dry to reduce the burning rate and allow uniform combustion. After all the samples were bombed, the gross energy, digestible and metabolisable energy were calculated.

2.2.4 Determination of fat content by Soxhlet method

a) Principle

Fat was extracted from dried sample with petrol ether and the dissolved fat was siphoned off with ether. The fat-free samples were re-weighed and the fat difference was calculated.

b) Methods

The Soxhlet extractor was fitted with a reflux condenser and flask. Thimbles and cotton wool were dried in the oven, weighed immediately to prevent absorption of moisture and stored in desiccators. Thimbles were labelled with a pencil. Approximately 3 g of dried samples were added to the thimble and weighed accurately. The weighed cotton wool was used as a stopper in the thimble and placed in the extractor. Petrol ether was added until it siphoned over and more were added. The aater temperature was adjusted until the ether boiled gently and the set-up was left for 12 hours. On the next day, the thimble was removed when the extractor barrel was emptied and left to drain until the ether was evaporated. Samples were dried in the oven to constant weight and allowed to cool in desiccators. Then, g fat/ 100 g of diets were calculated.

2.2.5 Quantification of proteins by Kjeldahl method

a) Principle

The Kjeldahl method was used to measure the nitrogen levels to determine the protein content in the diets. The nitrogen content of varies from 15 – 18% and by multiplying the nitrogen content with 6.25 the protein content was determined (Bradstreet, 1965). The three main processes in the Kjeldahl method can be divided into digestion, distillation and titration. The principal of this method involves the reduction of nitrogen to ammonium ions using sulphuric acid and oxidation of carbon to carbon dioxide. The chemical decomposition of the sample was known to be completed when the solution turned clear. The ammonium ions were then converted into ammonia gas through distillation with sodium hydroxide. The amount of ammonia gas trapped was converted back to ammonium ions in acidic buffer and titrated against a standard solution of sulphuric acid, a process known as *back titration*. A steam distillation apparatus designed by Markham (1942) was used. The end of the condenser was dipped into boric acid, allowing the ammonia to react with the acid and the remainder was titrated with sodium carbonate and methyl orange pH indicator.

b) Methods

Approximately 1.5 g of sample was ground, weighed on nitrogen-free paper and transferred to a digestion flask containing strong sulphuric acid. For each gram of sample, 20 ml of concentrated sulphuric acid was added and mixed well. Then, 5 ml of 30-35% hydrogen peroxide was added drop-wise to prevent an exothermic reaction which may cause an explosion. To this, 1 tablet of Kjeltabs CTC catalyst and a few anti-bumping granules were added to speed up reaction. The reactants were mixed then heated until the solution was clear. The clear solution was heated for another 20 minutes just below the boiling point to ensure that all the ammonia was converted to ammonium sulphate.

Before distillation, the sample was cooled on the rack. After cooling, 50 ml of distilled water was carefully added to the solution and transferred to a 100 ml volumetric flask. The solution was made up to a volume of 100 ml. Then, 5 ml aliquots were taken for distillation with the Markham apparatus. A series of 50 ml conical flasks filled with 10 ml indicator solution was prepared. One portion was diluted with 10 ml of water and used as a colour check for the end-point. Firstly, the apparatus was steamed out. The steam generator was connected to the steam jacket, the waste clip was closed, the stopper inserted and then the steam was let out for 10 – 15 minutes. The steam pressure was reduced by removing the Bunsen burner and cold water was added. The vacuum created by the cooling of the steam jacket caused the water to flush out, which was drained off by opening the waste clip.

After steaming out the apparatus, samples were ready to be distilled. The waste clip was closed, the stopper inserted and the steam generator was disconnected. A conical flask with a condenser was immersed under the indicator solution to trap gaseous ammonia that preceded the first drop of distillate. Then, 5 ml of sample was pipetted into the still and the tip of pipette was placed in the neck of the opening. Five millilitres of water was washed in and the stopper was replaced. After this, 10 ml of 40% NaOH was poured into the reservoir and the stopper was lifted up slightly, allowing NaOH to run gently into the digest. Water was left around the stopper to form a seal.

The steam generator was reconnected and distillation proceeded. Ten millilitres of distillate was collected after the indicator turned green by removing the tip of the condenser from the liquid, and distillation was continued for another 2 minutes. The outside of the condenser tip was washed and samples were set aside for titration. Heat

was removed from the steam generator and the liquid was flushed out. The reservoir and still were washed with distilled water and flushed out. The waste clip was opened to drain off excess water and the apparatus was then ready for the next sample.

The sharpness of the titration end-point was enhanced by comparing the intensity of methyl orange indicator and 1% boric acid as a reference solution. A standard solution of ammonium sulphate containing 1 mg nitrogen/ml was prepared in 2 ml aliquots. The acid in the biurette was standardised by titrating against ammonia in boric acid/indicator solution from the distillation of the standard solution. The amounts of nitrogen from the sample were calculated by noting the amount of acid required to titrate 2 mg of nitrogen.

2.3 Experimental design

2.3.1 Laboratory animals

All procedures were carried out according to the project license guidelines under the UK Home Office Animals Scientific Procedures Act, 1986. The animals were divided into 9 groups (8 mice per group), labelled and fed with the respective diets as in ***Table 2.5***. Small amounts (2% by weight) of corn oil (CO) were used in the low fat (LF) and low fat reference (LFR) diets in order to ensure an adequate intake of linoleic acid. The LFR group is a eucaloric group whereas the LF group is a hypercaloric diet. Palm olein (iodine value 56, PO, Archer Daniel Mills PLC, Erith, Kent) provided the sole source of fat in the high fat (HF) diet. EPA and DHA rich triacylglycerol concentrates (Croda Ltd, Hull) were substituted for 3% by weight of PO in the respective high fat diets. The first feeding study compared LFR, LF, HF, HFDHA and HFEPA diets. Pre-specified comparisons were made between: low fat and high fat hypercaloric groups with or without EPA or DHA. In the second study, high oleic sunflower oil (HOSO, provided by Archer Daniel Mills, Erith Kent), which consists mainly of triolein, was used as a comparator. In the 2nd feeding study which compared HOSO, PO, interesterified PO (IPO, supplied by Archer Daniel Mills, Erith Kent prepared from the same material as the PO) and lard (LARD, purchased from Sainsbury PLC) high fat diets. The experimental high fat milk was made by blending light condensed milk (LCM) with 8% (w/w) test fat and provided to the mice in jars separate from the pelleted diet; prespecified comparisons were made between. PO, IPO and LARD groups vs HOSO and between PO, IPO and LARD groups. Abbreviations of the groups are presented in ***Table 2.5***.

Table 2. 5: Abbreviations used for different types of groups fed different types of diets in this study for the thesis

Groups	Types of diets
Low fat reference (LFR)	2% Corn oil (CO) pellets
Low fat (LF)	2% CO pellets + LCM incorporated with 1% CO
High fat (HF)	18% Palm olein (PO) pellets + LCM incorporated with 8% PO
DHA (HFDHA)	15% PO, 3% Docosahexaenoic acid (DHA) pellets + LCM incorporated with 5% PO, 3% DHA
EPA (HFEPA)	15% PO, 3% Eicosapentaenoic acid (EPA) pellets + LCM incorporated with 5% PO, 3% EPA
High oleic sunflower oil (HOSO)	18% high oleic sunflower oil (HOSO) pellets + LCM incorporated with 8% HOSO
Palm olein (PO)	Similar to HF, a different name is used to differentiate the 1st from the 2nd study
Interesterified palm olein (IPO)	18% interesterified palm olein (IPO) pellets + LCM incorporated with 8% IPO
Lard (LARD)	18% lard pellets + LCM incorporated with 8% lard

LFR, LF and HF were used in Chapter 5, 8 and 10. HF, HFDHA and HFEPA were used in Chapter 6, 9 and 11. HOSO, PO and IPO were used in Chapter 7. LCM stands for light condensed milk

2.3.2 Feeding methods

It has been shown that overfeeding of high-fat liquid diet continuously at different time points can lead to the progression of NASH when compared to the mice fed *ad libitum* a solid high fat hypercaloric diet (Gaemers et al, 2011). For example, overfed animals with high fat liquid diets show characteristics of NASH such as obesity, hyperinsulinemia and loss of liver glycogen (Gaemers et al, 2011). In this thesis, mice were overfed *ad libitum* with condensed milk (CM) incorporated with different type of fats to match the solid food.

For the first week of study, mice were acclimatised with the pellets and had access to water *ad libitum* without the condensed milk. After the acclimatization period, all mice except for LFR mice were provided with condensed milk through custom made

feeding jars. Pellets and CM were replaced every Monday, Wednesday and Friday for 6 weeks. Body weights, pellet intake and CM consumption were recorded 3 times a week. An amount of diets equivalent to approximately 15% of their bodyweight per day was fed to the mice (Wolfensohn et al, 2003). By monitoring the growth of mice daily, mice were ensured to have healthy growth rates and no weight loss.

2.3.3 Dissection

After 7 weeks, mice were fasted overnight before culling. During sampling, blood samples were collected via decapitation and left to drain into a 2 ml sterile tube using a funnel. The blood was then left to coagulate at room temperature for 60 minutes and then centrifuged for 15 minutes at a speed of 350 g in a cooled bench-top centrifuged to obtain serum. Serum was then carefully pipetted from the top layer and immediately transferred to another sterile cryogenic tube, snap frozen in liquid nitrogen and stored in -80°C.

Liver samples and fat pads were collected and weighed. The liver was divided into 6 sections on a sterile petri dish placed on ice before being snap frozen in liquid nitrogen. Samples for histology were placed in formalin, without freezing. Other tissues such as soleus, plantaris and gastrocnemius muscles were obtained from both hind legs and weighed. All the collected samples were stored in -80°C freezer for further analyses.

After every dissection, all surfaces and equipment were washed with 70% (v/v) ethanol to keep cross-contamination to a minimal level. Liver samples needed for histology were stored in the formalin for 48 hours and sent to the histopathology laboratory in King's College Hospital, Denmark Hill for histological staining and liver scoring.

2.4 Histology

2.4.1 Tissue preparation

Livers were sectioned using the cryostat, a microtome inside a freezer at a constant temperature of -20 °C and set to cut at 7 µm. The liver specimen was embedded in Optimal Cutting Temperature (OCT) compound on a cylindrical block until it becomes frozen. The sections were then picked up on a glass slide (Hendley-Essex, microscope slides PTFE coated) ready for staining.

2.4.2 Fixing and hydration

Frozen sections were fixed in 4% paraformaldehyde (PFA) and rinsed in cold phosphate buffered saline (PBS). In the staining step, liver sections on the glass slide were covered with hematoxylin for 2 minutes and then rinsed under running water until the water turned clear for 2 minutes. Next, slides were dipped into blueing solution and allowed to stand in running water for another 2 minutes. Slides were immersed into 80% ethanol for 2 minutes followed by 5 minutes in eosin. This was followed by the dehydration step whereby slides were dipped 5 times in 80% ethanol to rinse out excess eosin, followed by 2 minutes in 95% ethanol and another 2 minutes in 95% ethanol, 2 minutes in 100% ethanol twice followed by 3 minutes in xylene for three times. Lastly, the slides with fixed, stained and dehydrated liver section was dotted with mounting gel (Permount) and covered with coverslips. Observations under the microscope showed nuclei which was stained dark blue (hematoxylin) and the cytoplasm was stained pink (eosin).

2.4.3 Statistical analyses

Histological evaluations were carried out by scoring the change observed in steatosis, inflammation and reticulin condensation in the liver. Analyses were preformed single-blinded by a recognised histopathologist in King’s College London, Denmark Hill. Histopathological scores for steatosis, inflammation and reticulin condensation are presented in counts and percentage within group with P values generated from Chi-square test where by P values less than 0.05 indicates statistically significance.

2.5 Serum analysis

Serum analysis (glucose, alkaline phosphatase, aspartate aminotransferase, alanine transaminase, non-esterified fatty acids, cholesterol and triacylglycerols) were carried out by a clinical chemist, Dr. Tracy Dew at KingsPath King's College London Hospital in Denmark Hill using laboratory diagnostics procedures. The parameters were determined by measuring the change of absorbance using the clinical analyser ADVIA 1650 (Bayer Diagnostics, Newbury, UK).

2.5.1 Determination of glucose

Glucose measurements are used as part of a panel of biomarkers for the diagnosis and management of diabetes mellitus which is also a common risk factor for non-alcoholic steatohepatitis (NASH).

In the sample, glucose was phosphorylated by the transfer of phosphate from adenosine triphophosphate (ATP) via the action of hexokinase. Glucose-6-phosphate formed in this reaction was oxidised by glucose-6-phosphate dehydrogenase. This was accompanied by the reduction of NAD^+ to NADH which resulted in the increase of absorbance at 340 nm which was proportional to the glucose concentration in the sample. The increase in absorbance was converted to glucose concentration by reference to a previously determined calibrator and reagent blank. The effects of any interfering substances were reduced by blanking sample using buffer and co-factors before adding the enzymes.

2.5.2 Determination of alkaline phosphatase (ALP)

The enzyme alkaline phosphatase (ALP) is an indicator of bone formation and is raised in association with increased bone turnover. The production of hepatic ALP is also increased in cholestasis by bile induction due to liver injury and thus a raised ALP may also act as a marker for hepatotoxicity. Para-nitrophenyl phosphate (PNPP) is an artificial substrate for ALP. ALP hydrolyses PNPP to form free phosphate and para-nitrophenol which is highly coloured (yellow). The reaction is monitored kinetically at 410 nm, the rate of increase in absorbance being directly proportional to ALP activity in the sample and expressed as IU/L by means of a conversion factor. 4-aminomethylpropanol (AMP) buffer maintains the required alkaline pH and acts as a phoshate acceptor, thus driving the reaction. Magnesium and zinc ions are present as ALP co-factors (Tietz et al, 1983).

2.5.3 Determination of aspartate aminotransferase (AST)

Aspartate transaminase (AST) is an intracellular (mitochondrial) enzyme present in most tissues, notably in the liver parenchymal cells, cardiac muscle and skeletal muscle. Raised levels of AST are associated with cell necrosis or increased cell leakage. AST is therefore markedly raised in hepatic inflammation or tissue damage and skeletal muscle damage and may be moderately raised in myocardial infarction. Reasonably, AST acts as a sensitive indicator of hepatitis, liver necrosis or liver transplant rejection and a relatively late indicator of myocardial infarction. The reaction is initiated by the addition of the substrate (2-oxoglutarate - contained in reagent 2) to the sample/co-enzyme (reagent 1) mixture.

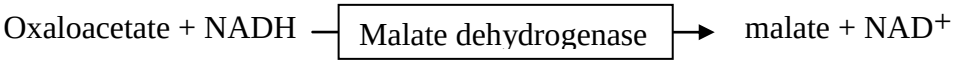

The rate of NADH consumption by the 2nd (linked) reaction is monitored at 340 nm and is directly proportional to the AST activity in the sample. Pre-incubation of the sample with the co-enzyme reagent removes any endogenous NADH by the conversion of oxaloacetate to malate by malate dehydrogenase which was added to the reagent (Jung et al, 1976).

2.5.4 Determination of alanine transaminase (ALT)

Alanine transaminase (ALT) is an intracellular (cytosolic) enzyme present in most tissues but notably in the liver parenchymal cells and skeletal muscle. Raised levels of ALT are associated with cell necrosis or increased cell leakage. ALT is therefore markedly raised in hepatic inflammation or tissue damage and skeletal muscle damage. ALT is thus a sensitive indicator of hepatitis, liver necrosis or liver transplant rejection. It is more specific for liver damage than AST (which is present to a much larger extent than ALT in cardiac muscle), and also more sensitive, being a cytosolic rather than mitochondrial enzyme. The reaction is initiated by the addition of the substrate (2-oxoglutarate - contained in reagent 2) to the sample/co-enzyme (reagent 1) mixture.

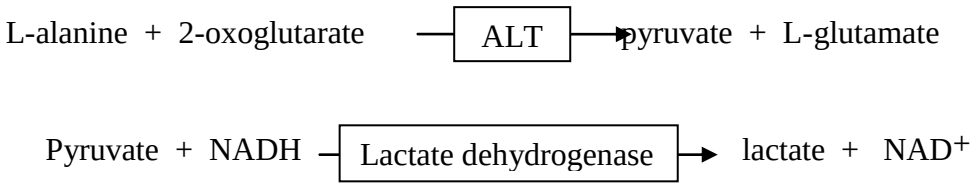

The rate of NADH consumption by the 2nd (linked) reaction is monitored at 340 nm and is directly proportional to the ALT activity in the sample. Pre-incubation of the sample with the co-enzyme reagent before the first measurement is taken to remove any endogenous NADH by the conversion of pyruvate to lactate by lactate dehydrogenase (Jung et al, 1976).

2.5.5 Determination of serum non-esterified fatty acids (NEFA)

NEFA in the blood is bound to albumin and is used as an important energy source of peripheral tissues. The amount of NEFA in serum depends on a balance between intake by the liver and peripheral tissues, and the release from adipose tissue. Serum NEFA levels are decreased by physical exercise, and increased by starvation, cold, fear or smoking and plays a key role in diabetes mellitus and insulin resistance. An increase in serum NEFA concentration is a risk marker of diabetes mellitus type 2 developments. In this assay NEFA in the sample was converted to acyl-coenzyme A, AMP and pyrophosphoric acid (PPi) by the action of acyl-coenzyme A synthetase (ACS), under coexistence with coenzyme A (CoA) and ATP. Obtained acyl-coenzyme A is oxidised and yields 2, 3-trans-enoyl-CoA and hydrogen peroxide by the action of acyl-coenzyme A oxidase (ACOD). In the presence of peroxide, the hydrogen peroxide formed yields a blue purple pigment by quantitative oxidation condensation with 3-methyl-N-ethyl-N-ß-hydroxyethyl-aniline (MEHA) and 4-amino-antipyrine (4-AA). Non-esterified fatty acids concentration is obtained by measuring absorbance of the blue purple colour (Okabe et al, 1980).

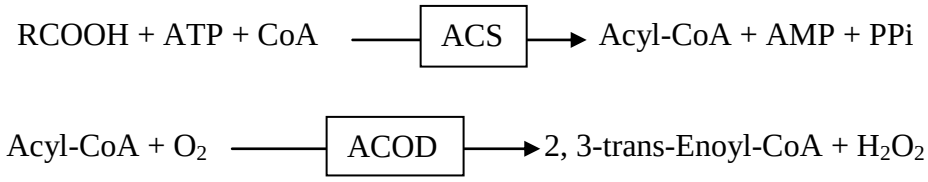

2.5.6 Determination of serum cholesterol

Serum cholesterol was determined by an enzymatic method using cholesterol esterase, oxidase and peroxidase in a chemiluminescent reaction to produce a red quinoneimine dye. The increase in absorbance is measured as an endpoint reaction at 505/694 nm.

2.5.7 Determination of serum triacylglycerols (TAG)

The Siemens Advia method for the measurement of TAG is an enzymatic assay. TAGs are converted to glycerol and free fatty acids by lipase. The glycerol is then converted to glycerol-3-phosphate by glycerol kinase followed by its conversion by glycerol-3-phosphate-oxidase to hydrogen peroxide. A coloured complex is formed from hydrogen peroxide, 4-aminophenazone and 4-chlorophenol under the catalytic influence of peroxidase. The absorbance of the complex is measured as an endpoint reaction at 505/694 nm.

2.5.8 Statistical analyses

Serum analyses were analysed using statistical software packages SPSS version 19. One-way analysis of variance (ANOVA) analyses followed by Tukey's multiple comparison tests were performed as required by the data. Results of food intake, body weights, organ weights and serum analyses were presented in mean with 95% confidence interval. Chi-square test was carried out for the histology scores. Fatty acid composition and concentrations of adipose tissue, non-esterified fatty acids, triacylglycerols, cholesteryl esters and phospholipids were presented in mean ± standard deviation and one way ANOVA with Tukey's multiple range test was used. P values less than 0.05 were considered as statistically significant.

2.6 Lipidomics

2.6.1 Extraction of lipids from liver samples (Folch method)

a) Principle

The protocol was carried out using Folch method (Folch, Lees & Stanley 1957) to extract lipids from liver tissues containing relatively low proportion of lipid compared to the proportion of water using chloroform-methanol (2:1 volume/volume) which acts as solvent. C-17 lipid standards were added to aid quantification. The Folch procedure also involved a wash with 0.9 % sodium chloride to remove protein contaminants.

b) Methods

2 ml of chloroform: methanol (2:1 by volume) was added to the weighed liver sample (approximately 100 mg) and homogenized with the internal standards in a Teflon lined screw-capped tube. After homogenizing the liver samples, the whole mixture was vortexed for 15 to 20 minutes at room temperature. The homogenate was then centrifuged to precipitate the solids. Next, the supernatant was collected by filtering out the solid upper phase and washed with 0.4 ml of 0.9 % of sodium chloride solution. Then the mixture was vortexed and centrifuged at low speeds, 350 g to separate the two phases. The upper layer was removed and the lower chloroform phase, containing the lipids, was evaporated under vacuum in a rotary evaporator. The dried residues were reconstituted in 0.5 ml chloroform and applied to solid phase extraction (SPE) cartridge in preparation for lipid class separation (Folch et al., 1957).

2.6.2 Lipid class separation using solid phase extraction (SPE)

a) Principle

Lipid class were separated on amino SPE cartridges using the techniques described by Kaluzny et al, (1985). This method allowed for the initial separation of neutral lipids, phospholipids and free fatty acids. The set up of the experiment is shown in ***Figure 2.1***. A second stage was then used to separate triacylglycerols and cholesterol sterols. By adding appropriate internal standards containing C-15 or C-17 fatty acids the amounts of each lipid class was quantified using gas liquid chromatography (GLC).

Figure 2. 1: The separation of lipid classes using solid phase extraction

b) Methods

Firstly, the aminopropyl cartridges were pre-washed twice with 2 ml hexane before use. Then, liver samples were applied to the columns and pulled through the chamber connected to the controllable vacuum port. Next, the dry lipid extracts were dissolved in 0.5 ml chloroform before being transferred to the columns.

In the columns, 4 ml of chloroform: propan-2-ol (2:1) was added and fraction A (TAG, cholesterol esters and cholesterol) was collected. Then, 4 ml of 2 % acetic acid in diethyl ether was added and fraction B (non-esterified fatty acids) was collected. Consequently, 4 ml of methanol was added to collect fraction C (phospholipids). Then, fraction A (collected in the first separation) was dried and re-dissolved in 0.2 ml of hexane. After that, a new column was placed beneath the existing column and 4 ml of hexane was added to collect fraction D (cholesterol esters). Next, 6 ml of 1 % diethyl ether and 10 % dichloromethane in hexane were added and fraction E (TAG) was extracted. Lastly, the solvents in the screw cap tubes were capped and evaporated using the rotary evaporator.

2.6.3 Methylation of lipids in the liver

a) Principle (Lepage & Roy 1986)

A low concentration of hydrochloric acid in methanol was used to minimise the formation of artifacts in this acid catalysed esterification reaction. Isomeric fatty acids were separated on a 60 m polar capillary column.

b) Methods

A solution of toluene:methanol, 20:80 (v/v) was made up in a glass beaker. Approximately 100 mg of liver sample was weighed and transferred to a glass tube with

a Teflon cap. Then, 2 ml of methanol:toulene solution was added to each sample. In a fume cupboard, 0.2 ml of acetyl chloride was added drop-wise with a glass dropper taking extra caution as the production of HCL causes an exothermic reaction. The glass tube was then sealed and heated for 2 hours at 60 ºC under water bath conditions. After 2 hours, the tubes were allowed to cool for an hour.

While waiting, anhydrous K_2CO_3 was powdered with a mortar and pestle and 6 g of K_2CO_3 were added to 100 ml distilled water to make solution of 6 % K_2CO_3 (aq). When the tubes were completely cooled, 5 ml of K_2CO_3 solution were added to the samples. Then the mixtures were vortexed and centrifuged at 5 ºC, 1500 g and 5 minutes. At this stage, 2 clear visible layers were observed and the upper phase was transferred to a clean glass vial with a glass pipette for gas chromatography (Agilent 7890/6890) analysis injected under split mode (50:1) using a 25 m BP60x SGE column 0.22 mm (SGE, Australia) with hydrogen as a carrier gas with a constant flow rate of 1 ml/min, injection temperature 250 ºC and detector temperature 280 ºC.

The gas chromatography was programmed to remain at 180 ºC for 14 minutes and then ramped at 15 ºC/min to 220 ºC and held for 10 minutes. The injection volume was 2 µL. Fatty acid methyl esters were identified by reference to the retention times of standards of known composition obtained from Sigma (Standards 189-1, 189-2, 189-3) and a secondary reference standard of MaxEPA (Seven seas Ltd, Hull, UK) for long chain n-3 fatty acids.

2.6.4 Determination of total fatty acids in adipose tissue

The fatty acid composition of adipose tissue was determined by direct methylation similar to methods in 2.6.3 (c) using 10 mg of adipose tissue. The fatty acid methyl esters were separated on an Agilent 7890/6890 gas chromatograph similar to conditions stated above.

2.7 Proteomics

Two-dimensional differential in-gel electrophoresis (2-D DIGE) was carried out to determine proteins altered in response to different diets for protein expression profiling. Following the lipidomics study, there were 3 distinct sets of comparisons: (1) LFR vs LF and HF groups, (2) HF vs HFDHA and HFEPA groups and (3) HOSO vs PO, IPO and LARD groups. Proteins samples were labelled with fluorescent dyes allowing one to differentiate between samples. The protein samples were first separated according to their isoelectric point (pI) and further separated according to their molecular mass also known as the 2nd dimension. The combination of these 2 parameters separate different proteins on a single gel, as many as several thousands.

To achieve this equal amount of protein from paired samples (control and treated) were labelled with Cy3 (a red dye) and Cy5 (a blue dye) DIGE fluorescent dyes, respectively. Pooled internal standards were included in each gel by mixing all the samples in one vial and labelling it with Cy2 (a yellow dye). By using the pooled internal standard in each gel, every protein on the gel was compared internally to the same standard. This aided matching between gels (Alban et al, 2003). CyDye differential gel electrophoresis enables a direct comparison between 3 samples in 1 gel and therefore reduces the gel to gel variation (Tonge *et al*, 2001). All 3 dyes were charge and mass matched and spectrally resolved (Alban et al, 2003). In other words, regardless of which CyDye the samples are labelled with, the same protein migrates to the same position.

After labelling, treated, control samples and internal standard were mixed and applied to the IPG gel strip. The proteins migrate along the IPG strip with the electric field and stay at their own pI position with no net charge. The pH value on the gel strip changes gradually along the strip which enhances the resolving power and loading capacity in the 1st dimension. Moreover, the isoelectric focusing step is only suitable for separating proteins with pI values between 3 and 10. Proteins with out-of-range (ie <pH 3 or >pH 10) values will be poorly separated by the IPG strips. Therefore it was important to ensure that the labelled samples are kept at a pH of 8.5.

Next, protein samples were separated by their molecular mass in the 2nd dimension of SDS polyacrylamide gel electrophoresis. SDS is an anionic detergent that denatures proteins and imparts a net negative charge to all proteins. The migration of proteins depends on their molecular mass and with an applied electric field the proteins move from the cathode to anode at different speeds. In order to minimise variations in

gel casting, commercially pre-cast DIGE gels (a low fluorescent 12.5% polyacrylamide gel) were used to achieve highly reproducible results.

For spot-picking, the gels were cast and separation of 250 µg proteins were visualised by Coomassie blue instead of silver stain. Although Coomassie blue stain (Neuhoff et al., 1988) is 50 times less sensitive compared to the silver stain (Heukeshoven & Denrick 1985), Coomassie stain is more compatible for subsequent peptide mass fingerprinting by mass spectrometry (Gharahdaghi et al, 1999).

Gels were scanned with an Ettan DIGE imager showing protein spots which were separated according to its isoelectric point and molecular weight. Single and overlaid images were obtained from ImageQuant software and subjected to DeCyder software for further statistical analyses. From the complex analysis of multiple gels, proteins of interest were picked automatically using the Ettan Spot Picker and each protein spot was identified by mass spectrometry. A diagrammatic summary of the procedure (***Figure 2.2***) was adapted from Applied biosystems (www.appliedbiomics.com/proteomics_2d_dige.html).

Figure 2. 2: A diagrammatic summary of the whole process of 2-D DIGE protein expression profiling.

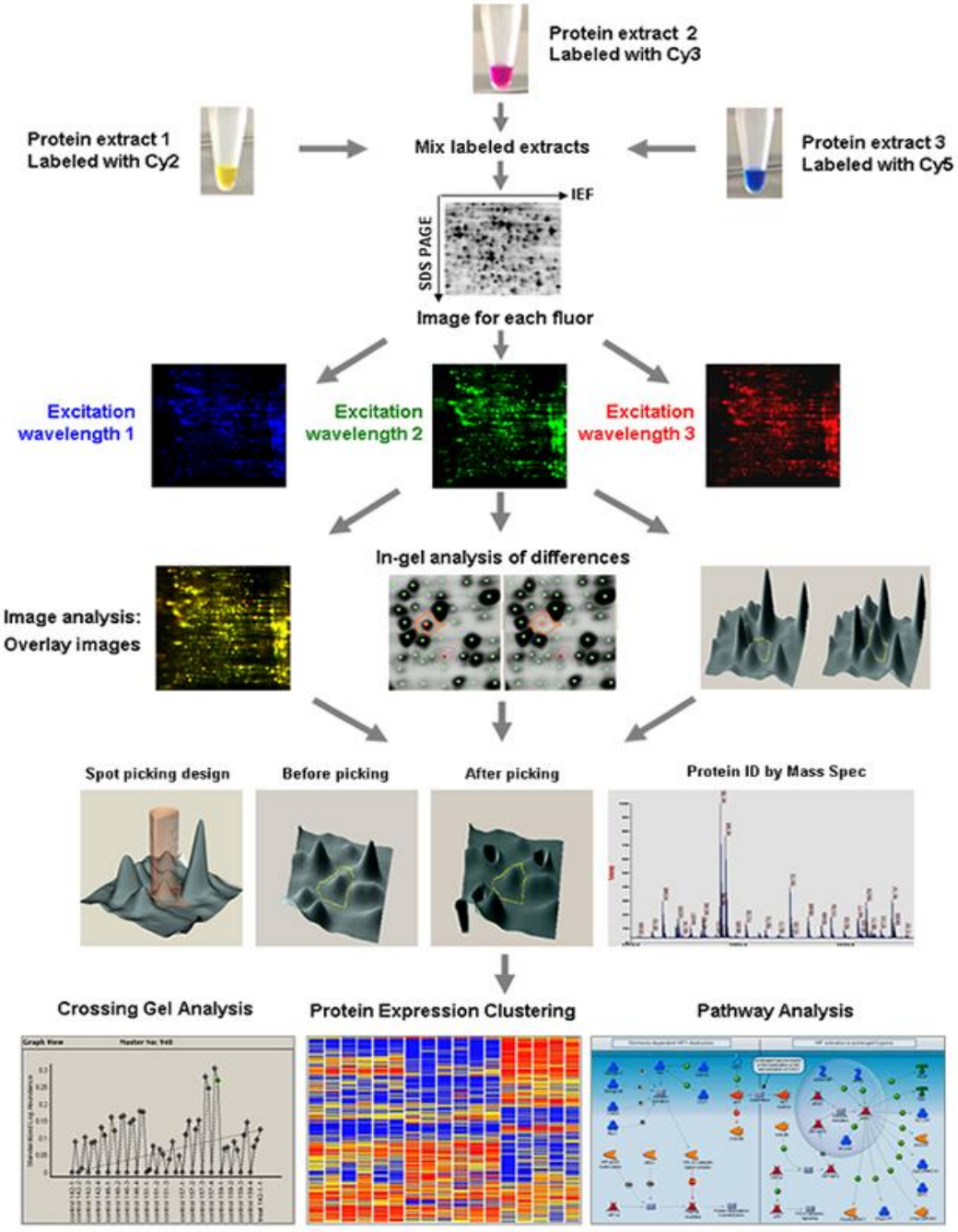

Source: Applied Biosystems. In this study for the thesis, crossing gel analysis and protein expression clustering was not carried out.

2.7.1 Sample preparation

Liver tissues were prepared in a planned randomization pattern (control; treated; treated; control) to decrease biasness. They were weighed four at a time to prevent the thawing of tissue which may degrade the protein in the sample. Approximately 100 mg of liver tissues were weighed individually in a sterile 2 ml tube and 2 x lysis buffer (containing DTT and IPG buffer; ***Table 2.6***) was added immediately to the tube with 2 mill balls. Samples were processed in batches of 20 to prevent clustering of protein homogenates from a single treatment group.

The ratio of liver weight to volume of 2x lysis buffer was set at 1:10 hence approximately 1 ml of buffer was added to 100 mg sample. Liver tissues were simultaneously disrupted using the tissue lyser for 30 seconds at 30 kilo-Hertz (***Figure 2.3***). The adapter sets were pre-cooled to 4°C before use to ensure that the samples were not affected by the heat generated during grinding. After homogenization, the samples were centrifuged at maximum speed for 15 minutes at 4°C and 15000 g to separate the protein homogenates from the insoluble material. Then, 100 to 150 µL of clear blue supernatant was transferred to a clean eppendorf tube in aliquots of 25 µL. Samples were stored in a -80ºC freezer, ready for the clean-up procedure.

Figure 2. 3: Liver tissue was homogenised in protein extraction buffer for 30 seconds at 30 kilo-Hertz in pre-cooled adapter racks

The hybridization oven for microarray chips in Section 2.8.2. Microarray chips were placed into the GeneChip Hybridization Oven 640 and the trays were loaded into the hybridization oven for incubation at 48°C for 16 hours.

2.7.2 Protein quantification before clean-up

a) Principles

For total protein quantification, the assay was performed with 2-D Quant Kit (GE Healthcare), which is designed to quantify precipitating proteins by excluding interfering substances in the solution due to the specific binding of copper ions to the protein. Therefore, precipitating proteins were re-suspended in a copper-containing solution, leaving the unbound copper to be measured with a colorimetric agent. This generated a linear graph with a negative gradient showing the inverse relationship between the colour density and protein concentration.

b) Methods

The first protein quantification was to ensure that the protein concentrations were within the range of 1-100 µg of protein in 1-100 µL of homogenate, which is important for the next step of clean- up samples. On average, 10 µg of sample, containing approximately 100 µg of protein was cleaned up in batches of 12.The procedure for protein quantification was carried out according to the protocol provided by GE Healthcare.

For this assay, 500 µL of precipitant was added to each tube, vortexed and incubated for 3 minutes at room temperature. This was followed by the addition of 500 µL of co-precipitant to each tube and mixed briefly. The tubes were then centrifuged at 10,000 g for 5 minutes for sedimentation of proteins. A small pellet was visible and the supernatant was decanted. These steps were repeated rapidly to avoid re-suspension of the pellet. Next, the tubes were repositioned carefully in the microcentrifuge with the cap-hinge and pellet facing outwards to bring the remaining liquid to the bottom of the tube. A micropipette was used to remove the remaining supernatant until there was no visible liquid in the tube.

In the next stage of the assay, 100 µL of copper solution and 400 µL of distilled water were added to each tube and vortexed briefly to dissolve the precipitated protein. Then, 1 ml of working colour reagent was added to each tube and vortexed immediately to ensure instantaneous mixing. Tubes were incubated at room temperature for 20 minutes. Then, 5 µL of samples including the BSA standards were transferred to a 96-well plate and transferred to a plate reader set at absorbance 480 nm, using water as a reference. The absorbance of the assay solution decreased with increasing protein concentration. A standard curve was generated by plotting a graph of absorbance

against quantity of protein. This standard curve was used to determine the protein concentration of the samples (***Table 2.6***).

Table 2. 6: Example of standard curve of BSA concentrations in serial dilutions with 2D-Quant kit

BSA standard (µL)	Protein (µg)	Absorbance at 480 nm
0	0	0.347
5	10	0.316
10	20	0.295
15	30	0.251
20	40	0.231
25	50	0.212

2.7.3 Protein clean-up

a) Principles

The 2-D Clean-up kit is designed to quantitate precipitated proteins while filtering out the interfering substances such as detergents, salts, lipids, phenolics and nucleic acids in the solution. Pelleted proteins were re-suspended in labelling buffer which is compatible with 1st dimension isoelectric focusing (IEF).

b) Methods

The standard procedure for the clean up process (2-D Clean-up Kit) was followed. First, 100 µl of protein sample was transferred to a 1.5 ml microcentrifuge tube and 300 µl of precipitant was added to the mixture, vortexed and incubated in ice for 15 minutes. This was followed by the addition of 300 µl of co-precipitant and vortexed briefly. The tubes in a microcentrifuge were centrifuged at 12,000 g for 5 minutes and a small pellet was visible after centrifugation. The supernatant was removed without disturbing the pellet. Tubes were repositioned with the cap-hinge and pellet facing outwards and centrifuged to bring the remaining liquid to the bottom of the tube. The remaining supernatant was removed with a micropipette.

A 40 µl volume of co-precipitant was layered on top of the pellet and the tube was left in ice for 5 minutes. Again, the tube was reposition carefully as before and centrifuged for 5 minutes. Next, 25 µl of distilled water was pipetted on top of each pellet and vortexed for 10 seconds. The pellet was dispersed but not dissolved in the water. Then, 1 ml of pre-chilled wash buffer and 5 µl of wash additive were added and vortexed until the pellet was fully dispersed. The tubes were incubated at -20°C for 30

minutes, vortexed for 30 seconds every 10 minutes. At this stage, the tubes were stored at -20°C for up to 1 week with minimal protein degradation.

After incubation, the tubes were centrifuged in a microcentrifuge at 12,000 g for 5 minutes. The supernatant was removed and discarded. The visible white pellet was allowed to air dry for 5 minutes, without over-drying to prevent the pellet from becoming difficult to re-suspend. The pellets were then re-suspended in 5 µl of labelling buffer until completely dissolved (***Table 2.7***). The pellets were then quantified and the concentration of protein was determined more accurately after the clean-up process.

Table 2. 7: Buffers prepared for DIGE sample preparation

Solutions for sample preparation			
Bromophenol blue solution (BPB)	1.00	% (w/v)	Bromophenol blue
	0.06	% (w/v)	Tris
2 x Lysis buffer	7.00	M	Urea
	2.00	M	Thiourea
	4.00	% (w/v)	CHAPS
	0.04	% (w/v)	BPB Solution
	2.00	% (w/v)	DTT
	2.00	% (w/v)	IPG Buffer ph 3-10
Labelling buffer	7.00	M	Urea
	2.00	M	Thiourea
	4.00	% (w/v)	CHAPS
	0.04	% (w/v)	BPB Solution
	30.00	nM	Tris

2.7.4 Protein quantification after clean-up

a) Principles

The Pierce assay was used in the 2nd protein quantification because it is a faster method compared to the 2-D Quant kit which is laborious. This Pierce assay is versatile and works with a wider range of detergents and reducing agents. Hence it is suitable for quantifying proteins in labelling buffer. The assay is based on the binding of dye metal complexes to proteins in an acidic solution. The measurable absorbance of 660 nm results from the binding of the reddish dye-metal complex (colour of the Pierce assay) turning green depending on the volume of the bound proteins. Proteins were quantified based on the basis of the absorbance obtained from a BSA standard protein dilutions assayed alongside the cleaned-up samples in a 96-well microplate.

b) Methods

First, 20 µl of each sample was transferred to a clean eppendorf tube. Samples were vortexed and centrifuged followed by the microplate procedure as mentioned in the protocol. Then, 5µl of each BSA standards with concentrations of 0.125, 0.250, 0.500, 0.750, 1.000, 1.500 and 2.000 µg/µl were pipetted into the microplate wells in duplicate (***Table 2.8)***. Consequently, 5µl of 1:20 dilutions of samples were pipetted into the labelled microplate wells followed by the addition of 150 µl of Protein Assay reagent into each well.

Table 2. 8: Example of standard curve of BSA concentrations in serial dilutions with the Pierce assay

BSA (µg/µL)	Abs (660nm)
0.000	0.045
0.125	0.093
0.250	0.115
0.500	0.172
0.750	0.225
1.000	0.285
1.500	0.378
2.000	0.505

A standard curve of absorbance at 660 nm against BSA standards and sample concentrations in µg/ml was plotted to determine the protein concentrations. From the standard curve, the protein concentrations were calculated and the volume of protein required for 50 µg of protein was calculated for protein labelling. The procedures were carried according to the protocol provided with the kit.

2.7.5 Protein labelling using CyDye

Before labelling, the samples were adjusted with 100 mM NaOH if necessary to a pH of 8.5 using pH indicator paper. Five microlitres of every CyDye dyes were reconstituted with 99.8% anhydrous dimethylformamide (DMF) to a concentration of 5 nmol/µL. The stock solutions of Cy2 (deep yellow), Cy3 (deep red) and Cy5 (deep blue) were stable at -20 °C for 3 months.

The working solution was prepared from the stock solution by allowing the CyDye in the -20°C freezer to warm for 5 minutes at room temperature. Then, 2 parts dye to 3 parts DMF were mixed in a new vial, vortexed vigorously and centrifuged for

30 seconds at 12,000 g. The final concentration of each CyDye was 400 pmol/µL and ready for labelling.

A volume of sample equivalent to 50 µg protein was transferred to a microcentrifuge tube and 1 µL of diluted CyDye was added to it. The samples and dye were mixed and centrifuged for 10 seconds and left on ice for 30 minutes in the dark. After 30 minutes, 1 µL of 10 mmol/L lysine was added to stop the reaction. Again, samples were mixed, centrifuged and left on ice for 10 minutes in the dark.

For the internal standards, the amount of protein required was calculated, depending on the number of gels in the experiment. For the comparison of LFR, LF, HF, HFDHA and HFEPA groups there were 20 gels in total and therefore a total of 40 samples were pooled as the internal standard. The final concentrations of dye-labelled samples and internal standards were 400 pmol per 50 µg protein. The dye-labelled samples and standards can be stored for 3 months in -80°C in the dark.

2.7.6 First dimension separation - Isoelectric focusing (IEF)

i) Pre-rehydration of IPG strips

Twenty four centimetres long Immobiline DryStrips and rehydration solution were used for cup loading of samples in an Immobiline DryStrip Reswelling Tray. Rehydration of IPG strips were carried out 6 hours before sample application. The re-swelling tray was levelled horizontally on the bench. Then, 450 µL of rehydration solution (***Table 2.9***) was pipetted into each groove of the re-swelling tray as a streak. The cover film on the IPG strip was removed and the strip was placed gel surface down. Air bubbles were removed by lifting the IPG strip carefully using forceps with bent tips and lowered carefully again. Then, 3 ml of DryStrip cover fluid was pipetted onto the IPG strip starting from the ends towards the centre. The sliding lid was closed and the whole tray was left over night (at least 6 hours) at room temperature.

ii) Isoelectric focusing (1st dimension separation)

The principal of isoelectric focusing allows the migration of proteins towards the anode and cathode along a pH gradient to meet their isoelectric point (pI) where the net charges are zero. The focusing effect takes place to avoid gain of charge when a protein diffuses away from its pI by migrating the protein back to its pI. From the 1st dimension separation, the pI of the proteins can be estimated with a calibration curve using protein markers. This method was used for preparative applications to purify the proteins in the

sample, ready for the 2nd dimension separation. The quality of 2-D separation can be determined by the pattern on graph of voltage against current

Samples were mixed with rehydration buffer and underwent rehydration loading overnight on 24 cm Immobiline DryStrips. After rehydration loading, the strips were transferred to a Ettan IPGphor Cup Loading Manifold (GE Healthcare) connected to the Ettan IPGphor Isoelectric Focusing System using the Ettan IPGphor II Control Software (version 1.01, Amersham Biosciences) following the manufacturer's instructions. More detailed steps on isoelectric focusing are provided in the GE protocol including the refocusing steps which were carried out before loading the samples onto the gels.

iii) Strip equilibration

The equilibration solution (***Table 2.9***) was prepared and the stock solution was aliquoted and stored at -20°C for further use. Then, 200 ml of equilibration buffer was thawed at room temperature. After this, 1 g of DTT and 2.5 g of iodoacetamide was weighed out separately.

After the IEF, the proteins on the IPG strips were refocused for 15 minutes before equilibration. The electrodes, loading cups and electrode pads were removed from the Manifold and the dry cover fluid was poured. Then, 1 g of DTT was added to 100 ml equilibration buffer, mixed thoroughly and poured into the manifold. The manifold was placed on an orbital shaker for 15 minutes. Next, 2.5 g of iodoacetamide was added to 100 ml equilibration buffer and the steps were repeated. Steps were taken to ensure strips were ensured not to stay longer than 15 minute in both equilibration solutions to avoid eluting part of the proteins from the strip.

Table 2. 9: Buffers for the rehydration of Immobiline DryStrips strips

IPG Strip Rehydration			
Rehydration solution	99.50	% (v/v)	DeStreak solution
	0.50	% (v/v)	Pharmalyte pH 3-10
Equilibration buffer	6.00	M	Urea
	2.00	% (v/v)	SDS
	50.00	M	Tris-Cl pH 8.8
	0.02	% (v/v)	BPB Solution
	30.00	% (v/v)	Glycerol

2.7.7 Second dimension separation - 2-dimensional difference gel electrophoresis (2D- DIGE)

i) Preparation for SDS running buffer and agarose sealing solution

SDS running buffer was prepared in advance by dissolving 0.25 mol/L Tris, 1.92 mol/L glycine and 1% SDS in MilliQ water to a final volume of 1 L using a magnetic stirrer. The SDS running buffer (10x concentrations) was stored at 4°C and later diluted before use. Besides that, agarose sealing solution was also prepared by mixing 0.5 g of 0.5% agarose, 200 µL 0.02% bromephenol blue and 10 ml of SDS running buffer (10 x concentrations) in MilliQ water to a final volume of 100 ml. Stock solution was aliquoted in to 15 ml centrifuge tubes and stored at room temperature.

ii) Procedure for 2nd dimension

For the Ettan DALTtwelve tank, the valve of tank was set to circulate and 950 ml running buffer (10x concentrations) was poured into the lower buffer tank. The tank was filled with 9.5 L of MilliQ water, set to 22°C and pump was set to 'ON' to allow the concentrated running buffer to mix in the tank.

The immobilized pH-gradient (IPG)-strips were transferred onto the 2nd dimension slab-gels and sealed with 0.5% (w/v) agarose solution. The gels were then slid into the slots of Ettan DALTtwelve System's electrophoresis tank followed by the 2nd dimension separation. The electrophoresis run was set according to the recommended run conditions: 1 Watt/gel for 1 hour followed by 17 Watt/gel for 5 hours.

2.7.8 Gel imaging

After the second dimension, the gels were removed from the tank and the surfaces were cleaned with water and wiped with lint-free tissue. The excess water on

the glass plates was removed with a glass plate squeegee and left to air dry to prevent streakiness on the surface.

The glass plates were scanned using the Ettan DIGE Imager with the imager control software which has a pre-set exposure and emission filter for each CyDye. A quick test scan was carried out randomly on a selected gel to determine the exposure times for each CyDye and the exposure areas were adjusted so that none of the areas on the gel presented protein spots that were over-saturated by referring to the pixel values. Target signals were achieved in pixel values ranging between 30,000 to 55,000 counts with exposure time for Cy2, Cy3 and Cy5 at 0.8, 0.3 and 0.5 seconds, respectively. All gels were scanned using the same exposure time and the images obtained were analysed using Ettan DIGE Imager.

After scanning, gels were cropped according to the region of interest using Image Quant Software.

2.7.9 Data analysis for proteomics

Data obtained from the scanned images were analysed using the DeCyder 2-D Differential Analysis Software with the DeCyder™ Extended Data Analysis Extension (GE Healthcare). The gel images were automatically loaded on to the batch processor and the area of interest was set to full image. The spot exclusion filter was set as follows: Slope > 1; Area > 100; Peak height < 100 or > 50,000 and Volume < 100.

Images were matched using Differential In-Gel Analyses (DIA). Among all the images, the one with the average number of spots was assigned as the Master gel. All other gels were matched to the Master gel using the Biological Variation Analysis (BVA) module. Each gel image was then assigned to a group and given a sample ID. After batch-processing, the gels were matched using the land marking option in the BVA module. Then, 10 clearly separated landmarks were used to match all gels to enhance the inter-gel matching accuracy. Thereafter, standard spot maps from each gel were matched using the Match function, followed by statistical analysis of protein abundance between samples using BVA module. One-way analysis of variance (ANOVA) analyses followed by Tukey's multiple comparison tests was carried out to retain spots with P Values < 0.05.

Spots of interest were selected and sent for further analyses to the Cambridge Proteomics Centre for identification by liquid chromatography tandem mass spectrometry (LC/MS-MS).

2.7.10 Preparative gels for spot-picking

i) Preparing cassettes with bind silane

The glass plates were cleaned with 5% Decon 90 solution overnight to remove any debris, gel pieces or keratin contamination. They were then rinsed with MilliQ water and wiped with lint-free tissue. Alternatively, water marks were avoided by letting the glass plates to air dry. Two self-adhesive internal reference marker stickers were applied on the short glass plate as shown in ***Figure 2.4.*** The spot picker camera identifies the internal reference markers.

Figure 2. 4: Positioning of the internal reference (IR) markers on the glass plate to ensure a precise excision when picking spot of interest

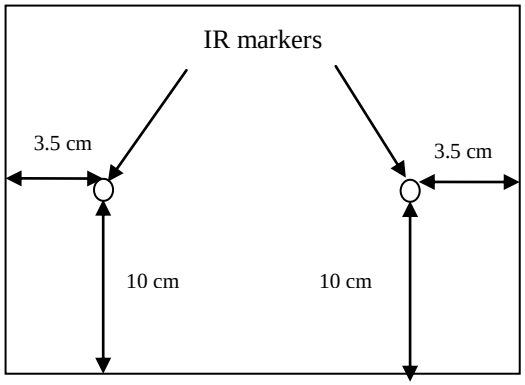

The bind-silane working solution was used for binding the gel to the glass plates and was made up of 8 ml of ethanol, 200 µL of acetic acid, 10 µL of bind-silane and 1.8 ml of MilliQ water. Then, 4 ml of the bind-silane solution was pipetted onto the plate and distributed equally over the plate with a lint-free tissue. The plates were covered to avoid dust contamination and left to dry for an hour. After 1 hour, the plates were polished with lint-free tissue and moistened with 2 ml of MilliQ water. Then, gels were cast on the same day using the Ettan DALTtwelve gel caster which can cast up to 14 gels. Instructions for gel casting can be referred to the protocol provided by GE

ii) Gel casting

The SDS gel buffer Tris-Cl pH 8.8 was prepared by dissolving 1.5 mol/L Tris-base and 0.4% SDS into 800 ml of MilliQ-water. The pH of the Tris buffer was adjusted to pH 8.8 with 4 mol/L hydrochloric acid. Then the buffer was made up to a final volume of 1 L and stored at 4°C. This was followed by the preparation of 10% ammonium persulfate (APS) solution. The APS solution was prepared fresh before use.

The 12.5% homogenous monomer gel casting solution was prepared fresh, de-gassed for 15 minutes while stirring and pre-cooled at 4°C. 175 ml of acrylamide, bis solution, was deionized with 3 g of mixed bed ion exchanger for 10 minutes and filtered before use. Then deionized acrylamide bis solution, Tris-HCL pH 8.8 and 100 % TEMED were dissolved in MilliQ-water. Lastly, 10% APS was added to the solution right before pouring into the gel caster.

For the displacing solution, Tris-Cl pH 8.8, 50 % glycerol and 0.02 % bromophenol blue solution were mixed and dissolved in MilliQ-water. After preparing all solutions required, the gel caster was assembled according to the manufacturer's protocol. Clear low fluorescent glass plates were placed alternately with separator sheets into the tilted caster resting on the supported legs. The gel caster was sealed in place and tightened evenly without applying too much pressure and the sealing gasket was compressed to prevent leakage. The caster was tip to the front and levelled horizontally on the bench.

Four ml of APS was added to the monomer gel casting solution and mixed gently to avoid air bubbles. The gel solution was poured directly into the gel caster immediately until it reached 3 cm below the upper edges of the casting cassettes and air-bubbles trapped in between the glass plates were removed. Displacing solution was poured to fill the V-chamber and the sloped bottom of the caster which will gave rise to the gel solution in the cassettes edges being 1cm below the upper edges whereby a thin blue layer was visible at the bottom of the cassettes. Then, 0.1% SDS overlay solution was sprayed over the casted gels immediately and covered with cling film to prevent loss of moisture from the gel. The gel caster was left at room temperature overnight to allow polymerisation and gel setting. The gels were either used immediately or stored in 1x SDS running buffer at 4° until required.

iii) Protein samples for preparative gels

For preparative gels, a total of 250 µg of pooled internal standard was used whereby 50 µg was labelled with Cy5 and 200 µg remains unlabelled. Under these measurements, optimum results were obtained when matching preparative gels to analytical DIGE gels. First and second dimension run were performed as described in ***Section 2.10.6*** and ***2.10.7*** with the exception that the low fluorescent gel cassettes were carefully separated allowing preparative gels to bind to the short glass plates. The gels

were rinsed in deionised water and stained with Deep Purple fluorescent stain following the protocol provided.

Briefly, the gels were fixed in pre-fixing solution for 45 minutes and left in fixing solution overnight. The next day, gels were placed in pre-buffering solution for 40 minutes and then replaced after 20 minutes followed by staining solution. After 1.5 hours, the gels were placed in washing solution for 15 minutes twice and soaked in acid solution for 10 minutes. Steps were carried out in re-sealable polyethylene bag covered with aluminium foil to prevent light on the orbital shaker. All post staining buffers and solutions are presented in ***Table 2.10***. The post stained gels were scanned on an Ettan DIGE Imager as described in ***Section 2.10.8***. The spot-maps were analysed and spots of interest were picked for protein identification.

Table 2. 10: Solutions for post staining of preparative DIGE gels

Post stain buffers and solutions			
Prefixing	15.00	% (v/v)	Ethanol
	10.00	% (v/v)	Glacial Acetic acid
Fixing/ acidification	15.00	% (v/v)	Ethanol
	1.00	% (v/v)	Citric acid
Prebuffering	6.20	% (w/v)	Boric acid
	3.80	% (w/v)	Sodium hydroxide
Staining	0.50	% (v/v)	Deep purple
	6.20	% (w/v)	Boric acid
	3.80	% (w/v)	Sodium hydroxide
Washing	15.00	% (v/v)	Ethanol

All buffers were prepared in deionised water

2.7.11 Spot picking

Proteins of interest in ***Chapter 3*** were picked with an automated robotic, namely the Ettan Spot Picker together with the Instrument Control Software. Firstly, spots of interest were detected on preparative gels based on its x and y coordinates in reference to the 2 marker spots (***Figure 2.6***). Then a 1.4 mm picker head was chosen for 1 mm gels and the robot's camera was calibrated according to the manufacturer's protocol. Briefly, a sheet of white paper was placed on the gel tray in the picker station and a camera calibration foot was placed on the picker head with a defined spot in the centre of the paper sheet. The picker head was directed to the recorded x and y coordinates and

then returned to its original position. The calibration was verified to be successful when picker head returned to the calibration foot 3 times consecutively.

After calibration 2 plate holders were placed in the tray filled with ultrapure water to 5 mm below the upper edges. A preparative gel was placed in the tray with the acidic corner close to the home position of picker head and fixed in place with plate holders. Then, 96 well digester plates with small holes in the bottom were placed into standard 96 well micro plates in the racks next to the gel tray. This was to prevent leakage when dispensing solution from the digester plates and avoid contamination of samples.

The height of picker head versus the horizontal position (z-coordinate) of the preparative gel was set and the picker head was moved towards a location outside the picking area for trial. The picker head was lowered until it touched the glass backing and further adjusted until a small gap of 1 to 2 mm was seen between the holder and picker head. This optimal position allows for precise excision of gel plugs without causing damage to the glass plates and therefore saved as gel z-coordinate. The horizontal location, x and y-coordinate of digester plates was adjusted if necessary.

The picking parameters were set according to the manufacturer's instructions and solutions for picking (ultrapure water and 20% ethanol) were prepared and used to prime the system before picking protein spots of interest. The pick list was uploaded and the software gave information on the volume of buffer required to pick all the spots. After priming, the system was set up and the picker head was positioned according to the micro-plates and rinse station. Once the picker head was placed appropriately in the rinse station, the picker head was manoeuvred according to the picking parameters. The gel plugs excised from the preparative gel were then transferred to 96 well micro plates and subjected to LC MS/MS analysis.

2.7.12 Mass spectrometry

All LC-MS/MS experiments were performed using an Eksigent NanoLC-1D Plus (Eksigent Technologies, Dublin, CA) HPLC system and Linear Trap Quadrupole (LTQ) Orbitrap mass spectrometer (ThermoFisher, Waltham, MA). Separation of peptides was performed by Dr. Mike Deery, using reverse-phase chromatography at a flow rate of 300 nL/min and a LC-Packings (Dionex, Sunnyvale, CA) PepMap 100 column (C18, 75 µM i.d. x 150 mm, 3 µM particle size). Peptides were loaded onto a pre-column (Dionex Acclaim PepMap 100 C18, 5 µ particle size, 100A, 300 µM i.d x

5mm) from the auto-sampler with 0.1% formic acid for 5 minutes at a flow rate of 10 µL/min. After this period, the ten port valve was switched to allow elution of peptides from the pre-column onto the analytical column. Solvent A was water + 0.1% formic acid and solvent B was acetonitrile + 0.1% formic acid. The gradient employed was 5-50% B in 40 minutes. The LC eluant was sprayed into the mass spectrometer by means of a New Objective nanospray source. All *m/z* values of eluting ions were measured in the Orbitrap mass analyzer, set at a resolution of 7500. Peptide ions with charge states of +2 and +3 were then isolated and fragmented in the LTQ linear ion trap by collision-induced dissociation and MS/MS spectra were acquired. The LTQ was to improve capacity, trapping efficiency and scan speed.

Post-run, the data was processed using Bioworks Browser (version 3.3.1 SP1, ThermoFisher). Briefly, all MS/MS data were converted to dta (text) files using the Sequest Batch Search tool (within Bioworks). The dta files were converted to a single mgf file using a SSH script in the SSH Secure Shell Client program (Version 3.2.9 Build 283, SSH Communications Corp.). These combined files were then submitted to the Mascot search algorithm (Matrix Science, London UK) and searched against the NCBI mouse database, using a fixed modification of carbamidomethyl and a variable modification of oxidation. All LC-MS/MS experiments were carried out by Dr. Mike Deery and his colleagues at the Cambridge Proteomics Centre, UK. Proteins in ***Chapter 3*** were picked by the robot and only proteins that were abundant in ***Chapter 7*** were picked by hand.

2.8 MiRNA expression in mice fed different types of dietary fats

2.8.1 Procedures of total RNA extraction

Frozen mouse liver samples (approximately 100 mg each) were submerged in 1 ml of TRIzol Reagent (Invitrogen Life Technologies, Paisley, UK) in a 2 ml microcentrifudge tube with 2 mill balls and homogenised for 60 seconds using an electrical tissue lyser (Qiagen). Five hundred µl of homogenate was transferred to clean 2 ml microcentrifuge tube and centrifuged at 12000 g for 10 minutes at 4°C in order to remove cell debris or unhomogenised particles from samples. The supernatant was transferred to a fresh tube and incubated for 5 minutes at room temperature.

After incubation, 100 µl of chloroform (0.2 ml of chloroform per 1 ml of TRIzol Reagent) was added, shaken vigorously by hand for 15 seconds and incubated for 3 minutes at room temperature. The solution was centrifuged at 12000 g for 15 minutes at 4°C and the aqueous and organic phases were observed. Then, 200 µl of aqueous phase was transferred to a fresh 0.6 ml microcentrifuge tube and 250 µl of 100% isopropanol (0.5 of isopropanol per 1 ml of Trizol used for initial homogenization) was added to precipitate RNA. The isopropanol mixture was incubated for 10 minutes at room temperature and centrifuged at 12000 g for 10 minutes at 4°C to pellet the precipitated RNA.

After formation of the RNA pellet, the supernatant was removed and the RNA pellet was washed with 500 µl of 75% ethanol (1 ml of ethanol per 1 ml of Trizol used for initial homogenization), centrifuged again at 7500 g for 5 minutes at 4°C and dried in the fume hood at room temperature for 30 minutes. The air-dried RNA pellet was dissolved in 40 µl of RNase-free water (Ambion) and the extracted RNA was resuspended in the RNase-free water. The dissolved RNA samples were aliquoted in 5 µl and stored at -80°C until further assessments of quantification and quality of RNA.

2.8.2 Measurement of RNA quantity and purity

Quantitation of RNA was performed using NanoDrop® ND-1000 Spectrophotometer with the selected module of "Nucleic Acid" according to the manufacturer's instructions. The NanoDrop® ND-1000 Spectrophotometer (***Figure 2.5***) provided not only RNA concentration i.e., calculated from absorbance at 260 nm, but also purity by observing the ratio of sample absorbance at 260 nm and 280 nm, respectively. The maximum absorbance of nucleic acid and proteins are 260 nm and 280 nm respectively.

In this method, 1 µl of extracted RNA sample was pippetted onto the lower measurement pedestal of the Nanodrop. The upper measurement pedestal was closed and the spectral measurement was then performed according to the operating software provided. The software automatically estimated the concentration (ng/µl) of nucleic acids and the ratio of absorbance 260 nm and 280 nm. The 260 nm/280 nm ratio indicates the purity of RNA which should be approximately 1.9-2.1. Low absorbance ratio of 260/280 means low concentration of nucleic acid. The sample's absorbance was obtained according to the following formula: Absorbance = -log (Intensity $_{sample}$/ Intensity $_{blank}$).

Figure 2. 5: The NanoDrop® ND-1000 Spectrophotometer used to measure RNA concentration and also purity of RNA by observing the ratio of sample absorbance at 260 nm and 280 nm

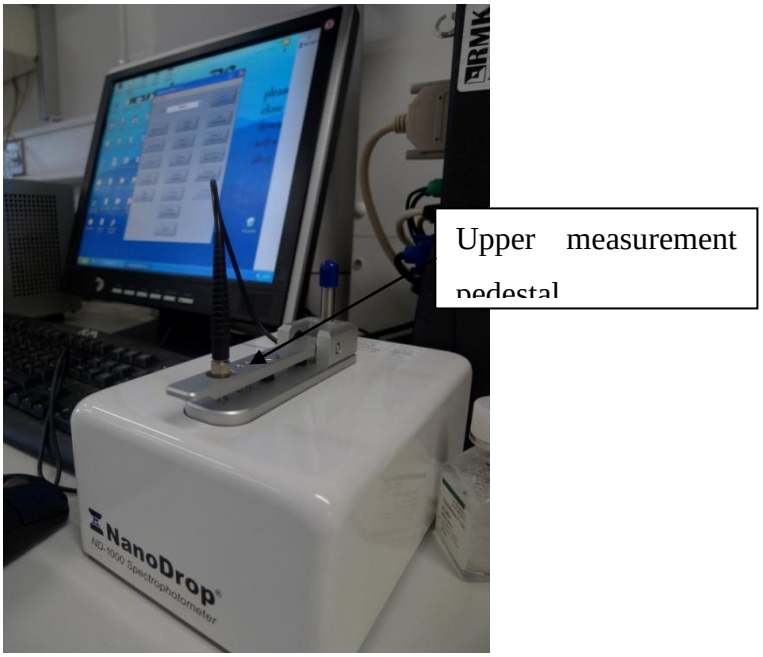

2.8.3 Measurement of quality of RNA

RNA quality was assessed using Agilent 2100 bioanalyzer RNA 6000 NanoChip. The concept of RNA quality assessment is based on miniaturized platform technologies. RNA samples were driven electrophoretically. RNA was microfabricated and separated according to their size by molecular sieving, and then detected by laser induced fluorescence detection.

Results were analysed by Agilent 2100 Bioanalyzer software which automatically generates a ribosomal ratio of 28S/18S ratio and RNA integrity number (RIN) as the presentation of RNA quality. The 28S/18S ratio of 2 is considered to indicate good quality. When RNA degradation occurs, the rRNA ratio will decrease. With the RNA integrity number (RIN), it has a systemic number from 1 to 10 to present the quality of RNA. For example, a RIN of 1 indicates the substantial degradation of RNA, whereas a RIN of 10 indicates the best RNA quality. The quality of RNA was also visually determined via electropherogram and gel-like image output was generated (***Figure 2.6***).

The procedures for estimating RNA quality included 3 steps of preparation. After an initial measurement of RNA concentration, the concentrations of samples were adjusted within 25-500 ng/µl to assess RNA quality using the bioanalyzer in 3 steps:

(i) *Gel preparation*

550 µl of RNA 6000 Nano gel matrix was placed into a spin filter and centrifuged at 1500 g for 10 minutes. After centrifugation, 65 µl filtered gel was aliquoted into 0.5 ml RNase-free microcentrifuge tubes.

(ii) Preparation of gel-dye mix

RNA 6000 Nano dye concentrate was left at room temperature for 30 minutes and vortexed for 10 seconds and spun down. 1 µl of dye was added into 65 µl of prepared filtered gel and mixed. The gel mixture was spun down at 13000 g for 10 minutes at room temperature.

(iii) Loading of Gel-dye mix, RNA 6000 Nano Marker, ladder and samples onto chip

Before loading the RNA 6000 Nano marker, ladder and samples, a new RNA chip was placed on the Chip Priming Station and 9 µl of gel-dye mix was loaded into the well with “G” marked. After closing the Chip Priming Station, pressing the plunger and releasing the clip, 9 µl of gel-dye mix in each of 2 additional gel-dye wells was loaded again. After loading the gel-dye mix, 5 µl of RNA 6000 Nano Marker (for each well) was pipetted into the Ladder well and into

each of 12 sample wells. Then, 1µl of ladder and 1µl in each of 12 samples wells was then loaded into the wells. After the completion of gel-dye mix, marker, ladder and samples loading, the chip was placed on the adapter and vortexed at 280 g for 1 minute. After vortexing, the chip was put in the bioanalyzer for assessment of RNA integrity.

Figure 2. 6: Visual determination via electropherogram and gel-like output generated from the bioanalyzer for quality check

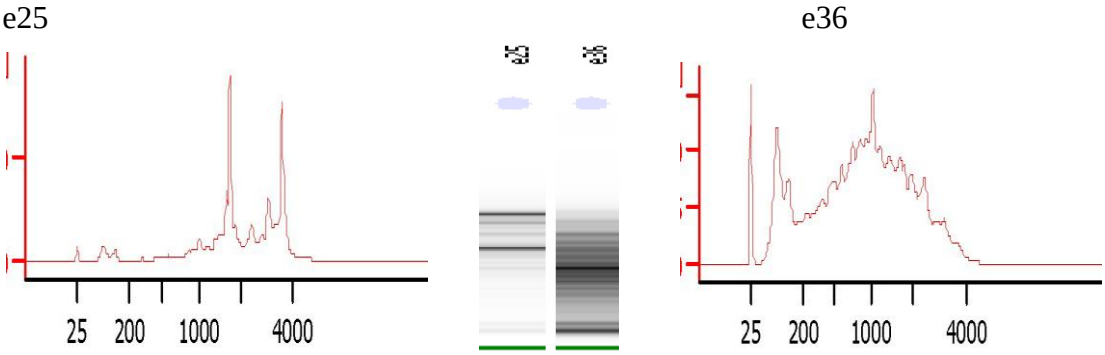

Image e25 represents good quality RNA whereas e26 represents RNA degradation. The 2 distinct peaks in e25 represent the 18S and 28S ribosomal. Ribosomal ratio of 28S/18S of 2 is considered to indicate good quality; and the ratio decreases if RNA quality is low.

2.9 Affymetrix miRNA Arrays

MiRNAs are short, single-stranded RNAs that regulate gene expression by partial complementary base pairing to specific mRNAs. MiRNAs are non-coding RNAs which is becoming an important component in investigating biological processes such as transcriptional gene silencing and translational repression.

The Affymetrix miRNA array consists of the most comprehensive miRNA assay system covering 71 organisms on a single array which includes human, mouse, rat, canine, monkey and additional 922 human small nuclear RNAs (snoRNAs and scaRNAs). SnoRNA and scaRNA are short non-translated RNAs that play a role in processing of ribosomal RNAs. In addition the Affymetrix array includes 4 copies of each miRNA probe distributed on the array. For each snoRNA and scaRNA, there are 11-probes. All 46,228 probe sets representing 6703 miRNA sequences are perfect match probes which mean the probes are complementary to the nucleic acid sequences of the miRNAs. The arrays are biotin labelled (FlashTag Biotin HSR) using a Genisphere RNA labelling kit. Sequences are from Sanger miRNA (V.11) or Ensembl databases and snoRNABase.

RNAs were subjected to a brief poly-A tailing reaction which is essential for translation and mRNA stability. The FlashTag Biotin HSR kit labels all RNA samples including low molecular weight RNA for analysis by Affymetrix GeneChip miRNA Arrays. The following step is the ligation of the biotinylated signal molecule to the target RNA samples at the 3’ end of the RNA. The ultrasensitive biotin labelling of the FlashTag Biotin HSR is due to Genisphere proprietary 3DNA dendrimer which is a branched structure of single and double-stranded DNA conjugated with numerous labels.

2.9.1 Labelling of RNA

In every experimental group, 6 samples of total RNA from individual mice were pooled in equal concentrations making up a total of 5000 ng of RNA and volumes were adjusted to 35 µl with Nuclease-Free water (***Table 2.11***). The labelling procedure started with poly (A) tailing followed by a ligation step as described:

(i) Poly (A) Tailing

From the pooled sample, 8 µl of RNA was transferred to ice and 2 µl of RNA Spike Control Oligos were added before returning samples to ice. Adenosine-5'-triphosphate (ATP) mix was diluted in 1 mM Tris according to the protocol

provided by the manufacturer. A master mix of 9 µl of 10x reaction buffer, 9 µl of 25 mM $MnCl_2$, 6 µl of diluted ATP mix and 6 µl of poly(A) polymerase (PAP) enzyme was prepared. Then, 5 µl of master mix was added to 10 µl RNA/Spike Control Oligos for a volume of 15 µl. Samples were microcentrifuged and incubated in a 37°C heat block for 15 minutes.

(ii) Ligation

Fifteen microlitres of tailed RNA was microcentrifuged and placed on ice. Then, 4 µl of 5x FlashTag Biotin Ligation mix was added followed by 2 µl of T4 DNA ligase. The samples were mixed gently, microcentrifuged and incubated at 25°C for 30 minutes. Next the reaction was stopped by adding 2.5 µl of HSR Stop solution, mixed and microcentrifuged. A total volume of 23.5 µl of biotin-labelled sample may be stored on ice for up to 6 hours or at -20°C for up to 2 weeks prior to hybridization on Affymetrix GeneChip miRNA arrays.

Table 2. 11: Samples pooled from the RNA extraction for microarray analysis

Samples	Absorbance ratio (260/280)		RNA concentrations (ng/µl)		
	1	2	1	2	Average
Pool LFR	2.10	2.07	142.03	143.71	142.87
Pool LF	2.10	2.10	136.62	137.02	136.82
Pool HF	2.10	2.07	153.26	153.46	153.36
Pool HFDHA	2.08	2.10	139.81	138.94	139.38
Pool HFEPA	2.11	2.10	141.58	142.42	142.00

2.9.2 Affymetrix GeneChip miRNA array procedure

a) Preparation of ovens, arrays and sample registration files

The Affymetrix Hybridization Oven 640 was set to 48°C. The arrays were unwrapped and placed on the bench top to warm to room temperature for 15 minutes. Each array was labelled. Then, a 200 µl unfiltered pipette tip was inserted into the upper right septum to allow for proper venting when the hybridization cocktail was injected. miRNA array library file package was installed and downloaded into the Affymetrix GeneChip Command Console (AGCC) software using the Command Console Library File importer tool. Samples and array information were uploaded into AGCC.

b) Hybridization

Eukaryotic Hybridization Controls were thawed completely for hybridization and then heated for 5 minutes at 65°C. A master mix of hybridization cocktail was prepared consisting of 50 µl 2x hybridization mix, 15 µl 27.5% formamide, 10 µl DMSO, 5 µl 20x eukaryotic hybridization controls and 1.7 µl control oligonucleotide B2. At this point, the total volume was 123.2 µl, which was incubated at 99°C for 5 minutes and then 45°C for 5 minutes. Thereafter, 100 µl of samples were aspirated and injected into the microarray chip. The pipette tip was removed from the upper right septum of the array. Both septa were covered with 1.5 inch Tough-Spots to minimize evaporation to prevent leaks. The microarray chips were then placed into the GeneChip Hybridization Oven 640 and the trays were loaded into the hybridization oven for incubation at 48°C for 16 hours.

c) Washing and staining

After 16 hours of hybridization, the arrays were removed from the oven and the Tough-spots were removed from the arrays. The hybridization cocktail was extracted from each microarray chip and transferred to a new tube. Each microarray chip was filled completely with Array Holding Buffer and allowed to equilibrate to room temperature before washing and staining. Vials were placed into sample holders on the fluidics station according to the manufacturer's protocol. The Fluidics Station 450 was washed and stained using fluidics script FS450_0003. The arrays were checked for air bubbles and it was ensured that there was no dust on the glass surface before scanning.

d) Scanning

All instructions for using the GeneChip Scanner 3000 7G and scanner arrays were referred to Affymetrix Command Console Software User Manual (pg 141). ***Figure***

2.7 shows the scanned image of the hybridized probe microarray, which is similar for all 5 microarray chips.

Figure 2. 7: Image of hybridized probe microarray with probes complementary to miRNA information of interest

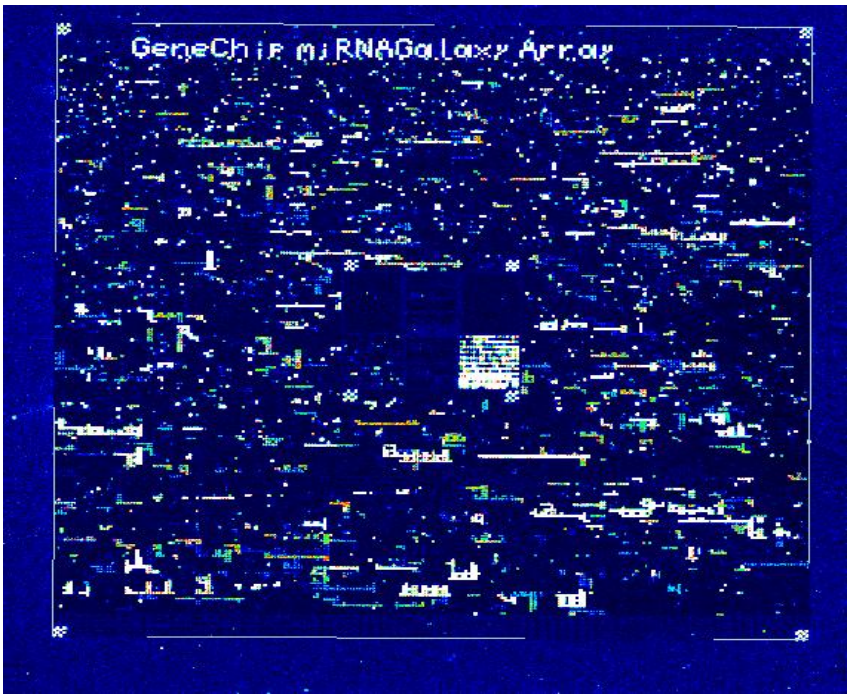

Every grid represents miRNA expression levels in fluorescence intensity, green intensity indicates down-regulated whereas red intensity indicates up-regulated miRNA expression in the treated group. Yellow indicates no change in miRNA expression.

e) Data analysis

Data summarization, normalization and quality control were analysed using the miRNA QC Tool software (version 1.1.1.0). The workflow used in miRNA QC Tool:

Detection	:	Background detection
Background adjustment	:	RMA Global Background Correction
Normalization	:	Quantile
Summarization	:	Median Polish

Each probe on the array was assayed for detection based on the Wilcoxon Rank-Sum test of the miRNA probe set signals, compared to the distribution signals from the background of Guanine-Cytosice (GC) content matched anti-genomic probes. $P \leq 0.06$ was considered to be detected above background hence a true detection and the P-value was generated using Fisher test. Therefore, with P-value > 0.06 were considered undetected due to the weak sample signal which was not able to discriminate from the background probes.

Normalization of data reduced the variability after employing background corrections (RMA Global) and summarization (Median Polish). Most normalization methods assume similar distribution of intensities between the 2 groups and the number of over expressed miRNAs is similar to the number of under expressed miRNAs. Quantile normalization was thus used to compare the probe intensities across microarray chips and ensured that the distributions of log intensities were comparable (Bolstad et al, 2003). Median polish is a summarization method that ignores outlier probe-level intensities (Biostatistics 2003).

An overview of data distribution as represented by the MA plot with green intensity ratio (M) plotted against the average intensity (A) is shown in ***Figure 2.8***. The MA plot shows the normalization of data generated from the 2 microarray chips ensures minimal technical biasness and to ensure hybridization efficiency. In general assumption, most miRNAs will not alter in expression and the majority of plots will thus be concentrated at 0 whereby Log (1) is 0. 'M' represents the log difference in intensities between the 2 chips and 'A' represents average intensities. The formula for M and A is as follows: $M=\log_2 R - \log_2 G$; $A= ½ \times (\log_2 R + \log_2 G)$.

Figure 2. 8: An overview of data distribution represented by MA plot with green intensity ratio (M) plotted against the average intensity (A).

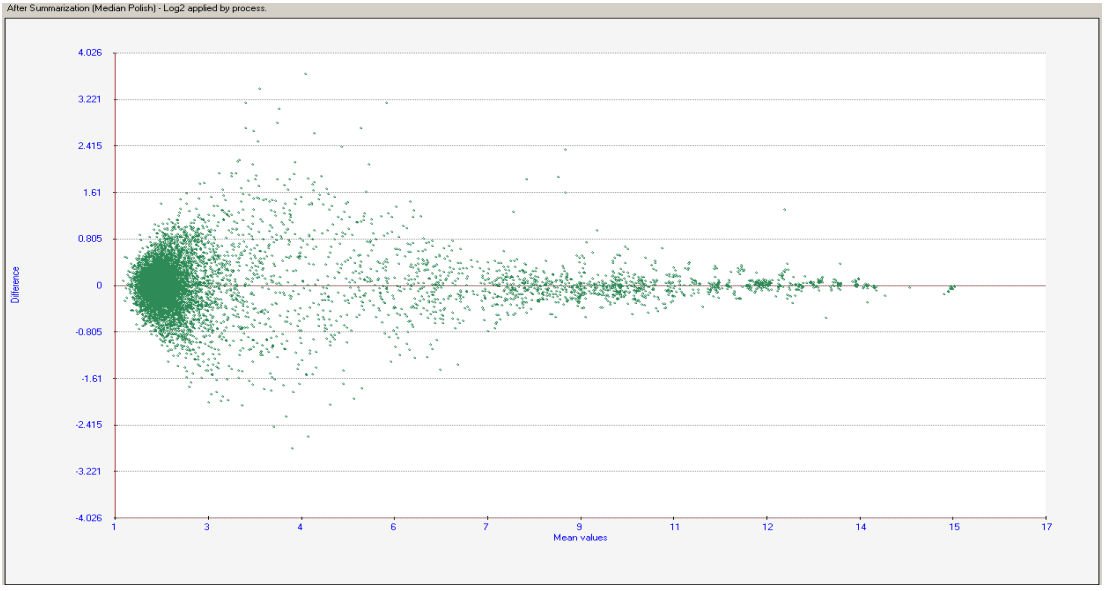

M on the y-axis represents green intensity ratio; A on the x-axis represents average intensities. Formula for $M=\log_2 R - \log_2 G$; $A= ½ \times (\log_2 R + \log_2 G)$.

From the list of miRNA generated from the microarray, only mouse miRNA were further analysed. Only miRNAs that were up regulated with relative intensities of >1.5 or down regulated with relative intensities of <0.5 were considered in the miRNA

selection for real-time RT-qPCR. Although there were no replicates of microarrays for statistical analysis, the selected miRNAs were validated with quantitative real-time RT-qPCR. Preliminary scrutiny of the data was carried out to indentify micro-RNAs suitable for verification by RT-qPCR. Subsequently it was revealed that the initial ranking of miRNAs were inaccurate. This was then corrected, and the data verified independently. The supposition that the array data displayed in this thesis is accurate is supported by the following observation: there was extremely good concordance of data when the array and RT-qPCR data were compared for the LFR versus HF study.

2.10 Quantitative real-time RT-qPCR miRNAs expression analysis

The miRNA microarray results were confirmed using real time RT-qPCR on independently derived RNAs from individual mice (n=6/group) for all 5 diet groups (i.e., LFR, LF, HF, HFDHA and HFEPA; ***Chapters 8***). Total RNA was isolated as described in ***Table 2.16*** and RT-qPCR was performed according to the manufacturer's protocol. On each 96-well plate, a small RNA assay for each cDNA sample, endogenous control and no template controls to evaluate background signal were allocated. At the beginning of the PCR reaction, products were allowed to amplify at a constant, exponential rate by ensuring that it did not compete with the primer binding. Excessive reagents and low enough concentrations of template and product were applied to prevent competition with primer as described in the manufacturer's protocol. Individual primers for each miRNAs were predesigned and validated using Applied Biosystems TaqMan by providing Applied Biosystems with the miRNA target sequence. Primers from the Applied Biosystems TaqMan assay are stem-loop structured because the miRNAs are short.

In this thesis, TaqMan (Applied Biosystems) was used for the detection of PCR products which generates fluorescence signal through the coupling of fluorogenic dye molecules and a quencher moiety to the same or different oligonucleotide substrates.

2.10.1 Sample preparation and RT-qPCR procedures

A two-step RT-PCR was carried out using TaqMan Small RNA assays. For the reverse transcription (RT) step, cDNA was reverse transcribed from RNA samples using a small RNA-specific, stem-loop RT primer from the TaqMan Small RNA Assays and reagents from TaqMan MicroRNA Reverse Transcription Kit. In the tube, the RT

master mix was prepared on ice using TaqMan MicroRNA reverse transcriptase kit (thawed) and allowing for 20% in excess volume to compensate for losses during pipetting. The components of RT master mix are indicated in ***Table 2.12***:

Table 2. 12: Components of reverse transcriptase (RT) master mix

Component	**Master mix volume per 15 µL reaction**
100 mM dNTPs (with dTTP)	0.15 µL
MultiScribe Reverse transcriptase, 50 U/µL	1.00 µL
10x reverse transcription buffer	1.50 µL
RNase inhibitor, 20 U/µL	0.19 µL
Nuclease-free water	4.16 µL
Total volume	7.00 µL

Each 15 µL reaction consists of 7 µL master mix, 3 µL of 5x RT primer and 5 µL RNA sample

The master mix solution was mixed gently, centrifuged and placed on ice ready for the RNA reaction. Each 15 µL RT reaction was combined with RT master mix with total RNA in the ratio of 7 µL RT master mix : 5µL total RNA (1 to 10 ng per reaction). Then, 12 µL of RT master mix containing total RNA was transferred to a 96-well reaction plate. Afterwards, 3 µL of 5x RT primer from each assay set was added into the corresponding well. The solution in the plates was sealed, mixed thoroughly and centrifuged to bring all solutions to the bottom of the wells. After 5 minutes of incubation on ice, samples were ready to be loaded onto the PTC-225 Peltier Thermal Cycler. The thermal cycler was set to 4 steps: (i) 30 minutes at16°C, (ii) 30 minutes at 42°C, (iii) 5 minutes at 85°C and (iv) hold until unloaded at 4°C. Finally, the RT run was performed. Immediately after the RT run, the PCR amplification step was continued.

For the PCR step, PCR products were amplified from cDNA using TaqMan Small RNA Assay and TaqMan Universal PCR Master Mix II. Then, 20 µL per reaction of qPCR reaction mix was prepared allowing for 20% excess to compensate for the volume loss during pipetting. After this, 1.5 ml microcentrifudge tube for each sample was quadruplicated and contained the following component indicated in ***Table: 2.13.***

Table 2. 13: Components required for polymerase chain reaction (PCR) step

Component	Volume per 20 µL reaction	
	Single reaction	**Three replicates**
TaqMan Small RNA Assay (20x)	1.00 µL	3.60 µL
Product from RT reaction[a]	1.33 µL	4.80 µL
TaqMan Universal PCR Master Mix II (2x)	10.00 µL	36.00 µL
Nuclease free water	7.67 µL	27.61 µL
Total volume	20.00 µL	72.01 µL

[a] *The maximum amount of RT product that can be added to the reaction. Primer was diluted to a minimum of 1:15 in the final qPCR reaction. Components of master mixes are listed in Table 2.13. Replicate volumes include 20% excess to compensate for volume loss during pipetting*

The microcentrifudge tube was capped and inverted several times to mix and then centrifuged briefly. 20 µL of the complete qPCR reaction mix, including assay and RT products was transferred into each of 4 wells on a 384-well plate using the Biomek FX Liquid handling robot (***Figure 2.9***). The plate was sealed, centrifuged and loaded onto the 7900 HT Fast RT-PCR System. The parameters on the real-time PCR were set for 40 cycles according to the following parameters:

Run mode: Standard

Sample volume: 20 µL

Thermal cycling conditions stated in Table 2.14

PCR efficiency was determined by referring to the real-time PCR plots whereby similar slopes have similar PCR efficiencies with minimal background noise.

Figure 2. 9: Biomek FX Liquid handling robot used to transfer 20 µL of the complete qPCR reaction mix, including assay and RT products into each of the 4 wells on a 384-well plate

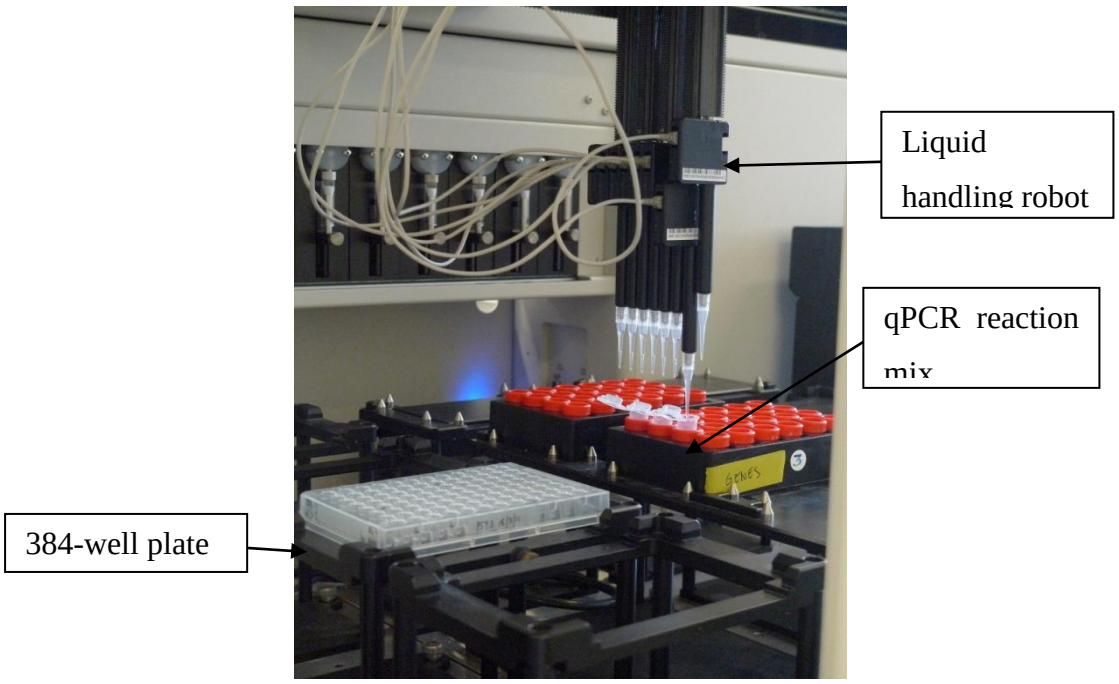

Table 2. 14: Conditions set-up for thermal cycling for real-time PCR

Step	Optional AmpErase UNG activity	Enzyme activation	PCR Cycle (40 cycles)	
	Hold	Hold	Denature	Anneal/extend
Temperature	50°C	95°C	95°C	60°C
Time	2 minutes	10 minutes	15 seconds	60 seconds

During PCR, the 5' nuclease assay process takes place whereby TaqMan minor grove binder (MGB) probe anneals to a complementary sequence between the forward and reverse primer sites. The TaqMan MGB probe contains a reporter dye linked to the 5` end of the probe, MGB at the 3'end of the probe and a non-fluorescent quencher at the 3'end of the probe. Probes that were intact suppress the reporter fluorescence by Forster-type energy transfer. Then probes that were hybridized to the target were cleaved by DNA polymerase which separates the reporter dye and the quencher dye. The separation between the reporter dye and the quencher dye increased the fluorescence by the reporter. The fluorescence signal increases when target sequence is complementary to the probe and therefore non-specific amplification is undetected. The total selected good quality and quantity RNA isolated individually from each group (***Table 2.15***).

2.10.2 Determining the Cycle threshold (Ct) by relative quantification

The amplification plot of the endogenous control used in this study is sno-234. The amplification plot is a graph of fluorescence signal against cycle number (***Figure 2.10***). As seen in the graph, there is little change in fluorescence in initial cycles of PCR and this defines the baseline of the amplification plot. In this study, a fixed threshold was set at 0.388, represented by the green horizontal line across the graph. The increase above the baseline indicates the accumulated PCR product. Ct is determined by the middle part of the exponential phase, normally between 25 and 35 cycles. Ct is the cycle number whereby the fluorescence signal reaches threshold level above background and this value is calculated by default using the ABI TaqMan program. The higher the initial sample volume, the sooner the accumulated sample is detected as a significant increase in fluorescence hence a lower Ct value. As seen in ***Figure 2.10***, the Ct values are reproducible due to the threshold set at the exponential phase of the PCR. At the exponential phase there is a linear relation between the log difference in fluorescence and cycle number. Each non-limiting reaction was run in quadruplicate. For every 4 samples, 2 mean Ct values were generated with 1 median Ct. For example, D30 is a contaminated sample but because median Ct was used in the calculations instead of the average Ct the outlier did not affect overall median Ct values. The difference between the normal and contaminated sample were 25.869 and 23.555 respectively**.** MiRNA expressions were quantified using the comparative C_T method referred to as $2^{-\Delta\Delta CT}$ method. Briefly, the median Ct of the endogenous control (snoRNA-234) was subtracted from each sample to obtain ΔCt. This was followed by the subtraction of ΔCt of each sample with the average ΔCt of the control group. The relative quantification presented the changes of the selected miRNAs relative to an endogenous control (snoRNA-234) and ΔCt of the control group. Tables for median Ct values and its standard deviation can be referred in ***Appendix 2.1*** to ***2.4.***

Table 2. 15: Individual RNA samples extracted from mice fed low fat reference (LFR), low fat (LF), high fat hypercaloric (HF), high fat hypercaloric DHA (HFDHA) or high fat EPA hypercaloric (HFEPA) ready for real-time qPCR

	Mouse no.	RIN	Absorbance ratio (260/280)		Ave RNA conc (ng/nL)	Dilution (1:10)	µL for 10ng of RNA	µL for 5ng RNA	Volume of H2O added to make 2.5µL
			1	2					
LFR	TABS 302	7.8	2.05	2.06	64.59	6.46	1.55	0.77	1.73
	TABS 303	4.6	2.1	2.08	191.74	19.17	0.52	0.26	2.24
	TABS 305	6.7	2.11	2.11	195.49	19.55	0.51	0.26	2.24
	TABS 306	6.3	2.11	2.1	276.90	27.69	0.36	0.18	2.32
	TABS 307	6.8	2.09	2.09	208.52	20.85	0.48	0.24	2.26
	TABS 308	7.3	2.11	2.09	224.47	22.45	0.45	0.22	2.28
LF	TABS 309	6.9	2.08	2.09	350.92	3.51	2.85	1.42	1.08
	TABS 310	6.5	2.08	2.09	244.94	24.49	0.41	0.20	2.30
	TABS 312	4.5	2.08	2.08	377.75	3.78	2.65	1.32	1.18
	TABS 313	7	2.11	2.13	214.63	21.46	0.47	0.23	2.27
	TABS 314	6.5	2.14	2.14	291.34	29.13	0.34	0.17	2.33
	TABS 316	7.6	2.08	2.08	232.37	23.24	0.43	0.22	2.28
HF	TABS 317	6	2.08	2.08	321.88	3.22	3.11	1.55	0.95
	TABS 320	4.5	2.08	2.08	325.38	3.25	3.07	1.54	0.96
	TABS 321	7.3	2.12	2.13	374.74	3.75	2.67	1.33	1.17
	TABS 322	6.6	2.14	2.14	262.89	26.29	0.38	0.19	2.31
	TABS 323	6.9	2.12	2.12	238.66	23.87	0.42	0.21	2.29
	TABS 324	7.9	2.13	2.13	333.27	3.33	3.00	1.50	1.00
HFDHA	TABS 326	5.3	2.12	2.1	306.71	3.07	3.26	1.63	0.87
	TABS 327	5.5	2.1	2.11	530.38	5.30	1.89	0.94	1.56
	TABS 328	5.8	2.09	2.09	430.86	4.31	2.32	1.16	1.34
	TABS 330	7.2	2.08	2.09	360.07	3.60	2.78	1.39	1.11
	TABS 331	7.1	2.13	2.14	266.37	26.64	0.38	0.19	2.31
	TABS 332	6.4	2.13	2.12	212.89	21.29	0.47	0.23	2.27
HFEPA	TABS 333	7.3	2.1	2.11	674.37	6.74	1.48	0.74	1.76
	TABS 334	6.1	2.13	2.13	301.47	3.01	3.32	1.66	0.84
	TABS 335	7.6	2.08	2.08	458.80	4.59	2.18	1.09	1.41
	TABS 337	6.9	2.09	2.08	436.31	4.36	2.29	1.15	1.35
	TABS 338	6.2	2.09	2.1	308.20	3.08	3.24	1.62	0.88
	TABS 340	6.3	2.12	2.13	352.27	3.52	2.84	1.42	1.08

RIN stands for RNA integrity number generated by Agilent for its bioanalyzer. Absorbance ratio (260/280) was obtained using Nanodrop. LFR (mice fed with 2% corn oil); LF (mice fed with 2% corn oil with condensed milk); HF (mice fed with 18% palm oil with condensed milk); HFDHA (mice fed with diet containing docosahexaenoic acid); HFEPA (mice fed with diet containing high fat hypercaloric eicosapentaenoic acid).

Figure 2. 10: Snapshot of the amplification plot of snoRNA-234, endogenous control generated from RT-qPCR

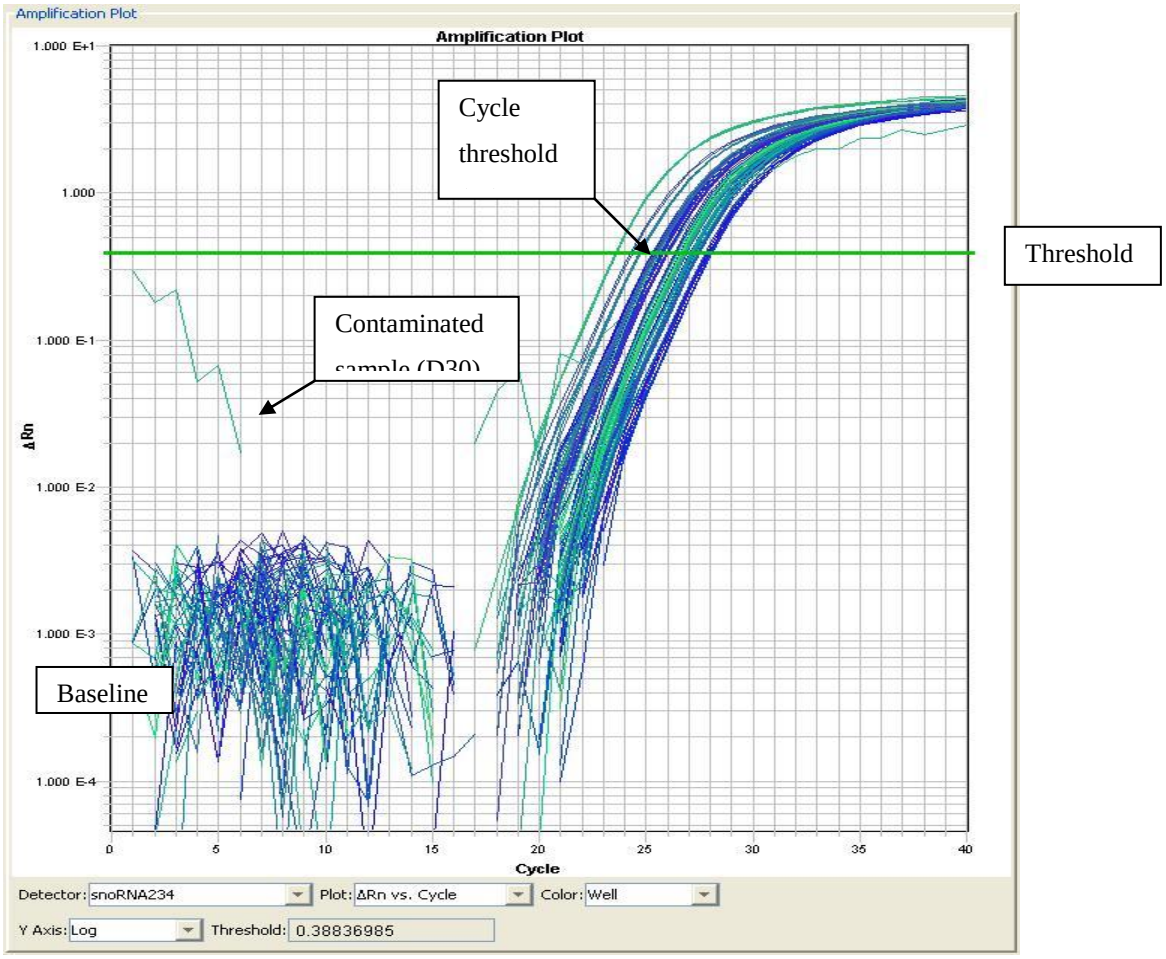

The amplification plot shows the fluorescence signal against cycle number. Baseline of graph shows there's little change in fluorescence in initial cycles of PCR. The fixed threshold is represented by green line parallel to x-axis. Ct values are determined at the exponential phase of the curve whereby the fluorescence signal reaches threshold level.

Chapter 3:

Preliminary study investigating the effects of an obesogenic diet through lipidomics and proteomics

3.1 Introduction

Non-alcoholic steatohepatitis (NASH) refers to the accumulation of fats in the liver with signs of inflammation and fibrosis which may lead to permanent liver scarring also known as cirrhosis (Neuschwander-Tetri 2005; Brunt 2005). Fatty liver can be induced experimentally by suppressing hepatic fatty liver oxidation under excessive fat intake (Cong et al, 2008). Although NASH is a highly prevalent disorder associated with insulin resistance, type 2 diabetes mellitus and obesity (Brunt 2009; Tiniakos et al, 2010; Ferreira et al, 2011), little is known about the effect of dietary fat composition on NASH.

Prospective studies in animals (Yamaguchi et al, 2007) and cells (Reid et al, 2008) showed that the accumulation of triacylglycerols (TAG) in the liver is driven by a high influx of non-esterified fatty acids (NEFA) into the liver. Fatty liver can be induced experimentally by suppressing hepatic fatty liver oxidation under excessive fat and carbohydrate intake. The elevated NEFA concentrations in the liver due to the uncontrollable and continuous stimulation of lipogenesis increases VLDL production (Minehira et al, 2008; Bijland et al, 2010). The inability to secrete VLDL from the liver contributes to hepatic steatosis (Bjorkegren et al, 2002), although there are other mechanisms as well (***Section 1.3***).

The objective of this study was to investigate the effects of a previously described obesogenic diet containing lard on the liver (Samuelsson et al, 2008) and to analyse the lipidomic profiles of fatty liver. Additionally, this study also aimed to undertake liver proteomic analyses comparing controls and obesogenic mice. Differences in liver histology between the controls and obesogenic mice were also compared. It was envisaged that after this study, the model would be used for studying the effects of dietary interventions, such as the modifying effects of low fat and obesogenic diets, EPA and DHA.

3.2 Methods

3.2.1 Animal models and materials

Female C57BL/6J mice were obtained from Charles River, UK and housed singly in raised bottom wired cages. Pelleted diets were obtained from Special Dietary Services. The obesogenic group mice in addition to the obesogenic pellets were allowed *ad libitum* access to full fat condensed milk (Carnation, Nestle). ***Table 3.1*** shows the nutritional composition of the pelleted diets and the condensed milk fed to controls and the obesogenic group. The notation 'obesogenic diet' and 'obesigenic group' will be used in this chapter interchangably, which is the same notation used by the original authors for the same diet.

Table 3. 1: Nutrient composition of diets for controls and obesogenic group mice

	Controls	**Obesogenic group**	
	Low fat chow	**Obesogenic chow**	**Condensed milk***
Protein (g/100 g)	15 (20%)	23 (22%)	8 (10%)
Carbohydrate (g/100 g)	57 (71%)	38 (34%)	55 (67%)
Fat (g/100 g)	3 (9%)	20 (44%)	8 (23%)
Energy (kcal/100 g)	301	414	310

Values in parentheses represent the % energy. Energy contents are calculated using Atwater factors of 4 kcal/g for protein, 3.75 kcal/g for carbohydrate and 9 kcal/g for fat. Lard was used as the test fat. indicates the full fat variety was used.*

3.2.2 Experimental design for pilot study

Female C57BL/6J mice approximately 100 days old were fed either the control or the obesogenic diet. After 6 weeks animals were killed, the liver frozen in liquid nitrogen and stored at -80°C until analysis. There were 10 mice in each group. The animals were caged in groups of five per cage and allowed *ad libitum* access to food and drink. Food intake was not measured. This study was carried out by Samuelsson et al, (2008) and for this thesis archival liver was obtained from the original first and last authors namely Dr. Anne Samuelsson and Dr. Paul Taylor, King's College London.

3.2.3 Analysis of tissue for histology and lipidomics

Histology using H&E stain was carried out on individual liver tissues and scored for steatosis, inflammation and reticulin condensation by Professor Bernard Portmann,

histologist from King's College Hospital. The scoring of liver tissues was carried out single-blindedly.

3.2.4 Lipidomics

Using methods as described in ***Chapter 2***, fatty acids were extracted from liver (Folch et al, 1957) and fractionated into non-esterified fatty acids (NEFA), triacylglycerols (TAG), cholesterol esters (CE) and phospholipids (PL) by solid phase extraction (Kaluzny et al, 1985). C-17 internal standards were added to quantify the fatty acids present in each fraction. All 4 fractions were methylated and loaded onto the gas chromatography to obtain individual fatty acid profile (Lepage & Roy 1986).

3.2.5 Analysis of tissue for proteomics

In this study, 2D-DIGE was used to determine protein expression (up-regulated or down-regulated) in the obesogenic and control group.

Before protein extraction, preliminary preparations involving tissue grinding and homogenization were performed. A sample grinding kit (Ettan, Amersham Biosciences) consisting of tubes with grinding resin and pestles were used to disrupt the liver tissues. Liver tissues were prepared in a planned randomization pattern (control; treated; treated; control) to decrease bias and weighed four at a time to prevent the thawing of tissue which may degrade the protein in the sample. Samples from each group (n=8/group) were pooled in pairs randomly.

The homogenized samples were then quantified using 2D-Quant kit (GE Healthcare) to measure the amount of precipitated proteins and also to ensure that the protein concentrations were within the range of 1-100 µL of protein in 1-100 µL of homogenate. Next, samples were cleaned up using the 2D- Clean up kit and quantified again with the Pierce assay to obtain 50 µg of protein from each sample for labelling.

Before labelling, the pH of the protein after clean-up was tested and the pH was 8.0. Therefore, to increase the alkalinity of the protein, labelling buffer was added to each sample giving a pH of 8.5. After that, 50 µg of each sample was labelled with 400 pmol of dye (Cy2, Cy3 and Cy3). Next the labelled samples were applied to the IPG gel strips for 1^{st} dimension run whereby the proteins migrate along the IPG strips with the electric field and stay at their own pI position with no net charge. After the 1^{st} dimension run, the IPG strips were transferred to the gel glass plates for separation by molecular mass in the 2^{nd} dimension of SDS polyacrylamide gel electrophoresis in the

Ettan DALTtwelve tank set at 1 Watt/gel for 1 hour followed by 17 Watt/gel for 5 hours. A more detailed procedure can be referred to the GE Healthcare protocol.

After scanning the analytical gels (n = 4), preparative gels for spot picking were cast. The proteins of interest selected for picking were matched at Auto Level 1 and were confirmed to have a significant value of $P<0.05$ with Student's T-test and at least ± 1.5 average ratio. The proteins of interest were picked using a robotic Gel Picker (GE healthcare) into a 96 well plate and then sealed for further analysis with LC-MS/MS. The gel plugs in the sealed plate was send to the Cambridge Proteomics Centre (Cambridge, UK) for protein identification using LC-MS/MS.

3.2.6 Statistical analysis

For lipidomics, data were analysed using SPSS version 18.0 by Independent Student's T-test. There were 9 mice in the control group and 10 mice in the obesogenic group. In histology, Chi-squared test was used to compare the differences in the frequency of certain distributions. For proteomics, Student's t-test was carried out using DeCyder between the controls and the obesogenic group. Significance was indicated when P value was equal to or less than 0.05.

3.3 Results

3.3.1 Histopathology

The staining of liver sections from the controls and obesogenic mice using hematoxylin and eosin are presented in ***Figure 3.1*** and the histological findings for the livers are presented in ***Table 3.2***. A greater number of mice with liver steatosis and reticulin condensation were found in the obesoegnic group with P<0.001 and P=0.002 respectively. Five out of 10 mice from the obesogenic group showed signs of steatosis at the top end of the scores compared to the controls where the majority of the mice livers were graded at the lower end of the scores. None of the mice from the control group showed signs of reticulin condensation compared to 70% of mice from the obesogenic group, which developed level 1 condensation in the reticulin. Furthermore, 30% of mice in the obesogenic group developed inflammation at level 2 compared to none in the controls. Overall, it appeared that histological conditions of non-alcoholic fatty liver disease were more severe in the obesogenic group in comparison to the controls.

3.3.2 Fatty acid concentrations and composition of hepatic non-esterified fatty acids

The accumulation of stearic acid (16:0) in the obesogenic group was significantly lower when compared with the controls (P<0.001) as shown in ***Table 3.3.*** Stearic acid was highest in the controls with 45% of the total NEFA fatty acids. Fatty acid composition of oleic acid (18:1n-9) contributed the highest proportion of monounsaturated fats (MUFA) in the obesogenic mice group (42%) and was significantly higher than controls (P<0.001). The proportion of linoleic acid (18:2n-6) was significantly higher (P=0.048) in the obesogenic group compared to the controls and there was no statistical significance in linolenic acid (18:3n-3). AA (20:4n-6) levels were significantly higher (P=0.011) in the obesogenic group when compared with the controls. In addition, EPA (20:5n-3) was significantly lower (P<0.001) in the obesogenic group (0.1%) compared to the controls (0.5%). In contrast, DHA was significantly higher in mice from the obesogenic group (2%) compared to controls with 0.8% (P=0.001). Besides that, adrenic acid (22:4n-6) was significantly lower in obesogenic mice compared with the controls (P=0.028). The total concentration (mg/g) of hepatic NEFA showed a significant increase in the obesogenic group compared to the controls (P<0.001).

3.3.3 Fatty acid concentrations and composition of hepatic triacylglycerols

The proportion of hepatic palmitic acid in obesogenic mice (29%) was significantly lower than the controls (26%; P<0.001) as shown in ***Table 3.4.*** Similar to NEFA fractions, the proportion of stearic acid in the obesogenic mice were half the proportion in the controls (P<0.001). Oleic acid showed the highest proportion in hepatic TAG concentrations and was significantly higher in the obesogenic (45%) group when compared with the controls (30%). Linoleic acid was significantly lower in obesogenic mice when compared to the controls with 11% and 14%, respectively (P=0.010). In addition, the proportion of linolenic acid was lower in obesogenic mice compared with the controls (P=0.033). Levels of EPA were significantly lower in obesogenic mice compared to the controls (P<0.001). In contrast, DHA was highest in obesogenic group with 3% followed by 1% in controls (P<0.001). AHA levels were 3 times lower in obesogenic group compared to controls (P<0.001). These findings were similar to NEFA composition. In concentrations terms, obesogenic mice accumulated the highest (52 mg/g) hepatic TAG when compared with 8 mg/g in controls.

3.3.4 Fatty acid concentrations and composition of hepatic cholesteryl esters

As seen in ***Table 3.5***, cholesteryl palmitate and palmitoleate were similar in both controls and obesogenic groups. However, cholesteryl stearate in controls accounted for a 2-fold increase in proportion to that found in the obesogenic group with significance at P<0.001. Cholesteryl oleate showed a 30% increase in the obesogenic mice group when compared with the controls. There was proportionately less cholesterol linoleate (18:2n-6) in animals fed with obesogenic diet when compared to controls (P<0.001). Both groups have similar proportions of AA (20:4n-6) derived from cholesterol linoleate (18:2n-6) which did not differ significantly. However, both controls and obesogenic groups have similar proportions of DHA. Similar to findings in NEFA and TAG concentrations, the obesogenic mice accumulated more fats when compared with the controls (P<0.001) (***Table 3.5***).

3.3.5 Fatty acid concentrations and composition of hepatic phospholipids

The data in ***Table 3.6*** shows that the proportion of palmitic acid (16:0) was significantly lower in obesogenic mice when compared to the controls (P<0.001). However, the proportion of palmitoleic acid was similar in both groups. In the obesogenic group, the proportion of stearic acid was 40% lower than the control group

(P<0.001). Oleic acid was significantly higher in the obesogenic group (8%) when compared with controls (6%: P=0.019). Obesogenic mice showed linoleic acid with a mean proportion of 6% and is significantly higher compared with controls (4%; P=0.010). In contrast, linolenic acid was higher in the obesogenic group (0.9%) when compared to 2.2% in the controls (P=0.002). As for the composition of AA (20:4n-6), obesogenic mice showed significantly higher levels by 2-fold in comparison to controls. EPA was similar in both groups but DHA was significantly higher in the obesogenic group (19%) when compared to the controls with 3.5% (P<0.001). In contrast to the findings in NEFA, TAG and CE fractions, PL concentrations expressed in mg/g was lower in the obesogenic mice when compared to the controls with P=0.001.

3.3.6 Protein expression in obesogenic mice using 2D-DIGE

A total of 2061 matching protein spots were detected on the master gel interfaces (n=4 gels) and 201 proteins were differentially expressed. Out of the 201 proteins, 18 proteins were confirmed to have a significant value of P<0.05 with Student's T-test and at least a 1.5 fold change (***Figure 3.2***). Of the 18 proteins, 5 were up-regulated and 13 were down-regulated (***Table 3.7***). Twelve of the 18 significantly expressed proteins were identified using LC-MS/MS. These 12 proteins were picked on the basis of high abundance and 3D peaks that were not overlapping (***Figure 3.3***) with significant difference of P<0.05 and average ratio of at least $\geq \pm 1.5$. The other 3 proteins with protein ID numbered 1563, 1845 and 1854 were selected for reference to confirm the results obtained from LC-MS/MS. These 3 proteins were picked by referring to the reference gel on SWISS 2D-PAGE. In total, 15 proteins were selected for identification with LC-MS/MS (***Figure 3.4***).

As shown in ***Table 3.8***, data revealed 5 Type II keratin subunit proteins and 10 other known proteins. However, there were no matches when comparing the results obtained from LC-MS/MS with the tentative protein spots identified by matching the preparative gel with the reference gel on SWISS 2D-PAGE. There are multiple reasons to why the proteins were not matched, one of which may be an error occurring during spot picking, whereby protein spots of interest were missed-picked by the robot. Furthermore, contamination by human keratin during gel handling would have caused apparent, ie, artificial changes in keratin abundance, whilst murine keratin contamination would have arisen from ongoing laboratory projects. Undoubtedly, one assumes that LC-MS/MS is the gold standard.

There are 6 categories of intermediate filament and Type 1 and Type 2 keratin subunit proteins are the most diverse, comprising of acidic and basic proteins respectively. Type II keratins are the basic counterpart of Type I keratins and Type II keratins bind to form acidic and basic heterodimers to make a keratin filament (Stewart 1990). Results from LC-MS/MS showed that keratin 4, 10, 6A, 73 and 75 were identified together with glutathione s-transferase omega 1 (GSTO1), quinoid dihydropteridine reductase (QDPR) and sepiapterin reductase (SPR). All proteins expressed differentially were up-regulated except for keratins type II and 6A, GSTO1 and QDPR which were down-regulated.

The abundance of keratin protein was of particular concern, especially as they were not identified in subsequent studies (***Chapter 7***). The failure to see changes in keratin in response to hypercaloric feeding in subsequent studies may have been due to a greater familiarisation of analytical techniques and the application of more refined methodology. Furthermore, we determined whether the keratins identified by LC-MS/MS would actually appear in the gels. However, there was marked discordance in the location of the keratins as identified by LC-MS/MS vs those located using the SWISSprot database. For example spot number 1812 had a pI of 4.72 and a molecular weight of 18.7 kDa by SWISSprot analyses. However, by LC-MS/MS the same spot number had a pI of 8.97 and a molecular weight of 66 kDa.

In summary, the analytical components of the data appeared to be marked by contamination.

3.3.7 Study limitations

This study was based on archival material and thus, there were no access to information on the liver weights of all the mice. Although, the composition of the condensed milk intake can be obtained there were no information on the amount ingested. Similarly, there was no information on the intakes of the pelleted diets. The lack of data on liver weights and dietary intakes limit the interpretation of the investigation.

Figure 3. 1: Hematoxylin and eosin staining of liver sections from mice fed either standard chow (top) or an obesogenic diet (bottom)

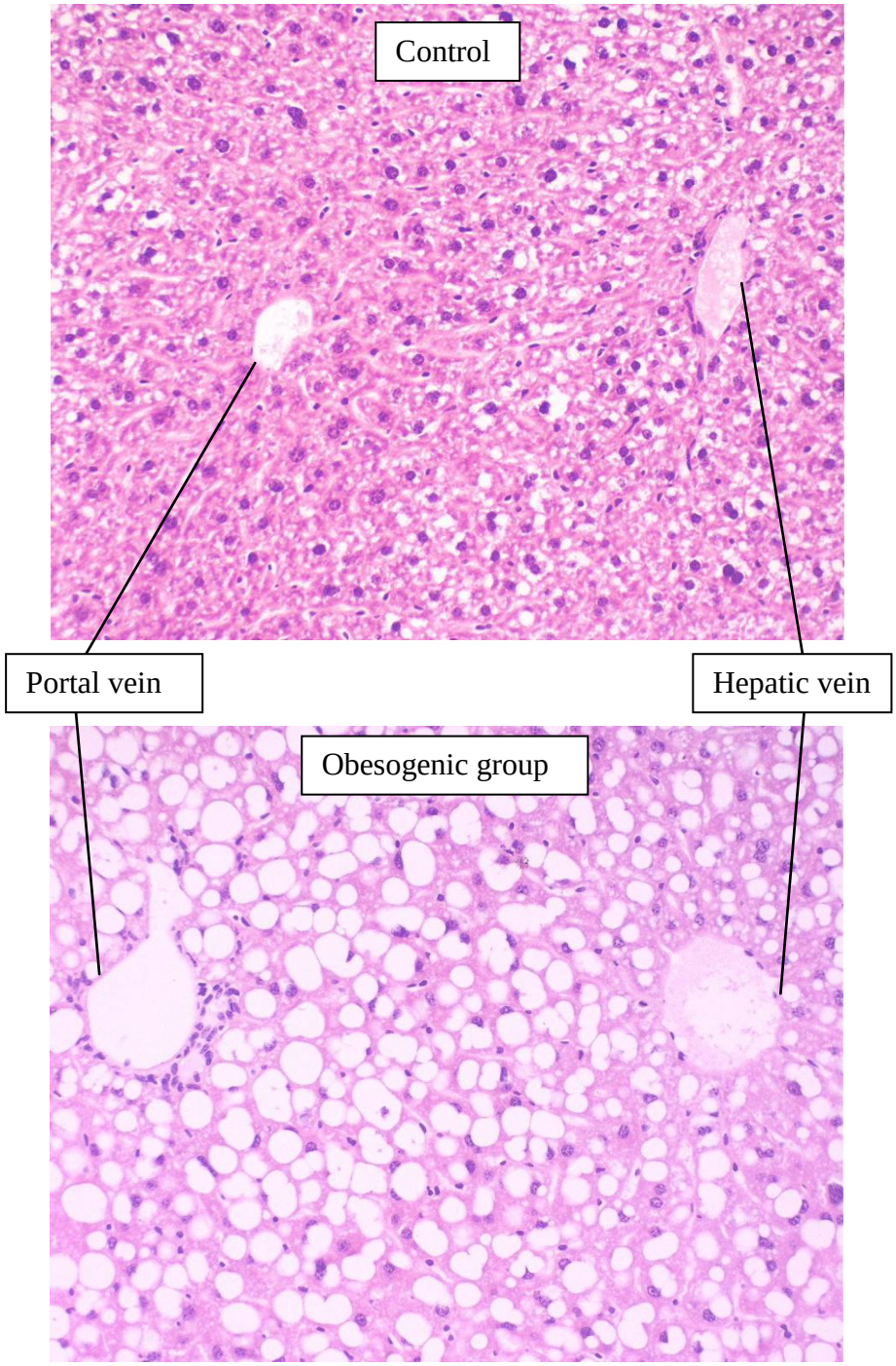

Representative micrograph shows the portal vein also known as Zone 1 is where the supply of oxygenated blood from hepatic arteries is highest. The hepatic vein represents Zone 3 where the oxygenation is poor. The white spaces between the cells represent the amount of fats in the liver.

Table 3. 2: Histopathology scores for steatosis, inflammation, ballooning and reticulin condensation of mice fed standard chow or an obesogenic diet

		Steatosis [a]					P value
		0	1	2	3	4	
Control (n=9)	Count	4	4	1	0	0	P<0.001
	% within group	44%	44%	11%	0%	0%	
Obesogenic (n=10)	Count	0	0	1	4	5	
	% within group	0%	0%	10%	40%	50%	

		Inflammation [b]					P value
		0	1	2	3	4	
Control (n=9)	Count	1	8	0	0	0	P=0.111
	% within group	11%	89%	0%	0%	0%	
Obesogenic (n=10)	Count	0	7	3	0	0	
	% within group	0%	70%	30%	0%	0%	

		Ballooning [c]					P value
		0	1	2	3	4	
Control (n=9)	Count	2	7	0	0	0	P=0.082
	% within group	22%	78%	0%	0%	0%	
Obesogenic (n=10)	Count	2	5	3	0	0%	
	% within group	20%	50%	30%	0%	0%	

		Reticulin condensation [d]					P value
		0	1	2	3	4	
Control (n=9)	Count	9	0	0	0	0	P=0.002
	% within group	100%	0%	0%	0%	0%	
Obesogenic (n=10)	Count	3	7	0	0	0	
	% within group	30%	70%	0%	0%	0%	

Values are expressed in counts and percentages. Chi-square test was used for statistical analysis between groups. The liver scores from 0 to 4 indicate:

a Steatosis: 0 = absent or occasional vacuoles; 1 = 5-25%; 2 = 25-50%; 3 = 50-75%

b Inflammation- 0 = absent; 1 = occasional cells; 2 = sparse cells; 3 = frequent cells

c Ballooning: 0 = absent; 1 = occasional cells; 2 = sparse cells; 3 = frequent cells

d Reticulin condensation: 0 = absent; 3 = present

Table 3. 3: Total fatty acid concentrations (mg/g) of hepatic non-esterified fatty acids (NEFA) of C57BL/6J female mice fed either standard chow or an obesogenic diet

NEFA fatty acids (weight %)	Controls (n=9)	Obesogenic (n=10)	P Values
16:0	29.3 ± 9.9	26.3 ± 1.0	P=0.347
16:1	4.7 ± 7.6	3.4 ± 0.6	P=0.615
18:0	44.9 ± 9.2	12.0 ± 2.6	P<0.001
18:1n-9	9.8 ± 5.0	42.2 ± 3.2	P<0.001
18:2n-6	7.0 ± 4.2	10.1 ± 1.8	P=0.048
18:3n-3	0.5 ± 0.3	0.5 ± 0.1	P=0.735
20:3n-6	0.4 ± 0.2	0.3 ± 0.1	P=0.395
20:4n-6	1.1 ± 0.9	2.0 ± 0.3	P=0.011
20:5n-3	0.5 ± 0.3	0.1 ± 0.1	P<0.001
22:4n-6	0.6 ± 0.5	0.2 ± 0.1	P=0.028
22:5n-6	0.3 ± 0.2	0.4 ± 0.2	P=0.204
22:5n-3	0.2 ± 0.2	0.3 ± 0.2	P=0.106
22:6n-3	0.8 ± 0.8	2.1 ± 0.6	P=0.001
mg/g	5.5 ± 1.8	13.7 ± 3.1	P<0.001

Values are expressed as mean ± standard deviation. Student's T-test was used; P values <0.05 indicates significant difference when compared to the controls

Table 3. 4: Total fatty acid concentrations (mg/g) and individual fatty acid composition (weight %) of hepatic triacylglycerols (TAG) of C57BL/6J female mice fed either standard chow or an obesogenic diet

TAG fatty acids (weight %)	Controls (n=9)	Obesogenic (n=10)	P Values
16:0	29.1 ± 1.1	25.5 ± 1.0	P<0.001
16:1	3.8 ± 0.3	3.8 ± 0.6	P=0.889
18:0	13.7 ± 3.6	7.3 ± 1.3	P<0.001
18:1n-9	30.4 ± 4.0	44.8 ± 3.2	P<0.001
18:2n-6	13.7 ± 2.3	10.8 ± 2.0	P=0.010
18:3n-3	0.8 ± 0.2	0.6 ± 0.1	P=0.033
20:3n-6	1.7 ± 1.9	0.4 ± 0.1	P=0.045
20:4n-6	1.9 ± 0.7	2.6 ± 0.3	P=0.005
20:5n-3	1.1 ± 0.7	0.1 ± 0.1	P<0.001
22:4n-6	1.7 ± 0.9	0.3 ± 0.2	P<0.001
22:5n-6	0.9 ± 0.5	0.5 ± 0.2	P=0.031
22:5n-3	0.3 ± 0.2	0.3 ± 0.2	P=0.591
22:6n-3	0.9 ± 0.4	3.0 ± 0.7	P<0.001
mg/g	8.1 ± 2.4	51.7 ± 21.9	P<0.001

Values are expressed as mean ± standard deviation. Student's T-test was used; P values <0.05 indicates significant difference when compared to the controls

Table 3. 5: Total fatty acid concentrations (mg/g) and individual fatty acid composition (weight %) of cholesterol esters (CE) of C57BL/6J female mice fed either standard chow or an obesogenic diet

CE fatty acids (weight %)	Controls (n=9)	Obesogenic (n=10)	P Values
16:0	27.0 ± 1.4	26.3 ± 3.3	P=0.535
16:1	4.0 ± 0.4	4.4 ± 1.5	P=0.456
18:0	8.3 ± 2.3	4.2 ± 1.4	P<0.001
18:1n-9	38.0 ± 2.4	49.5 ± 4.0	P<0.001
18:2n-6	17.1 ± 1.5	10.2 ± 4.1	P<0.001
18:3n-3	0.5 ± 0.5	0.6 ± 0.2	P=0.739
20:3n-6	0.1 ± 0.3	0.3 ± 0.1	P=0.037
20:4n-6	2.3 ± 1.8	1.6 ± 0.6	P=0.272
20:5n-3	0.0 ± 0.0	0.1 ± 0.0	P<0.001
22:4n-6	0.8 ± 0.6	0.3 ± 0.2	P=0.021
22:5n-6	0.5 ± 0.4	0.4 ± 0.2	P=0.763
22:5n-3	0.2 ± 0.2	0.3 ± 0.2	P=0.774
22:6n-3	1.1 ± 0.6	1.9 ± 0.9	P=0.054
mg/g	3.3 ± 1.4	24.2 ± 9.7	P<0.001

Values are expressed as mean ± standard deviation. Student's T-test was used; P values <0.05 indicates significant difference when compared to the controls

Table 3. 6: Total fatty acid concentrations (mg/g) and individual fatty acid composition (weight %) of hepatic phospholipids (PL) of C57BL/6J female mice fed either standard chow or an obesogenic diet

PL fatty acids (weight %)	Controls (n=9)	Obesogenic (n=10)	P Values
16:0	40.8 ± 7.8	27.0 ± 2.3	P<0.001
16:1	0.6 ± 0.7	1.0 ± 0.5	P=0.189
18:0	33.5 ± 6.1	19.8 ± 2.7	P<0.001
18:1n-9	6.1 ± 1.0	8.4 ± 2.4	P=0.019
18:2n-6	3.7 ± 2.0	5.7 ± 0.8	P=0.010
18:3n-3	2.2 ± 1.1	0.9 ± 0.2	P=0.002
20:3n-6	0.4 ± 0.5	0.4 ± 0.4	P=0.701
20:4n-6	6.1 ± 5.5	14.8 ± 5.4	P=0.003
20:5n-3	0.2 ± 0.2	0.2 ± 0.3	P=0.888
22:4n-6	1.2 ± 0.6	0.4 ± 0.1	P=0.001
22:5n-6	1.5 ± 0.8	2.0 ± 0.8	P=0.233
22:5n-3	0.3 ± 0.6	0.4 ± 0.1	P=0.658
22:6n-3	3.5 ± 3.8	19.0 ± 1.1	P<0.001
mg/g	27.5 ± 13.3	10.8 ± 2.3	P=0.001

Values are expressed as mean ± standard deviation. Student's T-test was used; P values <0.05 indicates significant difference when compared to the controls

Figure 3. 2: Flow chart of the selection of differential proteins in 2D-DIGE

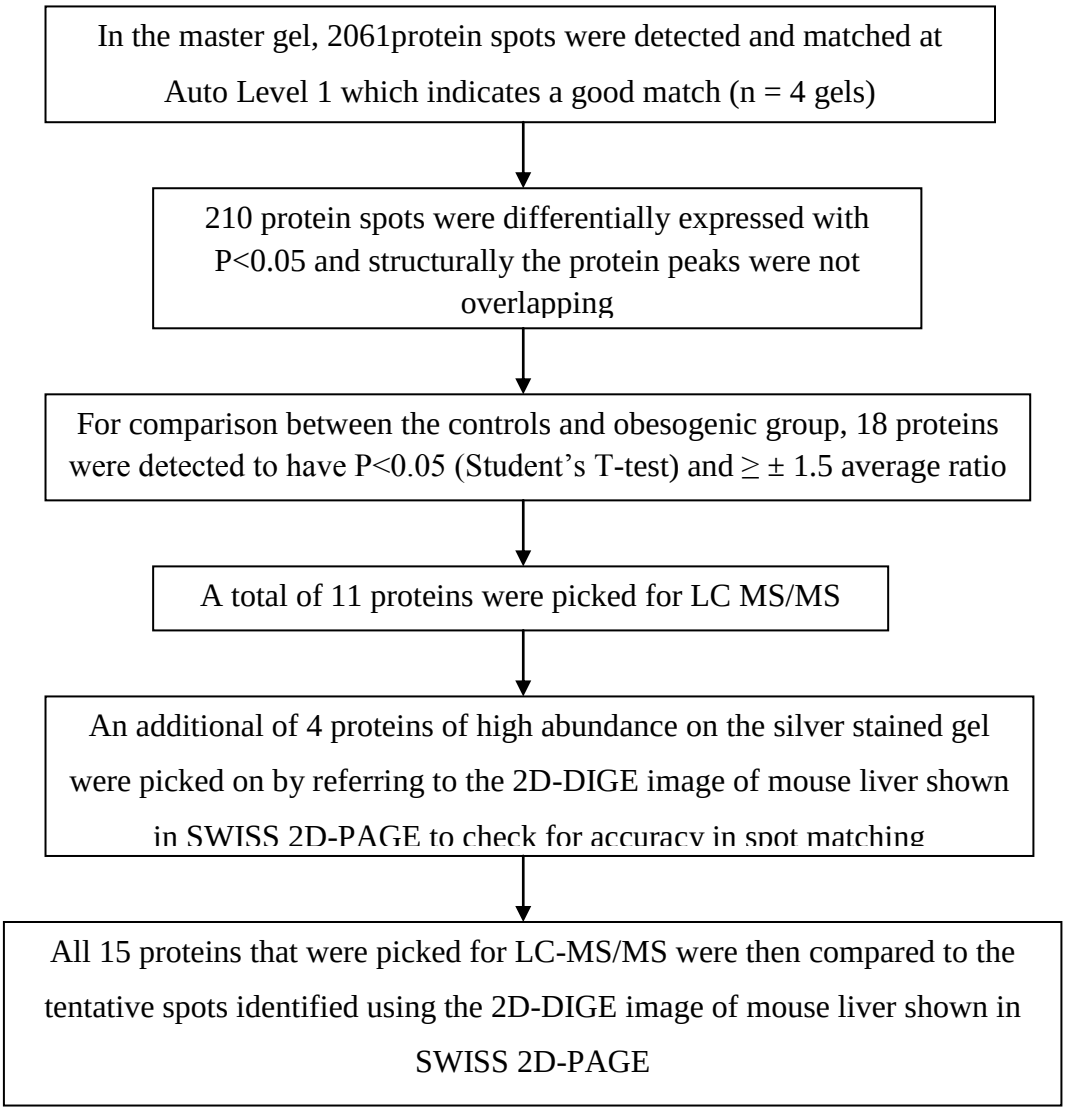

Figure 3. 3: 3-D representative images of proteins of interest which were differentially expressed in mice fed control or obesogenic diets

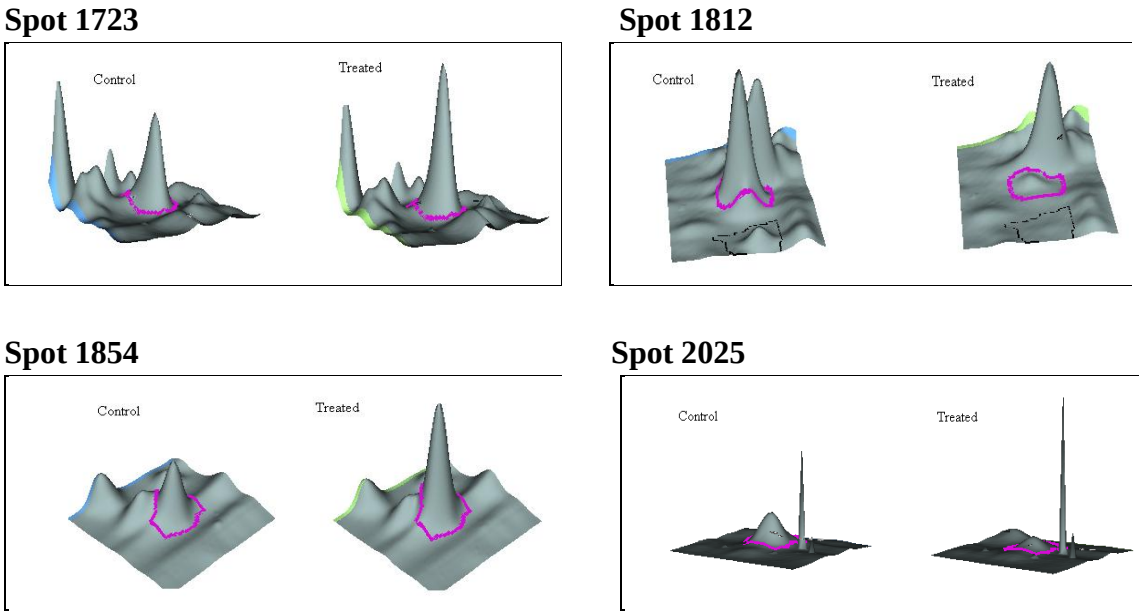

Images were generated by DeCyder version 6.5 and location of the spots on the gels is indicated by the purple ring around the peak. Within the box, the left peak image represents spots from control mice and the right represents the obesogenic mice.

Figure 3. 4: Protein spot map with contour lines and annotations on the proteins to be picked

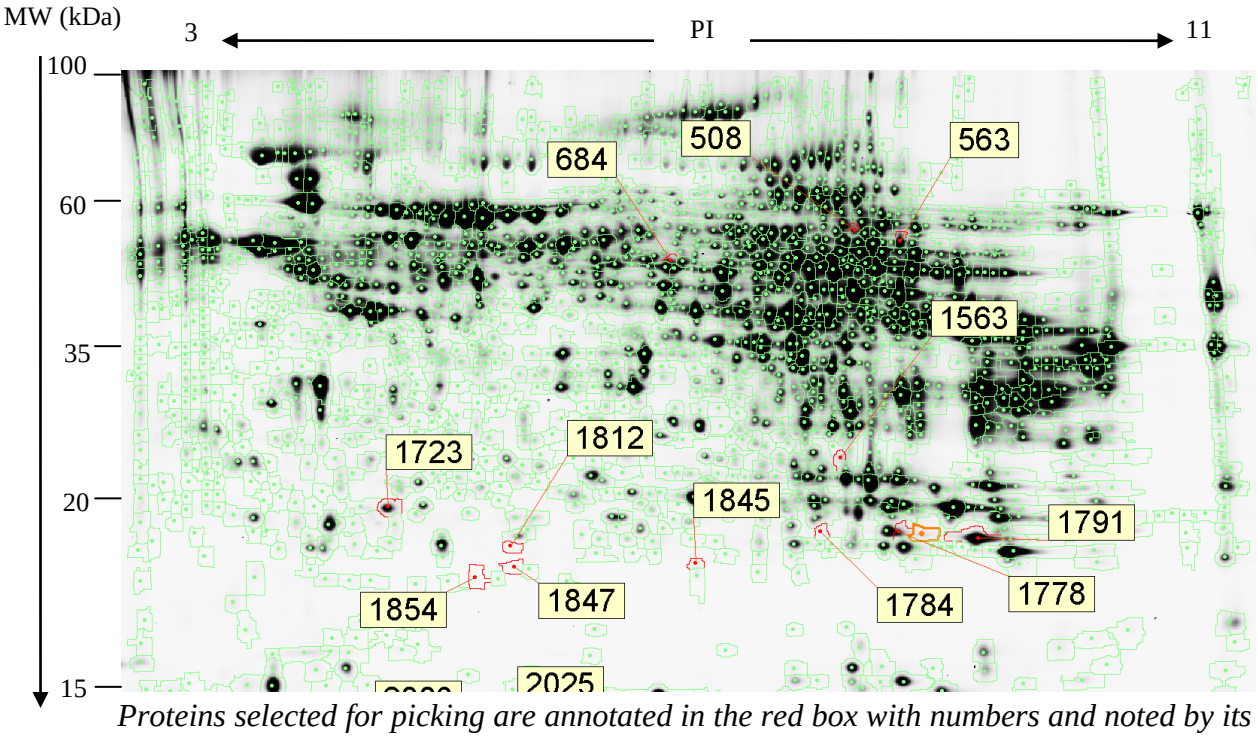

Proteins selected for picking are annotated in the red box with numbers and noted by its contour line around the spot. Spot 1993, 1003 and 2025 were partially or wholly cropped out of the gel due to unknown circumstances. Gel images were clear on screen and were used to compare with the reference gel on SWISS 2D-PAGE. All protein spots were confirmed to have a significant value of $P<0.05$ with Student's T-test and at least ± 1.5 average ratio except for

Table 3. 7: Proteins identified to be differentially expressed with statistical significance using Decyder when comparing controls with obesogenic mice

Spot ID	Swisprot			Protein identification	Controls vs Obesogenic	
	Accession number	pI	MW		P-Value	Average ratio
35	NF	NF	NF	NF	0.040	-1.81
508	P24270	7.72	59664	Catalase	0.026	1.57
563	P24549	7.91	54337	Retinal dehydrogenase	0.001	1.81
684	P11679	5.70	54434	Keratin, type II cytoskeletal 8	0.001	-1.84
1012	NF	NF	NF	NF	0.039	-2.09
1205	Q64374	5.16	33407	Regucalcin	0.022	-1.6
1566	NF	NF	NF	NF	0.026	-1.56
1645	NF	NF	NF	NF	0.021	-4.4
1723	NF	NF	NF	NF	0.007	1.59
1778	P11352	6.74	22179	Glutathione peroxidise 1	0.025	-1.52
1781	NF	NF	NF	NF	0.003	-1.83
1784	O08079	6.26	26252	Peroxiredoxin	0.037	-2.14
1791	P19157	8.13	23478	Glutathione S-transferase P1	0.010	-1.9
1812	P02762	4.72	18696	Major urinary protein 6	0.002	-4.75
1847	P11589	4.86	18710	Major urinary protein 2	0.038	-2.22
1993	P97450	5.40	8945	ATP synthase-coupling factor 6, mitochondrial	0.003	1.53
2003	P10639	4.80	11544	Thioredoxin	0.015	2.02
2025	P12787	5.01	12436	Cytchrome C oxidase	0.009	-2.08

Statistical test was carried out using Student's T-test. P-value with <0.05 indicates a significant difference between the groups. Average ratios with negative values indicate down-regulation of the protein in the experimental group and vice-versa.'NF' indicates that the protein spots were not found and, thus not matched to the reference gel on SWISS 2D-PAGE. The values for pI and MW were obtained from EXPASY.

Table 3. 8: The comparison between protein identification by LC-MS/MS

Protein ID	Accession number	Protein name	pI	MW (Da)	Protein score	% Coverage
508	P02535	**Keratin 10 (Type I)** *	4.91	52824	480	13.5
563	P04104	**Type II keratin subunit protein** *	8.97	65696	103	3.8
684	P04104	**Type II keratin subunit protein***	8.97	65696	207	3.8
1563	P04104	**Type II keratin subunit protein**	8.97	65696	143	3.7
1723	Q6NXH9	**Keratin 73***	8.36	59502	131	4.3
1778	Q3TTY5	**Keratin 2 epidermis***	8.23	71447	179	5.0
1784	O09131	**Glutathione S-transferase omega 1**	6.92	27708	333	39.6
1791	Q8BVI4	**Quinoid dihydropteridine reductase***	7.67	25782	389	33.6
1812	P04104	**Type II keratin subunit protein***	8.97	65696	282	5.7
1845	Q6NXH9	**Keratin 73**	8.36	59502	171	4.3
1847	P04104	**Type II keratin subunit protein***	8.97	65696	225	5.7
1854	Q8BGZ7	**Keratin type II cytoskeletal 75**	5.01	57978	167	5.4
1993	Q91XH5	**Sepiapterin reductase***	5.58	28208	199	23.0
2003	P07744	**Keratin 4***	9.08	44725	133	8.0
2025	P50446	**Keratin 6A***	8.04	59641	326	8.3

*All of the proteins identified were differentially expressed by at least 50% in the obesogenic group compared with the controls except for 1563, 1784, 1845 and 1854. These 4 proteins were identified to show the relevance of spot matching with the reference gel on SWISS 2D-PAGE. 'NF'indicates that the protein spots were not found and, thus not matched to the reference gel on SWISS 2D-PAGE. * indicates the proteins that were altered in the comparison of LFR vs LF or LFR vs HF groups. Protein score indicates how well the matching regions of polypeptides clusters are matched whereas the % coverage indicates how each of the polypeptides clusters match the protein. Proteins with the highest scores and % coverage were selected*

.

3.4 Discussion

3.4.1 Methodological considerations

Liver samples were obtained from those female mice used by Samuelsson et al, (2008) to develop methodological skills for lipidomics and proteomics. In the aforementioned study, the female mice were fed a palatable obesogenic diet (16% lard,

33% sugar), were hyperphagic and showed heavier body weights compared to the controls fed standard chow (3% fat, 7% sugar). The obesogenic mice also showed signs of hypertension, cardiovascular and metabolic dysfunction, loss of skeletal muscle mass, increased fasting insulin and elevated plasma glucose (Samuelsson et al, 2008). However, no data was obtained for either whole liver weight or food intakes.

For future studies in this thesis, it was proposed to obtain whole liver weight for the calculation of total lipids in the liver. The palatability of the semi-synthetic pelleted diets and milk intake will also be tested to ensure that the mice develop consistent growth patterns throughout the study (***Chapter 4***). The consumption of pellet and milk intakes will also be weighed for determining the energy intakes of each mouse caged individually and to measure the amount of fats ingested.

3.4.2 Lipid profile of obesogenic fed mice in comparison to controls and its histology

The overall lipid profile of non-esterified fatty acids (NEFA), triacylglycerols (TAG) and cholesterol esters (CE) in the obesogenic group showed a significant increase in the levels of fatty acids when compared with the controls with $P<0.05$ and this was also observed in the liver histology. Although mice in obesogenic group did not develop severe NASH, obesogenic diet markedly increased hepatic lipid accumulation mainly in NEFA, TAG and CE fractions. The TAG fraction showed a 6-fold increase with increases in oleic acid, arachidonic acid (AA) and docosahexaenoic acid (DHA) which was similar to the fatty acid profile in the NEFA fraction. There was a 7-fold increase in cholesterol esters with major increases in cholesteryl oleate, cholesteryl palmitate and cholesteryl linoleate. In the phospholipid fraction of the liver, there were large increases in the proportion of DHA and AA in the obesogenic group which may imply that there was increased synthesis of these fatty acids from linolenic and linoleic acids, respectively. The increased proportion of these long-chain polyunsaturated fatty acids may render the liver more prone to damage and metabolic disruption because of their higher susceptibility to oxidation (Hostetler et al, 2006).

Histological examination of the livers revealed that in the obesogenic mice there were features of mild steatosis but not severe non-alcoholic steatohepatitis (NASH). Notably, there was increased granularity of the hepatocyte cytoplasm with coarse amphophilic bodies resembling small Mallory bodies. Ninety percent of the mice from the obesogenic group presented signs of steatosis at the upper end of the scores

indicative of progression to steatohepatitis. These features were absent in the control animals.

3.4.3 Differential protein expression in mice fed obesogenic diets compared with controls identified by LC-MS/MS

Keratins are cytoskeletal proteins expressed in epithelial cells that represent the major subgroup of all intermediate filament proteins which are expressed as either type I or type II intermediate filament proteins (Moll et al, 1982). The functions of keratins are to modulate mechanical cell strength, cell signalling, cell differentiation and apoptosis (Kirfel et al, 2003; Snider et al, 2011). Alterations; both up- and down-regulation of keratins are commonly found in hepatocytes with ballooning, Mallory bodies and inflammation (Ludwig et al, 1980; Brunt 2004). The ballooned hepatocytes containing Mallory bodies are characteristics of NASH (Zatloukal et al, 2004), thus suggesting that keratin may influence or reflect the levels of inflammation and oxidative stress caused by obesogenic feeding.

However for this PhD, there was substantial contamination of the sample with keratins. The data in ***Table 3.7*** are probably invalid.

Quinoid dihydropteridine reductase (QDPR) is related to ferric reductase activity and at the mRNA level, QDPR is found to be up-regulated in liver during iron deficient growth conditions and down-regulated in condition when iron is excessive (Lee et al, 2000). In the aforementioned study, pigs were used as experimental animals and no studies on hepatic dysfunction related to QDPR have been carried out in mice. In this study for the thesis, using a mouse model, QDPR was 90% down-regulated in the obesogenic group when compared with the controls.

In future work, it is proposed that a comprehensive analysis of the proteins expressed in the liver will be carried out and the causal factors for the mismatch between the SWISS 2D-PAGE reference gel and LC-MS/MS will be determined. Further, technical development in this method will be improvised in order to pick proteins that are specifically related to liver diseases induced by dietary fats.

Chapter 4:

Methodological development and optimization of animal feed to develop hypercaloric fed mice

4.1 Experiment 1: Introduction

Animals have a preference for hypercaloric foods as a natural behaviour for the regulation of body temperature and energy storage, thus consuming more calories than needed (Takeda et al, 2001). The palatability of such diets is dependent on factors such as flavour (Ishii et al, 2003; Forestell & LoLordo 2003) and texture (Kadohisa et al, 2005). In a previous study by Samuelsson et al, (2008), mice were fed with a hypercaloric diet (average 16% fat, 33% sugar) comprising of both the pellets and condensed milk. The controls were fed standard chow containing on average 3% fat and 7% sugar, which included the pellets without the condensed milk. ***Table 3.1*** shows the break-down of both the fat and sugar energy composition derived from the pellet and milk. The condensed milk was provided to the mice in a jar for easy consumption. It was also highly palatable.

The obesogenic diet was fed to maternal mice in one study as a novel model for developmental programming to investigate metabolic and cardiovascular function on the offspring (Samuelsson et al, 2008). The aforementioned study reported that the maternal mice fed on the obesogenic diet were hyperphagic, increased their body weights and abdominal fat pads. These maternal mice also developed hypertension and endothelial dysfunction. Consequently, the offsprings exposed to the influence of maternal programming developed similar problems as the dams (Samuelsson et al, 2008). The livers of these maternal mice were used in the preliminary study as described in ***Chapter 3***. The term obesogenic is used in the study by Samuelsson et al, (2008) to differentiate the hypercaloric groups subsequently used for the thesis (***Chapters 5, 11***). In fact, both the obesogenic and hypercaloric diets are similar except for the different types of fats used, namely lard and palm oil, respectively.

In ***Chapter 3***, we showed that the obesogenic diet used by Samuelsson et al, (2008) caused liver inflammation and mild steatosis in mice compared to the controls. Unfortunately, we were unable to calculate the energy intake of the mice and the composition of fat intakes derived from the obesogenic and control diets. Therefore, to obtain a more accurate measure of energy and fat intakes of mice fed obesogenic diets, we prepared our own hypercaloric semi-synthetic pelleted diets prepared in the food laboratory and then measured the energy intake derived from the pellets and condensed milk separately. We hypothesised that the mice would consume equal amounts of pelleted diets and condensed milk as measured over one week.

4.1.1 Animal models and materials

28 days old juvenile male C57BL/6J mice were obtained from Charles River, UK and house in Utemp1284 standard cages (Techniplast, UK) enriched with nesting materials such as paper strips, a cardboard roll and wood shavings. The nesting materials were necessary for activity (van de Weerd et al., 1997) and environmental enrichment (Olsson & Dahlborn 2002). The platform of the cage was layered with wood chips. Light condensed milk incorporated with 8% (w/w) palm oil was contained in jars. A detailed list of materials is contained in ***Chapter 2***.

4.1.2 Methods

A total of 8 mice were divided into 2 groups (ie, n = 4 per group) and mice were fed on either the standard chow or 18% (w/w) palm oil pellets plus condensed milk enriched with 8% (w/w) palm oil. Mice fed with the palm oil plus condensed milk diet were called the hypercaloric group and mice fed on the standard chow were the controls. Mice were acclimatized for 3 days on standard chow followed by one week of feeding with either hypercaloric pellets plus condensed milk or standard chow. Diets used for these studies are described in ***Table 2.1 and***. ***2.2.*** The ears of the mice were crimped for identification when measuring individual food intake.

Mice were weighed and randomized into 2 cages to either the control or hypercaloric group. All diets and water were fed *ad libitum*. The nutrient compositions of the semi-synthetic pelleted diet and condensed milk incorporated with palm oil are presented in ***Table 2.1 and 2.2***. Body weights, food and condensed milk intake of mice were weighed daily for 7 days. The moisture absorbance of pellet and condensed milk was also tested. Mice were fasted overnight before culling. Liver and fat pads were collected and snap frozen in liquid nitrogen. Weights of soleus, plantaris and gastrocnemius muscles were recorded.

4.1.3 Results

During the acclimatization period, body weights and feed intake of mice were recorded. It was observed that there was moderate contamination of the condensed milk with wood chips which made the measurement of the food intake laborious. There was no overt change in weight (ie, an indication of hydration) of the food pellets or condensed milk when left for 24 hours (data not presented for brevity).

Figure 4.1 showed that mice from both groups gained body weight gradually throughout when fed on the control and hypercaloric diets. Mice fed the hypercaloric diet showed similar body weights when compared to the controls. There were no significant difference in weights of liver, adipose tissue and the total hind limb muscles (***Table 4.1***). The total weights of hind limb muscles included soleus, plantaris and gastrocnemius muscles.

The energy intakes of mice in the hypercaloric group were mainly derived from condensed milk (***Table 4.2***). The calculated total energy intake in mice fed the control and hypercaloric diet was relatively comparable (***Figure 4.2).*** The mean energy intake of the hypercaloric group was 58 kcal/week compared to 41 kcal/week in the control group (***Figure 4.3***). Mice in the hypercaloric group consumed a significantly higher proportion of the total condensed milk compared to the pellets (***Figure 4.4***).

Figure 4. 1: Mean body weights of mice fed either a control or a hypercaloric diet from acclimatization period to feeding and fasted state

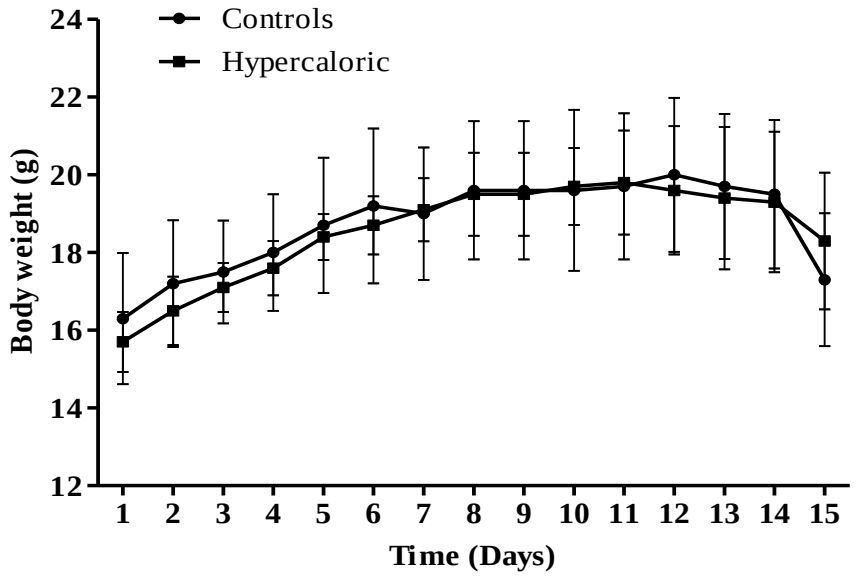

Body weights are presented in mean ± standard deviation. Day 1-7, Acclimatization period; Day 7-14, Feeding period; Day14-15, Fasting period.

Table 4. 1: Organ weights (g) soleus:plantaris ratio and total hind limb muscles of mice after 6 days of feeding

Organs (g)	Groups	n	Mean	95% Confidence Interval Bounds		P Value
				Lower	Upper	
Liver	Controls	4	0.692	0.529	0.856	P=0.613
	Hypercaloric	4	0.732	0.562	0.901	
Adipose tissues	Controls	4	0.164	0.120	0.207	P=0.071
	Hypercaloric	4	0.290	0.111	0.469	
Soleus	Controls	4	0.006	0.005	0.007	P=0.705
	Hypercaloric	4	0.006	0.004	0.007	
Plantaris	Controls	4	0.010	0.009	0.011	P=0.097
	Hypercaloric	4	0.012	0.009	0.014	
Gastrocnemius	Controls	4	0.083	0.072	0.094	P=1.000
	Hypercaloric	4	0.083	0.073	0.093	
Soleus:Plantaris ratio	Controls	4	0.600	0.488	0.713	P=0.179
	Hypercaloric	4	0.505	0.341	0.669	
Total hind limbs muscles	Controls	4	0.099	0.087	0.112	P=0.827
	Hypercaloric	4	0.101	0.088	0.113	

Values are expressed as mean with 95% CI. Independent Student's t-test was used. Total hind limb muscles refer to the sum of soleus, plantaris and gastrocnemius muscle weights are combined left and right

Table 4. 2: The energy intake of mice over 6 days in control group fed standard chow and from hypercaloric animals

Time (Day)	Control	Hypercaloric	
	Feed consumed (g)	Feed consumed (g)	Condensed milk consumed (g)
1	14.0	0.4	23.8
2	12.1	1.2	14.7
3	12.2	0.6	17.5
4	12.1	0.7	21.6
5	12.1	1.0	17.5
6	12.2	1.3	12.0

A full fat condensed milk was used instead of the light condensed milk

Figure 4. 2: Energy intakes of the mice over 6 days during the feeding period with either control or hypercaloric diets

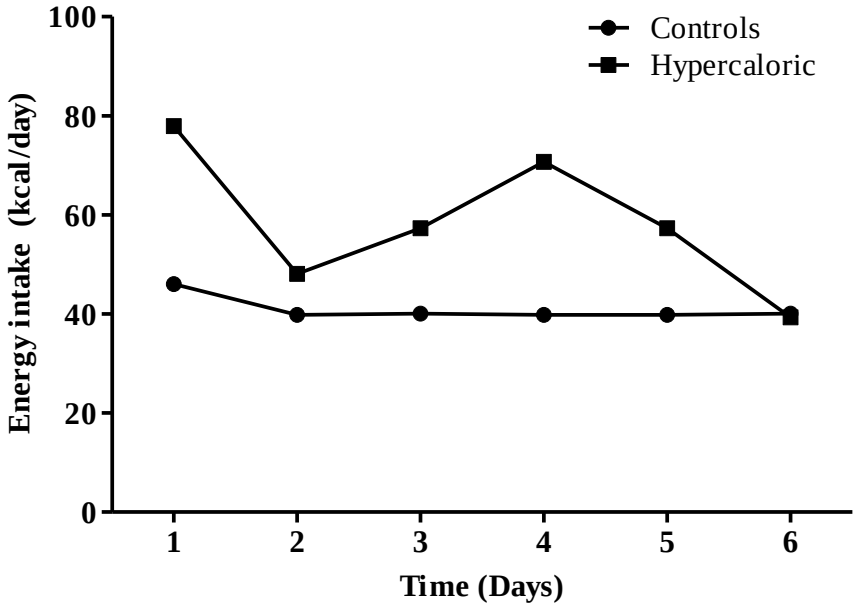

Mean energy intake is presented without standard deviation because there was only one cage per group (n = 4 per group).

Figure 4. 3: Mean energy intake over 6 days of control and hypercaloric mice.

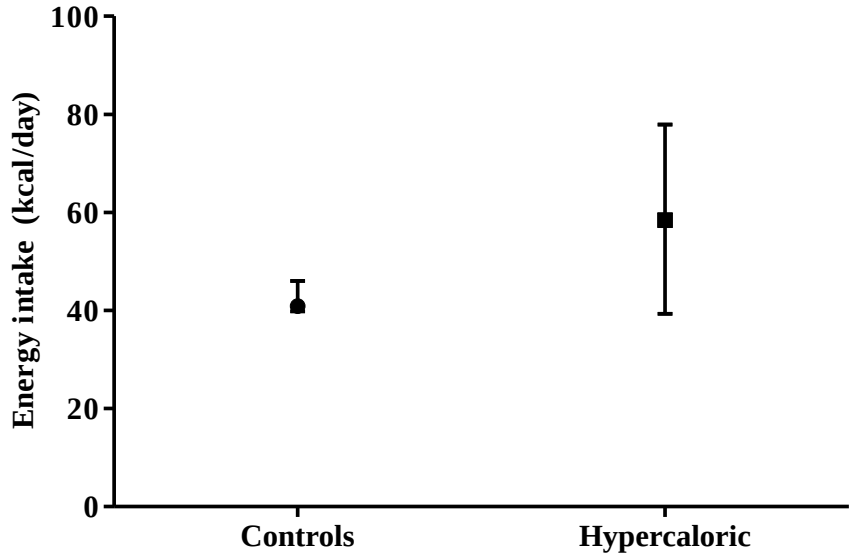

Data is presented in mean with 95% confidence interval over the period of 6 days of feeding

Figure 4. 4: The total mean energy intake of mice over 6 days in control or hypercaloric group derived from milk and pellet intake

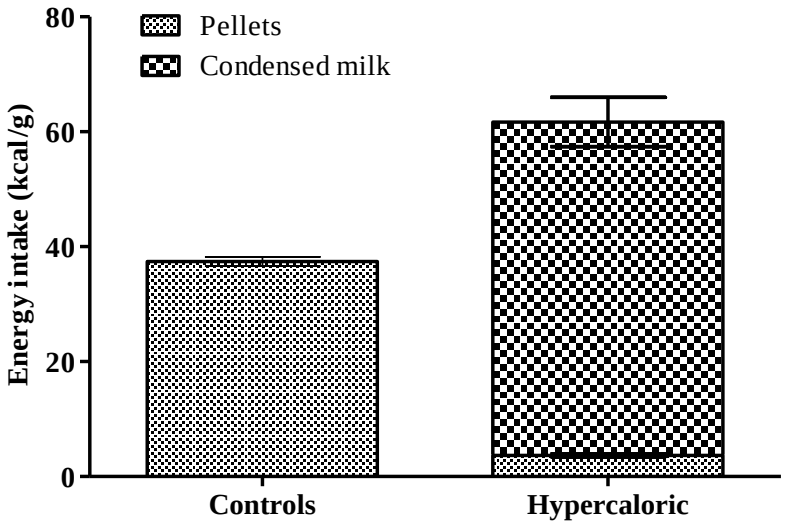

Data is presented in mean ± standard deviation

4.1.4 Discussion

Both the control and hypercaloric diets supported growth over a short period of feeding and there were no differences in lean tissue as represented by the muscle weights. There were no statistically differences in body, liver and adipose tissue weights which may be due to the short period of feeding. Consumption of the hypercaloric diet resulted in an increased energy intake by 40% mainly contributed by the palm oil enriched condensed milk.

The findings for this PhD indicate that it will be necessary to modify the fatty acid composition of the condensed milk as well as the pelleted diet in order to test the hypothesis that different dietary fatty acids influence NASH. This is because when condensed milk is added alongside the pelleted feed in the hypercaloric diet, the mice showed a significantly higher preference towards the condensed milk. By incorporating the test fats into the condensed milk, the effects of dietary fats on the liver can be investigated.

4.2 Experiment 2: Introduction

Experiment 2 was to further confirm the finding in ***Experiment 1*** in this section that the full fat variety of condensed milk was responsible for the increased food intake rather than the composition of the pelleted diet. Therefore, I aimed to test the hypothesis that the acclimatization to the pelleted diet prior to the introduction of condensed milk would result in increased pellet consumption when condensed milk is introduced. In ***Experiment 2***, I will be comparing the energy intake in mice fed standard chow with and without condensed milk. In addition, I will also compare the energy intake between the mice fed a low fat pelleted diet (2% corn oil) with condensed milk and mice fed a hypercaloric pelleted diet (18% palm oil) with condensed milk. I also reduced wood chips and paper contamination in the milk jar to increase the accuracy of measuring food intake.

4.2.1 Animals and materials

C57BL/6J male mice were housed in raised bottom wired cages containing cardboard rolls and an aluminium tin to contain the milk jar.

4.2.2 Methods

A total of 16 C57BL/6J mice were acclimatized without condensed milk for one week. Mice were then allocated to either one of the following 4 groups: standard chow, standard chow with access to condensed milk, low fat pellet (2% corn oil) or hypercaloric pellet (18% palm oil) with access to condensed milk. The condensed milk used in this study is the full fat variety instead of the light condensed milk. The groups were identified as (1) Controls (2) Controls with condensed milk (3) Low fat (4) hypercaloric groups. Full details of the diets and their detailed composition are found in ***Chapter 2*** and ***Table 2.1, 2.2 and 2.4.*** Weights of mice, pellet and condensed milk intake were recorded every day for 3 weeks. In order to avoid contamination of condensed milk in the jar, mice were placed in raised wire-bottomed cages. After 3 weeks, feeding jars were removed and mice were fasted overnight before culling. Liver tissues were collected and muscle weights were recorded similar to procedures in ***Experiment 1*** (***Section 4.1.3***).

4.2.3 Results

The weights of adipose tissue in the controls with condensed milk group were significantly higher compared to the controls and low fat group (P=0.005). Interestingly, the adipose tissue weight in the controls with condensed milk group was 2 fold higher compared with the hypercaloric group. There were no significant changes in the weights of liver, soleus, plantaris, gantrocnemius and total hind limb weights (***Table 4.3***).

Animals fed the pelleted diet (either control or hypercaloric) with condensed milk *ad-libitum* showed increased energy intakes and growth rates that did not differ significantly (***Figure 4.5***). The increased energy intake of these groups was mainly a consequence of increased condensed milk consumption (***Figure 4.6***), which is high in sugar/carbohydrate. In the present study no contamination of the condensed milk occurred due to the use of raised cages. There was less contamination in the milk jars which increased reliability of feed intake measurement. Other observations included mice building a nest in the aluminium tin by removing scraps of paper from the cardboard roll. This nesting behaviour was consistent throughout the whole experiment; as observed when old rolls were replaced with new ones.

Table 4. 3: Organ weights (g), soleus:plantaris ratio and total hind limb muscles of mice in the controls, controls with condensed milk, low fat and hypercaloric groups

Organs (g)	Groups	n	Mean	95% Confidence Interval Bounds		P Value
				Lower	Upper	
Liver	Controls	4	0.662	0.574	0.749	0.177
	Controls with condensed milk	4	0.723	0.616	0.829	
	Low fat	4	0.622	0.507	0.736	
	Hypercaloric	4	0.720	0.586	0.854	
Adipose tissue	Controls	4	0.152 [a]	0.052	0.252	0.005
	Controls with condensed milk	4	0.481 [b]	0.255	0.707	
	Low fat	4	0.101 [a]	0.077	0.125	
	Hypercaloric	4	0.280 [a,b]	0.038	0.598	
Soleus	Controls	4	0.015	0.009	0.021	0.396
	Controls with condensed milk	4	0.014	0.009	0.019	
	Low fat	4	0.010	0.001	0.019	
	Hypercaloric	4	0.011	0.003	0.018	
Plantaris	Controls	4	0.015	0.007	0.022	0.344
	Controls with condensed milk	4	0.016	0.011	0.021	
	Low fat	4	0.013	0.010	0.017	
	Hypercaloric	4	0.017	0.016	0.019	
Gastrocnemius	Controls	4	0.090	0.055	0.124	0.206
	Controls with condensed milk	4	0.103	0.096	0.110	
	Low fat	4	0.097	0.087	0.107	
	Hypercaloric	4	0.110	0.090	0.130	
Soleus : Plantaris ratio	Controls	4	1.110	0.413	1.808	0.406
	Controls with condensed milk	4	0.882	0.603	1.160	
	Low fat	4	0.841	0.034	1.715	
	Hypercaloric	4	0.620	0.143	1.097	
Total hind limb muscles	Controls	4	0.119	0.087	0.150	0.198
	Controls with condensed milk	4	0.133	0.125	0.140	
	Low fat	4	0.121	0.107	0.134	
	Hypercaloric	4	0.138	0.113	0.163	

Values are expressed as mean with 95% CI. One way analysis of variance (ANOVA) and Tukey's multiple range test was used. Values with different superscripts indicate significant differences between treatments.

Figure 4. 5: Body weights of mice in controls, controls with condensed milk, low fat and hypercaloric groups from acclimatization period to feeding and fasted state

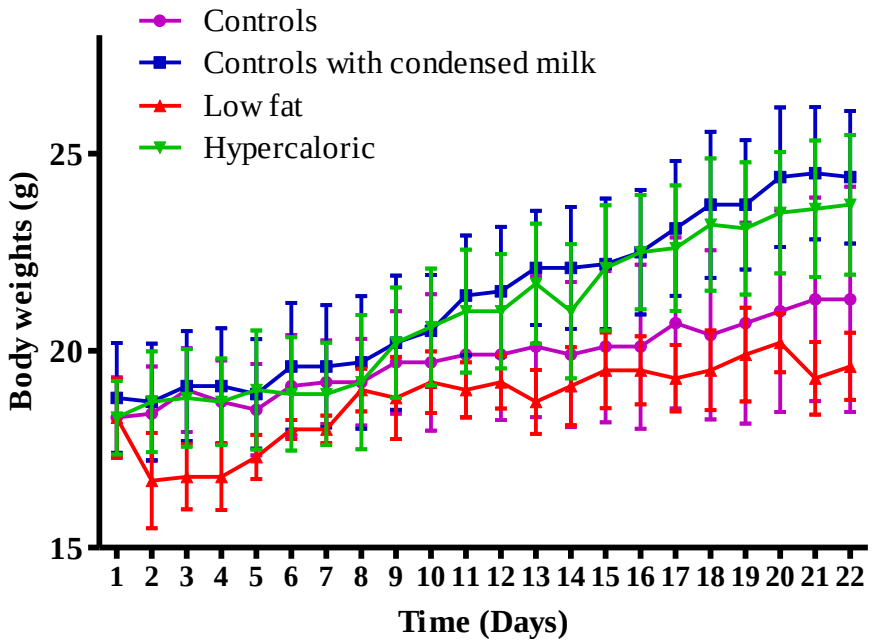

Time line: Day 1-7, without milk; Day 7-21, Feeding period; Day 21-22, Fasted overnight. Data are shown as mean ± standard deviation of 4 observations in each group.

Figure 4. 6: Energy intake in week 2 and 3 of mice in controls, controls with condensed milk, low fat and hypercaloric groups from acclimatization period to feeding and fasted state

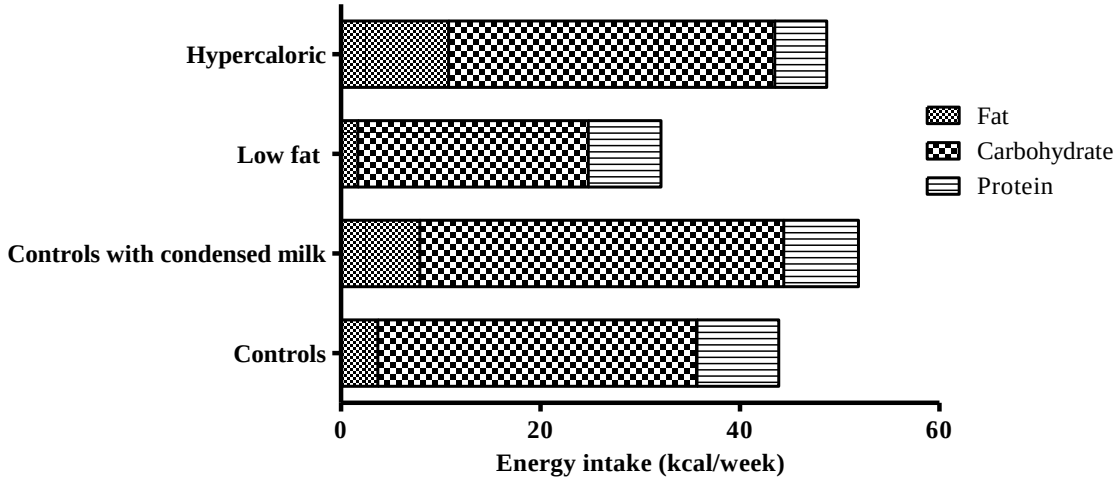

4.2.4 Discussion

The results in ***Experiment 2*** show the consumption of condensed milk by mice was significantly higher compared to the pelleted diet despite acclimatizing the mice with pelleted diets. The acclimatization of mice on only the pelleted diets did not increase pelleted diet intake when condensed milk was added to the diet in week 2. This was observed in all 3 groups; controls with condensed milk, low fat and the hypercaloric group whereby condensed milk was provided in the diet. The results of ***Experiment 2*** indicated that it is necessary to modify the fat composition of the condensed milk as well as the pelleted diet in order to investigate the effects of dietary fats in the diets of mice. In the subsequent main studies, test fats of known concentrations will be incorporated to *light* condensed milk which has 0% fat to match the fat content in the pellets. By increasing the fat content in the *light* condensed milk, the fat content will be more proportionate to the carbohydrate/sugar content in the light condensed milk thus, comparable to the ratio of fat to carbohydrate/sugar in the semi-synthetic hypercaloric diet. Therefore, all condensed milk mentioned in ***Chapter 5*** to ***8*** are *light* condensed milk incorporated with different types of fats. Detailed composition of all the diets are contained in ***Chapter 2*** in ***Table 2.1, 2.2*** and ***2.4.***

In 2 weeks of feeding period, the weight of adipose tissue showed a 50% increase in mice fed the control with condensed milk compared to the mice fed the hypercaloric diet which contains 18% (w/w) palm oil. However, the weight of adipose tissue in the hypercaloric group was not significantly different when compared to the low fat and control group. In simple terms, it can be suggested that the fatty acid concentration in the adipose tissue of the hypercaloric group is higher than the controls which mimics the diets provided to the respective group. This expected observation suggested that the fatty acid profile of the adipose tissue in the study for the thesis may reflect the fatty acid profile of the dietary fats provided. In the subsequent main studies (***Chapter 5 and 6***), fatty acid profiles of adipose tissue will be investigated to compare with the dietary fat intakes.

Lastly, raised bottom cages with cardboard roll will be used to prevent mice from gnawing on bedding. Jars containing condensed milk will be placed in an aluminium container to allow accurate measure of condensed milk spillage. The food intake measurements were as accurate as possible, to generate a reliable and more coherent interpretation of fatty acid profiles in the liver and adipose tissue of mice.

Chapter 5:

The effects of overfeeding with diets high or low in fat on the pattern of fatty acid accumulation in the liver lipid fractions

5.1 Introduction

Fat accumulation in the liver occurs when hepatic fatty acid oxidation is suppressed and/or there is excessive delivery of triacylglycerol (TAG) to the liver from chylomicrons (Yasunaga et al, 2007) or an excessive flux of non-esterified fatty acids (NEFA) from adipose tissue (Larter et al, 2009; Stanton et al, 2011) resulting in hepatic TAG synthesis. Overfeeding in humans (Klein et al, 1998; Grau & Bonet 2009) and animals (Gaemers et al 2011; ***Chapter 3***) is associated with the development of fatty liver and the progression to non-alcoholic steatohepatitis (NASH) and can be achieved by overfeeding a diet high in fat and sugar.

Although liver biopsy is the gold standard measure for the diagnosis of liver disease (Brunt & Tiniakos 2010), there are limitations associated with morbidity associated with the biopsy procedure (Myers et al, 2008). Therefore, a less invasive method is required to distinguish steatosis from NASH to avoid permanent liver damage. The effectiveness of histological scoring systems (Brunt et al, 1999; Merat et al, 2008) and analyses of serum liver enzymes (Mathiesen et al, 1999; Sorrentino et al, 2004) related to NASH are well-established but unreliable in diagnosis of early-stage NASH. Furthermore, there is a need to identify whether there are differences in the pattern of fatty acid accumulation in the various liver lipid fractions which are NEFA, TAG, cholesteryl esters and phospholipids.

In the fed state, excess carbohydrate is converted to fatty acids (mainly palmitic and oleic acids) in the liver and stored as TAG in adipose tissue. TAG can also be derived from chylomicrons and chylomicrons containing saturated fatty acids (SFA) may be metabolized slower than PUFA (Green et al, 1984). However, this may depend on the chain length of the fatty acids (Leyton et al, 1987) and their physical properties (Berry, 2009). In the fed state, insulin inhibits hormone sensitive lipase (HSL) in adipose tissue which in turn inhibits the supply of NEFA from the adipose tissue to the liver (Reid et al., 2008). This may be a potential protective mechanism by the action of HSL to prevent further accumulation of fat in the liver.

In the fasting state, TAG in adipose tissue is hydrolyzed and mobilized into plasma causing an influx of NEFA to the liver. In the liver, NEFA has two main fates, either beta-oxidation takes place to generate energy including the formation of ketone bodies which can be used as an energy source for extrahepatic tissues including the brain (Heijboer et al, 2005) or, if oxidation is suppressed, re-esterification from TAG (Postic & Girard 2008). The liver is the primary site for cholesterol metabolism and is

interlinked with TAG metabolism. Both TAG and cholesteryl esters (CE) accumulate within the hepatocyte and their accumulation normally results in the formation and secretion of lipoproteins. Very low density lipoproteins (VLDL) are predominantly rich in TAG but also contain some CE (Redgrave 1970). Inhibition of cholesterol synthesis by HMGCoA reductase inhibitors decreases VLDL secretion, whereas in *vitro* studies suggest that oleic acid promotes VLDL formation and secretion. The normal process is for fat synthesised within the liver to be exported as VLDL for use by muscle or storage in adipose tissue. In mammals, the accumulation of fat within the liver generally reflects and imbalance between TAG synthesis and secretion; for example in acute starvation. One of the pathological features of associated with fatty liver is the ballooning of hepatocytes which is believed to be a consequence of an imbalance between phosphatidylcholine and phosphotidylethanolamine, and is associated with inflammation (Li et al, 2006).

Excess energy from carbohydrate stimulates *de novo* lipogenesis in the liver whereas excess energy from fat may lead to direct accumulation of lipid within the liver even though it suppresses *de novo* lipogenesis. Fat accumulation in the liver cause insulin resistance (Ning et al, 2011) and, therefore, the normal suppression of lipolysis following food intake may not occur and the increased flux of NEFA would further drive increased TAG accumulation. It is currently uncertain whether the suppression of hepatic TAG synthesis would reduce hepatic fat accumulation on a high fat diet. Eicosapentaenoic acid (20:5n-3, EPA) and docosahexaenoic acid (22:6n-3, DHA) are known to suppress hepatic TAG synthesis. It is uncertain whether they have favourable effects in the context of a hypercaloric diet on fat accumulation within the liver.

It was hypothesised that a hypercaloric diet consisting of *ad libitum* access to condensed milk (CM) and a high saturated and monounsaturated fat diet would exacerbate fat accumulation in the liver compared to one low in fat/high in sugar and that EPA and DHA would reverse this effect. To test this hypothesis mice were randomly allocated to five diets (n=8 per group); a low fat reference (LFR) and 4 hypercaloric diets where the animals had access to pelleted diet and condensed milk that were low in fat (LF group) or high in fat (HF) with or without additional EPA (HFEPA) and DHA (HFDHA).

Research questions

1. Does the addition of fat to a hypercaloric diet alter the pattern of lipid accumulation in the liver?
2. Do EPA and DHA alter the pattern of fat accumulation in the liver?

Aims and objectives

To conduct a parallel designed feeding trial of 7 weeks duration in mice and to assess the pattern of fatty acids accumulation in the liver lipid fractions.

5.2 Methods

5.2.1 Animal models and materials

Male C57BL/6J 28-day-old mice obtained from Charles River, UK were housed singly in raised bottom wired cages and acclimatised for one week. They were then randomly allocated into 5 treatment groups (n=8): low fat reference (LFR), low fat hypercaloric (LF) or high fat (HF) or high fat with EPA or DHA (HFEPA and HFDHA respectively). The animals were fed on pelleted diet for 1 week and then on pelleted diet + condensed milk except of the eucaloric group, who received pelleted diet only. Growth rates and food intakes were monitored and after 7 weeks, food was withdrawn in the evening, the animal euthanized the following morning and blood and tissue collected. Blood samples were collected via cardiac puncture under anaesthesia and whole blood was processed to obtain serum after cervical dislocation. Liver, epididymal fat pads, soleus, plantaris and gastrocnemius muscles were collected, blotted dry and weights were recorded. All tissues were sectioned into separate vials before being rapidly frozen in liquid nitrogen and stored at -70°C until analysis.

5.2.2 Diets

Semi-synthetic pelleted diets were prepared as described ***Chapter 2*** and the freeze dried pellets were stored at 4°C. In order to meet essential fatty acids requirements in the low fat groups, the diet contained 2% by weight corn oil. The high fat pelleted diets contained 18% fat by weight palm olein or 15% palm olein + 3% EPA triacylglycerol concentrate or 15% palm oil + 3% DHA triacylglycerol concentrate. Animals allocated to the low fat hypercaloric diet received a condensed milk containing 1% fat prepared by blending low fat condensed milk (Carnation Light) with corn oil

(99:1). The animals on the high fat hypercaloric diet received a blend 92:8 by volume of low fat condensed milk and test oil (ie, palm olein, or palm olein + EPA or palm olein + DHA).

5.2.3 Analysis of tissue

Samples of liver were taken for histology (haematoxylin and eosin staining) and scored for steatosis, inflammation and reticulin condensation, by Prof. B Portmann (KCL). Serum was analysed for insulin, glucose, cholesterol, triglycerides, NEFA and liver enzymes ALT, AST and ALP by routine methods. Lipids were extracted from liver (Folch et al, 1957) and fractionated into non-esterified fatty acid (NEFA), triacylglycerol (TAG), cholesteryl ester (CE) and phospholipid (PL) fractions in the presence of C17 containing internal standards to facilitate quantitation. These fractions were reacted with HCL in methanol: toluene to form methyl esters which were analysed by capillary gas chromatography as described in ***Chapter 2***. Epididymal fat pads were directly methylated without any separation into lipid class as they consist almost entirely of TAG.

5.2.4 Statistical analysis

Repeated measure ANOVA was used to compare growth values and dietary intake. Other data were analysed using one way analysis of variance (ANOVA). Tukey's multiple range tests was used to make comparisons between diets. Dunnet's test was used to compare energy intakes of mice from LFR group to all other groups. Chi-squared test was used to compare differences in the frequency of certain observations.

5.3 Results

5.3.1 Food intake

Energy intake from solid food declined when there was access to condensed milk in both LF and HF group but remained relatively constant in the LFR group (***Figure 5.1*** and ***Appendix 5.1***). Total energy intake was 17 kcal/d higher on the HF than the LF group which in turn was greater than the LFR. The higher energy density of the HF condensed milk was mainly responsible for this difference in energy intake. The average intakes of energy with 95% CI were 80 kcal/week (74, 86) on the LFR, 94 kcal/week (88, 99) on LF, 105 kcal/week (99, 110) on the HF, 109 kcal/week (98, 119) on HFDHA and 106 kcal/week (100,111) on HFEPA group. Energy intakes from solid food and condensed milk are shown in ***Appendix 5.2*** and ***5.3*** respectively. The contribution to energy intake from solid food declined markedly on introduction of condensed milk so that the condensed milk was providing about 90% of the energy intake.

Figure 5. 1: Total energy intake (kcal/week) from the consumption of all sources during run-in and over 6 weeks of feeding period in low fat reference (LFR), low fat (LF), high fat (HF), high fat DHA (HFDHA) and high fat EPA (HFEPA) groups.

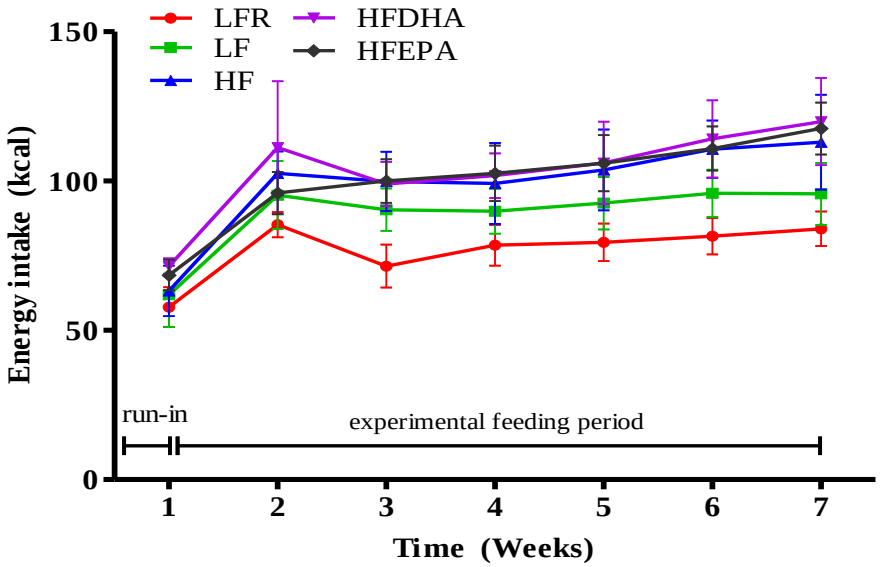

Mean values ± SD, 8 animals/group. Repeated measures ANOVA shows significant difference between diets P<0.0001. LFR diet is significantly different from all other diets (Dunnett's test P<0.05). There are no significant differences between high fat diets. The energy intake on the LF diet is 13 kcal/day (95% CI 5, 21) lower than on the high fat diets (P<0.01).

5.3.2 Body and organ weights

Generally the animals appeared to remain in good health throughout the study as shown in the growth rates of the animals (***Figure 5.2*** and ***Appendix 5.4***). At the end of the study body weights increased in the LF and HF groups, respectively (both P<0.001) compared with the LFR group. The weight gain was only 3.6 g greater in the HF group compared to the LF group even though the additional energy intake 546 kcal over the 6 week feeding period would be predicted to result in an increase in weight of about 54.6 g (assuming each additional 10 kcal results in a 1 g weight gain) (***Appendix 5.5***). Epididymal fat pad weights were correspondingly higher in the HF group compared to the LF group but the liver weights did not differ. The weight gain in the LF group compared to the LFR group was 4.6 g whereas the additional energy intake of 160 kcal would predict an increase weight by 16 g. These findings would suggest that the efficiency of energy utilisation was lower on the high fat diet than on the low fat diet. The excess energy was presumably lost as heat.

Plantaris and gastrocnemius muscles were significantly lower in the LFR group compared to the others which was reflected in the significant decrease in the total hind limb muscles (***Table 5.1***). No other differences were noted in body and organ weights.

Figure 5. 2: Body weights (g) during run-in and over 6 weeks of feeding period in low fat reference (LFR), low fat (LF), high fat (HF), high fat DHA (HFDHA) and high fat EPA (HFEPA) groups.

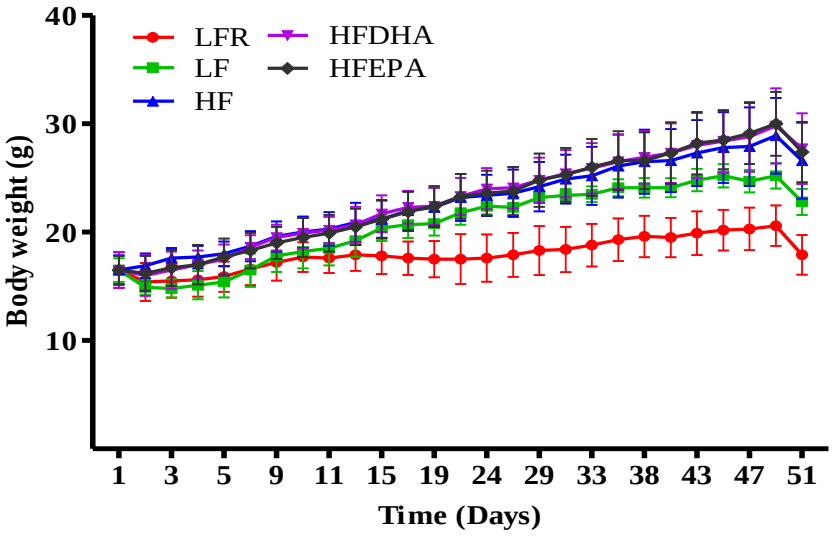

Mean value ± SD, 8 animals/group. There is a significant effect of diet on weight gain (P<0.001). At day 50, the weight of LFR group is significantly lower than all other groups (P<0.01). There are no differences between HF groups. Body weight of HF groups at day 50 is 3.6 g (95% CI 0.9, 6.5) greater than LF group.

Table 5. 1: Organ weights (mg) soleus:plantaris ratio and total hind limb muscles of mice after 7 weeks of feeding low fat reference diet (LFR), low fat (LF) , low fat (LF), high fat (HF), high fat DHA (HFDHA) and high fat EPA (HFEPA) diets..

Organs (mg)	LFR	LF	HF	HFDHA	HFEPA	Statistical significance
Liver	681[a] (557,806)	880[b] (799,962)	919[b] (831,1006)	977[b] (880,1075)	921[b] (815,1027)	P<0.001
Epididymal adipose tissue	134[a] (95,174)	326[a] (239,413)	1033[b] (741,1325)	940[b] (647,1235)	903[b] (591,1215)	P<0.001
Soleus	7 (5,9)	8 (7,9)	8 (6,9)	8 (6,9)	8 (7,8)	P=0.914
Plantaris	12[a] (11,14)	15[b] (14,17)	15[a,b] (13,17)	16[b] (14,17)	16[b] (15,17)	P=0.014
Gastrocnemius	84[a] (73,96)	106[b] (99,113)	109[b] (100,118)	110[b] (101,118)	114[b] (110,118)	P<0.001
Soleus:plantaris	0.572 (0.421,0.724)	0.502 (0.453,0.551)	0.507 (0.448,0.565)	0.490 (0.425,0.555)	0.502 (0.457,0.547)	P=0.455
Total hind limb muscles	104[a] (90,118)	129[b] (120,138)	132[b] (120,144)	133[b] (124,141)	138[b] (134,141)	P<0.001

Mean values with 95% CI. Data were analysed by one way analysis of variance (ANOVA) and values with different superscripts indicate significant differences (P<0.05) between treatment using Tukey's multiple range test.

5.3.3 Blood biochemistry

Blood biochemistry in the animals is shown in ***Table 5.2***. Animals in the LF and HF group had fasting plasma glucose concentrations in excess of 7.1 mmol/L indicating impaired glucose tolerance compared with 5.2 mmol/L in the LFR group. The mean plasma glucose concentrations was greater in the LF group (11.9 mmol/L) compared with the LFR, HFDHA and HFEPA groups. Fasting insulin values were low (<1 IU/L) and partial haemolysis of the sample may have resulted in the low values. Serum cholesterol concentrations tended to be lower in the LFR group compared to the HF group but this fell short of statistical significance. Triacylglycerol were greater in the HFDHA and HFEPA groups compared to the LF. These findings were opposite to what was expected. However, no correction was made for glycerol in the assay and as the animals had been fasted overnight there could be a significant contribution from glycerol as a result of increased hydrolysis of lipids from adipose tissue.

Results for the liver enzymes are shown in ***Table 5.2*** Normal values in C57BL/6J mice model in the age range of 1 to 2 months were reported by Mazzaccara et al, (2008), to ALP 160, AST 105 and ALT 60 IU/L. AST values were higher in the present study. ALT values were unremarkable and ALP values were higher in the LFR group compared to the HFEPA and HFDHA group.

Table 5. 2: Fasting serum insulin, glucose, cholesterol, triacylglycerols (TAG), non-esterified fatty acids (NEFA concentrations and activities of alkaline phosphatase (ALP), aspartate transaminase (AST) and alanine transaminase (ALT) in mice fed either low fat reference (LFR), low fat (LF), high fat (HF), high fat DHA (HFDHA) or high fat EPA (HFEPA) diets

Serum analytes	LFR	LF	HF	HFDHA	HFEPA	P Anova
Insulin (ng/ml)	0.4 (0.1,0.7)	0.3 (0.2,0.5)	0.3 (0.2,0.3)	0.3 (0.2,0.3)	0.3 (0.2,0.4)	P = 0.458
Glucose (mmol/L)	5.2[a] (2.5,8.0)	11.9[b] (5.9,17.9)	8.2[a,b] (4.5,12.0)	5.1[a] (3.1,7.1)	4.3[a] (3.0,5.7)	P = 0.007
Cholesterol (mmol/L)	1.8 (1.3,2.4)	2.8 (1.9,3.6)	3.0 (2.2,3.8)	2.7 (2.0,3.3)	2.6 (2.4,2.7)	P = 0.098
Triacylglycerol (mmol/L)	0.7[a,b] (0.6,0.9)	0.6[a] (0.5,0.8)	0.7[a,b] (0.4,1.0)	1.4[c] (0.8,1.9)	1.3[b,c] (0.8,1.7)	P = 0.003
NEFA (mmol/L)	1.5 (1.0,2.0)	1.1 (1.0,1.3)	1.3 (0.8,1.8)	1.2 (1.0,1.3)	1.2 (1.1,1.4)	P = 0.336
ALP (IU/L)	155[b] (29,282)	90[a,b] (53,126)	79[a,b] (30,128)	62[a] (46,79)	59[a] (52,67)	P = 0.037
AST (IU/L)	433 (195,1060)	246 (61,553)	309 (67,684)	177 (106,249)	173 (63,283)	P = 0.646
ALT (IU/L)	31 (10,73)	19 (0,37)	21 (3,40)	20 (10,30)	19 (8,29)	P = 0.812

Mean values with 95% C, 8 animals/group. Data were analysed by one way analysis of variance (ANOVA) and values with different superscripts indicate significant differences (P<0.05) between treatments using Tukey's multiple range test.

5.3.4 Histopathology

The histopathological findings on the liver are shown in ***Table 5.3***. Steatosis was more frequent and severe in the LFR group compared to the HF and HFDHA group. Signs of inflammation were less frequent in all HF groups especially, HFDHA, compared to LF and LFR groups. Generally, the HFDHA group showed fewer histopathological abnormalities compared to the other groups. Examples of sections from animals fed the LF and LFR diets are shown in ***Figure 5.3***. The presence of large lipid droplets was very evident in the LFR group.

Figure 5. 3: Panel A shows liver section from a mouse fed the hypercaloric low fat diet and Panel B shows one from the low fat reference diet stained with haemotoxylin and eosin (400x magnification)

PANEL A

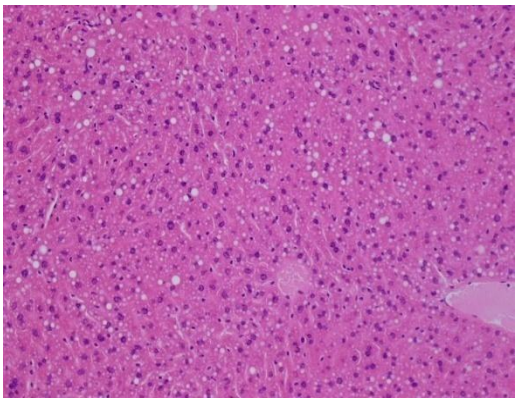

PANEL B

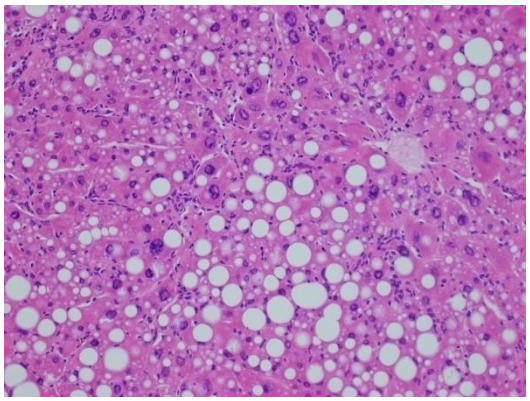

Table 5. 3: Histopathology scores for steatosis, inflammation and reticulin condensation of mice fed either low fat reference (LFR), low fat (LF), high fat (HF), high fat DHA (HFDHA) or high fat EPA (HFEPA) diets

	Scores	LFR (n=8)	LF (n=8)	HF (n=8)	HFDHA (n=8)	HFEPA (n=8)	P Anova (Tukey's)
Steatosis	0 (0%)	0 (0%)	1 (13%)	1 (13%)	3 (38%)	0 (0%)	P=0.001
	1 (5-25%)	2 (25%)	4 (50%)	4 (50%)	5 (63%)	4 (50%)	
	2 (25-50%)	0 (0%)	1 (13%)	3 (38%)	0 (0%)	3 (38%)	
	3 (50-75%)	2 (25%)	1 (13%)	0 (0%)	0 (0%)	1 (13%)	
	4 (>75%)	4 (50%)	1 (13%)	0 (0%)	0 (0%)	0 (0%)	
	Mean	3.1 ± 1.3^{a}	$1.6 \pm 1.30^{a,b}$	1.3 ± 0.7^{b}	0.6 ± 0.5^{b}	$1.6 \pm 0.^{7a,b}$	
Inflammation	0 (Absent)	0 (0%)	4 (50%)	5 (63%)	7 (88%)	6 (75%)	P=0.004
	1 (Occasional)	3 (38%)	2 (25%)	3 (38%)	1 (13%)	1 (13%)	
	2 (Sparse)	1 (13%)	0 (0%)	0 (0%)	0 (0%)	0 (0%)	
	3 (Frequent)	4 (50%)	0 (0%)	0 (0%)	0 (0%)	1 (13%)	
	4 (Most)	0 (0%)	2 (25%)	0 (0%)	0 (0%)	0 (0%)	
	Mean	2.1 ± 1.0^{a}	$1.3 \pm 1.8^{a,b}$	0.4 ± 0.5^{b}	0.1 ± 0.4^{b}	1.1 ± 0.4^{b}	
Reticulin condensation	0 (Absent)	3 (38%)	4 (50%)	4 (50%)	4 (50%)	3 (38%)	P=0.274
	1 (Occasional)	1 (13%)	2 (25%)	3 (38%)	4 (50%)	4 (50%)	
	2 (Sparse)	0 (0%)	0 (0%)	1 (13%)	0 (0%)	0 (0%)	
	3 (Frequent)	3 (38%)	0 (0%)	0 (0%)	0 (0%)	1 (13%)	
	4 (Most)	1 (13%)	2 (25%)	0 (0%)	0 (0%)	0 (0%)	
	Mean	1.8 ± 1.7	1.3 ± 1.8	0.6 ± 0.7	0.5 ± 0.5	0.9 ± 1.0	

Values are expressed in counts (%) or mean score ± SD

5.3.5 Fatty acid composition (weight %) of adipose tissue

The fatty acid composition of the dietary fat was compared with that of adipose tissue (***Figure 5.4*** and ***Appendix 5.6***). It is often assumed that the composition of adipose tissue mirrors that of the dietary fat. However, the proportion of palmitic acid was lower and that of oleic acid (18:1n-9) in the adipose tissue than in the HF diet indicating that a substantial proportion 16:0 had been chain elongated and desaturated to form 18:1n-9. In contrast, in the animals fed EPA and DHA, the proportion of palmitic acid was similar to that provided in the diet. This would indicate that EPA and DHA inhibited the conversion of palmitic acid to oleic acid. DHA accumulated in adipose tissue on the DHA diet but there was only a small increased in EPA in adipose tissue on the EPA diet. The proportion of palmitoleic acid (16:1n-7) in epididymal adipose fats was greater in the LF and LFR group compared to the HF groups. This fatty acid believed to be an indicator of *de novo* synthesis of lipid from carbohydrate. There were statistically significant differences between diets in stearic acid (18:0), linoleic acid (18:2n-6), dihomo-gamma linolenic acid (DGLA; 20:3n-6), clupanodonic acid (22:5n-3) and docosahexaenoic acid (DHA; 22:6n-3)

Figure 5. 4: Fatty acids composition (weight %) derived from adipose tissue and diets of mice fed either low fat reference, low fat, high fat, high fat DHA or high fat EPA diets.

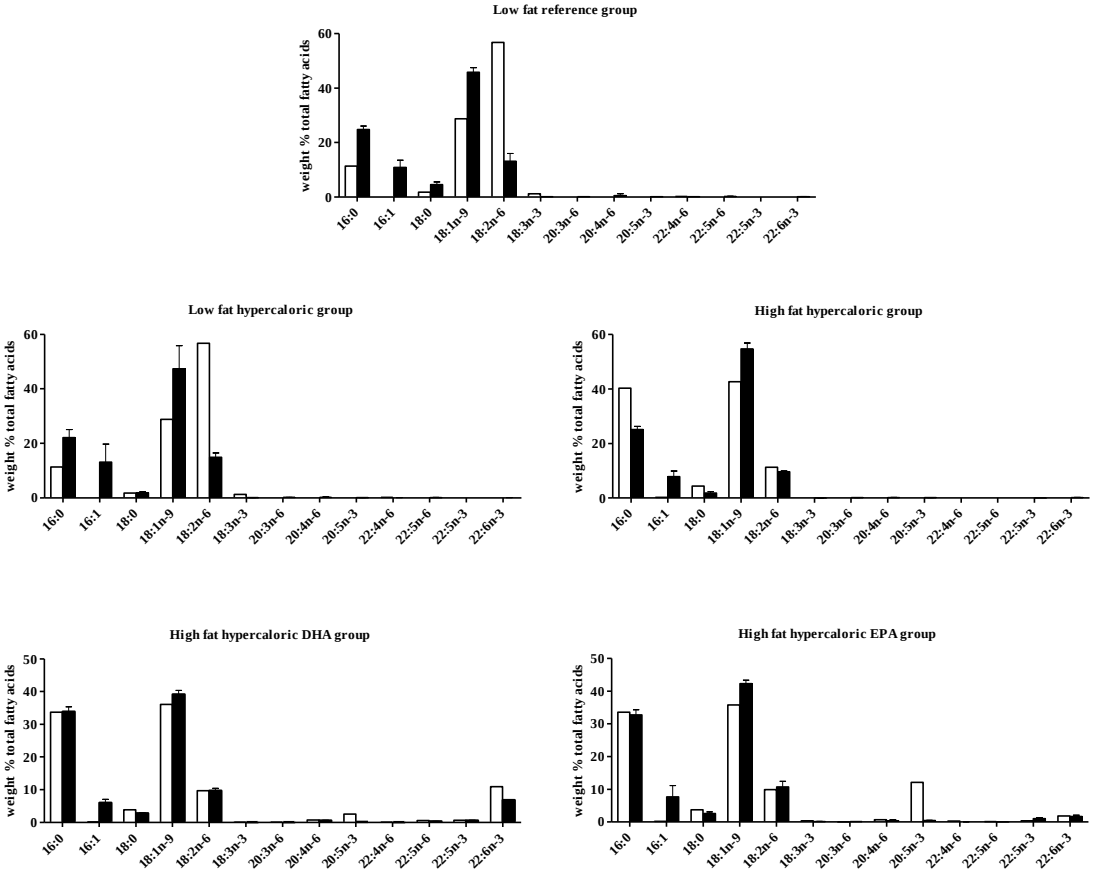

Mean values ± SD, 8 animals/group. Open bar, dietary fat, filled bar, adipose tissue.

5.3.6 Total lipids and the proportions in different lipid fractions

The concentrations of hepatic lipid fractions are shown in ***Table 5.4.*** NEFA concentrations were higher in the LFR group compared with the other groups. TAG concentrations were higher in the HFEPA group compared to the LF and HFDHA group. Cholesteryl ester concentrations were highest in the LF group and greater in the HF group compared to the HFDHA and HFEPA group. Phospholipid concentrations were high in the HF group compared to the LF and HFDHA group and highest in the LFR and HF group. When the results were expressed on a per liver basis (***Figure 5.5***), the differences were smaller because the LF over-feeding caused an increase in liver weight compared with the LFR group and the difference between the LF and HF groups in total lipids/liver was more marked as overfeeding with HF which increased both liver

size and liver fat concentration. It was decided therefore to only make further comparisons on a concentration basis rather than a per liver basis.

Figure 5. 5: Hepatic lipid concentrations expressed mg fatty acid /liver in mice fed either low fat reference (LFR), low fat (LF), high fat (HF), high fat DHA (HFDHA) or high fat EPA (HFEPA) diets.

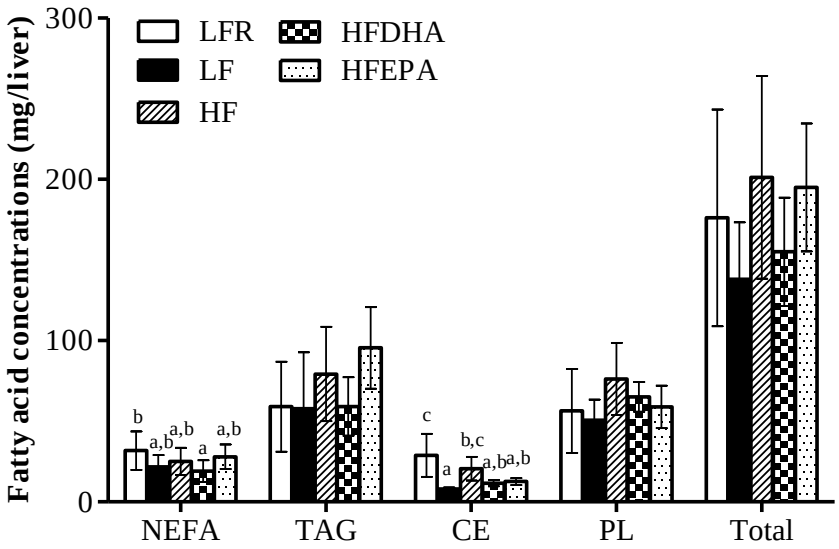

Mean values ± SD, 8 animals/group. Open bar, LFR; filled bar, LF; hatched, HF; checked, HFDHA; dots, HFEPA. Data were analysed by one way analysis of variance. Bars with different superscripts indicate significant differences (P<0.05) between treatments using Tukey's multiple range test.

Table 5. 4: Lipid content of non-esterified fatty acids (NEFA), triacylglycerols (TAG), cholesteryl esters (CE) and phospholipids (PL) expressed in mg/g fatty acids in mice fed either low fat reference (LFR), low fat (LF), high fat (HF), high fat DHA (HFDHA) or high fat EPA (HFEPA) diets.

Fatty acid concentrations	**LFR**	**LF**	**HF**	**HFDHA**	**HFEPA**	**Statistical significance**
NEFA	46.2 ^{c} ± 9.7	24.9 ^{a,b} ± 8.7	27.0 ^{a,b} ± 6.7	19.3 ^{a} ± 5.7	29.7 ^{b} ± 5.6	P=0.005
TAG	84.0 ^{a,b} ± 25.9	54.5 ^{a} ± 26.0	96.7 ^{a,b} ± 34.1	63.5 ^{a} ± 15.2	102.9 ^{b} ± 19.6	P=0.014
CE	41.5 ^{c} ± 12.5	9.3 ^{a} ± 1.0	22.2 ^{b} ± 5.6	11.9 ^{a} ± 1.7	13.8 ^{a,b} ± 1.2	P<0.001
PL	76.1 ^{a,b} ± 17.0	57.6 ^{a} ± 11.9	83.0 ^{b} ± 18.3	67.5 ^{a,b} ± 2.2	64.7 ^{a,b} ± 15.6	P=0.010
Total	247.9 ^{c} ± 47.9	156.0 ^{a} ± 37.8	228.8^{c} ± 57.3	162.2 ^{a,b} ± 22.0	211.5 ^{b,c} ± 29.4	P<0.001

Mean values ± SD; 8 animals/group. Data were analysed by one way analysis of variance. Values with different superscripts indicate significant differences (P<0.05) between treatments using Tukey's multiple range test.

5.3.7 Fatty acid concentrations by degree of unsaturation in liver lipid fractions

The concentrations of lipids according to degree of unsaturation by lipid classes are shown in ***Figure 5.6***. SFA concentrations in NEFA were lower in LF, HF and HFDHA compared to LFR and HFEPA. In the TAG fraction, SFA concentrations were greater in HFEPA and HF when compared to LFR, LF and HFDHA. In the CE fraction, SFA concentrations were significantly lower in LF when compared to LFR and HF.

MUFA concentrations were significantly higher in LFR group in NEFA and CE fractions when compared to other groups whereas those in HFDHA and HFEPA showed the lowest concentration (***Figure 5.6***). In TAG fraction, MUFA was lowest in HFDHA group when compared to the other groups whereas HF was significantly greater when compared to others but showed no statistical difference when compared to HFEPA. In PL, MUFA was significantly lower in HFDHA and HFEPA when compared to HF.

PUFA concentrations in NEFA were greater in the LFR group compared to the other groups (***Figure 5.6***). In the TAG fraction, PUFA concentrations were highest in the HFDHA and HFEPA groups compared to the LF group. In the CE fraction, PUFA concentrations were highest in the LFR group compared to all other groups but lower in the LF group compared to HF. There were no differences in concentration of PUFA in PL fraction.

Figure 5. 6: Fatty acid concentrations (mg/g) derived from NEFA, TAG, CE and PL fractions classified into saturated fats (SFA), monounsaturated fatty acids (MUFA) and polyunsaturated fatty acids (PUFA) in mice fed either low fat reference (LFR), low fat (LF), high fat (HF), high fat DHA (HFDHA) or high fat EPA (HFEPA) diets

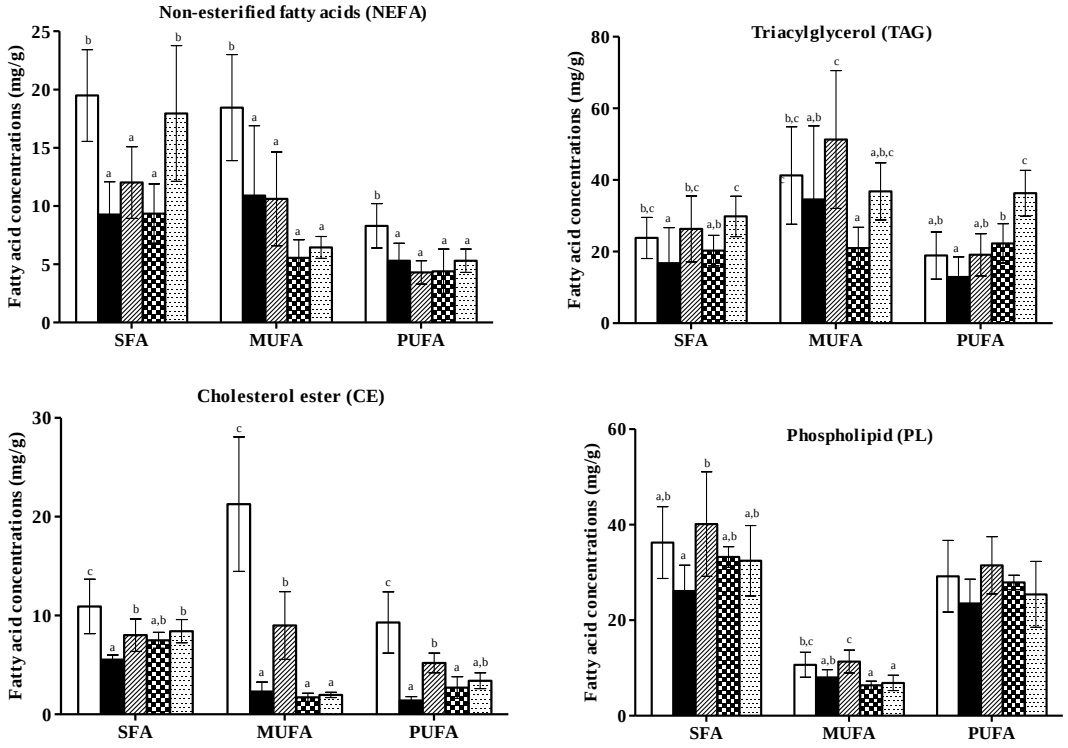

Mean values ± SD, 8 animals/group. Open bar, LFR; filled bar, LF; hatched, HF; checked, HFDHA; dots, HFEPA. Saturated fatty acids (SFA), monounsaturated fatty acids (MUFA), polyunsaturated fatty acids (PUFA). Data were analysed by one way analysis of variance.. Bars with different superscripts indicate significant differences ($P<0.05$) between treatments using Tukey's multiple range test.

5.3.8 Short and long chain PUFA concentrations in different lipid classes

There were major differences in the concentration of long-chain polyunsaturated fatty acids between treatments (***Figure 5.7***). The addition of EPA and DHA increased n-3 LCP and decrease n-6 LCP in all fractions. The concentration of n-3 LCP was greater in NEFA, TAG, CE and phospholipid in HFPO, HFDHA and HFEPA compared to LFR and LF. The lowest concentration on n-3 LCP was found in the LFR and LF group in all fractions, which would correspond with the lower level of 18:3n-3, but the concentration of n-6 LCP was correspondingly greater. The LFR and LF group led to a markedly higher concentration of n-6 LCP in the NEFA, TAG and PL fractions compared to HFPO, HFDHA and HFEPA. High fat feeding showed an increase in n-3 LCP and a decrease in n-6 LCP in all fractions when compared to LFR and LF groups.

Figure 5. 7: Fatty acid concentrations (mg/g) derived from NEFA, TAG, CE and PL fractions classified into linolenic acid (18:3n-3), linoleic acid (18:2n-6), n-3 long chain PUFA (n-3 LCP) and n-6 long chain PUFA (n-6 LCP) in mice fed either low fat reference (LFR), low fat (LF), high fat (HF), high fat DHA (HFDHA) or high fat EPA (HFEPA) diets.

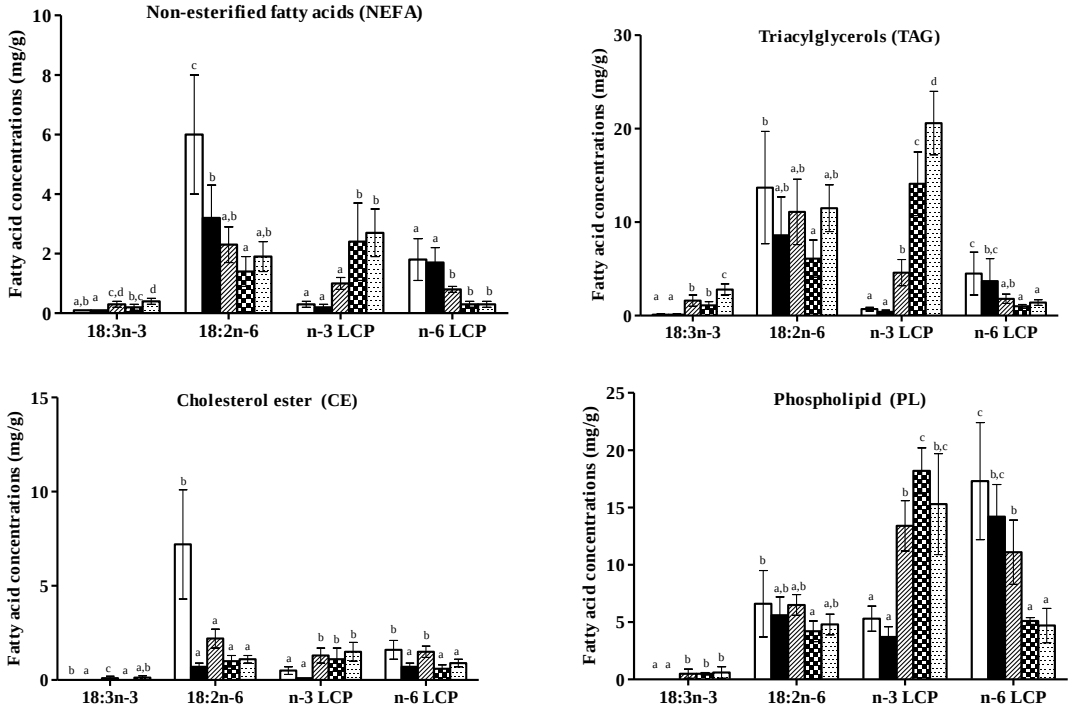

Mean values ± SD, 8 animals/group. Open bar, LFR; filled bar, LF; hatched, HF; checked, HFDHA; dots, HFEPA. Linolenic acids (18:3n-3), linoleic acid (18:2n-6), long chain polyunsaturated fatty acids (LCP). Data were analysed by one way analysis of variance. Bars with different superscripts indicate significant differences (P<0.05) between treatments using Tukey's multiple range test.

5.3.9 Major individual fatty acid concentrations in NEFA, TAG, PL and CE fractions

In the NEFA fraction, the concentration of palmitic acid (16:0) was significantly higher in HFEPA when compared with LF and HFDHA groups (P<0.001) (***Figure 5.8***). As with adipose tissue, the proportion of palmitic acid (16:0) in the liver was greater in the HFDHA than in the HF group whereas the concentration of palmitoleic acid (16:1) was lower. Stearic acid concentrations were also higher in the LFR and HFEPA groups compared with the other groups. The concentration of oleic (18:1n-9) and linoleic acid (18:2n-6) was significantly higher in LFR compared to LF, HF, HFDHA and HFEPA groups. The HFDHA group had significantly lower concentrations of linoleic acid (18:2n-6) when compared to the LF group. In addition, arachidonic acid (AA; 20:4n-6) concentrations were significantly higher in the LFR and LF groups when compared to HF and even more so HFDHA and HFEPA groups. As expected, DHA and EPA concentrations were highest in mice fed DHA and EPA, respectively. However, there was a higher concentration of DHA in the HF compared to the LF group.

In the TAG fraction, the concentration of palmitic acid was significantly higher in the HFEPA group compared to the LF group (***Figure 5.8***). Palmitoleic acid was significantly lower in the HFDHA group compared to the HF group. In accord with the findings in the NEFA fraction, stearic acid concentration was higher in HFEPA compared to LF, HF and HFDHA. Oleic acid concentrations were significantly higher in the HF group compared to the HFDHA group. EPA concentrations were markedly higher in HFEPA compared to the other groups. DHA concentrations were greater in the order of HFDHA> HFEPA> HF compared to the LF and LFR groups.

In the cholesteryl ester fraction, cholesteryl oleate and linoleate concentrations were both higher in the LFR group compared to the other groups (***Figure 5.8***). Cholesteryl palmitate concentrations were greater in the HF compare to the LF group and cholesteryl oleate concentrations were greater in the HF group compared to LF, HFDHA and HFEPA groups. Cholesteryl docosahexaenoate concentrations were greater in the order HFDHA>HFEPA>HF compared to the LF and LFR groups. The concentration of cholesteryl arachidonate was correspondingly lower.

In the phospholipid fraction, palmitic acid (16:0) concentrations were significantly lower in the LF group vs the HF group but were significantly lower in the HFEPA and HFDHA group when compared to HF group (***Figure 5.8***). Arachidonic acid concentrations were lower in the HFEPA and HFDHA groups and those of EPA and

DHA were higher. The concentration of DHA was notably higher in the HF group compared to the LF group.

Figure 5. 8: Concentration of different fatty acids (mg/g liver) in major lipid classes in mice fed either low fat reference (LFR), low fat (LF), high fat (HF), high fat DHA (HFDHA) or high fat EPA (HFEPA) diets.

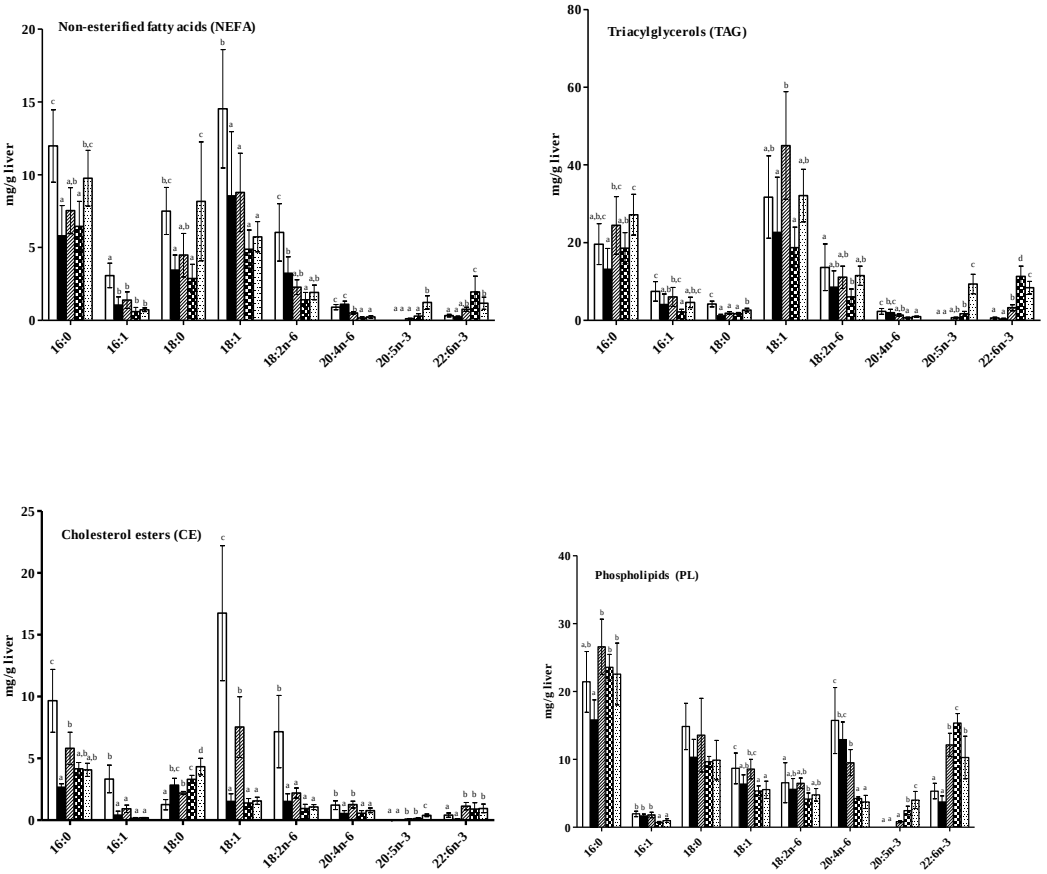

Mean values ± SD, 8 animals/group. Open bar, LFR; filled bar, LF; hatched, HF; checked, HFDHA; dots, HFEPA. Data were analysed by one way analysis of variance. Bars with different superscripts indicate significant differences ($P<0.05$) between treatments using Tukeys multiple range test.

5.4 Discussion

The aim of this study was to see if a high fat diet exacerbated NASH in this overfeeding model. High fat feeding increased energy intakes (kcal/week) and this was a consequence of the higher energy density of the diet. The animals on the high fat diet accumulated more epididymal adipose tissue and fattier livers compared to the overfed animals on the low fat diet. However, the addition of DHA to the high fat diet decreased the fat content of the liver to that similar on the LF diet. The addition of EPA to the high fat diet did not decrease liver fat. The findings, therefore, suggest that DHA but not EPA reduces fat accumulation in the liver. This finding is also consistent with the absence of histological abnormalities in the HFDHA group.

The expansion of the cholesteryl ester pool was mainly due to increased proportions of cholesteryl oleate and linoleate. Unexpectedly, there was no evidence to indicate that the HF worsened liver damage as judged by liver enzymes and histology. Indeed, the histology indicated more inflammation (P=0.015), steatosis and reticulin condensation in mice fed the LFR diet than the LF diets and the least in HF, HFDHA and HFEPA groups.

Adipose tissue composition did not entirely represent the dietary fat in the HF group, the proportion of palmitic acid was lower and that of oleic acid was higher. The lack of similarity in the fatty acid composition of adipose tissue compared to the dietary fat signifies modification of dietary fatty acids in adipose tissue and contribution from *de novo* lipogenesis particularly in the low fat high carbohydrate groups. For example, palmitic acid accounted for about 40% of the fatty acids in palm olein but only 25% in adipose tissue and oleic acid accounted for 43% in palm olein but 55% in adipose tissue. As palmitoleic acid was not provided in the diet it must have been synthesised from palmitic acid and the proportion in adipose tissue was about 8%. This still leaves about 7% palmitic acid unaccounted and a higher than expected proportion of oleic acid in adipose tissue. In the LF group, the linoleic acid accounted from about 57% of the dietary fat but about 15% of the adipose tissue. This would suggest that only about a quarter of the fat in adipose tissue was derived directly from dietary fat and remaining amount would have been synthesised *de novo.* These findings also lend support to the idea that adipose tissue composition is a poor indicator of dietary saturated fat intake and that the effect of overfeeding is primarily to increase palmitic and oleic acid synthesis, which are the same as the major fatty acids in palm olein. The addition of EPA and DHA to the diet results in a higher proportion of 16:0 in adipose fatty acids.

This probably was a consequence of decrease chain length and desaturation in oleic acid caused by competitive inhibitor by n-3 LCP.

Hepatic NEFA concentrations were greater in the mice fed the reference diet which is low in fat (2 % corn oil) and without condensed milk (CM). This may be due to larger amounts of fatty acids being released from adipose tissue to the liver when the animals were fasted prior to sacrifice because of their lower energy reserves. Plasma NEFA concentration represent the influx of fatty acids from adipose tissue and the spill over of fatty acids released during lipolysis which are not trapped by fatty acid binding proteins (Sniderman et al, 1998). On the low fat diets, the composition of hepatic NEFA was quite similar to that of adipose tissue which is consistent with it being derived mainly from the lipolysis of adipose. However, the proportion of oleic acid in this fraction was lower than that in adipose tissue. The hepatic NEFA probably reflect the composition of the metabolically active pool of fatty acids that feed into esterified lipid synthesis and fat oxidation. The lower proportion of oleic acid could indicate a more rapid utilisation of this fatty acid for beta-oxidation. Indeed, tracer studies indicate a higher rate of beta-oxidation of oleic acid vs palmitic acid (Leyton et al, 1987).

The regulation of hepatic TAG biosynthesis under various nutritional states has been extensively studied in the liver (Mayes & Felts 1967; Menahan et al, 1983; Takahashi et al, 2003; Turner et al, 2003). An average mouse liver (1 to 1.5 g) is able to incorporate 200 to 300 nmol of glycerol into TAG per min and is dependent on the fatty acids present (Greenspan et al, 1982). Results of hepatic TAG suggested a significantly rapid desaturation of stearic to oleic acid in all 3 groups that were 3 times lower when compared to the NEFA profile. HF group showed a higher desaturation of stearic to oleic acid when compared to the LFR and LF respectively. The raised levels of oleic acid in TAG liver of HF group may be the reason for the insignificant increase in serum cholesterol (Bonanome et al, 1992). A high proportion of stearic acid instead of palmitic acid was converted to oleic acid (Bonanome et al, 1992; Emken et al, 1993) or stearic acid was synthesised *de novo* from carbohydrate. Oleic acid is relatively stable to oxidation compared with PUFA. On the other hand, a reduced proportion of stearic acid (C18:0) and increased proportion of oleic acid (C18:1n-9) increased the proportions of long-chain PUFA (AA and DHA) in HF mice. This suggest that high fat palm oil diet had the effect of increasing fatty acid desaturation which increases susceptibility to lipid oxidation in vivo (Valencak & Ruf 2011).

Fatty acids are converted to cholesteryl esters by the action of the enzyme acetyl-Coenzyme-A acetyltransferase (ACAT). This enzyme exists in different forms but has high specificity for oleic and linoleic acid with linoleic acid being the preferred substrate. There was proportionately least cholesteryl linoleate in animals fed the LF diet, followed by the HF and then the LFR diet. Previous research has shown that oleic acid feeding resulted in the accumulation of cholestryl oleate in the liver whereas palmitic acid resulted in a much lower accumulation of cholesteryl oleate (Takeuchi et al, 1999). Cholesteryl oleate accounted for 40%, 33% and 16% of cholesteryl esters in the LFR, HF and LF mice respectively.

In hepatic phospholipds, there were marked differences in the balance of n-6/n-3 long chain polyunsaturated fatty acids The elevated DHA concentrations in the HF fed mice is in agreement with the finding in the pilot study and suggests that conversion of linolenic acid to DHA may be enhanced on a high fat diet in the presence of a high sugar intake, presumably because linolenic acid is spared from oxidation.

The findings of this study do not support the hypothesis that an increased intake of palmitic and oleic acids exacerbates NASH compared with carbohydrate overfeeding. The higher proportion of C20-22 polyunsaturated fatty acids in the HF group indicates that the high fat and/or high sugar diet promotes their synthesis from linolenic acid and this deserves further investigation.

Chapter 6:

The effects of triacylglycerol structure of palmitic acid rich fats on liver lipids in mice fed hypercaloric high fat diets

6.1 Introduction

It has been suggest that animal fats, such as lard, which are high in saturated fatty acids, exacerbate fatty liver disease. Palm oil is now the major vegetable oil produced globally being produced mainly in Malaysia and Indonesia. Palm oil is high in palmitic acid (16:0) but is also high in the oleic acid (18:1n-9) and unlike coconut oil contains significant amounts of the essential fatty acid linoleic acid (18:2n-6). Although palm oil is regarded as a saturated fat, it may have different properties from animal fats because of its triglyceride structure where the palmitic acid is in the *sn*-1 and *sn*-3 positions and the unsaturated fatty acids are present in the *sn*-2 position mainly as 1,3 dipalmityl-2 oleoyl-*sn*-glycerol and 1,2 dioleoyl, 3- palmityl-*sn*-glycerol. Lard, contains a similar proportion of saturated fatty acids and unsaturated fatty acids compared to palm olein but is characterised by a high proportion (about 70%) of palmitic acid in the *sn-2* position of the TAG mainly as 1,3 dioleoyl-2-palmityl-*sn*-glucerol.

Interesterification is a process that does not affect the fatty acid composition but redistributes fatty acids in the three positions of TAG. Interesterification can be directed to place fatty acids in certain positions using enzymes, for example Betapol™, which is an interesterified fat made from palm olein that consists mainly of oleic, palmitic and oleic acid in sn-1, 2 and 3 respectively (OPO) and is used in the manufacture of infant formula because of its higher digestibility. More commonly interesterification involves randomization of vegetable oils either using a chemical catalyst such as sodium methoxide or bacterial derived enzymes. The randomization results in fatty acids being equally distributed among the three position of the triacylglycerol. The process is widely used by the food industry to make higher melting fats that are favoured for the functional characteristics in making margarine and bakery products. This technique is now in widespread in Europe when it was decided to avoid using the process of partial hydrogenations, which generates trans-fatty acid.

Palmitic acid in the *sn*-2 position of TAG as in lard is very well absorbed in rats (Kayden et al, 1967) whereas as randomized lard is less well absorbed (Boquillon et al, 1977). Furthermore, the fatty acids in the *sn*-2 position are retained in that position upon absorption, and TAG synthesis in the intestine retains the same fatty acid as in the *sn*-2 MAG (Small et al, 1991). Thus lard which is rich in (oleic, palmitic, oleic acid) OPO gives rise to chylomicron TAG that is rich in OPO. Sanders et al, (2011) have recently demonstrated differences in postprandial lipaemia between palm olein, interesterificd palm olein and lard and confirmed that there are differences in the structural

composition of the newly absorbed fat in human volunteers. The effects of altered stereospecific TAG structure on liver lipids are uncertain.

It was hypothesised that the stereospecific location of palmitic acid in TAG may result in a different pattern of fat accumulation in the liver. In order to test this hypothesis, an experiment was conducted using the high fat overfeeding model described in ***Chapter 5*** but substituting different fats.

6.2 Methods

6.2.1 Dietary fats

The four test fats compared were: high oleic sunflower oil (HOSO, Archer Daniel Mills, Erith, UK), native palm olein (PO, iodine value 56) (Archer Daniel Mills, Erith, UK) interesterified palm olein (IPO, made from the same batch of oil as the PO) and lard (Sainsbury PLC, UK). The fatty acid composition of the oil and the TAG molecular species were determined by high resolution gas chromatography by the European laboratories of Archer Daniel Mills (Hamburg, Germany). The fatty acid composition of the experimental fats was confirmed at King's College London following HCl-catalysed methylation to form methyl esters by capillary gas liquid chromatography (GLC) using a BP70 column (25 m x 220 µm x 0.25 µm; SGE Analytical Science, Victoria, Australia) on an Agilent 6890 (Agilent Technologies, Cheshire, United Kingdom).

Fatty acid methyl standards were obtained from Sigma (Poole, Dorset). The proportions of fatty acids in the *sn*-2 position of the TAG were determined following incubation of the TAG with porcine lipase (Type VI-S, from porcine pancreas, EC 3.1.1.3, 100,000 units, Sigma, Poole, Dorset, UK), separation of the 2-mono-acylglycerol and analysis of its fatty acid composition were conducted by Androulla Filippou (King's College London). The test fat (50 mg) dissolved in heptane (50 µL) was incubated with 0.5 ml sodium cholate and 1 g/L 1 M Tris pH 8.0 at 40°C, 0.2 ml $CaCl_2$ (220 g/L water, pre-incubated at 40°C) followed by 200 µl (20,000 units) lipase dissolved in TRIS buffer, the tube was immediately vortex mixed following the addition of lipase and incubated at 40°C in a shaking water bath for 1 min, removed and vortex mixed for 2 min, cooled on ice and 1 ml hydrochloric acid (6 N) and 3 ml diethyl ether added. The upper phase was collected and dried under nitrogen and the residue dissolved in heptane and applied to a Silica Gel G TLC (0.5 mm) plate and developed in

(hexane:diethyl-ether:formic acid glacial (140:60:4 by volume). Following development, the plates were sprayed with 5 mg 2'7'-dichlorofluorescein/L methanol water (95:5 by volume) and bands visualized under a *uv* light source. A standard of 2-mono-oleoyl-glycerol (Sigma, Poole, Dorset, UK) was used to identify the monacylglycerol band. The bands were scraped from the TLC plate and methylated with 2 ml methanol: toluene (80:20 by volume) containing 50 g/L HCl by incubation at 60°C for 2 h. The methyl esters were recovered from the upper phase following the addition of 6 ml potassium carbonate for GLC analysis.

The composition of the experimental fats of both palm olein fractions had a similar fatty acid composition but the native PO consisted mainly of 1, 3 dipalmityl-2 oleoyl-*sn*-glycerol and 1, 2 dioleoyl, 3- palmityl-*sn*-glycerol. The proportions of palmitic acid at the *sn*-2 position were 0.6 mol% in HOSO, 9.2 mol% in PO, 39.1 mol% in IPO and 70.5 mol% in lard. The lard contained a similar proportion of saturated fatty acid (47.0 *vs*. 47.8 mol %) and oleic acid (39.2 *vs*. 39.6 mol %) compared to PO and IPO but contained more stearic acid (16.2 *vs*. 4.0 mol %) and less palmitic acid (29.1 *vs.* 42.5 mol %) (***Table 6.1***).

Differential scanning calorimetry (Reading Scientific Services Ltd; Reading, UK) showed lard to have single melting point peak at 32.9°C and the IPO to have two melting point peaks at 16.6°C and 38.2°C; measurement of the solid fat content by NMR (Reading Scientific Services Ltd; Reading, UK) of lard and IPO gave values of 7.9% and 9.7% at 32°C, 4.8% and 4.7% at 37°C and 2.7% and 2.2% at 42°C respectively. PO had a single melting peak at 13.3°C and was fully melted at that temperature; neither PO nor HOSO contained solid fats above 32°C.

Table 6. 1: Proportions of fatty acids in the total fat, in the sn-2 position and the triacylglycerol (TAG) composition of the experimental fats

Fatty acids		Mol %			
		HOSO	**PO**	**IPO**	**Lard**
14:0	total	0.1	1.3	1.3	1.7
	sn-2	0.0	0.6	1.2	3.3
16:0	total	4.4	42.5	42.5	29.1
	sn-2	0.6	9.2	39.1	70.5
16:1	total	0.1	0.2	0.2	2.8
	sn-2	0.0	0.0	0.3	3.2
18:0	total	2.8	4.0	4.0	16.2
	sn-2	0.3	1.6	5.6	5.0
18:1n-9	total	80.5	39.6	39.6	39.2
	sn-2	87.8	69.1	43.0	14.1
18:2n-6	total	10.6	10.8	10.8	8.6
	sn-2	11.3	19.5	10.8	3.9

Carbon Number	TAG species	Mol %			
		HOSO	**PO**	**IPO**	**Lard**
46:0	MPP/PMP	0.0	0.2	0.7	0.2
46:1	MOM/OMM	0.0	0.1	0.5	0.2
48:0	PPP	0.0	0.8	7.8	0.8
48:1	MOP/OPM	0.0	1.6	1.5	1.2
48:2	MLP/LMP	0.0	0.4	0.6	0.5
50:0	PPS/PSP	0.0	0.2	2.2	2.8
50:1	POP/PPO	0.6	29.4	22.6	8.6
50:2	PLP/LPP	0.2	9.3	6.6	3.3
52:0	PSS/SPS	0.0	0.0	0.3	4.0
52:1	POS/PSO/SPO	0.5	5.1	4.2	22.9
52:2	POO/OPO	10.8	23.0	22.3	23.2
52:2	PLS/PSL/LPS	0.0	2.0	0.0	8.1
52:3	PLO/LPO/LOP	1.8	9.9	11.2	11.0
54:0	SSS	0.0	0.0	0.0	0.4
54:1	SOS/SSO	0.0	0.6	0.5	1.6
54:2	SOO/SOP	6.8	2.6	2.1	3.9
54:2	SLS/LSS	0.0	0.0	0.0	0.5
54:3	OOO	76.8	3.5	6.2	3.4
54:3	SLO/OSL/LOS	0.0	1.2	1.1	2.7
56:2	AOO/OAO	0.0	0.2	0.0	0.0
	Diacylglycerol	2.4	9.9	9.8	0.7

Taken from Sanders et al, (2011). A, arachidic acid; L, linoleic acid; M, myristic acid; O, oleic acid; P, palm olein; S, stearic acid.

6.2.2 Animal models and materials

Male C57BL/6J mice were obtained from Charles River, UK and housed singly in raised bottom wired cages. Semi-synthetic diets containing 18% by weight fat were prepared in a food lab free from contamination: the fat was provided by the test fats, high oleic sunflower oil (HOSO), the palm oil (PO), interesterified palm oil (IPO) and the lard (see ***Table 2.3***). The dough like consistency diets was formed into pellets by hand and frozen for 12 hours in -40°C before transferring to the freeze-drier for 3 days. The freeze-dried pellets were then stored in 4°C cold room until experimentation. Condensed milk containing 8% (w/w) of the test fat was freshly prepared by mixing *Carnation Light* (contains no fat) in a ratio of 92:8 by volume with the test fat on the day of feeding to mice in respective groups. The composition of the test milk is shown in ***Table 2.4***. Source of materials and detailed list of ingredients for all diets are provided in ***Chapter 2***.

6.2.3 Experimental design

A parallel design was used to compare 32 animals randomly allocated to 4 treatments (8/group): HOSO (control), PO, IPO and lard. For 6 weeks, animals were allowed *ad libitum* access to the respective pellets and CM. After 6 weeks on the experimental diet, the animals were euthanized.

Blood samples were collected via cardiac puncture under anaesthesia and whole blood was processed to obtain serum after cervical dislocation. Liver, epididymal fat pads, soleus, plantaris and gastrocnemius muscles were collected, blotted dry and weights were recorded. All tissues were sectioned into separate vials before being rapidly frozen in liquid nitrogen and stored in -70°C until analysis.

6.2.4 Analysis of tissue

The methods used for analyses are described in detail in ***Chapter 2***, briefly lipids were extracted from liver (Folch et al, 1957) and fractionated into non-esterified fatty acids (NEFA), triacylglycerols (TAG), cholesteryl esters (CE) and phospholipids (PL) by solid phase extraction (Kaluzny et al, 1985). Heptadecanoic acid (C-17) containing internal standards were added to quantify the fatty acids present in each fraction. All 4 fractions were methylated and loaded onto the gas chromatograph to obtain individual fatty acid profiles using acid catalysis with HCl (Lepage & Roy 1986). Epididymal fat pads (~50 mg) were treated with 2 ml of a 5% solution of HCl in methanol:toluene

(80:40 by volume) at 60°C for 2 hours to yield fatty acid methyl esters which were collected from the upper phase following the addition of 4 ml 6% potassium carbonate solution. The upper phase was diluted with hexane and analysed by gas chromatography. The hind limb muscles (soleus, plantaris and gastrocnemius) were weighed and recorded to determine if there were signs of muscle loss during the feeding period.

6.2.5 Statistical analysis

Data were analysed using SPSS version 18.0 by analysis of variance (ANOVA). Tukey's multiple range tests was used to make comparisons between diets when the overall F value was $P<0.05$. Chi-squared test was used to compare the differences in the frequency of certain distributions.

6.3 Results

6.3.1 Food intake

Energy intakes during the study are shown in ***Figure 6.1*** and ***Appendix 6.1.*** Initially there were small differences in energy intakes between groups but by week 5 these differences had disappeared and the overall energy intake for the 6 week period did not differ between groups. Average energy intakes with 95% CI were 104 kcal/week (98, 109) in the HOSO group, 109 kcal/week (102, 116) in the PO group, 113 kcal/week (108,117) in the IPO group and 109 kcal/week in the lard group. Energy intakes were similar in the PO group to that reported in ***Chapter 5*** for the HF diet, which had an identical composition. Energy intakes from solid food and condensed milk are shown in ***Appendix 6.2*** and ***6.3***, respectively. In all groups, the contribution to energy intake from solid food was less than that from condensed milk in which the condensed milk provided 70% - 80% of the energy intake.

Figure 6. 1: Energy intake (kcal/week) from consumption of all sources over 6 weeks of feeding period in mice fed either a high fat high oleic sunflower oil (HOSO), palm olein (PO), interesterified palm olein (IPO) or lard diet

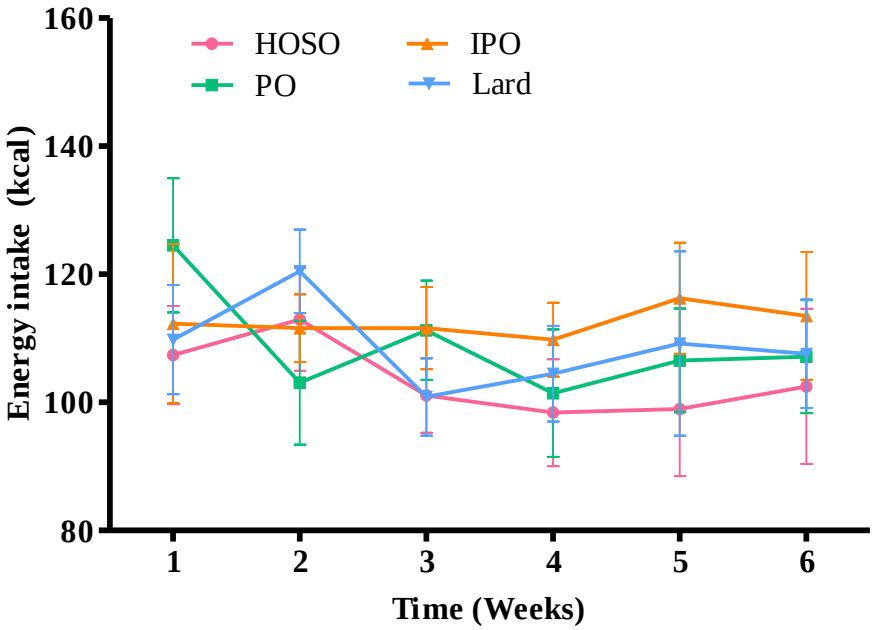

Mean values ± SD for 8 animals/group. Data were analysed by repeated measures ANOVA. No significant differences in energy intake between groups

6.3.2 Body and organ weights

Body weights increased by 2.4, 2.5, 2.6 and 2.3 g in the HOSO, PO, IPO and lard groups, respectively but did not differ significantly between groups (***Figure 6.2*** and ***Appendix 6.4***). The animals appeared to be in good health throughout the study and did not show significant weight loss in all groups (***Appendix 6.5***).

There was a significant difference in liver (P=0.047) with the liver weight being highest in the IPO group (***Table 6.2***). Total limb muscle weights tended to be marginally lower in the HOSO but not in adipose tissue and muscle weights or in ratio of soleus: plantaris ratio between treatments. However, the liver weights and adipose tissue weight were significantly highest in animals fed on IPO and lowest in HOSO group.

Table 6. 2: Organ weights (g) after 6 weeks of overfeeding either high oleic sunflower oil (HOSO), palm olein (PO), interesterified palm olein (IPO) or lard diets.

	HOSO	PO	IPO	Lard	P Anova
Liver (mg)	771 (706,837)	817 (740,895)	904 (832,976)	825 (736,914)	P = 0.047
Epididymal adipose tissue (mg)	340 (139,541)	414 (185,644)	468 (226,709)	410 (211,609)	P = 0.797
Soleus muscle (mg)	12 (11,13)	12 (10,14)	12 (10,14)	12 (10,15)	P = 0.961
Plantaris muscle (mg)	23 (21,25)	22 (20,24)	24 (22,26)	24 (22,26)	P = 0.327
Gastrocnemius muscle(mg)	174 (165,183)	178 (172,184)	181 (172,190)	174 (159,190)	P = 0.635
Soleus:plantaris ratio	0.513 (0.476,0.550)	0.554 (0.466,0.641)	0.507 (0.438,0.575)	0.508 (0.410,0.606)	P = 0.710
Total hind limb muscles (mg)	197[a] (187,207)	213 [a,b] (205,220)	217 [b] (206,228)	211 [a,b] (194,228)	P = 0.050

Values are expressed as mean with 95% CI. Data are analysed by one way analysis of variance. Values with different superscripts indicate significant differences between treatments using Tukey's multiple range tests. Total hind limbs are summations of the soleus, plantaris and gastrocnemius muscles.

Figure 6. 2: Body weights (g) over the 6 weeks feeding period in mice fed either a high oleic sunflower oil (HOSO), palm olein (PO), interesterified palm olein (IPO) or lard diets.

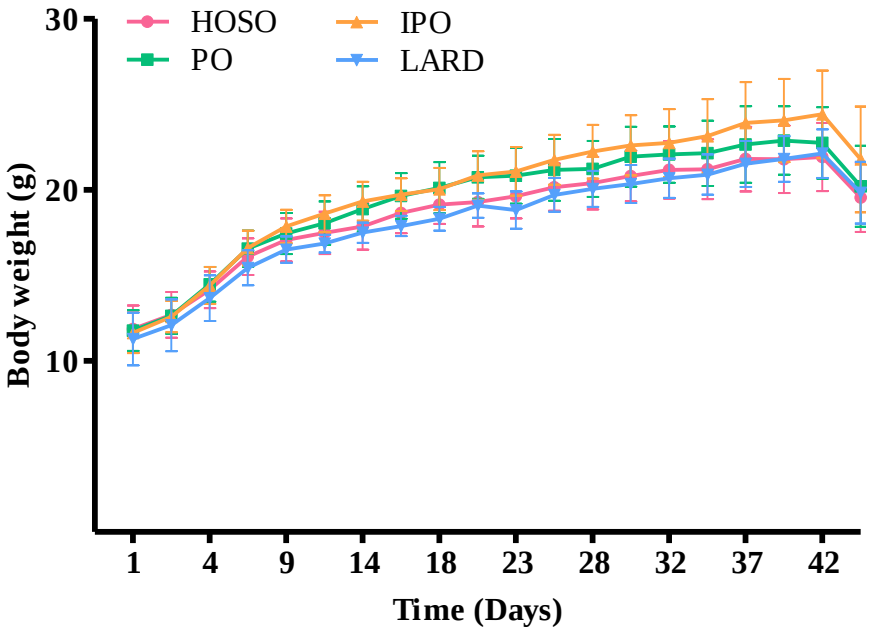

No significant differences in body weights between groups. Repeated measures ANOVA. Mean values ± SD for 8 animals /group.

6.3.3 Blood biochemistry

There was a tendency for plasma glucose concentrations to be high in all group (>7.0 mmol/L) (***Table 6.3*****).** However, there were no differences between treatments in serum lipids, liver enzymes alkaline phosphatase (ALP), aspartate aminotransferase (AST), alanine aminotransferase (ALT) and were unremarkable.

Table 6. 3: Serum analyses of insulin, glucose, cholesterol, triacylglycerols (TAG) and non-esterified fatty acids (NEFA) in mice fed either a high fat high oleic sunflower oil (HOSO), palm olein (PO), interesterified palm (IPO) or lard diest

	HOSO	**PO**	**IPO**	**Lard**	**P Anova**
Insulin (ng/ml)	0.6 (0.1,1.0)	0.5 (0.2,0.9)	0.5 (0.3,0.7)	0.4 (0.3,0.5)	P=0.820
Glucose (mmol/L)	8.9 (7.4,10.3)	10.0 (3.6,16.4)	8.9 (7.4,10.3)	8.9 (7.4,10.4)	P=0.904
Cholesterol (mmol/L)	4.4 (3.9,4.8)	5.4 (1.0,9.8)	4.9 (3.8,5.9)	5.1 (4.7,5.5)	P=0.808
Triacylglycerol (mmol/L)	0.7 (0.6,0.8)	1.1 (0.2,2.0)	1.3 (0.5,2.1)	1.0 (0.8,1.3)	P=0.209
NEFA (mmol/L)	1.5 (1.0,2.0)	2.4 (0.2,4.6)	2.2 (1.4,2.9)	1.6 (1.1,2.0)	P=0.368
ALP (IU/L)	138 (76,200)	125 (4,245)	92 (37,147)	98 (77,118)	P=0.597
AST (IU/L)	200 (134,266)	363 (87,639)	233 (161,305)	213 (153,273)	P=0.162
ALT (IU/L)	31 (16,46)	31 (7,55)	38 (15,61)	24 (14,33)	P=0.429

Values are expressed as mean with 95% CI. Data are analysed by one way analysis of variance. Values with different superscripts indicate significant differences between treatments using Tukey's multiple range tests.

6.3.4 Fatty acids composition of adipose tissue

The fatty acid composition of the epidydimal adipose tissue compared to the dietary fat for the respective diets are showed in ***Figure 6.3*** and ***Appendix 6.6***. The fatty acid composition of the HOSO adipose tissue generally mirrored that of the diet except that the proportion of palmitic acid was greater than in the diet. In agreement with the findings in ***Chapter 5***, the PO diet resulted in a lower proportion of palmitic acid in adipose tissue than in the diet and a correspondingly higher proportion of oleic acid. IPO results in a higher proportion of palmitic acid compared to PO (23.8 vs 27.3%) and lower proportion of linoleic acid (7.9 vs. 9.9%). The proportion of stearic acid was greater in the lard fed animals than in the other groups. In contrast to the PO fed animals, the proportion of palmitic acid was similar to that provided in the diet on the lard diet. Adipose tissue from the PO fed animals contained significantly more docosahexaenoic acid (0.3%) compared with the other diets (<0.1%).

Figure 6. 3: Fatty acids composition (weight %) of adipose tissue of C57BL/6J male mice fed either a high oleic sunflower oil HOSO), palm olein (PO), interesterified palm olein (IPO) or lard diets.

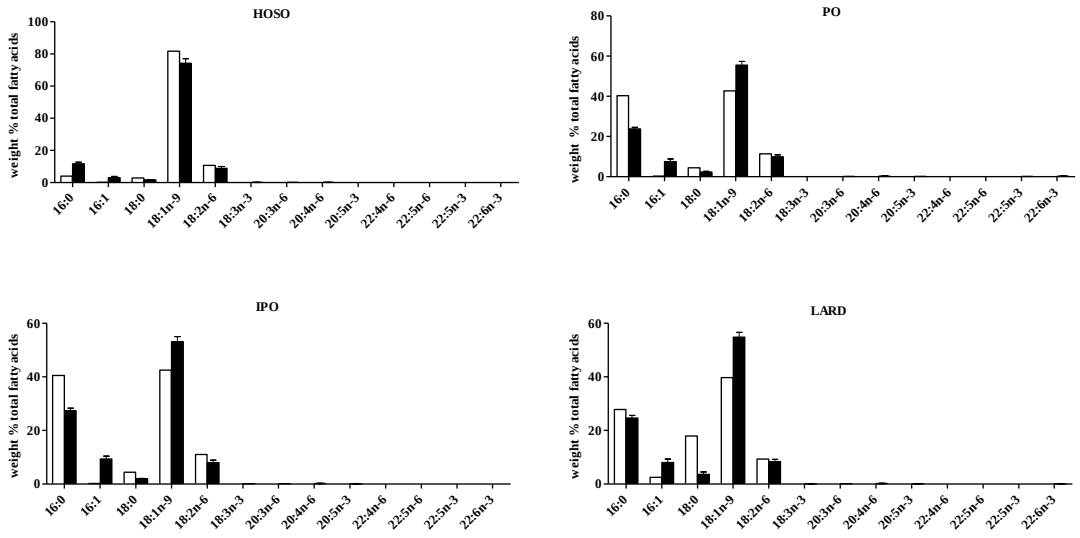

Mean values ± SD, 8 animals/ group. Open bar, dietary fat, filled bar, adipose tissue

6.3.5 Total liver lipids and proportions in different class

The lipid concentrations expressed as fatty acids in the different lipid fractions did not differ between treatments when expressed per gram tissue (***Table 6.4***). However, when expressed on a per liver basis, the difference between the IPO diet and other diets became significant albeit for only PL (***Figure 6.4***).

Table 6. 4: Liver lipid concentrations as mg fatty acids/g liver in mice fed either a high fat high oleic sunflower oil (HOSO), palm olein (PO), interesterified palm olein (IPO) or lard diets)

Fatty acids	HOSO	PO	IPO	Lard	Statistical significance
NEFA	13.6 ± 3.7	11.8 ± 3.6	9.8 ± 3.7	9.5 ± 1.7	P=0.070
TAG	50.3 ± 7.8	54.5 ± 16.9	36.5 ± 11.8	34.6 ± 6.2	P=0.090
CE	31.8 ±10.5	31.9 ± 7.5	38.1 ± 10.9	32.6 ± 7.7	P=0.489
PL	60.4 ± 3.5	60.4 ± 5.8	71.5 ± 12.1	63.4 ± 10.5	P=0.057

Mean values± SD, 8 animals /group except for PO n=7. Data were analysed by one-way analysis of variance

Figure 6. 4: Fatty acid concentrations (mg/ liver) in different liver lipid fractions in mice overfed high oleic sunflower oil (HOSO) palm oil (PO), interesterified palm oil (IPO) or lard.

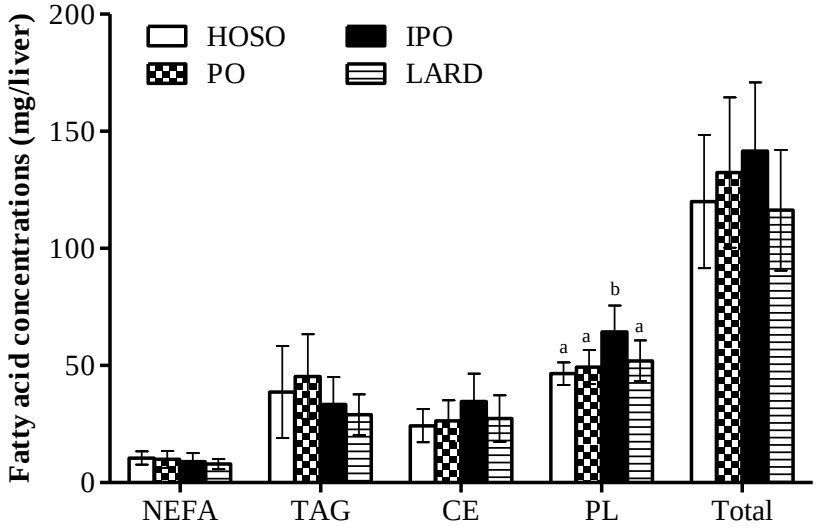

Mean ± SD; n=8 animals/group. Open bar, HOSO; checked, PO; filled bar, IPO; line, lard. Data were analysed by one way analysis of variance (ANOVA). Bars with different superscripts indicate significant differences (P<0.05) between treatments using Tukey's multiple range test.

6.3.6 Fatty acids concentrations by degree of unsaturated in liver lipid fractions

The concentrations of fatty acid classes in the various lipid fractions are shown in ***Figure 6.5***. The concentration of PUFA in the NEFA, TAG and CE fractions were greater in the PO compared with IPO and lard diet. In contrast, the concentration of MUFA was greater in the cholesteryl esters and phosholipids on the IPO compared to PO. The concentration of SFA was lower on the HOSO diet compared with the other diets in the phospholipid fraction

Figure 6. 5: Lipid concentrations according to degree of unsaturation in the major liver lipid gractions of mice overfed either high oleic sunflower oil (HOSO), palm olein, interesterified palm (IPO) or lard diets.

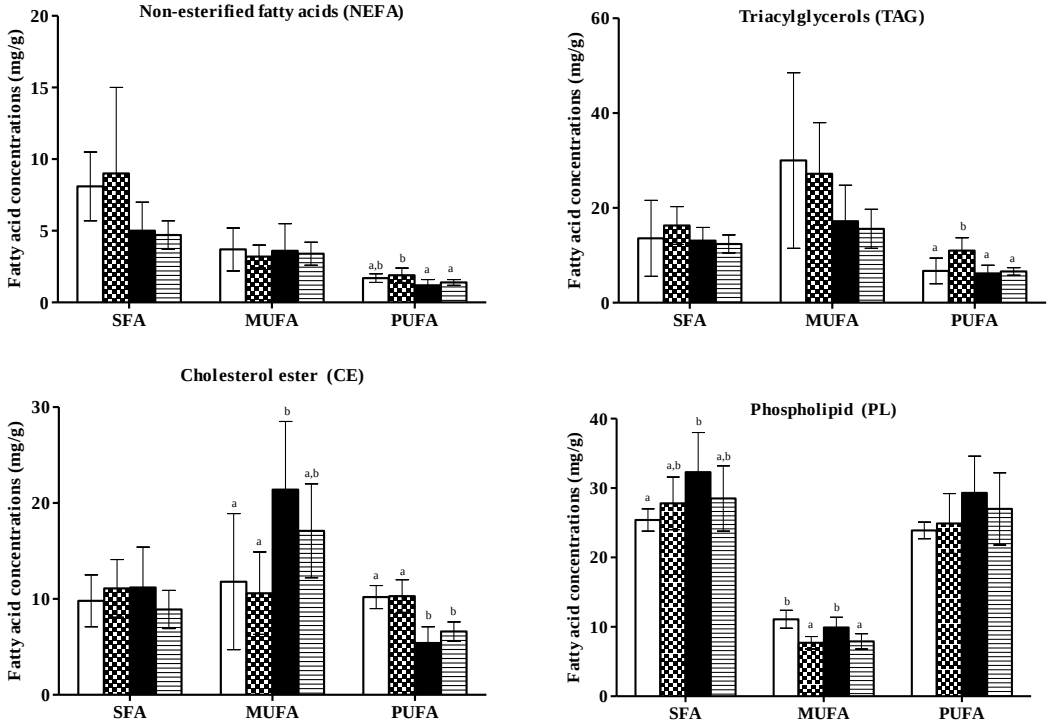

Mean ± SD; n=8 animals/group. Open bar, HOSO; checked, PO; filled bar, IPO; line, lard. Data were analysed by one way analysis of variance (ANOVA). Bars with different superscripts indicate significant differences (P<0.05) between treatments using Tukey's multiple range test.

NEFA= non-esterified fatty acids; TAG= triacylglcyerols; CE=cholesteryl esters; PL=phospholipids; SFA=saturated fatty acids; MUFA= monounsaturated fatty acids; PUFA= polyunsaturated fatty acids.

6.3.7 Fatty acids concentrations in distribution of short and long chain PUFA

The distribution of short and long chain polyunsaturated (LCP) fatty acids in different lipid classes is shown in ***Figure 6.6***. These results indicate substantial differences between treatments the palmitate fat rich diet. The proportion of n-3 LCP was greater in NEFA, TAG, CE and phospholipid in PO compared to HOSO, IPO and lard diets. The lowest proportion on n-3 LCP was found in the HOSO group in all fractions but the proportion of n-6 LCP was correspondingly greater. The proportion of n-6 LCP in the phospholipid fraction was greater in the IPO group compared to PO and lard.

Figure 6. 6 : Fatty acid concentrations (mg/g) of parent and long-chain polyunsaturated (LCP) n-3 and n-6 fatty acids in hepatic NEFA, TAG, CE and PL fractions in mice overfed either a high oleic sunflower oil (HOSO), palm oil (PO), interesterified palm (IPO) or lard diets.

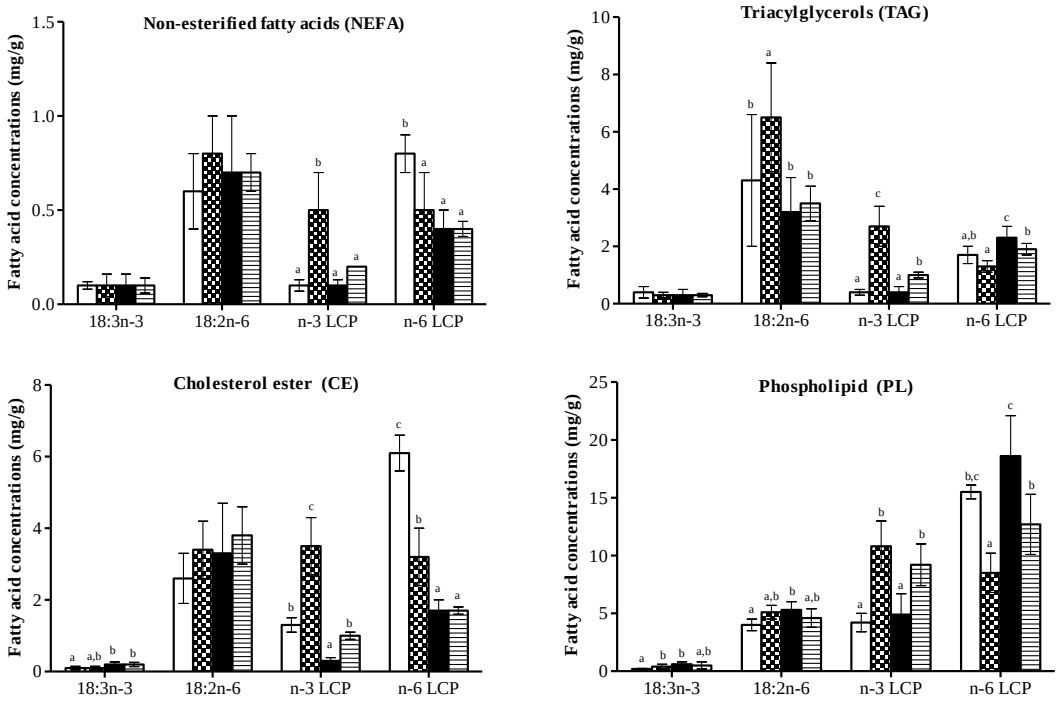

Mean ± SD; n=8 animals/group. Open bar, HOSO; checked, PO; filled bar, IPO; line, lard. Data were analysed by one way analysis of variance (ANOVA). Bars with different superscripts indicate significant differences (P<0.05) between treatments using Tukey's multiple range test.

6.3.8 Concentrations of major fatty acids in hepatic NEFA, TAG, PL and CE fractions

The concentrations of the major fatty acids in the liver lipid classes are shown in ***Figure 6.7***. The concentration of arachidonic acid (20:4n-6) was significantly greater in HOSO in NEFA when compared to the other groups. However, the concentrations of EPA and DHA were significantly greater in the PO group compared to the HOSO group and the IPO and lard groups.

For the TAG fraction, the concentration of palmitoleic acid was greater in PO, IPO and lard groups when compared to HOSO (***Figure 6.7***). As expected the concentrations of oleic acid was greater in the HOSO group but was also greater in the PO group compared to the lard group. The concentation of linoleic acid was highest in PO group in comparison to the other groups. Consistent with the finding in NEFA, the proportion of DHA were notably higher in the PO group compared with other groups.

As expected cholesteryl palmitate was significantly lower in the HOSO group compared with the other groups (***Figure 6.7***). However, cholesteryl oleate concentrations were higher in the IPO and lard groups compared with the HOSO and PO groups. Cholesteryl arachidonate concentrations were greater in the HOSO and PO groups compared with the other groups and the concentration of cholesteryl docosahexaenoate was notably high in the PO group, a finding that is consistent with ***Chapter 5***.

In the PL fraction, the concentrations of palmitic acid (16:0) were significantly lower in the HOSO group compared to the other groups (***Figure 6.7***). Oleic acid concentrations tended to be slightly high in the HOSO group. However, arachidonic acid concentrations were lower in the PO group compared to the other groups. The concentrations of DHA were higher in the PO and lard groups compared to the other groups.

Figure 6. 7: Major fatty acid concentration in different hepatic lipid fractions in mice overfed either a high oleic sunflower oil (HOSO), palm oil (PO), interesterified palm (IPO) or lard diets.

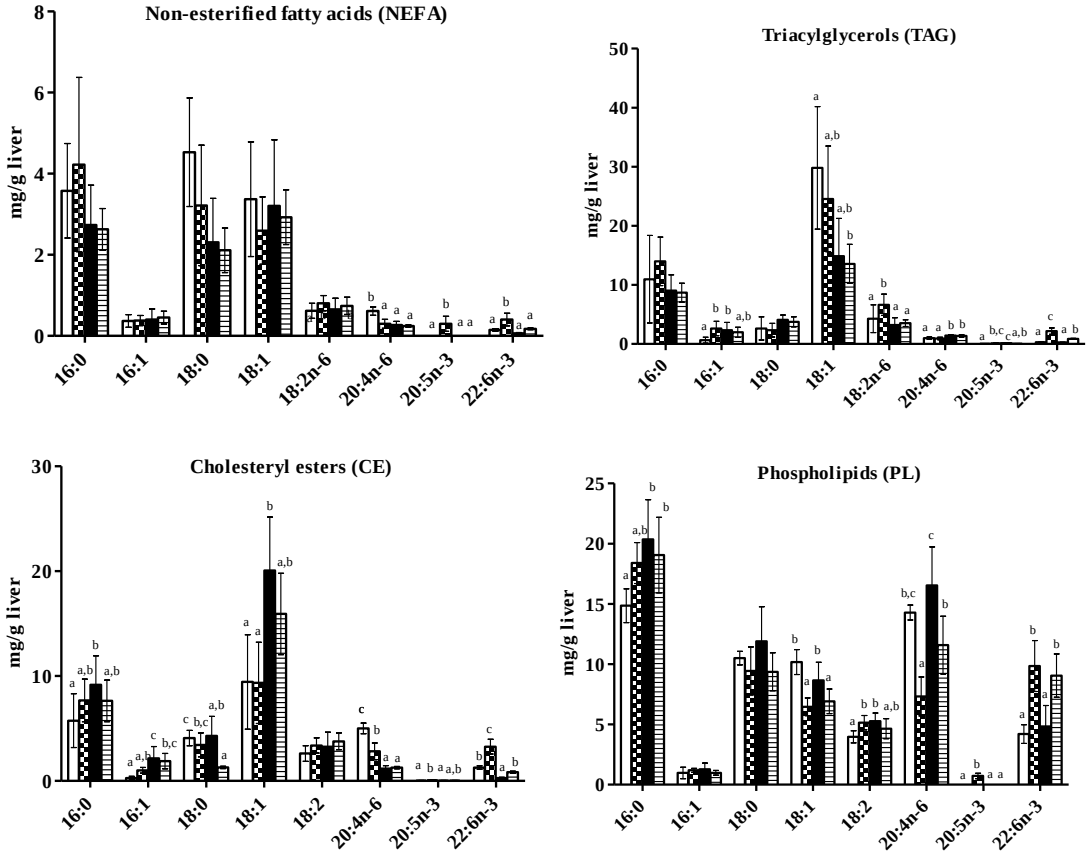

Mean ± SD; n=8 animals/group. Open bar, HOSO; checked, PO; filled bar, IPO; line, lard. Data were analysed by one way analysis of variance (ANOVA). Bars with different superscripts indicate significant differences (P<0.05) between treatments using Tukey's multiple range test.

6.4 Discussion

This study set out to determine whether the stereospecific structure of TAG influenced its subsequent metabolism in the liver. Overall, there were no differences in the proportions of total lipids in the various classes. However, there were significant differences in the allocation of various fatty acids to the various fractions notable between PO and IPO, which had virtually identical fatty acid composition. This study showed clear differences between PO and IPO on the fatty acids species in NEFA (palmitic acid and long-chain n-3 polyunsaturated fatty acids), in TAG (palmitic acid, oleic and long-chain n-3 polyunsaturated fatty acids) and cholesteryl esters (oleic acid, linoleic acid and long-chain n-3 polyunsaturated fatty acids) and phospholipids (palmitic acid, arachidonic acid and long-chain n-3 polyunsaturated fatty acids). As the fatty acid composition of the PO and IPO was similar and food intakes and growth rates were similar between the diets, the only likely explanation is the TAG structure. Furthermore, the lard diet showed similar effects on hepatic TAG and cholesteryl esters. The findings from this study are original in that they indicate that TAG structure influences hepatic lipid metabolism. As far as can be ascertained, this has not previously been reported.

It was hypothesised that there may be differences in adipose tissue fatty acid composition between PO and IPO. The proportion of palmitic acid was indeed lower in the PO vs the IPO and linoleic acid proportions were higher.

A consistent finding in this study and in the study reported in ***Chapter 5*** is the higher proportion of long-chain n-3 polyunsaturated fatty acids in hepatic lipids after palm oil feeding. This diet was devoid of long-chain n-3 polyunsaturated fatty acids and so these long-chain n-3 polyunsaturated fatty acids must have been synthesised from linolenic acid. There were only trace amounts of linolenic in the test oils and thus the main source of linolenic acid would be that associated with the milk or with the casein that was used to make the solid diet. The amounts of linolenic acid provided by the different diets would be similar. Therefore, the results of this study indicate that the capacity to convert linolenic acid to long-chain n-3 polyunsaturated fatty acids is favourably influenced by the amount of palmitic acid in the *sn*-1 and *sn*-3 position. This may be a consequence of competition for beta-oxidation with the higher concentration of palmitic acid sparing linolenic acid from oxidation and thus allowing it to be converted to longer chain derivatives. Lard, however, did not result in lower concentrations of DHA in phospholipids whereas IPO resulted in more arachidonic acid

and less DHA than PO. These findings may be of biological significance given the importance of arachidonic acid in eicosanoid formation and docosahexaenoic acid as a structural lipid in the brain and retina and require confirmation in another study.

Chapter 7:

Differential protein expression in low and high fat hypercaloric feeding

7.1 Introduction

The accumulation of triacylglycerols (TAGs) from lipids synthesised in the liver and influx of non-esterified fatty acids (NEFA) released from adipose tissue resulting in hepatic inflammation may cause steatosis and if not treated, may lead to NASH. The emerging interest among researchers in investigating the reversible state of NASH, which may further lead to the progression of permanent liver cirrhosis, is crucial due to the high prevalence of this disease.

The pathogenesis and the mechanisms of NASH are still being elucidated. Proteomic studies show that hepatic steatosis induced by high fat diets leads to the up-regulation of arginase 1 and down-regulation of endothelial nitric oxide synthase, whereby both proteins are involved in nitric oxide metabolism (Eccleston et al, 2011). Other proteins are also down-regulated (for example peroxiredoxin, glutathione S-transferase P1) or up-regulated (for example succinate semialdehyde dehydrogenase, glutathione synthetase and selenium binding protein) due to oxidative stress and/or induced by high fat feeding (Schmid et al, 2004; Douette et al, 2005; Kirpich et al, 2011). Some of these alteration in the liver also include perturbations in NEFA uptake from adipose tissue to the liver (Srivastava & Chan 2007), hepatic TAG accumulation in the liver (Lin et al, 2005) and hepatic liver inflammation (Lieber et al, 2004). Proteins associated with lipid metabolism such as fatty acid synthase (Jiang et al, 2009) and peroxisome proliferator-activated receptor-α (PPAR-α) (Abdelmegeed et al, 2010) are significantly down- and up-regulated, respectively, in response to high fat feeding. Furthermore, studies have also shown that insulin resistance is highly correlated with hepatic steatosis induced by high fat feeding (de Roos et al, 2009; Fiorentino et al, 2010). The complexities of hepatic steatosis induced by high fat feeding are multi-factorial and interrelated between several pathways which are yet to be discovered.

In studies whereby DHA and EPA are investigated independently, the biological effects on the liver have been inconsistent. Selective studies have suggested that EPA lowers hepatic epoxide hydrolase, which influences the inflammatory pathways whereas DHA affects lipoprotein metabolism (Pan et al, 2004) in relation to oxidative stress (Gonzalez-Periz et al, 2006; Mavrommatis et al, 2010; Li et al, 2011). EPA also alleviates saturated fat-induced insulin resistance by increasing hepatic fatty acid oxidation and decreasing inflammation (Kalupahana et al, 2010; El-Mowafy et al, 2011). Furthermore, DHA shows a stronger hepatic TAG-lowering effect compared to EPA due to a higher suppression of TAG synthesis (Gotoh et al, 2009), exhibited via the

reduction of insulin resistance through the increase of plasma adiponectin (Vemuri et al, 2007). Although both DHA and EPA are essential fatty acids, as individual fatty acids, they have differential effects on hepatic metabolism which requires further investigation

In this study, we addressed the hypothesis that proteomics can determine those proteins which change in response to high fat diets and n-3-polyunsaturated fatty acids. This will identify key regulatory proteins such as enzymes or structural proteins such as those which contribute to the mircroarchitecture. Protein expression studies do not specifically identify if changes occur via transcription (ie alterations in mRNA levels) alone but also those affected by perturbations in translation and/or proteolysis. Greater insights related to the cause of NASH using proteomics have been performed extensively in previous studies (Baranova et al, 2007; Rodriguez-Suarez et al, 2010; Burlamaqui et al, 2011). However, these aforementioned studies have limitations whereby none have examined hypercaloric diets in response to liver damage.

The advancement in proteomics techniques provides pattern recognition of biomarkers that are important for the early diagnosis of NASH. The discovery of clinically helpful biomarkers also allows for a better understanding of molecular mechanisms in the pathogenesis of NASH and its progression from simple steatosis to liver cirrhosis (Baranova et al, 2007). However, the underlying mechanisms of NASH remains incomplete and no mice model fully shows the clinical features of NASH observed in humans (Ariz et al, 2010). To gain a greater mechanistic insight into the processes that contribute to the changes in hepatic lipid profile of mice fed low fat (LF) and high fat (HF) hypercaloric diets, 2D-DIGE was used to identify proteins that were differentially expressed. Another aim of this study was to investigate if dietary EPA and DHA ameliorate changes in the expression of proteins in the liver induced by hypercaloric feeding.

7.2 Methods

Animal work, experimental diets and designs are outlined in ***Chapter 2***. All materials and methods for proteomics are described in ***Chapter 2*** and ***5***. The following sections provide information specific to this study. In this present experimental design, the 5 groups involved were low fat reference (LFR), low fat hypercaloric (LF), high fat hypercaloric (HF), high fat hypercaloric plus DHA (HFDHA) and high fat hypercaloric plus EPA (HFEPA) groups. Briefly, the LFR diet contained 2% corn oil whereas LF hypercaloric diet contained 2% corn oil plus condensed milk (CM). In addition, the HF hypercaloric diet contained 18% palm oil plus condensed milk (CM) and the HFDHA diet consisted of 15% palm oil and 3% DHA. Lastly, the HFEPA diet consisted of 15% palm oil and 3% EPA. Diets used for this study are described in ***Table 2.1*** and ***2.2.*** *Light* condensed milk has zero fat and was incorporated with 8% of fat (see ***Table 2.4*** for composition of light condensed milk and high fat (8% w/w) condensed milk.

7.2.1 DIGE experiment

All standard procedures were carried out according to the DIGE protocol provided by GE Healthcare. However, optimisation steps were applied to the samples accordingly, to obtain results that were shown in this chapter.

7.2.2 Liver preparation and solubilisation for DIGE

Protein extraction was carried out on individual mice liver samples and 2x lysis buffer containing 7 M urea and 2 M thiourea were used to solubilise proteins in the fatty liver because it has been tested to yield high extraction efficiency resulting in reproducible protein expression patterns (Zhou et al, 2005). Thiourea allows solubilisation of hydrophobic proteins which is essential due to the limited concentration of liver proteins. The concentration of proteins in the liver is estimated to be 150-250 mg/g liver tissue.

After tissue homogenization, proteins were quantified with the 2D-Quant kit before the clean-up procedure to ensure that proteins were not degraded during homogenization. Then the clean-up procedure was performed, followed by final protein quantification with the Pierce assay.

7.2.3 Two-dimensional gel electrophoresis and image acquisition

The 1st dimension separation was carried out on immobilized pH gradient (IPG) strips from pH 3 to 11. After equilibration, the strips were transferred to the slab gels (12.1% acrylamide and 0.38% bisacrylamide) for the 2nd dimension separation and run with anode (buffer based on piperidinopropionamide) and cathode (0.25 M Tris, 1.92 M glycine, 1% w/v SDS) buffer in an Ettan DALTtwelve electrophoresis unit for 5 hours. Proteins were detected using silver stain compatible to LC-MS/MS (Yan et al, 2000). Gels were scanned using an Ettan DIGE Imager.

7.2.4 Data analysis and statistical test

Assisted image analysis was performed using the DeCyder software (GE Healthcare). The average spot volume is directly related to the protein abundance and was thus used for data analysis. Statistical analysis of one way analysis of variance (ANOVA) was carried out and Tukey's multiple range tests was also carried out among the 5 groups. Protein spots were detected using DeCyder and confirmed to be matched on Auto level 1 which indicates a strong match across the gels. Protein spots were identified as *"TRUE"* if they were high in abundance and non-overlapping proteins. Only proteins that were abundant in volume were selected as proteins of interest because proteins spots could be subsequently picked by hand on the silver stained preparative gel. Proteins discussed in this study were selected for further identification based on its abundance and 3-D images using DeCyder.

The limitation in using DeCyder for statistical analysis is that P-values were not generated when analysis of variance (ANOVA) was used and therefore data was analysed using SPSS for multiple groups. Comparisons between (i) LFR vs LF, (ii) LFR vs HF, (iii) LF vs HF, (iv) HF vs HFDHA and (v) HF vs HFEPA were also discussed.

7.2.5 Experimental design for DIGE analysis

To minimize batch variation, the treatment groups with a sample size of 8 animals per group were subdivided into 2 groups of 4 and randomly assigned to 2 of the 3 batches. A control group was included in each batch. Therefore, each group of 4 represented one experimental block.

After allocating samples into experimental blocks, a symmetrical dye swap was applied. First and second dimension separations were run in 2 batches and all samples were spread evenly across the 2 batches to reduce biasness resulting from technical

influences. The randomization of Dye labelling and application of controls, treated and internal standards on IPG strips for 20 gels are shown in ***Table 7.1***. The internal standards consisted of all samples and were run in all gels to minimise gel to gel variations (Gorg et al, 2004).

Table 7. 1: The randomization of CyDye labelling and application of controls, treated and internal standards on 24 cm IPG strips

Gel	Sample/ Cy3	Label	Concentration (µL of 50 µg)	Sample/ Cy5	Label	Concentration (µL of 50 µg)	Internal standard/Cy2	24 cm IPG strip no.
1	**A1**	301	2.91	B1	309	1.97	Pool	36058
2	**B2**	310	1.99	C1	317	1.69	Pool	36059
3	**C2**	318	2.67	D1	325	1.97	Pool	34170
4	**D2**	326	2.08	E1	333	2.25	Pool	34171
5	**E2**	334	1.98	A2	302	2.75	Pool	36051
6	**A3**	303	1.66	C3	319	1.71	Pool	36052
7	**C4**	320	1.80	E3	335	2.37	Pool	36053
8	**E4**	336	2.24	B3	311	1.30	Pool	36054
9	**B4**	312	1.55	D3	327	1.75	Pool	36055
10	**D4**	328	1.53	A4	304	2.35	Pool	36056
11	**A5**	305	3.09	D5	329	2.18	Pool	96623
12	**D6**	330	2.01	B5	313	2.69	Pool	98330
13	**B6**	314	1.86	E5	337	2.62	Pool	98331
14	**E6**	338	2.49	C5	321	2.70	Pool	98333
15	**C6**	322	2.51	A6	306	2.39	Pool	98334
16	**A7**	307	1.79	E7	339	2.13	Pool	98335
17	**E8**	340	2.78	D7	331	2.18	Pool	98336
18	**D8**	332	1.84	C7	323	1.70	Pool	98337
19	**C8**	324	2.64	B7	315	1.31	Pool	98338
20	**B8**	316	2.98	A8	308	2.11	Pool	98339

A=LFR, B=LF, C=HF, D=HFDHA, E=HFEPA; there were 8 animals/group. The numberings next to the letter represent the individual mice from respective groups. The internal standards are represented by Cy2 (yellow) and the controls and treated samples were either dyed in Cy3 (red) or Cy5 (blue).

7.3 Results from 2D-DIGE

7.3.1 Scanned images from 2D-DIGE

From the 1st and 2nd dimension separation, the protein spots seen on the gel images were scanned with the Ettan DIGE Imager. These gel images are presented as an overlaid image comprising of the treated, controls and internal standards (***Figure 7.1***). Spot quantitation was carried out on overlaid Cy2 (pooled internal standard)/ Cy5 or Cy2 (treated samples) on each gel, followed by gel to gel matching. Every protein spot is assigned a volume ratio by DeCyder which is expressed as protein abundance. The protein abundance is generated from the volume ratio between the internal standard and treated sample from the same gel. Using the relative sample as a reference, the DeCyder determines the abundance of specific protein spots (ie. same spot number) (Uwakwe 2004). By comparing all the protein spots to the same pooled internal standard there is no need for normalization (Uwakwe 2004; Marouga et al, 2005).

Figure 7. 1: Overlaid image (top left) of protein spots from all 3 scans comprising of controls, either low or high fat hypercaloric sample and internal standards

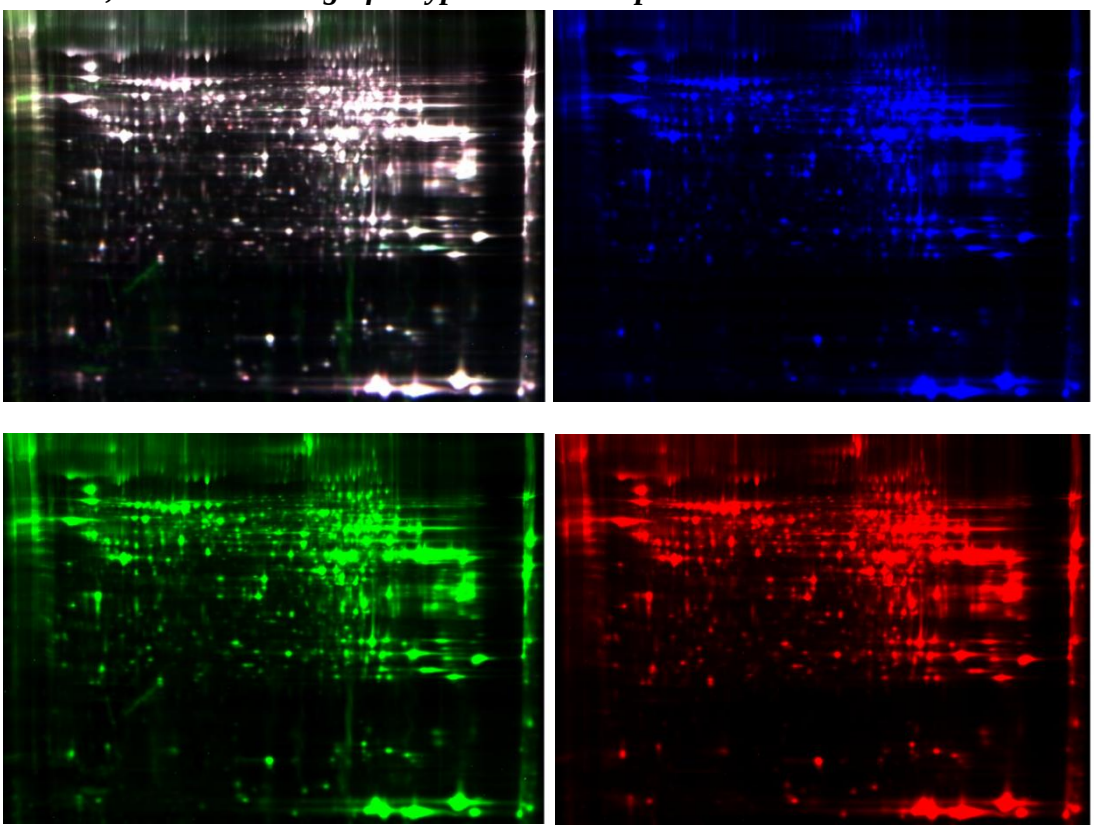

Controls are labelled with Cy5; blue, low or high fat hypercaloric sample stained with Cy3; red and internal standards with Cy2; yellowish green in this image

7.3.2 Preliminary data analyses

Of the 3291 protein spots on the master gel, 306 proteins were matched at Auto Level 1 among 20 gels by DeCyder (***Figure 7.2***). Ninety one protein spots were high in abundance and structurally the protein peaks were not overlapping. Of these 64 were proteins of interest matched on Auto Level 1. The proteins identified at Auto Level 1 were matched speculatively with the reference gel image of mouse liver in the SWISS-2D PAGE (Sanchez et al, 2001) before confirming by LC-MS/MS. Seventeen protein spots were tentatively identified using SWISS-2D PAGE of mouse liver in Expasy Bioinformatics Resource Portal based on its abundance (***Table 7.2***) and its 3D-peak images (***Figure 7.3***). However, only 6 of the 17 proteins were selected for LC-MS/MS because not all the protein spots identified using SWISS-2D PAGE were stained abundantly in the preparative gel. The other 8 proteins selected for validation using LC-MS/MS were based on their abundance on the preparative gel and reference to SWISS 2D-PAGE gel. A total of 14 proteins were analysed using LC-MS/MS.

Preparative gels were cast and stained with a silver preparation which is 50 times more sensitive compared to the Coomassie Brilliant Blue stain that detects only approximately 50 ng of protein (Winkler et al, 2007). In this study, the protein spots were picked by hand and therefore only protein spots that were visible and abundant on the preparative gels were selected for subsequent verification by LC-MS/MS. Sixty four protein spots were identified when scanning the analytical gel using DeCyder (***Figure 7.4***) whereas in the preparative gel stained with silver stain only 56 of the 64 protein spots of interest were visible (***Figure 7.5***). The protein spot map was made clearer by adding contour lines around the protein spot (***Figure 7.6***).

Figure 7. 2: Flow chart of image analysis and spot selection when comparing LFR vs LF and LFR vs HF

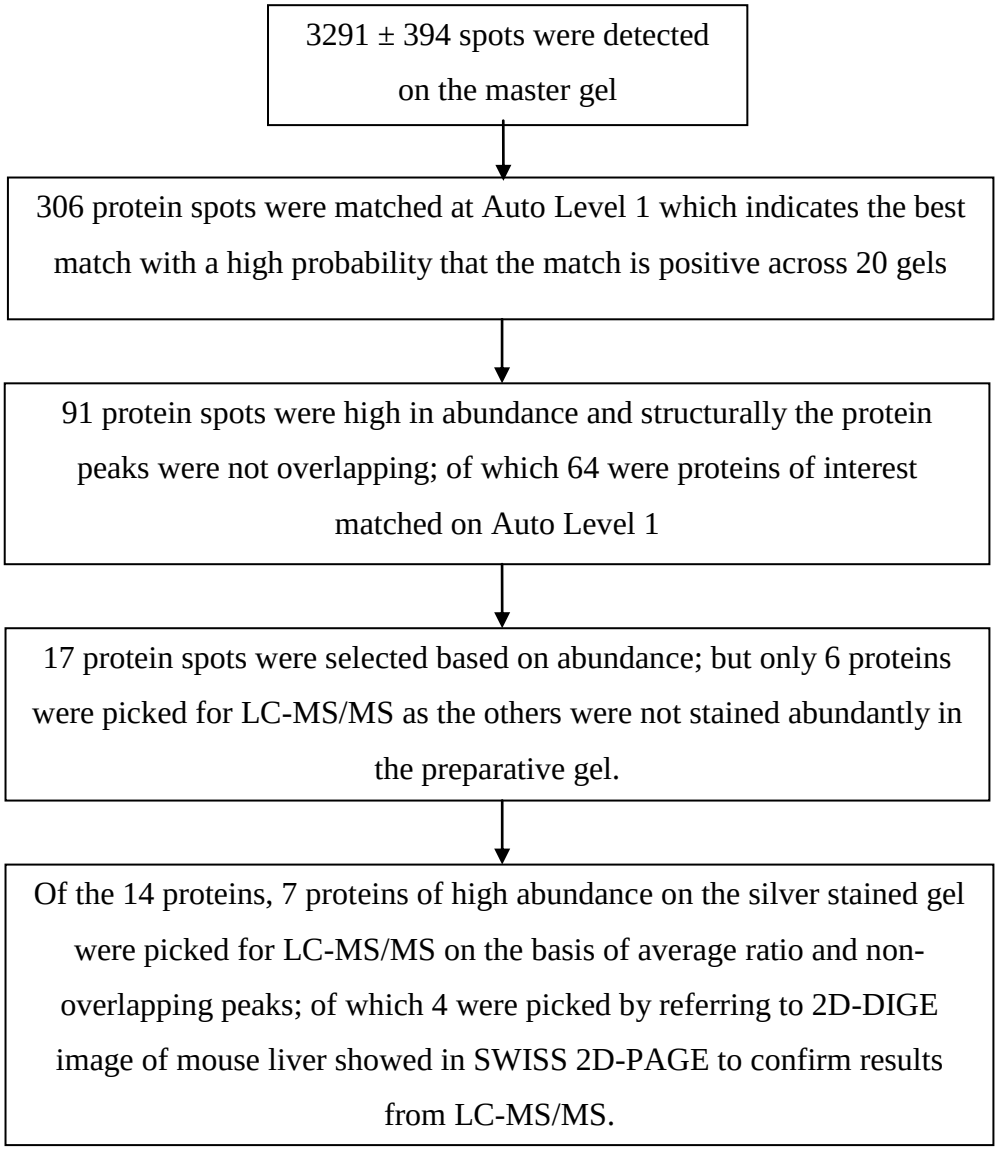

Figure 7. 3: Proteins of interest which were differentially expressed in mice fed low fat reference (LFR), low fat (LF) and high fat (HF) diets

Spot 1728 Spot 1846

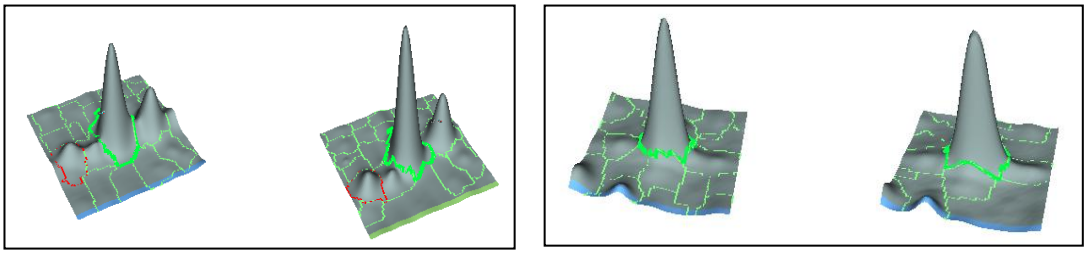

Represenatative images were generated by DeCyder version 6.5 and location of the spots on the gels are indicated by the green ring around the peak. Within the box, the left peak image represents spots from LFR mice and the right represents either the low fat or high fat groups

Figure 7. 4: Protein spots from the analytical gel with annotation on the proteins of interest

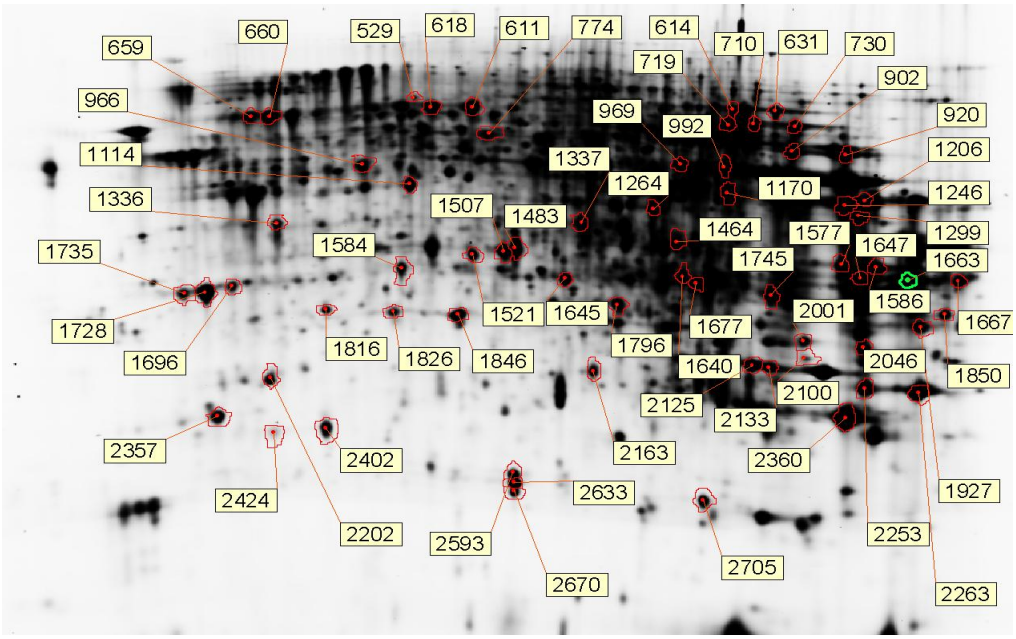

The protein spots circled in red are protein of interest (n=64) with non-overlapping protein peaks

Figure 7. 5: Post staining of preparative gels used for picking proteins of interest

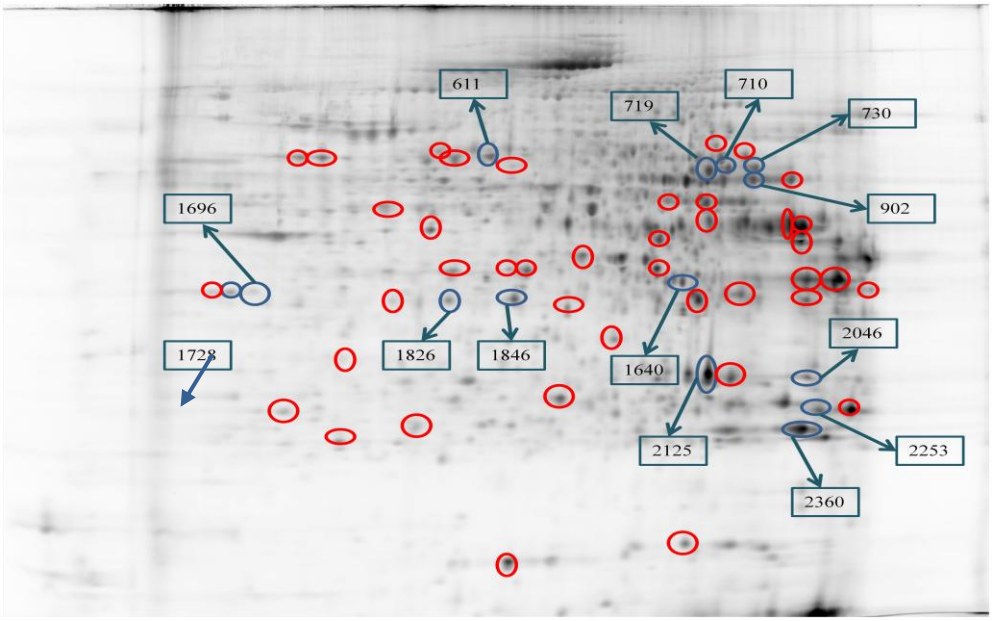

Protein spots of interest were detected on the preparative gel whereby 14 spots circled in blue were picked for LC-MS/MS. The spots circled in red were proteins of interest that were not picked. Proteins of interest picked were within the inclusion criteria of P<0.05 and at least a 1.5 fold change. Numbers in the box signify the spot identification given by DeCyder

Figure 7. 6: Protein spot map with contour lines and annotations on the proteins to be picked

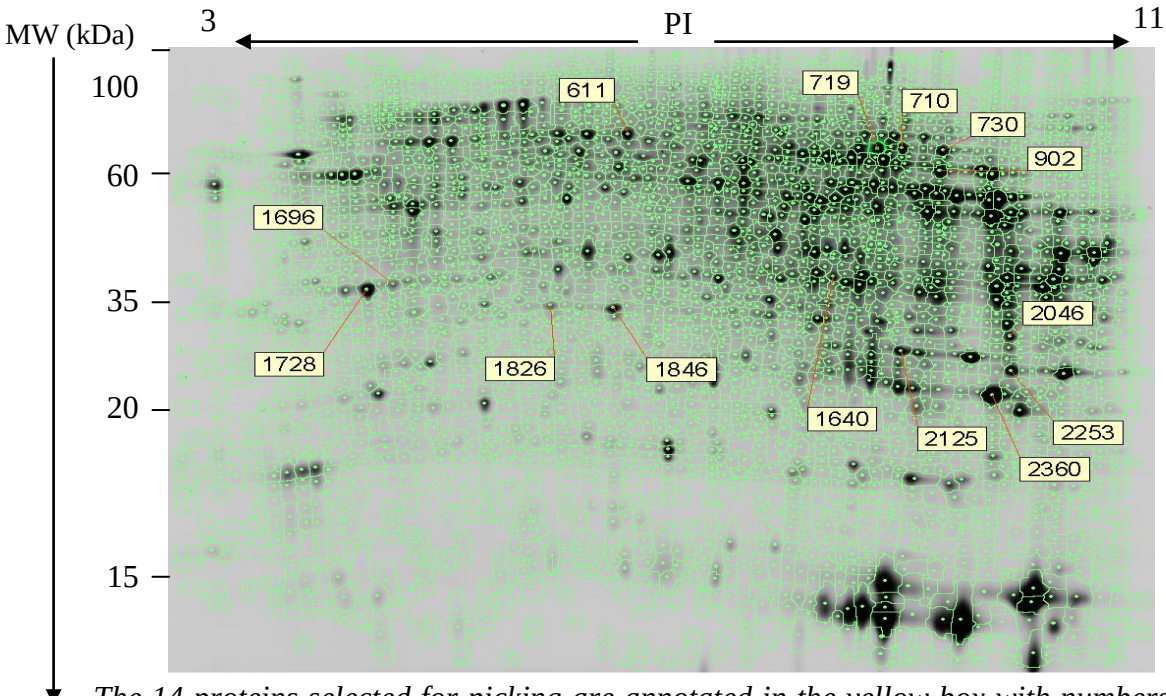

The 14 proteins selected for picking are annotated in the yellow box with numbers and noted by its contour line around the spot. Numbers signify the spot identification given by DeCyder.

7.3.3 Protein identification with LC-MS/MS

Fourteen selected proteins were digested with trypsin and peptides were analysed using LC-MS/MS by Dr. Mike Deery in Cambridge Proteomics Center, Cambridge UK. The MASCOT algorithm (Matrix Science) was used and searched against the NCBI mouse database. The accesssion number represents the unique identification number for the protein identified in the NCBI mouse database. Data from the LC-MS/MS analysis which included molecular weights, isoelectric point, protein scores and % coverage are shown in ***Table 7.3***. Data for the relative abundance of individual proteins are shown in ***Table 7.4***.

ANOVA showed that most of those proteins in ***Table 7.4*** were significantly altered by the various dietary interventions ($P<0.011$ to 0.001) except protein spots 1826 and 2253 ($P>0.05$). In the following text we describe first the effects of hypercaloric feeding with the LF and HF diets followed by the effects of DHA and EPA. In these descriptions we use the names of the identified proteins as we have every confidence in their assignments.

Ornithine transcarbamylase (OTC), regucalcin and malate dehydrogenase were found to be up-regulated between 40 and 130% when comparing LF with LFR (***Table 7.4***).

In the comparison for HF vs LFR, the up-regulated proteins were Isoform 1 of epoxide hydrolase 2 (EPHX2), catalase (CAT), ATP synthase subunit alpha (ATP5a1), OTC and regucalcin (RGN); changes ranged from 80 to 120% (***Table 7.4***).

Carbonic anhydrase 3 (CAR3) was down-regulated by 40% in HF when compared with LFR group. In addition, catalase, ATP5a1 and electron transfer flavoprotein subunit beta were up-regulated by 30 to 70% when comparing LF vs HF groups (***Table 7.4***).

Catalase was also found to be up-regulated by 40% in the HFDHA group when compared to HF group mice (***Table 7.4***).

Malate dehydrogenase (MDH1) and glutathione S-transferase A3 (GSTPA3) were picked for LC-MS/MS analyses despite not reaching statistical significance because they were found abundant on the preparative gel and were also identified to be proteins related to lipid and glucose metabolism when matched with the reference gel on SWISS 2D-PAGE.

The proteins identified with LC-MS/MS (***Table 7.3***) were compared to the protein spots that were matched with the reference gel on SWISS 2D-PAGE (***Table***

7.2). Protein spots matched with the reference gel showed only 64% accuracy. Therefore, the tentative protein spots shown in ***Table 7.2*** were deemed unreliable and were not used in the analysis to generate pathways in GeneGo.

Table 7. 2: Proteins identified tentatively using SWISS 2D-PAGE

Spot ID	Accession number	pI	MW		Tentative protein identification
611	P17563	5.87	52514	SBP1	Selenium binding protein 1
618	NF	NF	NF	NF	NF
719	P24270	7.72	59664	CAT	Catalase
902	P26443	6.71	55913	DHE3	Glutamate dehydrogenase 1
920	NF	NF	NF	NF	NF
992	P26443	6.71	55913	DHE3	Glutamate dehydrogenase 1
1170	NF	NF	NF	NF	NF
1264	P99023	7.53	42826	THIM	3-ketoacyl-CoA thiolase, mitochondrial
1337	P99016	6.43	41076	IVD	Isovaleryl-CoA dehydrogenase
1521	-	-	NF	NF	NF
1584	NF	NF	NF	NF	NF
1586	NF	NF	NF	NF	NF
1640	P11725	6.66	36123	OTC	Ornithine transcarbamylase, mitochondrial
1696	Q64374	5.16	33407	RGN	Regucalcin
2125	P16015	6.97	29235	CAR3	Carbonic anhydrase 3
2357	NF	NF	NF	NF	NF
2633	P08228	6.03	15811	SODC	Superoxide dismutase

Statistical test was carried out using Student's T-test. P-value with <0.05 indicates a significant difference between the groups and Average ratios with negative values indicate down-regulation of the protein in the experimental group and vice-versa. NF indicates that the protein was not found when matched to the reference gel on SWISS 2D-PAGE.The values of pI and MW are theoretical values obtained from ExPASy.

Table 7. 3: The protein identification by LC-MS/MS

Protein ID	Accession number (LC-MS/MS)	Protein identification from LC-MS/MS	pI	MW	Protein score	% Coverage
611	P34914	Isoform 1 of Epoxide hydrolase 2*	5.85	63045	1762	56.5
710	P24270	Catalase[&]	7.72	60043	1862	58.3
719	P24270	Catalase*	7.72	60043	1911	59.8
730	P24270	Catalase	7.72	60043	1803	60.0
902	Q03265	ATP synthase subunit alpha, mitochondrial*[#]	9.22	59830	1653	49.7
1640	P11725	Ornithine transcarbamylase, mitochondrial*	8.81	39854	1536	76.3
1696	Q64374	Regucalcin*	5.15	33899	1092	66.6
1728	Q64374	Regucalcin	5.15	33899	2840	73.9
1826	P14152	Malate dehydrogenase, cytoplasmic[#]	6.16	36659	906	47.3
1846	P14152	Malate dehydrogenase, cytoplasmic[#]	6.16	36659	948	47.9
2046	Q9DCW4	Electron transfer flavoprotein subunit beta[#]	8.24	27834	1105	63.5
2125	P16015	Carbonic anhydrase 3*	6.89	29633	1159	53.8
2253	P30115	Glutathione S-transferase A3	8.76	25401	728	61.5
2360	P19157	Glutathione S-transferase P1	7.68	23765	738	60.0

*PI stands for Isoelectric point and MW stands for molecular weight of protein. * indicates the proteins that were altered in the comparison of LFR vs LF or LFR vs HF groups. [&] indicates the protein was altered in the comparison of HF vs HFDHA.. [#]indicates the proteins that were not matched between the SWISSprot and LC-MS/MS. Protein score indicates how well the matching regions of polypeptides clusters are matched whereas the % coverage indicates how each of the polypeptides clusters match the protein. Proteins with the highest scores and % coverage were selected.*

Table 7. 4 : Protein abundance identified and validated with LC-MS/MS in mice fed either low fat reference (LFR), low fat (LF), high fat (HF), high fat DHA (HFDHA) or high fat EPA (HFEPA) diets

Protein name	**Spot number**	**LFR**	**LF**	**HF**	**HFDHA**	**HFEPA**	**P Anova**
Isoform 1 of Epoxide hydrolase 2	611	0.61 ^{a} ± 0.06	0.94 ^{a,b} ± 0.06	1.33 ^{b,c} ± 0.03	1.62 ^{c} ± 0.03	1.45 ^{b,c} ± 0.03	P<0.001
Catalase	710	0.72 ^{a,b} ± 0.02	0.63 ^{a} ± 0.03	0.88 ^{b,c} ± 0.03	1.23 ^{d} ± 0.02	1.12 ^{c,d} ± 0.01	P<0.001
Catalase	719	0.64 ^{a} ± 0.03	0.73 ^{a} ± 0.03	1.13 ^{b} ± 0.04	1.40 ^{b} ± 0.01	1.23 ^{b} ± 0.02	P<0.001
Catalase	730	0.83 ^{a,b} ± 0.04	0.76 ^{a} ± 0.09	1.16 ^{a,b,c} ± 0.03	1.60 ^{c} ± 0.03	1.32 ^{b,c} ± 0.02	P<0.001
ATP synthase subunit alpha, mitochondrial	902	0.52 ^{a} ± 0.02	0.63 ^{a} ± 0.05	1.10 ^{b} ± 0.02	1.20 ^{b} ± 0.02	1.23 ^{b} ± 0.04	P<0.001
Ornithine carbamoyltransferase	1640	0.73 ^{a} ± 0.02	1.00 ^{b} ± 0.04	1.30 ^{b,c} ± 0.03	1.59 ^{c} ± 0.03	1.38 ^{c} ± 0.03	P<0.001
Regucalcin	1696	0.52 ^{a} ± 0.09	1.02 ^{b} ± 0.06	1.16 ^{b} ± 0.02	1.06 ^{b} ± 0.02	0.88 ^{a,b} ± 0.04	P=0.001
Regucalcin	1728	0.51 ^{a} ± 0.12	1.00 ^{a,b} ± 0.07	1.19 ^{b} ± 0.03	1.09 ^{b} ± 0.03	1.00 ^{a,b} ± 0.05	P=0.008
Malate dehydrogenase, cytoplasmic	1826	0.64 ± 0.12	1.05 ± 0.06	1.02 ± 0.03	1.02 ± 0.05	0.74 ± 0.04	P=0.146
Malate dehydrogenase, cytoplasmic	1846	0.50 ^{a} ± 0.15	1.17 ^{b} ± 0.06	1.42 ^{b} ± 0.03	1.29 ^{b} ± 0.01	0.93 ^{a,b} ± 0.05	P=0.004
Electron transfer flavoprotein subunit beta	2046	0.95 ^{a,b} ± 0.03	0.88 ^{a} ± 0.03	1.16 ^{b,c} ± 0.01	1.28 ^{c} ± 0.02	1.13 ^{b,c} ± 0.01	P<0.001
Carbonic anhydrase 3	2125	1.35 ^{b} ± 0.03	1.12 ^{a,b} ± 0.05	0.86 ^{a} ± 0.03	0.81 ^{a} ± 0.04	0.79 ^{a} ± 0.05	P=0.001
Glutathione S-transferase A3	2253	0.79 ± 0.07	0.98 ± 0.09	1.10 ± 0.06	0.71 ± 0.03	0.74 ± 0.03	P=0.177
Glutathione S-transferase P1	2360	0.65 ^{a} ± 0.11	0.71 ^{a,b} ± 0.10	1.18 ^{a,b} ± 0.05	1.64 ^{b} ± 0.07	1.37 ^{a,b} ± 0.08	P=0.011

All data are expressed as standardized protein abundance ± standard errors. One way analysis of variance (ANOVA) and Tukey's multiple range test was used. Values with different superscripts indicate significant differences between treatments.

7.3.4 Functional analysis of selected proteins

The use of the bioinformatics software tool GeneGo allowed for the analysis of protein expression data in the context of regulatory networks, cellular pathways and biological functions (Beyer et al, 2007). Together with the statistical analysis obtained from the regulatory networks, the biological functions were linked to identify the possible pathways related to the effects of LF and HF hypercaloric diets on the liver. In this study, GeneGo was used to identify the selected protein networks, only using the tentative proteins assigned by LC-MS/MS. It was thought prudent to exclude proteins assigned by SWISSprot and these proteins were deemed to be speculative. Thus only isoform 1 of epoxide hydrolase, catalase, ornithine transcarbamylase, ATP synthase subunit alpha, regucalcin and carbonic anhydrase 3 were input into GeneGo. The use of GeneGo to analyse affected pathways in proteomic studies on the liver has been used before (Remily-Wood et al, 2011; Nikolsky et al, 2009).

The process networks associated with the selected proteins were identified by their *P-Value* and *Ratio*. The *Ratio* indicates the number of selected proteins against the number of proteins identified in all other studies involving the selected proteins. There were few associations between the selected proteins but a relatively high significance of pathways and processes when referred to each individual protein (***Table 7.5***).

The main process network associated with the significantly expressed protein was related to the response of hypoxia and oxidative stress ($P<0.001$) (***Table 7.6***). The top 10 diseases associated with the significantly expressed proteins were of high significance ($P<0.0001$) in comparison to other studies available in the GeneGo database (***Table 7.7***). The list of diseases was shown to be related to neuron disease, nerve dysfunction and urinary problems. The legend for the nodes used in the network clusters are shown in ***Figure 7.7***. The network clusters of the picked proteins and the predicted functional proteins are presented in ***Figure 7.8*** to ***7.11.***

Briefly, proteins such as ornithine transcarbamylase (OTC) is involved in the urea cycle (***Figure 7.8***) and carbonic anhydrase 3 (CAR3) plays an important role in the reversible hydration of carbon dioxide and nitrogen metabolism (***Figure 7.9***; Kim et al, 2001). However with only a few proteins identified to have been altered by hypercaloric feeding, any in-depth discussion in using pathway analysis would be imprudent.

Table 7. 5: Protein networks extracted from GeneGo bioinformatics software associated with the selected proteins identified by LC-MS/MS

Pathway networks	P Value	Ratio
Nitrogen metabolism	2.09E-02	*1/35
Nitrogen metabolism/ Rodent version	2.15E-02	*1/36
Urea cycle	4.14E-02	*1/70
Aspartate and asparagines metabolism	4.31E-02	*1/73
(L)-Arginine metabolism	4.49E-02	*1/76
HETE and HPETE biosynthesis and metabolism	4.72E-02	*1/80
Heme metabolism	5.53E-02	*1/94
Arginine metabolism (Rodent version)	5.70E-02	*1/97
Oxidative phosphorylation	6.16E-02	*1/105
ATP/ITP metabolism	7.12E-02	*1/122

Only 6 proteins were fed into the GeneGo analysis and they were assigned via LC-MS/MS as SWISSprot was deemed unreliable. The 6 proteins were as follows isoform 1 of epoxide hydrolase, catalase, ornithine transcarbamylase, ATP synthase subunit alpha, regucalcin and carbonic anhydrase 3

Table 7. 6: Process networks associated with the protein networks (refer to Table 7.5)

Process networks	P Value	Ratio
Response to hypoxia and oxidative stress	2.29E-05	*1/163

Only 6 proteins were fed into the GeneGo analysis and they were assigned via LC-MS/MS as SWISSprot was deemed unreliable. The 6 proteins were as follows isoform 1 of epoxide hydrolase, catalase, ornithine transcarbamylase, ATP synthase subunit alpha, regucalcin and carbonic anhydrase 3

Table 7. 7: Diseases associated with the selected proteins and tentative proteins extracted from GeneGo bioinformatics software

Diseases	P Value	Ratio
Ornithine transcarbamylase Deficiency Disease	4. 67E-04	*1/1
Acatalasia	4. 67E-04	*1/1
Urea Cycle disorders, Inborn	1.89E-03	*1/4
Metabolism, Inborn errors	2.40E-03	*3/659
Hyperammonemia	2.80E-03	*1/6
Hearing loss, noise-induced	6.06E-03	*1/13
Neurma, Acoustic	7.45E-03	*1/16
Cranial Nerve Neoplasms	7.45E-03	*1/16
Vestibulocochlear nerve diseases	7.45E-03	*1/16
Retrocochlear Diseases	7.45E-03	*1/16

Only 6 proteins were fed into the GeneGo analysis and they were assigned via LC-MS/MS as SWISSprot was deemed unreliable. The 6 proteins were as follows isoform 1 of epoxide hydrolase, catalase, ornithine transcarbamylase, ATP synthase subunit alpha, regucalcin and carbonic anhydrase 3

Figure 7. 7: Legends for the following protein network cluster as constructed by GeneGo. Nodes are presented in different colours and shapes to represent the origin and direction of regulation of protein.

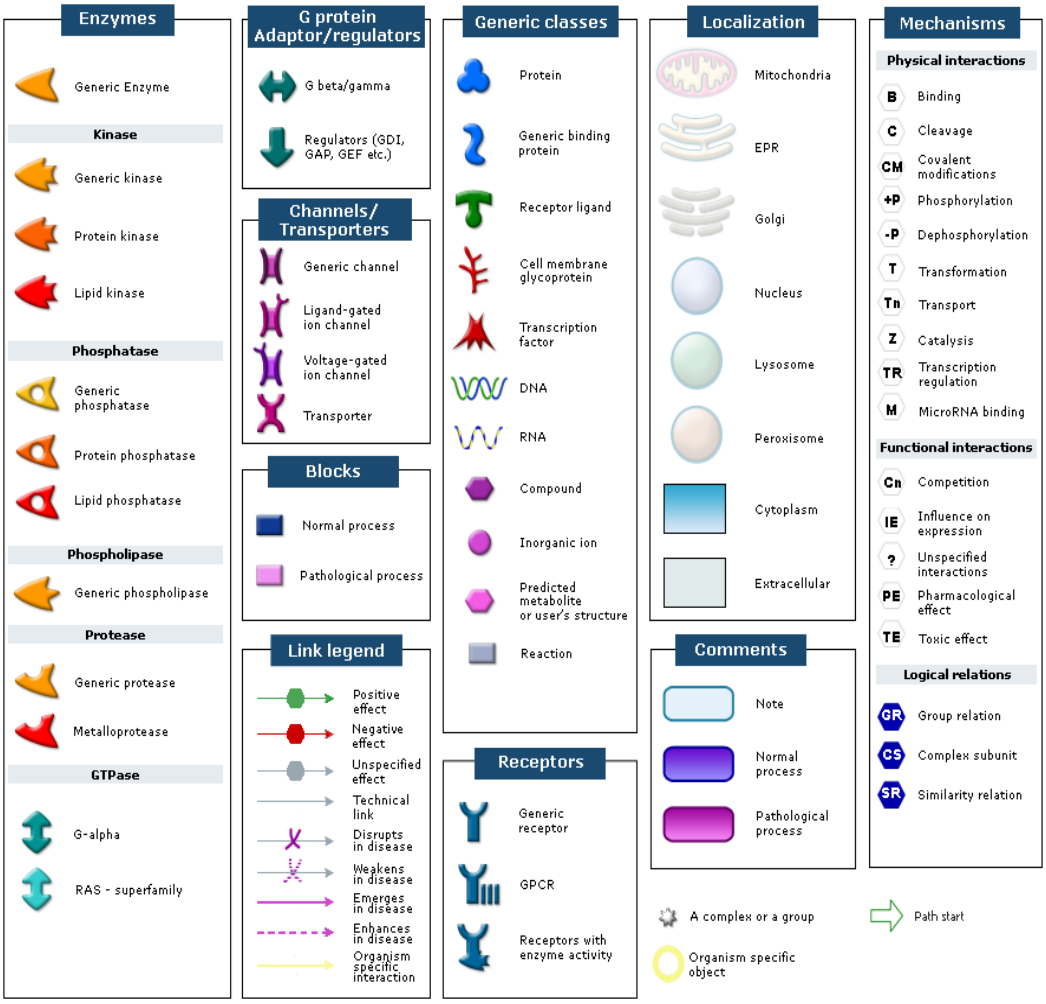

Source: GeneGo

Figure 7. 8: Ornithine transcarbamylase (OTC) as the picked protein in relation to the urea cycle

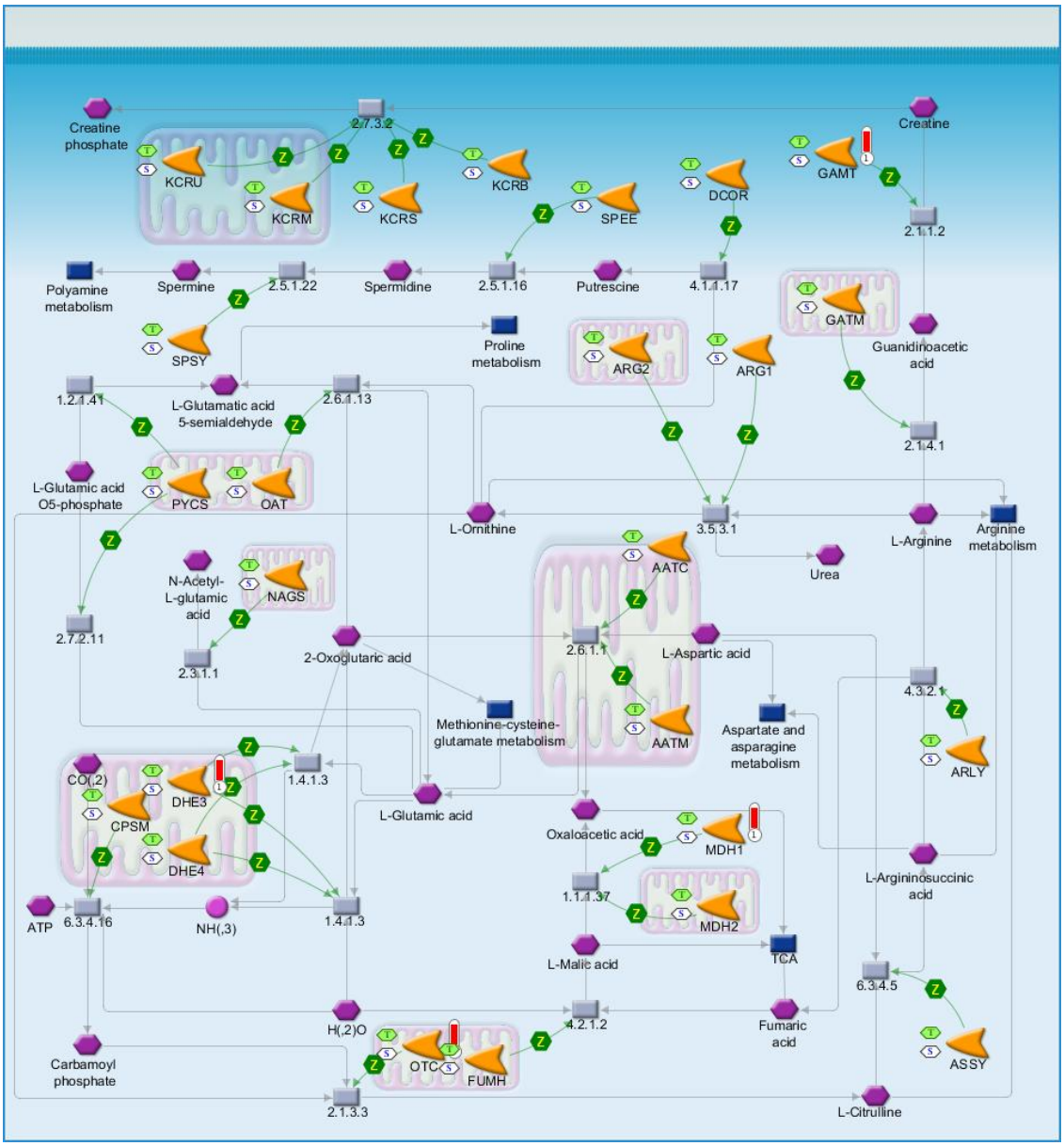

All legends are presented in Figure 7.7. The hexagons with letter T represents liver (tissue), S represents mouse (species), D represents liver (diseases). Source: GeneGo

Figure 7. 9: Carbonic anhydrase 3 (CAR3) in relation to nitrogen metabolism in mice

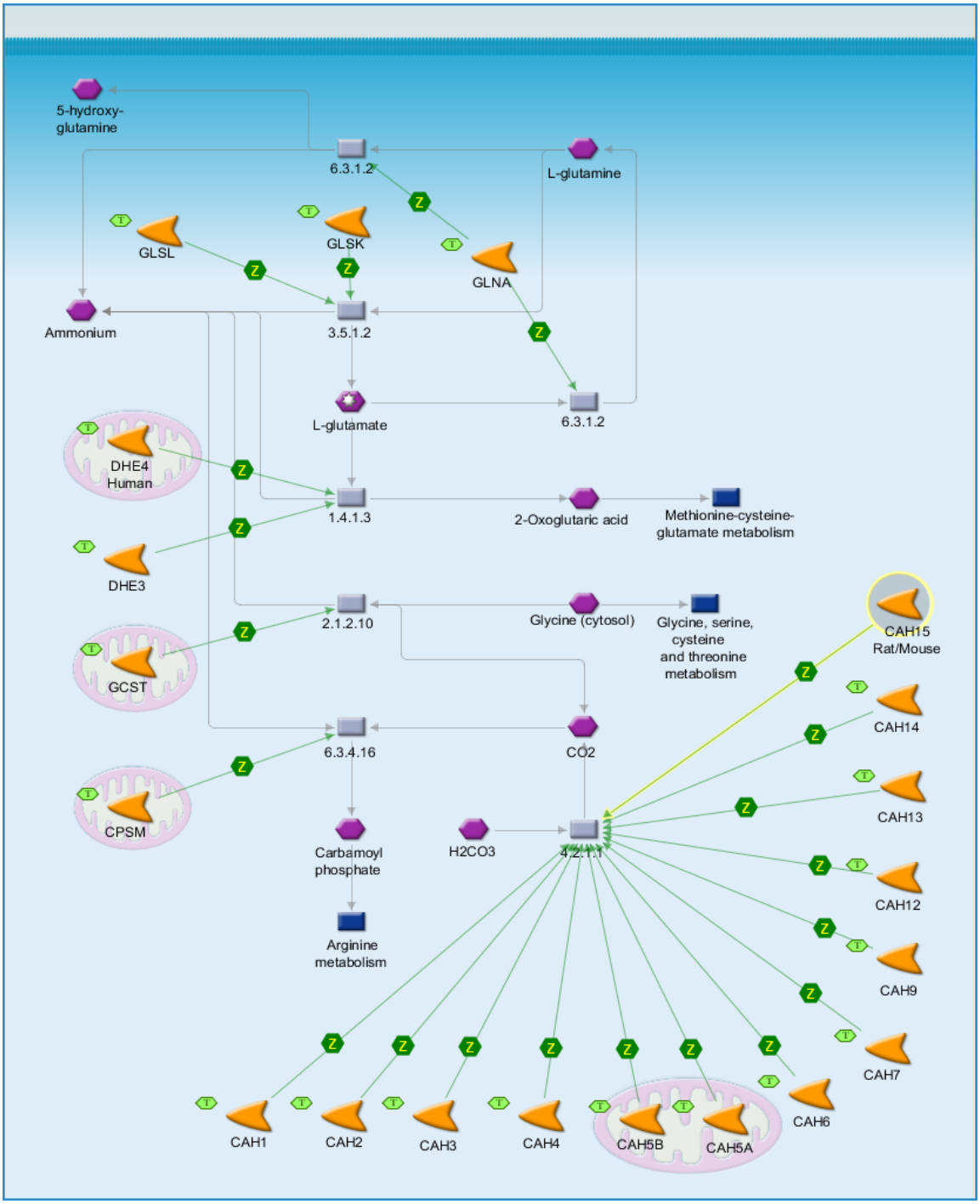

All legends are presented in Figure 7.7. The hexagons with letter T represents liver (tissue), S represents mouse (species), D represents liver (diseases). Refer to figure 7.7 for legend on respective nodes. Source: GeneGo

Figure 7. 10: *Ornithine transcarbamylase (OTC) involved in aspartate and asparagines metabolism*

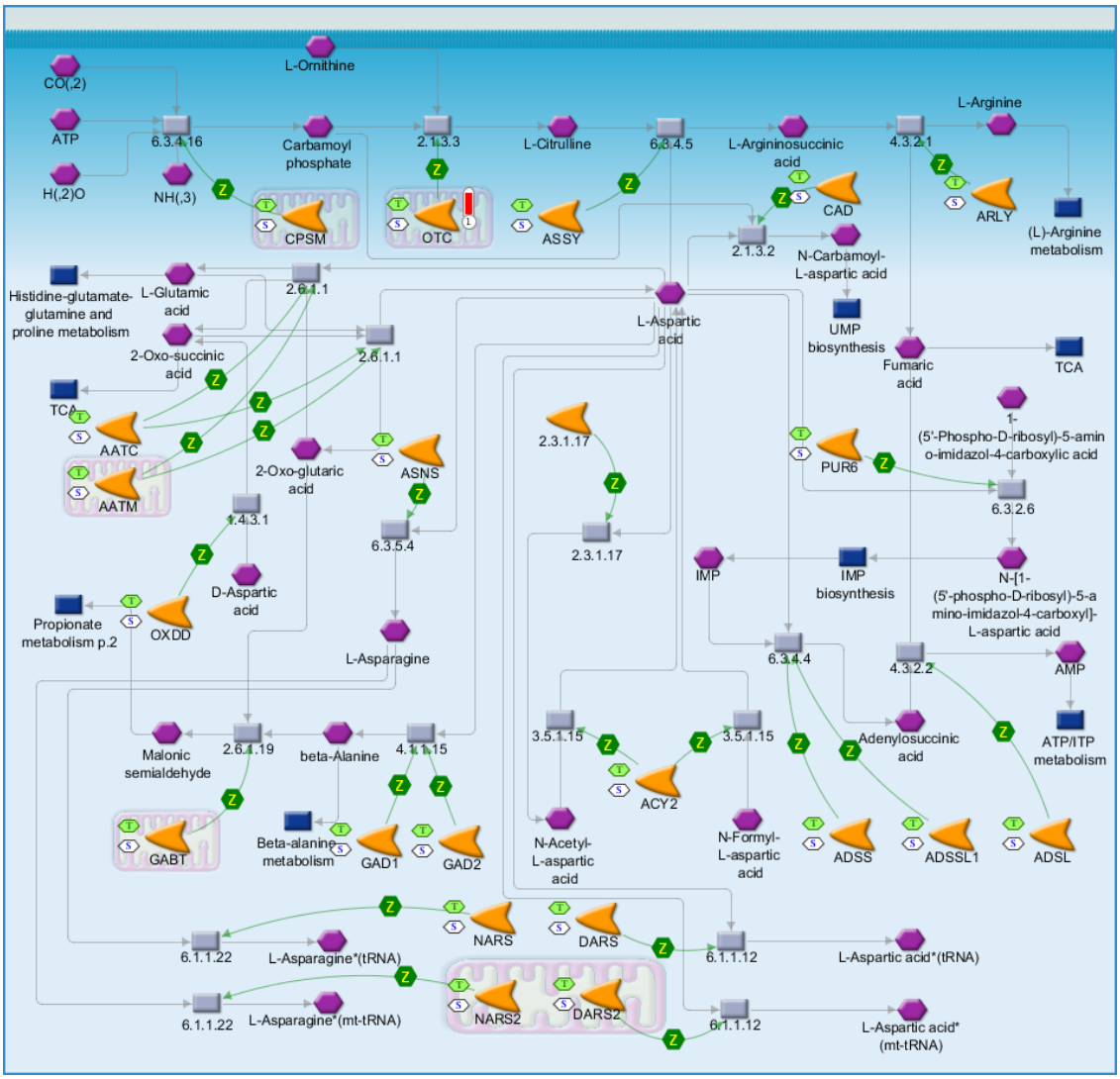

All legends are presented in Figure 7.7. The hexagons with letter T represents liver (tissue), S represents mouse (species), D represents liver (diseases). Source: GeneGo

Figure 7. 11: Ornithine transcarbamylase (OTC) involved in (L)-Arginine metabolism

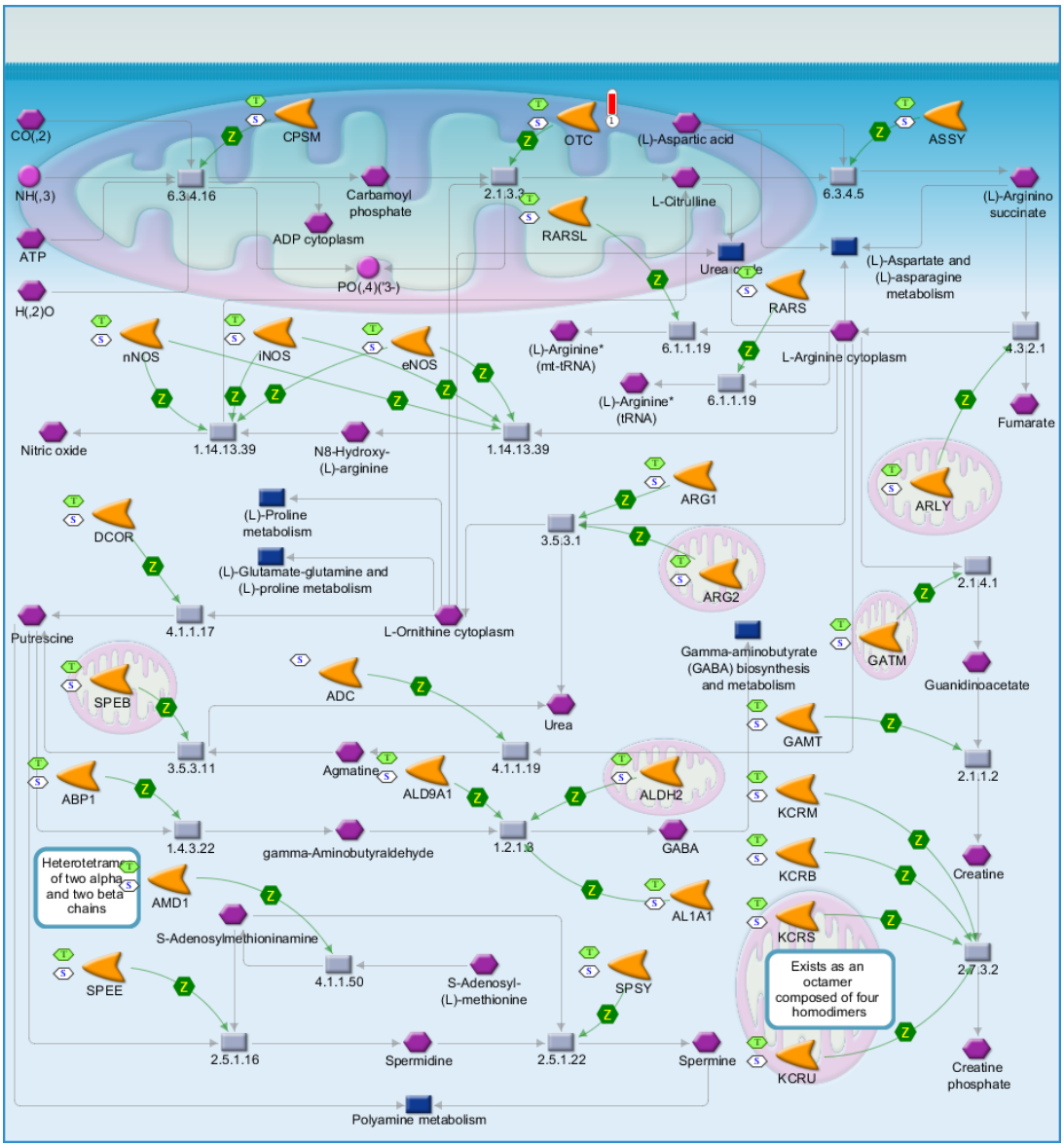

All legends are presented in Figure 7.7. The hexagons with letter T represents liver (tissue), S represents mouse (species), D represents liver (diseases). Source: GeneGo

7.4 Discussion

7.4.1 Methodological considerations

In these studies both LF and HF mice were fed high hypercaloric diets with condensed milk whereas LFR mice was the reference group fed with a low fat pelleted diet, without access to the condensed milk. Changes in protein expression in mice liver was identified using 2D-DIGE which is the most frequently used gel-based technique in clinical proteomics with good reproducibility (Marouga et al, 2005). From the 2D gels, proteins of interest were picked for identification by liquid chromatography tandem mass spectrometry (LC-MS/MS). Proteins were selected for LC-MS/MS on the basis of their average volume ratio and if there was a significant difference of $P<0.05$ when compared to the control group. Only non-overlapping protein spots and only those which could be picked by hand manually were considered for further confirmation by LC-MS/MS in this study.

In addition, non-overlapping proteins that were highly matched on Decyder at Auto Level 1 in the LF and HF groups when compared to the LFR group were tentatively identified using the reference mouse liver gel in SWISS 2D-PAGE. The tentative molecular weight (MW) and isoelectric point (PI) of the proteins were obtained from the reference gel on SWISS 2D-PAGE. To ensure that the tentative proteins were identified accurately, 4 proteins were randomly picked along-side to confirm the protein spots on the reference gel. However, the results obtained from LC-MS/MS showed that the identification of picked protein spots were only 64% accurate when compared to those on the reference gel on 2D-image on SWISS 2D-PAGE.

We assumed that the remaining protein spots that were differentially expressed and identified from the SWISS 2D-PAGE database, but not validated by LC-MS/MS, were not reliable. They were thus not fed into the GeneGo database for pathway analysis.

Although proteomic methods are considered to be reliable, there is still room for optimisation and such advancements in proteomic techniques incur a high cost and therefore may not necessarily be used effectively and broadly in clinical practice. A more precise and sensitive detection system may be required to identify the majority of the proteins affected by LF and HF hypercaloric diets in the liver. The clarification of how the protein profiles are modified as a consequence of the LF and HF hypercaloric diets on the liver is important in further investigating the progression of steatosis to NASH.

7.4.2 Biological implications of altered protein in liver due to hypercaloric feeding

The following section is a discussion on the specific proteins that altered in the metabolic pathways. To reiterate the points above, proteins were identified by LC-MS/MS and speculative proteins identified with SWISSprot are not discussed.

Mice in the LF and HF groups had increased liver size when compared to the LFR mice, also known as hepatomegaly (***Section 5.3.2***). Interestingly, total fats in the whole liver of LF and HF mice were not higher when compared to LFR mice but there was a significantly higher liver and adipose tissue weight in the HF group mice compared to the LF group. In concentration terms, hepatic NEFA was not significantly different when comparing LF and HF groups (***Section 5.3.9***) whereas hepatic TAG was significantly higher in HF mice when compared to LF mice (***Section 5.3.9***). Similarly, both hepatic CE and PL were significantly higher in HF fed mice compared to the LF fed mice. The significant increase in hepatic NEFA is mainly due to oleic and palmitic acid which is also reflected in the hepatic TAG fatty acid profile. The significant increase of hepatic CE in HF group is pre-dominantly caused by cholesteryl oleate, linoleate and plamitoleate esters. Lastly, in the PL species, there was a significant increase in palmitic, stearic acids and DHA in mice fed HF diets compared to the LF mice. These findings suggest that a high saturated fat intake does not exacerbate NASH (for further details please refer to ***Chapter 5***).

In the proteomics aspect of this chapter, proteins identified by LC-MS/MS shown to alter in response to HF hypercaloric feeding were as follows: isoform 1 of epoxide hydrolase 2 (EPHX), catalase, ATP synthase subunit-alpha mitochondrial (ATP5α1), ornithine transcarbamylase-mitochondrial (OTC), regucalcin and carbonic anhydrase 3 (CAR3). In the comparison between LFR and LF, OTC and regucalcin were up-regulated. EPHX, catalase, ATP5α1, OTC and regucalcin were up-regulated significantly in the comparison between LFR vs HF groups. CAR3 was significantly down-regulated in both HF and LF groups when compared to LFR. Only catalase was up-regulated when comparing HFDHA with the HF group.

7.4.3 Proteins involved in urea cycle: ornithine transcarbamylase (OTC)

Metabolic steps involved in urea excretion occur in the liver through a series of reactions between the mitochondria and cytosol. Ornithine transcarbamylase (OTC) is a catalyst responsible for the formation of L-citrulline in the 2nd step of the urea cycle in

the mitochondria (Morizono et al, 1997). A mutation in the OTC gene was shown to cause disordered urea synthesis (Stratford-Perricaudet et al, 1990; Brusilow & Maestri 1996). In this study for the thesis, OTC was found to be significantly up-regulated in the HF and LF group when compared to the LFR group but there was insufficient time to examine plasma ammonia levels. This merits further investigation. The up-regulation of OTC in the HF and LF mice may be due to the increase urea cycle activity in the mitochondria necessary for muscles to replenish the energy through the glucose-alanine cycle during the fasting state.

7.4.4 Protein involved in glucose metabolism: carbonic anhydrase III (CAR3)

Carbonic anhydrase III (CAR3) is a cytosolic protein found in skeletal muscle and liver (Tweedie & Edwards 1989) that catalyzes the interconversion of carbon dioxide and carbonic acid to generate hydrogen and bicarbonate ions which maintain pH balance (Sanyal 1984). CAR3 plays a role in hepatic *de novo* lipogenesis by utilizing bicarbonate required by acetyl-CoA carboxylase (Lynch et al., 1995) and CAR3 inhibitors have been demonstrated to reduce *de novo* lipogenesis in hepatocytes (Herbert & Coulson 1984). Besides that, CAR3 functions as an oxygen radical scavenger thus protecting cells from oxidative damage (Raisanen et al, 1999).

Changes in CAR3 together with glutathione S-transferase pi 1 (GSTP1) and catalase were found to be markers for pre-cancerous conditions in liver tissue (Kuo et al, 2003). Up-regulation of CAR3 is associated with liver fatty acid oxidation and down-regulation of this protein may lead to liver damage (Henkel et al, 2006). Changes in hepatic CAR3 is also commonly associated with amino acid or protein deprivation. For example, the lack of methionine and cysteine in the diet may be result in the up-regulation of GSTP1 and CAR3 (Ronchi et al, 2004) in the liver. Although CAR3 is significantly reduced in hepatocellular carcinoma induced mice, the reduction was inconsistent throughout the lobular liver structure when immunohistochemical analysis was carried out (Elchuri et al, 2007). Therefore, the mechanism causing the reduction of hepatic CAR3 in hepatocellular carcinoma remains unclear (Kim et al, 2004).

In this study, CAR3 in HF mice was down-regulated when compared with mice from the LFR group. This may indicate the decreased activity of *de novo* lipogenesis developed in HF mice due to the HF hypercaloric diet in comparison to LFR mice. However, no studies till this date have investigated how the different types of dietary fats affect the down- or up-regulation of CAR3.

7.4.5 Proteins involved in oxidative stress induced by HF hypercaloric diet: catalase (CAT)

Catalase functions as a catalyst for decomposition of hydrogen peroxide to water and oxygen to prevent toxicity of hydrogen peroxide, which may cause cell damage (Imlay 2003). Therefore, up-regulation of catalase in both LFR vs HF is correlated with low oxidative stress. Mice lacking catalase tended to develop Type II diabetes due to the high concentrations of hydrogen peroxide (Goth 2008). Furthermore, mice induced with NASH presented decreased levels of catalase activity compared with chow fed mice and in the absence of glutathione, detrimental hydroxyl radicals were disposed more slowly (Haque et al, 2010). Similar findings were found in ob/ob mice when hepatic steatosis was attenuated by feeding green tea extracts causing decreased adipose lipogenesis and enhanced hepatic antioxidant defences which resulted in increased hepatic catalase and glutathione peroxidase activity (Park et al, 2011). In addition, catalase is up-regulated in steatosis, indicating high activity to prevent hepatic oxidative stress (Bujanda et al, 2008) along with the increments of superoxide dismutase, glutathione peroxidise and nitric oxide synthase. In this study for the thesis, there was a significant up-regulation in HF group when compared to LFR group. Therefore, the HF group mice may have been prevented from hepatic oxidative stress as suggested by Bujanda et al, (2008). However, overall antioxidant status was not measured in these studies though this could be the focus of future investigations in this area.

7.4.6 Protein involves in maintaining cell homeostatis: regucalcin (RGN)

Regucalcin (RGN) plays an important role in maintaining cell homeostasis by regulating Ca^{2+} signalling in the liver. For example, the expression of mRNA RGN was found to increase 30 minutes after the administration of 5 to 30 mg per 100 g body weight of calcium to mice (Murata & Yamaguchi 1997). Furthermore, the inhibitory effect of RGN on protein kinase C that is activated by Transcription Factor-2 may phosphorylate activators of transcription thus leading to an increased expression in cancer cells (Yamasaki et al, 2009). Hepatic RGN is also shown to be stimulated by insulin (Nakashima & Yamaguchi 2006) and estrogens (Yamaguchi & Oishi 1995). RGN also regulates nuclear function in liver cells (Yamaguchi 2000).

The increased RGN expression in the HF and LF when compared to LFR group may have enhanced glucose utilization, via Ca^{2+} signalling pathway which is regulated

by RGN and stimulated by insulin (Yamaguchi et al, 1995). Unfortunately in this study, the aspects of calcium ions were not investigated.

7.4.7 Protein involve in transporting ATP: ATP synthase subunit-alpha (ATP5α1)

The ATP synthase subunit alpha (ATP5α1) is a mitochondrial membrane ATP synthase that functions as an ion carrier in the electron transport complex (Lee et al, 1990). ATP5α1 combines ATP synthesis and/or hydrolysis across the membrane via the ATPase proton in the presence of a proton gradient to produce ATP from ADP (Tappenden et al, 2011). ATP5α1 in mice liver was up-regulated in the HF group when compared with the LFR mice, which implies a higher rate of ATP synthesis indicating greater coordination in the regulating mitochondrial proliferating, and gene expression related to oxidative phosphorylation (Di Liegro et al, 2000). However, it is difficult to relate these findings to the characteristics changes in the whole liver of LF or HF fed mice as the aforementioned studies by Di Liegro et al, (2000) were specifically carried out in liver mitochondria.

7.4.8 Biological implications of altered protein in liver due to EPA and/or DHA

Polyunsaturated n-3 fatty acids such as DHA and EPA are known to be protective against high fat hypercaloric diet induced hepatic steatosis and inflammation in the liver, but the mechanism of which these individual fatty acids function in the liver is still unclear. Work in this thesis tested the hypothesis that the protective effects of EPA and DHA would be reflected in the protein profiles and in particular would identify proteins which have been previously ascribed to EPA or DHA-induced effects.

Furthermore in ***Chapter 5***, hepatic NEFA and TAG profiles of mice from the HFDHA group were markedly reduced compared to either the HFEPA or HF groups. The significant reduction of fats deposited in the liver was mainly due to the reduction of oleic acid. Although there were no other detectable alterations besides catalase in the protein expression when comparing mice fed the HFDHA hypercaloric diet versus HF diet, the effects of DHA in reducing oleic acid concentration in NEFA and TAG fractions in the liver may be an important aspect in this study and requires further investigation.

A study by Polozova & Salem (2007) showed that dietary DHA is more likely to be metabolised by the liver compared to dietary oleic acid. The uptake of dietary DHA

in the liver may be redistributed to the brain and retinal tissues where DHA is the predominant n-3 polyunsaturated fatty acid (Sinclair & Crawford 1972). The role of DHA in regulating LDL metabolism may mediate via lipoproteins as transporters for n-3 polyunsaturated fatty acids to the target organs rather than monounsaturated fatty acids (Polozova et al, 2006).

In contrast, one study showed that fish oil, but not pure DHA, significantly lowered hepatic epoxide hydrolase levels, an inflammatory response protein in mice fed DHA when compared to mice fed high-oleic sunflower oil (Mavrommatis et al, 2010). This may explain the role of EPA in lowering expoxide hydrolase more rapidly compared to DHA. However, there were no significant differences shown in this protein for the studies in the thesis, even though this protein was identifiable in the SWISSprot reference gel.

Catalase was detected to be up-regulated in HFDHA group when compared to the HF group. This may indicate a high decomposition rate of hydrogen peroxide to water and oxygen to prevent toxicity of hydrogen peroxide in the presence of DHA. However, there were no significant changes in the plasma levels of insulin, glucose, cholesterol, triacylglycerols (TAG), non-esterified fatty acids (NEFA) and liver enzymes (ALP, AST and ALT) when comparing HFDHA and HFEPA with HF group mice (***Section 5.3.3***).

Mice fed a high-fat fish oil diet for 3 weeks present significant increases in peroxisomal beta-oxidation and catalase activity in both liver and myocardium (De Craemer et al, 1994). Further investigations were carried out by the aforementioned study by De Craemer et al, (1994) whereby 2% of DHA administered to healthy mice was shown to induce significant increases in catalase protein of the myocardium after 3 weeks but there were no changes in catalase protein in the liver. In addition, there were no changes in the peroxisomes of myocardium and liver indicating that DHA dosage used in the study by De Craemer et al, (1996) did not disrupt fatty acid metabolism in the liver. In addition, Demoz et al, (1992) showed that hepatic acyl-CoA oxidase and catalase activities increased by 50% and 30% respectively in EPA administered mice. In this study for the PhD, catalase was significantly increased in HFDHA when compared with HF group. Catalase in the HFDHA group was consistently higher compared to the HFEPA group.

Consistently in ***Chapter 5***, DHA seem to show a higher effect in lowering TAG synthesis in the liver compared to EPA. Further studies are required to target protein expressions affecting hepatic fatty oxidation and synthesis.

7.5 Conclusion

In this study for the thesis, proteins shown to be differentially expressed using 2-D DIGE were selected for validation by LC-MS/MS. However, the concordance of agreement was poor. Nevertheless some proteins identified by LC-MS/MS play an important role in cellular respiration, ketone and carboxylic acid metabolism syndrome, generation of precursor metabolites and energy generation.

It is noteworthy that, proteins such as glutathione S-transferases were shown to be significantly down-regulated in other studies examining the liver in response to high fat feeding and hepatic steatosis (Kirpich et al, 2011). Moreover, glutathione S-transferases are known to be up-regulated in the liver due to increased hepatic inflammation and oxidative stress (Fernandes et al, 1996; Lee et al, 2009). Although both the proteins were identified by LC-MS/MS in this study for the thesis, they were not differentially expressed in the liver in response to feeding hypercaloric low or high fat diets. Future work may require a longer period of time to see the differential effects of hypercaloric feeding on liver protein profiles.

However, the precise molecular mechanisms for the effects of the HF hypercaloric diet on the liver are still unclear. Future work is required to comprehend the influence of dietary fats on liver metabolism in this chapter.

CHAPTER 8:

The differential expression of microRNA (miRNA) in the liver of mice fed with low fat or high fat hypercaloric diets containing eicosapentaenoic or docosahexaenoic acid

8.1 Introduction

Various studies have shown that hypercaloric diets predispose the liver to both the suppression of hepatic fatty acid oxidation and an excessive influx of fatty acids from adipose tissue to the liver, causing steatohepatitis also commonly called NASH (Dolganiuc et al, 2009; Estep et al, 2010; Stanton et al, 2011). Understanding this process is highly relevant particularly when steatohepatitis can lead to the progression of other risk factors such as liver fibrosis, cirrhosis and hepatocellular carcinoma with corresponding increases in morbidity and mortality (Bugianesi et al, 2002; Bailey et al, 2002; Pais et al, 2010; Sanyal 2011). It has been proposed that the development and progression of NASH is highly dependent on the different types of fats consumed (Hussein et al, 2007; Vallim & Salter et al, 2010) and the degree of hepatic inflammation (Harmon et al, 2011). The preceding events that lead to the inflammatory response are also poorly defined but are thought to involve cytokines, adipokines, PPAR-alpha signalling and a variety of other factors (Czaja 2004). Many of these mechanisms are mediated by changes in mRNA expression.

The n-3 polyunsaturated fatty acids, mainly EPA and DHA, are extremely important in down-regulating inflammatory genes and stimulating fatty acid oxidation (Yusufi et al, 2003; Shaw et al, 2007; Gorjao et al, 2009). EPA and DHA are both anti-thrombotic, hypolipidemic and inhibitors of cholesterol and lipoprotein formation in the liver (Deckelbaum et al, 2006). The protective effects of EPA and DHA against liver inflammation and a reduction in TAG synthesis in the liver are in part mediated by the expression of mRNA such as SREBP1-c (Kajikawa et al, 2009). However, hitherto no studies have examined differential effects of EPA or DHA on gene expression in the liver. In this regard, it is important to highlight the fact that mRNA levels *per se* do not dictate the subsequent expression of proteins within a cell. Apart from rates of translation and post-transcriptional modification of proteins, the microRNAs have a pivotal role in modulating mRNA.

These miRNAs are small (~22 nucleotides) non-coding RNA molecules which regulate mRNA expression via post-transcriptional control through poly (A) tail removal (Kojima et al, 2010), and binding to un-translated 3' regions. The miRNAs have been proposed to modulate the metabolic pathways related to liver inflammation and hepatic fatty acid accumulation (Hand et al, 2009; Padgett et al, 2009).

Studies have shown the commonly re-occurring miRNAs in liver such as miR-10 (Zheng et al, 2010), miR-21 (Meng et al, 2007), miR-122 (Xu et al, 2010, Lewis &

Jopling 2010), miR-199 (Shen et al, 2010) and miR-200 (Murakami et al, 2011) are related to liver fibrosis and hepatocellular carcinoma which are features of chronic NASH or its ensuing consequences. Furthermore hepatocellular inflammation is also associated with perturbations in miRNA (Brunt et al, 2001; Dolganiuc et al, 2009). Various animal models have shown that NASH related to methionine and choline deficient (MCD) (Dolganiuc et al, 2009) and high fat diets (Ahn et al, 2011) cause changes in selective miRNAs in the liver. For example, MCD diet regimens resulted in either the up-regulation of miR-705 and miR-1224 or down-regulation of miR-182, miR-183 and miR-199a-3p (Dolganiuc et al, 2009). However, there are no studies in which microRNA arrays have been investigated with respect to hypercaloric feeding of low and high fat diets with the inclusion of EPA and DHA.

We hypothesised that there is differential expression of miRNA in mice fed hypercaloric diets with different lipid compositions. In the ensuing studies, all diets had adequate protein, carbohydrate and micro-nutrients to minimize factors that may affect the accumulation of hepatic fats. The miRNA expression profiles were generated with microarray chips and then changes in selected miRNAs were further validated using RT-qPCR. We also hypothesised that the mice fed with either supplemental DHA or EPA or both will present an improved miRNA profile compared with mice fed a HF hypercaloric diet without any n-3 polyunsaturated fats.

8.2 Materials and methods

Animal work, diets and experimental designs are outlined in ***Chapter 2***. All materials and methods including the manufacturer and make of the products for miRNA experiments are also listed in ***Chapter 2***. The following sections provide information specific to this chapter. There were 5 groups of animals: a single LFR (Low fat reference) and 4 hypercaloric groups namely, LF (low fat), HF (high fat), high fat DHA (HFDHA) and high fat EPA (HFEPA) groups. In simple terms, the hypercaloric diets were supplemented with condensed milk (light fat version) incorporated with either corn oil in the LF group, palm oil in the HF group, palm oil with DHA or palm oil with EPA (for detailed composition of the diets see ***Chapter 2***).

8.2.1 RNA extraction, hybridization and selection for miRNA microarray

Total liver RNA was isolated with TRIzol LS Reagent as described in the manufacturer's protocol. The quantity and quality of RNA was assessed using the

Nanodrop spectrophotometer and Agilent bioanalyser, respectively. After ensuring the quality and quantity of the RNA present in the samples was satisfactory, approx 170 ng RNA from each sample (n=6 per group) was pooled to provide an aliquot containing 1000 ng of sample. Then nuclease-free water was added to each pooled sample to make a final volume of 35 µL. Thereafter, 1000 ng of total RNA was labelled with FlashTag Biotin HSR kit and hybridized in the Affymetrix Hybridization Oven 640 for subsequent analysis by Affymetrix GeneChip miRNA arrays. After 16 hours of hybridization, the hybridization cocktail (***Section 2.8***) was extracted from the array to a new tube and filled with array holding buffer and allowed to equilibrate before washing and staining. The Affymetrix Fluidics station 450 was used for the washing and staining process.

The hybridization signals on the microarray chips were detected with the GeneChip Scanner 3000 7G. Data was summarized, normalized and checked for quality control using miRNA QC Tool Software version 1.1.1.0. Statistical analysis was carried out between the miRNA probe sets and background probes. The detection are said to be "*TRUE"* when $P \leq 0.06$.

Specifications of the miRNA arrays used in this study were as follow (information was obtained from Affymetrix):

Chip type	: Affymetrix chip for miRNA
Probe pairs for miRNA	: 4 identical probes
Probe pairs for sno/scaRNA	: 11 probes
Oligonucleotide probe length	: less than or equals to 25-mer
Hybridization controls	: bioB, bioC, bioD and cre
Control sequences	: 22 control probe sets (10 probes/set)
Background probes	: 95 antigenomic probe sets

8.2.2 Real-time reverse transcriptase-quantitative polymerase chain reaction, (real time RT-qPCR)

The selected miRNAs, namely miR-199a-5p, 200b, 324-5p, 21*, 31*, 345-3p, 451 and 466f, were normalized against snoRNA-234 (endogenous control). Specific primer sequences for each miRNA were ordered from Applied Biosystems which are designed to be similar to each independent stem-loop sequence identified in the Sanger Institute miRBase (release 10.0) but the primer sequences were not revealed by the company. The miRNAs selected for verification was on the basis of the microarray data.

MiRNA microarray results were validated using RT-qPCR on independently derived RNAs from individual mice. A 2-step RT-qPCR was carried out using TaqMan Small RNA assays. In the reverse transcription (RT) step, reagents from TaqMan MicroRNA Reverse Transcription (RT) kit were used and cDNAs were reverse transcribed from RNA using a small RNA-specific, stem-loop RT primer. Each 15 µL RT reaction was combined with RT master mix with total RNA in the ratio of 7µL RT master mix : 5 µL total RNA (1 to 10 ng per reaction). Then, 12 µL of total RNA with RT master mix was transferred to a 96-well reaction plate and loaded onto a PTC-225 Peltier Thermal Cycler set to 4 steps as mentioned in ***Section 2.9***.

Immediately after the RT run, PCR amplification was continued using TaqMan Universal PCR Master Mix II. For this 20 µL per reaction of qPCR reaction mix was prepared accordingly (***Section 2.9)*** and transferred into 4 wells of 384-well plate using the Biomek FX Beckman Coultier Liquid handling robot. All samples were run in quadruplicate. Plates were sealed, centrifuged and loaded onto the 7900 HT Fast RT-PCR Systems. First-strand cDNA samples were amplified for 40 cycles (95°C for 5 sec, 60°C for 5sec, 72°C for 22 sec). Quantitative real-time RT-PCR and analysis was carried out using the ABI Prism 7000 sequence detection systems.

The amounts of initial template cDNA for the target miRNA were quantified by applying the threshold cycle to the standard curve. The final results for the expression levels of target miRNAs were normalized to the expression of snoRNA-234 by referring to its standard curve as quantified using real-time RT-qPCR. The $2^{-\Delta\Delta CT}$ method was used to calculate the relative quantification (RQ) of intensities indicating fold change between the groups. The median Ct of the 4 samples normalized to controls was used for comparing Ct values as shown in ***Appendix 2.1*** and ***2.2.***

8.2.3 Statistical analyses

Microarray data was summarized and normalized using the miRNA QC Tool Software version 1.1.1.0 which applies Student's t-test for its P-values. Cycle threshold and relative quantification of the selected miRNAs generated from real time RT-qPCR were analysed using analysis of variance (ANOVA) with Tukey's post hoc test.

8.3 Results

8.3.1 Microarray analyses for microRNAs

One microarray chip was used for each group using pooled good quality RNAs from 6 mice per group. The microarray data in its log form of intensity were then normalized against the log intensity of the background probes within the arrays to counter technical biasness in order to identify real biological differences between groups. An overview of data distribution was represented by the MA plots, with intensity ratio (M) plotted against the average intensity (A). An example of the MA plots of HF vs HFEPA is presented in ***Figure 8.1***. The assumption that most miRNAs do not change in their expression mean that the clustering of the miRNAs around the 0 point of the X-axis indicates normalized data. As seen in the MA plots, there were no distinct outliers (***Figure 8.1***).

In this chapter there were 4 sets of comparisons of interest (i) LFR vs LF group (ii) LFR vs HF group (iii) HF vs HFDHA group (iv) HF vs HFEPA group. After data normalization, the intensities of the hybridized probes were filtered according to its species and only mouse miRNA were subsequently analysed. There were 609 mouse miRNAs and 259 miRNAs were detected as a "*TRUE*" miRNA with $P \leq 0.06$ (***Figure 8.2***). Relative intensities were estimated by calculating the difference in log 2 intensities between the groups followed by the antilog of the difference obtained.

For the comparison between LFR and LF groups, a total of 25 miRNAs had fold change of >1.5 and 16 miRNAs had a fold change of <0.5 (***Table 8.1***). For the comparison between LFR and HF groups, there were 23 miRNAs with fold change > 1.5 and 20 miRNAs with fold change <0.5 (***Table 8.2***). Furthermore, for the comparison between HF and HFDHA, a total of 9 miRNAs had fold change of >1.5 and 6 miRNAs had fold changes of <0.5 (***Table 8.3***). For the comparison between HF and HFEPA groups, there were 22 miRNAs with fold change > 1.5 and 5 miRNAs with fold changes <0.5 (***Table 8.4***).

Referring to the Venn diagram (***Figure 8.3***), there were 25 miRNAs expressed in the comparisons between LFR vs LF and LFR vs HF. For the comparison between HF vs HFDHA and HF vs HFEEPA, the Venn diagram (***Figure 8.4***) showed that there were 4 miRNAs similarly expressed in both the comparisons. The miRNAs expressed in both comparisons are shown in ***Table 8.5*** and ***8.6***.

8.3.2 Quantification of miRNA with RT-qPCR

The sequence of the selected miRNAs which were required for the design of stem-loop RT and real-time PCR assays for quantitation of mature miRNA expression by Applied Biosystems TaqMan (***Table 8.7***). In this study a small RNA namely snoRNA-234 was used as the endogenous control due to its relatively constant expression levels in liver tissues (Huang et al, 2005). Furthermore, sno-234 shows relatively high abundance and low variation in liver tissues of mice (Chen et al, 2005; Chen et al, 2007).

8.3.3 MiRNA expression by RT-qPCR

MiR-200b, miR-21* and miR-31* were significantly down-regulated in the LF group when compared to the LFR group by -76%, -33% and -57% respectively ($P<0.01$ to $P<0.001$; ***Figure 8.5***). In the HF group, miR-199a-5p, miR-200b, miR-324-3p, miR-21*, miR-31*, miR-345-3p and miR-466f were significantly down-regulated by -86%, -86%, -51%, -76%, -76%, -72% and -62%, respectively when compared to the LFR group ($P<0.05$ to $P<0.001$; ***Figure 8.5***).

In addition, a comparison between LF and HF treated groups (ie, the effects of high fat hypercaloric feeding) showed that miR-21* and miR-466f were significantly reduced when HF is compared to LF group ($P<0.01$; ***Figure 8.5***).

8.3.4 MiRNA expression by RT-qPCR in comparison with microarray data

The comparison between RT-qPCR and the microarray data showed similar trends in the expressions for miR-200b, miR-21*, miR-31*, miR-345-3p and miR-466f in all comparisons (***Figure 8.6***). However, opposite effects were seen in miR-324-3p for all comparisons and exceptionally miR-200b showed an opposite effect in HF vs HFDHA (***Figure 8.6***). The array and RT-qPCR data for miR-451 appeared to be dissimilar in the comparison of LFR vs HF and HF vs HFEPA. There were also a slight difference in miR-199a-5p between RT-qPCR and the microarray data when comparing HF vs HFDHA and HFEPA.

Figure 8. 1: MA plot of microarray data from HF and HFEPA groups

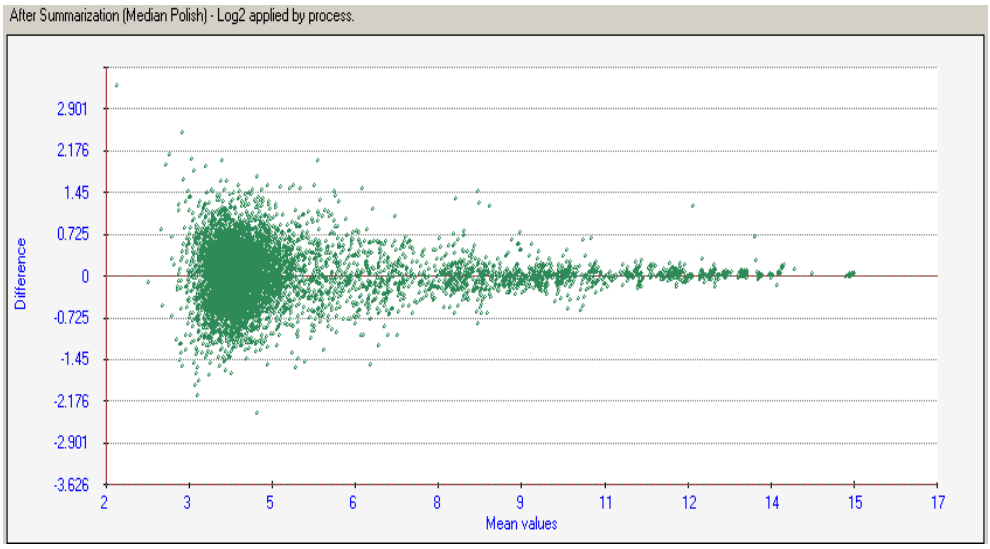

M is green intensity ratio on the y-axis; A is average intensities on the x-axis. Formula for $M=log_2R- log_2G$; $A= ½ x (log_2R + log_2G)$.

Figure 8. 2: Flow chart of miRNA analysis for LFR, LF and HF groups

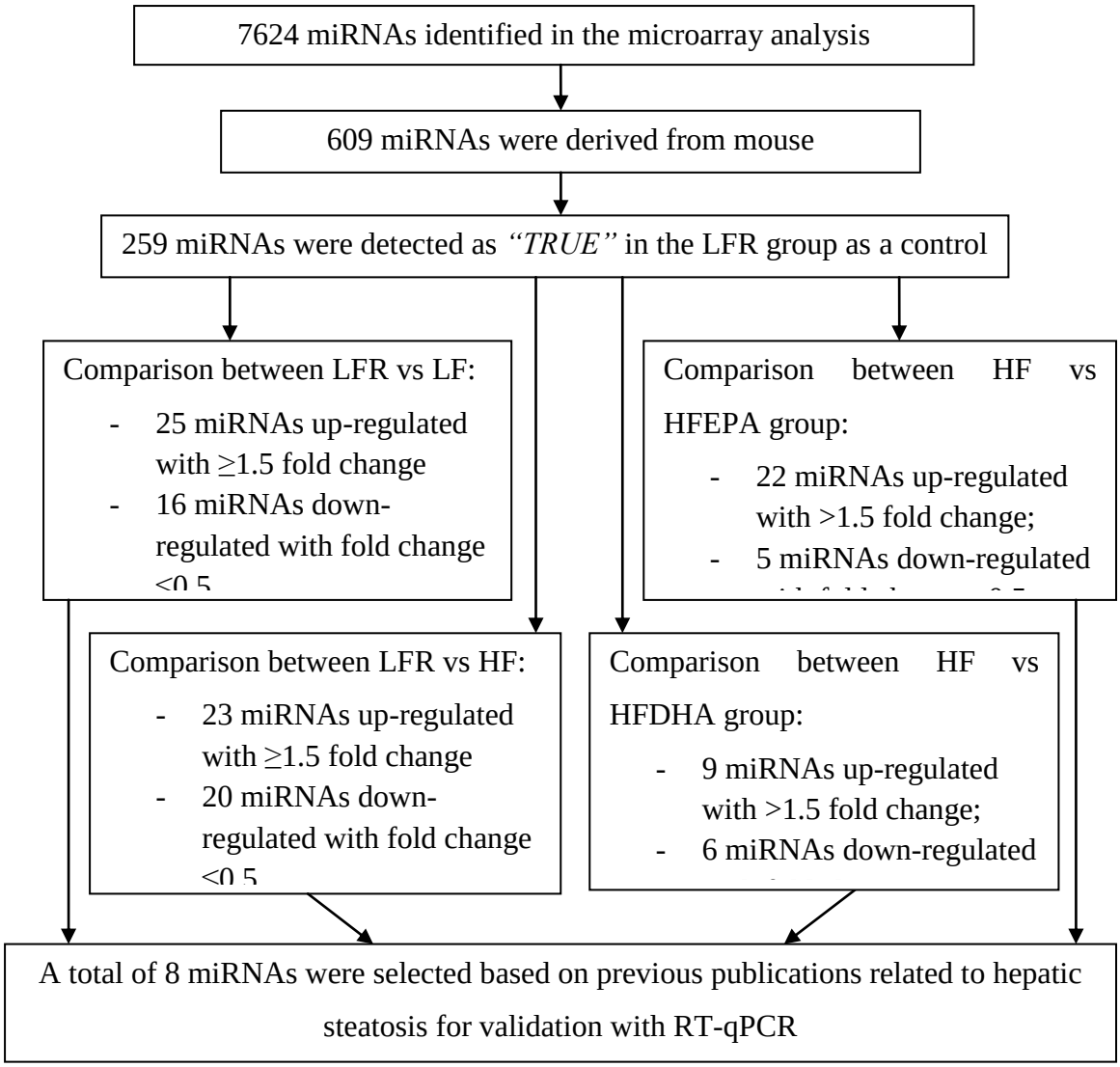

Table 8. 1: List of mouse miRNAs altered (increased or decreased by at least 50%) when comparing LFR vs LF groups

Probe Set Name	Log_2 (LFR intensities)	Absolute LFR intensities	P-value LFR	Log_2 (LF intensities)	Absolute LF intensities	P-value LF	Relative quantification (RQ) Intensities
mmu-miR-494	7.33	160	2.50E-07	9.56	754	2.10E-08	4.70
mmu-miR-744	7.59	193	1.00E-06	9.23	600	3.80E-08	3.11
mmu-miR-762	11.46	2816	4.60E-08	13.03	8346	4.60E-08	2.96
mmu-miR-714	7.93	245	0.00021	9.45	700	6.50E-07	2.86
mmu-miR-720	6.64	100	1.30E-06	8.09	272	2.10E-08	2.73
mmu-miR-203	7.17	144	1.90E-07	8.36	329	7.10E-08	2.29
mmu-let-7g	8.6	387	2.10E-08	9.79	885	2.10E-08	2.29
mmu-let-7f	8.32	320	2.10E-08	9.4	677	2.10E-08	2.12
mmu-miR-455	8.98	505	2.10E-08	10.05	1062	2.10E-08	2.10
mmu-miR-328	5.72	53	0.00378	6.7	104	0.00037	1.98
mmu-miR-1195	9.63	790	2.50E-07	10.55	1499	2.10E-08	1.90
mmu-miR-193	8.02	260	2.10E-08	8.92	485	2.10E-08	1.86
mmu-miR-101a	4.34	20	0.05493	5.13	35	0.00945	1.72
mmu-miR-101b	7.04	132	7.10E-08	7.81	224	2.10E-08	1.70
mmu-miR-193*	7.58	191	2.10E-08	8.33	323	2.10E-08	1.69
mmu-miR-148b	4.79	28	0.0018	5.52	46	0.00068	1.66
mmu-miR-139-3p	5.22	37	0.03828	5.92	61	0.00355	1.63
mmu-miR-712	5.65	50	0.00662	6.35	82	0.00073	1.63
mmu-miR-188-5p	4.61	24	0.03773	5.3	39	0.00163	1.62
mmu-miR-467a	4.47	22	0.03977	5.13	35	0.00539	1.58
mmu-miR-26b	5.46	44	0.00014	6.1	69	5.70E-08	1.56
mmu-miR-148a	8.17	289	2.10E-08	8.81	448	2.10E-08	1.55
mmu-miR-324-3p	5.12	35	0.0226	5.74	53	0.00379	1.54
mmu-miR-139-5p	8.57	380	2.10E-08	9.17	575	2.10E-08	1.51
mmu-miR-486	8.05	264	1.00E-06	8.63	397	2.50E-07	1.50
mmu-miR-497	8.18	290	2.10E-08	7.14	141	2.10E-08	0.49
mmu-miR-199a-3p	9.04	525	2.10E-08	7.97	251	3.50E-07	0.48
mmu-miR-214	9.38	668	2.10E-08	8.31	317	2.50E-07	0.47
mmu-miR-181d	5.58	48	7.20E-05	4.51	23	0.07144	0.47
mmu-miR-379	5.25	38	0.0033	4.12	17	0.11965	0.45
mmu-miR-18a	7.4	169	1.90E-07	6.2	73	3.30E-05	0.43
mmu-miR-199b*	5.61	49	6.40E-06	4.35	20	0.23945	0.42
mmu-miR-183	5.41	42	0.0004	4.14	18	0.33365	0.42
mmu-miR-708	5.29	39	5.70E-05	3.95	16	0.58027	0.40

mmu-miR-200c	7.76	217	2.10E-08	6.42	86	3.30E-06	0.40
mmu-miR-146b	5.22	37	0.0004	3.83	14	0.27355	0.38
mmu-miR-199a-5p	9.17	577	2.10E-08	7.76	217	2.10E-08	0.38
mmu-miR-362-5p	6.8	111	1.00E-06	5.38	42	0.00044	0.37
mmu-miR-34a	8.79	441	2.10E-08	7.24	152	2.10E-08	0.34
mmu-miR-214*	5.67	51	0.00025	3.84	14	0.66624	0.28
mmu-miR-200a	7.73	212	2.10E-08	5.72	53	0.00011	0.25

**indicates that the miRNA arises from the 3'arm of miRNA; without the star it means the miRNA arises from 5'arm of miRNA. Similarly, 5p and 3p indicates that the miRNA is derived from the 5' and 3' end respectively. miRNA with the same number but different letters are derived from the same sequence. Green indicates up-regulated miRNAs whereas red indicates down regulated miRNAs. Absolute intensities = 2^ Log_2Intensities; Relative intensities = Absolute intensities of treated samples/Absolute intensities of controls. MiRNAs selected are within the criteria of a "TRUE" detection in LFR group, and >1.5 fold change or <0.5 fold change between groups.*

Table 8. 2: List of mouse miRNAs identified when comparing HF with LFR mice group

Probe Set Name	Log_2 (LFR intensities)	Absolute LFR intensities	P-value LFR	Log_2 (HF intensities)	Absolute HF intensities	P-value HF	Relative quantification (RQ) Intensities
mmu-miR-455	8.98	505	2.10E-08	10.49	1438	2.10E-08	2.85
mmu-let-7g	8.60	387	2.10E-08	10.00	1027	2.10E-08	2.65
mmu-miR-744	7.59	193	1.00E-06	8.76	434	2.50E-07	2.25
mmu-let-7f	8.32	320	2.10E-08	9.49	718	2.10E-08	2.24
mmu-miR-203	7.17	144	1.90E-07	8.27	309	2.10E-08	2.15
mmu-miR-193	8.02	260	2.10E-08	9.09	547	2.10E-08	2.10
mmu-miR-148b	4.79	28	0.00180	5.76	54	0.00026	1.95
mmu-miR-720	6.64	100	1.30E-06	7.55	188	2.10E-08	1.88
mmu-miR-101b	7.04	132	7.10E-08	7.95	247	2.10E-08	1.87
mmu-miR-193*	7.58	191	2.10E-08	8.46	352	2.10E-08	1.84
mmu-miR-705	8.01	258	4.00E-06	8.86	463	6.50E-07	1.80
mmu-miR-714	7.93	245	0.000210	8.73	423	1.80E-05	1.73
mmu-miR-291b-5p	4.77	27	0.0328	5.54	47	0.00857	1.70
mmu-miR-328	5.72	53	0.00378	6.48	89	0.00035	1.70
mmu-miR-324-3p	5.12	35	0.0226	5.87	59	0.0017	1.69
mmu-miR-1195	9.63	790	2.50E-07	10.36	1310	2.10E-08	1.66
mmu-miR-486	8.05	264	1.00E-06	8.74	427	1.30E-07	1.61
mmu-miR-22*	5.58	48	1.80E-05	6.26	77	7.10E-06	1.60
mmu-miR-455*	5.00	32	0.00432	5.67	51	0.00036	1.59
mmu-let-7d*	5.94	62	1.40E-06	6.61	97	4.60E-07	1.58
mmu-miR-361	8.51	364	2.10E-08	9.16	572	2.10E-08	1.57
mmu-miR-146a	8.04	263	2.10E-08	8.68	411	2.10E-08	1.56
mmu-miR-92a	10.02	1037	2.10E-08	10.65	1604	2.10E-08	1.55
mmu-miR-199b	9.12	557	2.10E-08	8.11	275	2.10E-08	0.49
mmu-miR-384-5p	4.70	26	0.0178	3.69	13	0.39211	0.49
mmu-miR-541	5.30	39	0.000250	4.23	19	0.34877	0.48
mmu-miR-181c	5.24	38	0.00365	4.16	18	0.236	0.47
mmu-miR-503	6.16	72	0.000360	5.04	33	0.08493	0.46
mmu-miR-199b*	5.61	49	6.40E-06	4.40	21	0.29115	0.43
mmu-miR-301a	4.93	31	0.00731	3.70	13	0.58965	0.43
mmu-miR-764-5p	5.01	32	0.00739	3.78	14	0.51246	0.43
mmu-miR-200c	7.76	217	2.10E-08	6.53	92	7.70E-06	0.43
mmu-miR-183	5.41	42	0.000400	4.16	18	0.20933	0.42
mmu-miR-711	5.51	46	0.00423	4.24	19	0.22206	0.41

mmu-miR-214*	5.67	51	0.00025	4.39	21	0.18961	0.41
mmu-miR-200b	6.25	76	3.50E-07	4.84	29	0.00534	0.38
mmu-miR-214	9.38	668	2.10E-08	7.96	250	2.20E-06	0.37
mmu-miR-199a-5p	9.17	577	2.10E-08	7.74	214	2.10E-08	0.37
mmu-miR-379	5.25	38	0.0033	3.82	14	0.35736	0.37
mmu-miR-362-3p	5.03	33	0.004	3.50	11	0.92355	0.35
mmu-miR-146b	5.22	37	0.0004	3.56	12	0.66668	0.32
mmu-miR-497	8.18	290	2.10E-08	6.24	75	1.40E-06	0.26
mmu-miR-200a	7.73	212	2.10E-08	5.31	40	0.00263	0.19

**indicates that the miRNA arises from the 3'arm of miRNA; without the star it means the miRNA arises from 5'arm of miRNA. Similarly, 5p and 3p indicates that the miRNA is derived from the 5' and 3' end respectively. miRNA with the same number but different letters are derived from the same sequence. Green indicates up-regulated miRNAs whereas red indicates down regulated miRNAs. Absolute intensities = 2^ Log_2Intensities; Relative intensities = Absolute intensities of treated samples/Absolute intensities of controls. MiRNAs selected are within the criteria of a "TRUE" detection in LFR group, and >1.5 fold change or <0.5 fold change between groups.*

Table 8. 3: List of mice miRNAs altered (increased or decreased by at least 50%) when comparing HF vs HFDHA groups

ProbeSet Name	Log_2 (HF intensities)	Absolute HF intensities	P-value HF	Log_2 (HFDHA intensities)	Absolute HFDHA intensities	P-value HFDHA	Relative intensities
mmu-miR-689	6.92	121	0.007006	7.83	228	0.002189	1.88
mmu-miR-483	4.65	25	0.005256	5.54	47	0.007972	1.86
mmu-miR-719	4.50	23	0.017164	5.28	39	0.000299	1.72
mmu-miR-501-3p	4.42	21	0.035683	5.20	37	0.00481	1.72
mmu-miR-872*	4.85	29	0.031088	5.54	47	0.005325	1.61
mmu-miR-497	6.24	75	1.38E-06	6.89	118	2.33E-07	1.57
mmu-miR-466f-5p	5.55	47	0.000419	6.19	73	1.44E-05	1.56
mmu-miR-188-5p	4.96	31	0.021397	5.57	47	0.000908	1.53
mmu-miR-326	4.88	29	0.038338	5.48	45	0.017652	1.52
mmu-miR-551b	4.90	30	0.034338	3.87	15	0.621309	0.49
mmu-miR-297a	4.81	28	0.017439	3.71	13	0.384216	0.47
mmu-miR-451	6.66	101	5.52E-08	5.32	40	0.00049	0.39
mmu-miR-10a	6.99	127	2.55E-06	5.48	45	0.000471	0.35
mmu-miR-149	7.30	157	5.23E-05	5.50	45	0.007379	0.29
mmu-miR-708*	4.75	27	0.043956	2.93	8	0.570898	0.28

**indicates that the miRNA arises from the 3'arm of miRNA; without the star it means the miRNA arises from 5'arm of miRNA. Similarly, 5p and 3p indicates that the miRNA is derived from the 5' and 3' end respectively. miRNA with the same number but different letters are derived from the same sequence. Green indicates up-regulated miRNAs where as red indicates down-regulated miRNAs. Absolute intensities = 2^ Log_2Intensities; Relative intensities = Absolute intensities of treated samples/Absolute intensities of controls. MiRNAs selected are within the criteria of a true detection in HF group, and >1.5 fold change or <0.5 fold change between groups*

Table 8. 4: List of mice miRNAs altered (increased or decreased by at least 50%) when comparing HF vs HFEPA groups

ProbeSet Name	Log2(HF intensities)	Absolute HF intensities	P-value HF	Log2(HFEPA intensities)	Absolute HFEPA intensities	P-value HFEPA	Relative intensities
mmu-miR-483	4.65	25	0.00526	6.22	75	2.00E-05	2.98
mmu-miR-466f-5p	5.55	47	0.00042	7.07	134	2.10E-08	2.87
mmu-miR-494	7.80	223	2.05E-08	9.08	542	2.10E-08	2.43
mmu-miR-762	11.72	3369	4.59E-08	12.94	7885	4.60E-08	2.34
mmu-miR-467d*	5.00	32	0.00459	6.07	67	6.20E-06	2.10
mmu-miR-667	4.73	27	0.05133	5.79	55	0.00258	2.09
mmu-miR-699	5.23	37	0.03063	6.28	78	0.00119	2.08
mmu-let-7b*	4.91	30	0.04202	5.89	59	1.10E-06	1.97
mmu-miR-92a*	5.04	33	0.01369	5.99	64	0.00011	1.94
mmu-miR-669c	5.99	63	2.60E-05	6.81	112	3.40E-06	1.77
mmu-miR-574-5p	7.61	195	1.33E-07	8.35	326	2.10E-08	1.67
mmu-miR-327	5.68	51	0.00118	6.38	83	7.70E-06	1.62
mmu-miR-21*	4.97	31	0.00684	5.66	51	0.00181	1.62
mmu-miR-690	13.12	8873	2.05E-08	13.81	14333	2.10E-08	1.62
mmu-miR-501-3p	4.42	21	0.03568	5.09	34	0.00361	1.59
mmu-miR-685	7.39	168	2.05E-08	8.04	264	2.10E-08	1.57
mmu-miR-29b	5.81	56	7.31E-06	6.45	88	1.00E-07	1.56
mmu-miR-714	8.73	423	1.77E-05	9.37	661	6.50E-07	1.56
mmu-miR-671-5p	6.44	87	0.00823	7.06	133	0.00113	1.53
mmu-miR-324-5p	5.82	57	0.00311	6.42	86	0.00161	1.52
mmu-miR-150	6.78	110	3.86E-06	7.38	166	2.10E-08	1.51
mmu-miR-31*	6.81	112	9.72E-07	5.79	55	8.70E-05	0.49
mmu-miR-149	7.30	157	5.23E-05	6.27	77	0.00192	0.49
mmu-miR-542-5p	4.70	26	0.01869	3.54	12	0.43233	0.45
mmu-miR-302c*	4.48	22	0.00688	3.17	9	0.12995	0.40
mmu-miR-345-3p	5.86	58	0.00212	4.44	22	0.06662	0.37

**indicates that the miRNA arises from the 3'arm of miRNA; without the star it means the miRNA arises from 5'arm of miRNA. Similarly, 5p and 3p indicates that the miRNA is derived from the 5' and 3' end respectively. miRNA with the same number but different letters are derived from the same sequence. Green indicates up-regulated miRNAs where as red indicates down-regulated miRNAs. Absolute intensities = 2^ Log_2Intensities; Relative intensities = Absolute intensities of treated samples/Absolute intensities of controls. MiRNAs selected are within the criteria of a true detection in HF group, and >1.5 fold change or <0.5 fold change between groups*

Figure 8. 3: Venn diagram of regulated miRNAs in both HF vs LF

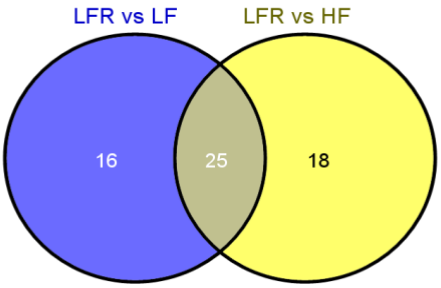

Table 8. 5: List of regulated miRNAs overlapping and expressed individually when comparing between (LF vs LFR) and (HF vs LFR)

miRNAs in LFR vs LF	*miRNAs in common*	*miRNAs in LFR vs HF*
mmu-miR-494	mmu-miR-744	mmu-miR-705
mmu-miR-762	mmu-miR-714	mmu-miR-291b-5p
mmu-miR-101a	mmu-miR-720	mmu-miR-22*
mmu-miR-139-3p	mmu-miR-203	mmu-miR-455*
mmu-miR-712	mmu-let-7g	mmu-let-7d*
mmu-miR-188-5p	mmu-let-7f	mmu-miR-361
mmu-miR-467a	mmu-miR-455	mmu-miR-146a
mmu-miR-26b	mmu-miR-328	mmu-miR-92a
mmu-miR-148a	mmu-miR-1195	mmu-miR-199b
mmu-miR-139-5p	mmu-miR-193	mmu-miR-384-5p
mmu-miR-199a-3p	mmu-miR-101b	mmu-miR-541
mmu-miR-181d	mmu-miR-193*	mmu-miR-181c
mmu-miR-18a	mmu-miR-148b	mmu-miR-503
mmu-miR-708	mmu-miR-324-3p	mmu-miR-301a
mmu-miR-362-5p	mmu-miR-486	mmu-miR-764-5p
mmu-miR-34a	mmu-miR-497	mmu-miR-711
	mmu-miR-214	mmu-miR-200b
	mmu-miR-379	mmu-miR-362-3p
	mmu-miR-199b*	
	mmu-miR-183	
	mmu-miR-200c	
	mmu-miR-146b	
	mmu-miR-199a-5p	
	mmu-miR-214*	
	mmu-miR-200a	

The yellow highlighted miRNAs were validated with RT-qPCR

Figure 8. 4: Venn diagram of miRNAs that were overlapping when comparing HFDHA vs HF and HFEPA vs HF groups.

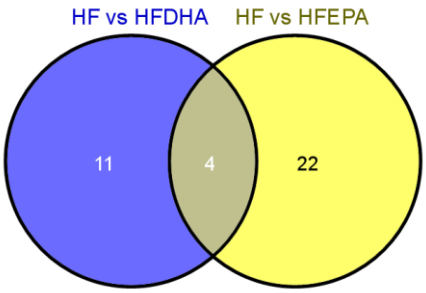

Table 8. 6: List of miRNAs overlapping and exprressed individually when comparing between (HF vs HFDHA) and (HF vs HFEPA) groups

miRNAs in HF vs HFDHA	*miRNAs in common*	*miRNAs in HF vs HFEPA*
mmu-miR-689	mmu-miR-483	mmu-miR-494
mmu-miR-719	mmu-miR-501-3p	mmu-miR-762
mmu-miR-872*	mmu-miR-466f-5p	mmu-miR-467d*
mmu-miR-497	mmu-miR-149	mmu-miR-667
mmu-miR-188-5p		mmu-miR-699
mmu-miR-326		mmu-let-7b*
mmu-miR-551b		mmu-miR-92a*
mmu-miR-297a		mmu-miR-669c
mmu-miR-451		mmu-miR-574-5p
mmu-miR-10a		mmu-miR-327
mmu-miR-708*		mmu-miR-21*
		mmu-miR-690
		mmu-miR-685
		mmu-miR-29b
		mmu-miR-714
		mmu-miR-671-5p
		mmu-miR-324-5p
		mmu-miR-150
		mmu-miR-31*
		mmu-miR-542-5p
		mmu-miR-302c*
		mmu-miR-345-3p

The yellow highlighted miRNAs were validated with RT-qPCR

Table 8. 7: miRNA sequence selected for validation with real-time RT-qPCR for LFR, LF and HF groups

Probe set name	Sequence
mmu-miR-199a-5p	CCCAGUGUUCAGACUACCUGUUC
mmu-miR-200b	UAAUACUGCCUGGUAAUGAUGA
mmu-miR-324-3p	CCACUGCCCCAGGUGCUGCU
mmu-miR-21*	CAACAGCAGUCGAUGGGCUGUC
mmu-miR-31*	UGCUAUGCCAACAUAUUGCCAUC
mmu-miR-345-3p	CCUGAACUAGGGGUCUGGAGAC
mmu-miR-451	AAACCGUUACCAUUACUGAGUU
mmu-miR-466f	UACGUGUGUGUGCAUGUGCAUG

The miRNAs selected for RT-qPCR were related to hepatic steatosis and consequently NASH based on previous studies. Source from Applied Biosystems

Figure 8. 5: The relative intensities of miR-199a-5p, miR-200b, miR-324-3p and miR-21* validated with RT-qPCR for LFR, LF and HF groups

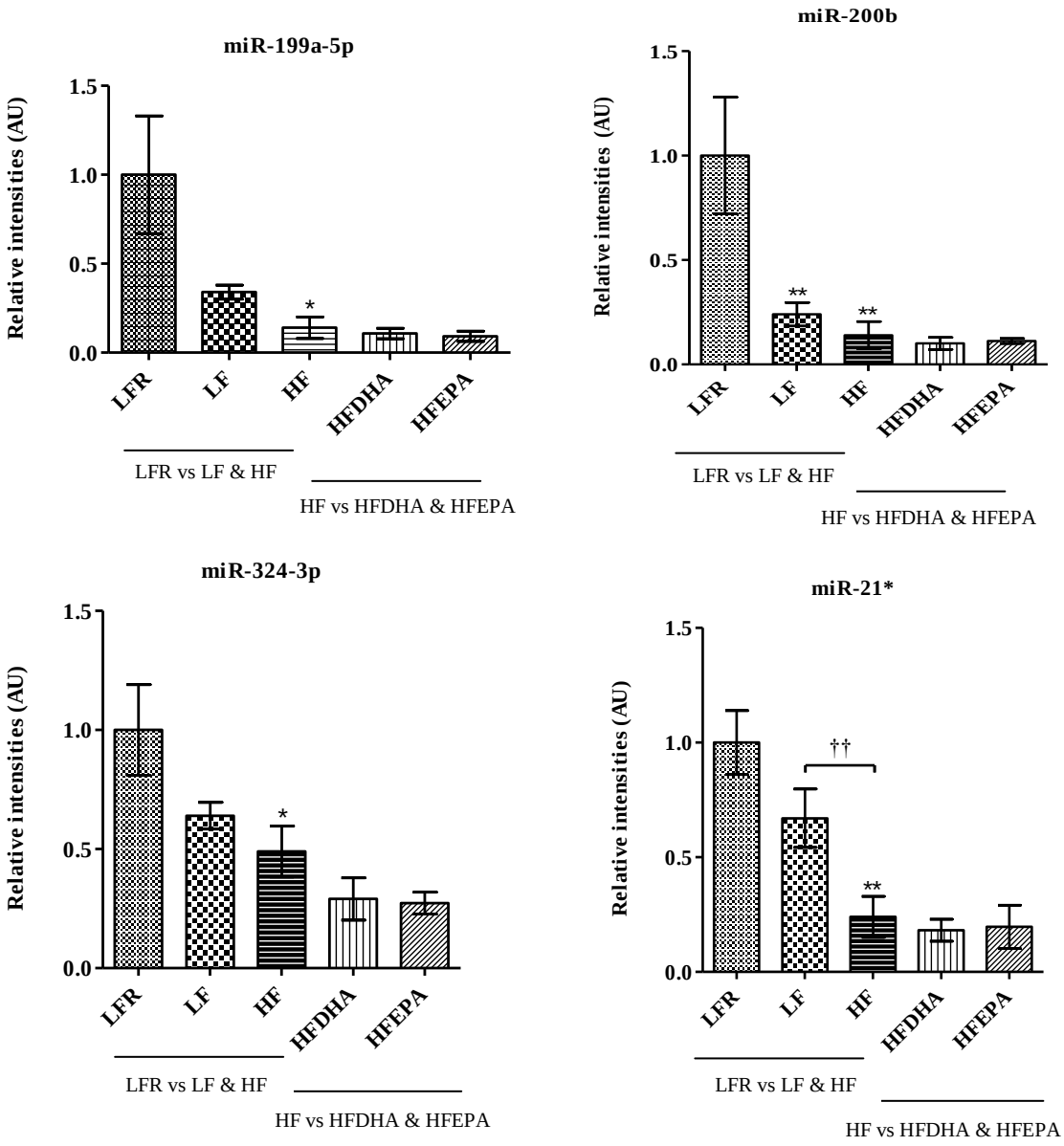

to be continued

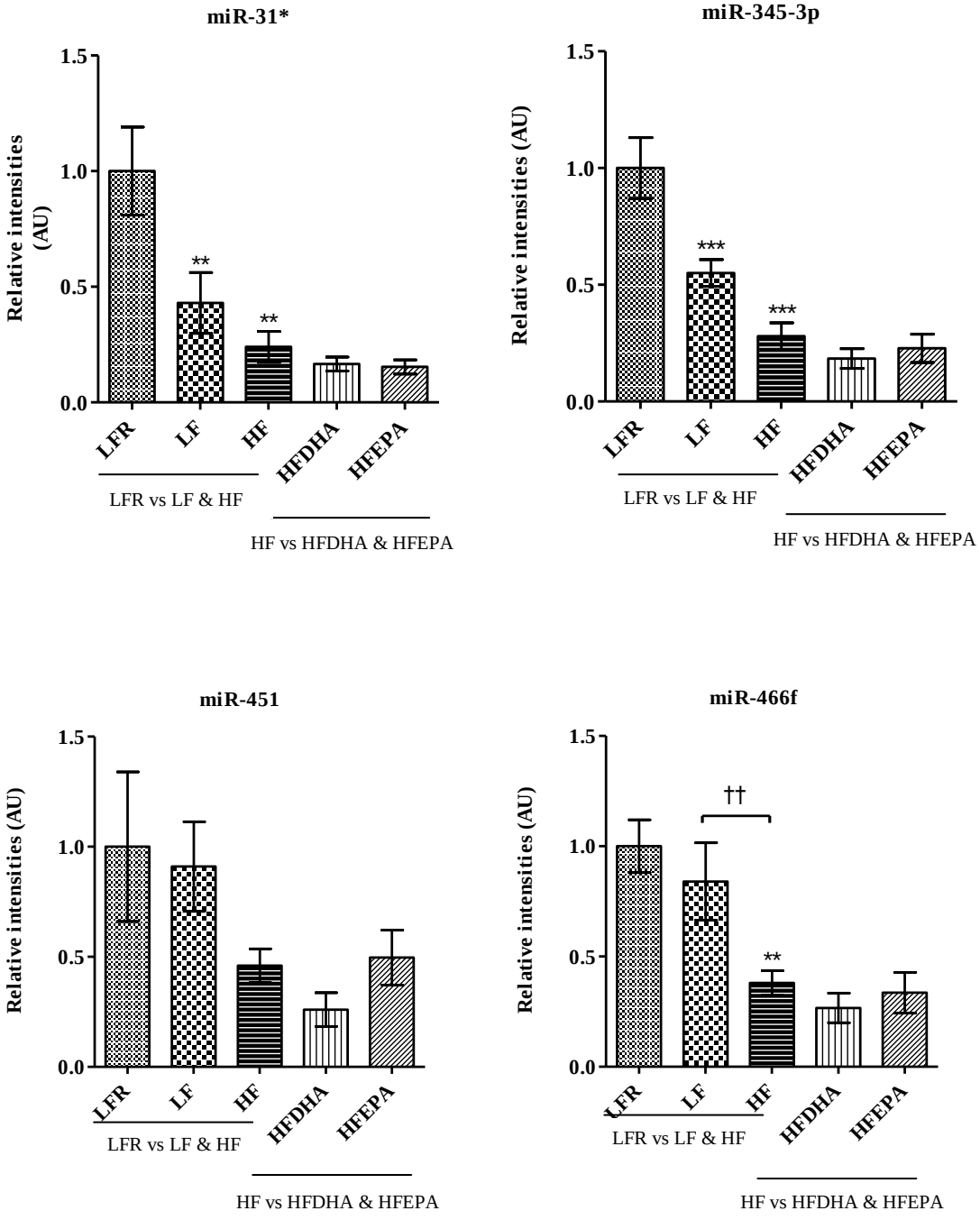

Data are mean ± SEM (n=6 per group). Differences between the mean of 5 groups were estimated with analysis of variance (ANOVA) followed by Tukey's test. ANOVA values for miR-199a-5p, 200b, 324-3p, miR-21, miR-31, 345-3p, 451 and 466f when comparing all 5 groups were P=0.001, <0.001, <0.001, <0.001, <0.001, <0.001, 0.040 and <0.001 respectively.

*A comparison between LFR vs LF and HF groups was carried out. The significant differences between the LFR control group and either the LF or HF group are as follows: * = P<0.05, ** = P<0.01 and *** = P<0.001. Differences between the LF and HF groups are displayed with a horizontal bar over the two groups where ††= P<0.01. There were no significant differences when comparing HF vs HFDHA and HFEPA.*

Figure 8. 6: Changes in miRNAs in LF and HF groups compared to the LFR group and changes in HFDHA and HFEPA groups compared to HF group using either microarrays or RT-qPCR

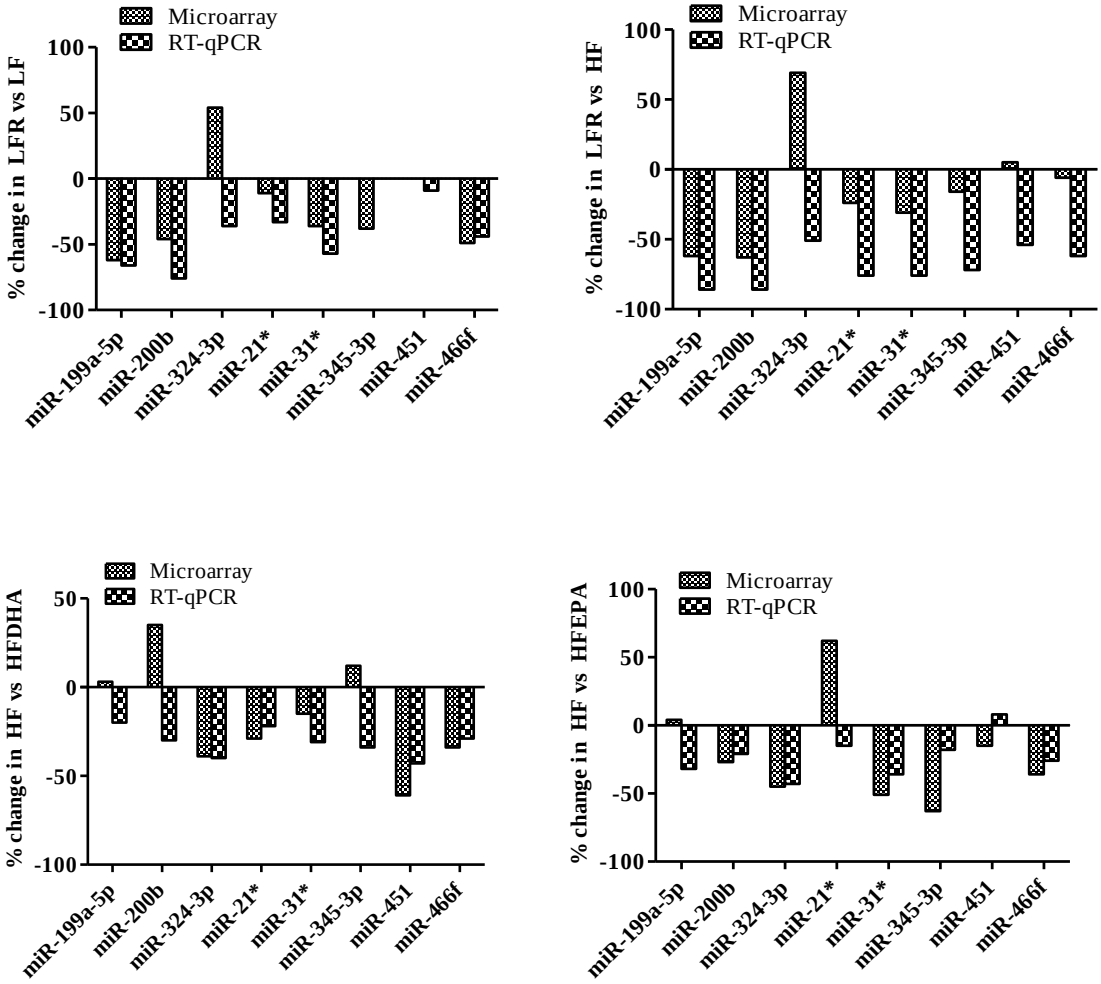

8.4 Discussion

8.4.1 Methodological considerations

Initial studies with microarrays used one microarray chip per group hence there were no statistical analyses between treatments. Subsequently, specific miRNAs were selected for verification by RT-PCR. Most verification studies are based on a number of premises namely (a) the intensity of the signals are "TRUE"; (b) they alter by least a defined amount, (c) they are deemed to be of metabolic significance based on existing bimolecular information, (d) they have been reported to alter in different diseases or conditions. It is tempting just to select those which display the greatest changes, but this may not have a firm foundation that relates to the existing knowledge base nor be related to hepatic pathology. For example, miR-494 shows a 4.7 fold increase in the HF hypercaloric diet but there is very little information on its function. There are only 6 papers on the pathology of murine miR-494, which are all related to gastric cancer. On the other hand, there are 177 papers on miRNA 21*. Whilst miR-494, 200a and 455 have not been examined in mouse liver, miR-199a-5p (Kanda et al, 2010), 31* (Zhang et al, 2011) have.

The normalization of the data in RT-qPCR is essential in order to obtain relative intensities in miRNAs expression which are close to real biological changes. SnoRNA's are commonly used as an endogenous control for normalizing microarray miRNA expression data because they are closer in length to miRNAs, expressed abundantly across various tissues and most importantly they are unlikely to be related to other miRNA regulatory pathways (Kiss 2002). SnoRNA-234 was selected due to its consistency of expression (i.e., least variability) across experimental conditions compared to snoRNA135, 142, 202 and 251 (Applied Biosystems;weblink:http://www3.appliedbiosystems.com/cms/groups/mcb_marketing/documents/generaldocuments/cms_044972.pdf). These stable small RNAs have been used as controls in other studies such as those of Mestdagh et al, (2009) and Meyer et al, (2010).

Although miR-21*, 31*, 345-3p, 451 and 466f were not overtly altered within the array studies, comparing LFR vs LF and LFR vs HF, we wanted to confirm the results by RT-qPCR. There are numerous studies based on these miRNAs. For example, miR-21* was up-regulated in mouse hepatocytes exposed to ionizing radiation which led to liver carcinogenesis (Zhu et al, 2010).

8.4.2 Comparison between the array and RT-qPCR

The comparison between the results from the microarray and RT-qPCR studies showed that directional changes in miR-200b, miR-21*, miR-31*, miR345-3p and miR-466f were generally consistent, with the exception of miR-324-3p. MiR-324-3p showed divergent changes when using either the array (up-regulation) or RT-qPCR (down-regulation). The opposite effect was also seen in miR-200b when comparing HF vs HFDHA.

Overall there is a good concordance of data measured by either the arrays or RT-qPCR. However, it is difficult to explain why there were divergent results using either the array or RT-qPCR for miR-324-3p. One reason could be due to the sensitivity of both the methods. This is not unusual since Abruzzo et al, (2005), Bhusari et al, (2006) and Ach et al, (2008) showed inconsistencies in results generated by both microarray and RT-qPCR. The other explanation is that the primers for the RT-qPCR were not correctly provided or were unstable. However, the company which provided the primers (Applied Biosystems) was not able to reveal the primer sequence. Moreover, the primers were stable as they were manufactured about 1.5 weeks before use. Nevertheless, RT-qPCR is considered the gold standard method for quantitative analysis.

There are a number of approaches in which one can analyse the data from either the array and/or the RT-qPCR. For example, one could analyse those miRNAs that show common changes within the context of pathway analysis or one could interpret the data in terms of individual miRNAs that have been shown to alter in specific pathologies related to either lipid oxidation, hepatic steatosis or overfeeding. Here, the latter approach is adopted since several studies have shown that more than 30% of all mRNAs can be regulated by a single miRNA (Valencia-Sanchez 2006; Nilsen 2007, Tzur et al, 2009). Furthermore, miRNAs regulate translation and mRNA degradation which can results in at least a 80% reduction in mRNA levels causing a decrease in protein synthesis in selective studies (Guo et al, 2010). MiRNA affects translation by preventing the elongation step of protein synthesis or by inhibiting the ability of ribosomes to bind targeted mRNAs (Pawlicki et al, 2008).

In the following section, attention is focused on those miRNAs confirmed to have altered by RT-qPCR, though an equally valid approach would be to focus on the 25 miRNAs differentially expressed in the comparison of LFR vs LF, or others shown to alter in the comparison of LFR vs HF or LF vs HF groups. However, the miRNA

study was carried out at the end of the thesis so it was not possible to validate all 25 of the miRNAs by RT-qPCR due to time constraints.

8.4.3 Influence of hypercaloric diets on miRNA expressions

The over-expression of miR-199 and miR-200 families have been linked to the progression of liver fibrosis by Murakami et al, (2011). The aforementioned study determined that 4 out of 11 miR-199 and miR-200 families were significantly elevated in liver fibrosis when compared with controls; namely miR-199a, 199a*, 200a and 200b (Murakami et al, 2011). The predicted target genes for miR-199 and miR-200 have been proposed to include inflammation related genes (FAS, NFKB1), cytokines (IL-6, IL-8, TNF-α) and fibrosis related genes (FGFR1, SOCS1) (Murakami et al, 2011). For this chapter, miR-199a-5p and miR-200b in the HF group were down-regulated significantly when compared to the control LFR group as detected by RT-qPCR. If miRNA can down-regulate mRNA, one can speculate that the down-regulated miR-199a-5p and 200b may be responsible for an up-regulation of inflammatory related genes. However, no increase in inflammation was seen in liver of the HF group when compared to the LFR group. Rather there was a reduction in inflammation scores. The high fat hypercaloric mice may have developed a protective mechanism in overcoming suppression of hepatic fatty acid oxidation causing the reduced signs of inflammation in the HF group mice as shown in the liver histology presented in ***Section 5.3.5***. For example, hepatic inflammatory scores in the HF group revealed 63% of animals with no signs of inflammation, whereas in the LFR group 63% of the mice showed inflammation at scores 2 and 3.

In the normal process of liver regeneration, quiescent liver cells enter the cell cycle, non-parenchymal and parenchymal cells (hepatocytes) divide and liver restores proper formation. The removal of mouse liver by 60% causes the remaining liver to grow back to its original mass in approximately 1 week (Zimmermann 2004). During liver regeneration, miR-21 was found to be the regulator of hepatocyte proliferation and it directly inhibited B-cell translocation gene (Btg2), a cell cycle inhibitor that is essential for DNA synthesis in hepatocytes (Song et al, 2010). The over-expression of miR-21 inhibited NF-kappaB signalling and miR-21 was up-regulated during early stages of liver regeneration (Marquez et al, 2010). In this study chapter, miR-21 was significantly down-regulated in the high-fat hypercaloric (HF group) mice compared to the high-carbohydrate (LF group) hypercaloric mice. In addition, miR-21 in both the LF

and HF group were significantly down-regulated when compared to the LFR group. Potentially, the up-regulation of miR-21 may be dependent on the rate of normal liver cell proliferation; the more severe the damage in the liver, the higher the degree of miR-21 expression to regenerate the liver. Therefore, the down-regulation of miR-21 in both the LF and HF groups may imply the imposition of less severe liver damage compared to the LFR group. This was supported by the histology scores in ***Section 5.3.4***

A study by Zhang et al, (2011) showed that miR-31 increased in oesophageal squamous cell carcinoma tissue compared to normal controls by promoting colony formation, migration and invasion. However, there are no other reports on how miR-31 in the liver responds to high fat diets. Targets of miR-31 include tumour suppressor mRNAs such as epithelial membrane protein1 (EMP1), kinase suppressor of ras 2 (KSR2) and regulator of G-protein signalling 4 (RGS4). Similarly, miR-31 was significantly up-regulated in hepatocellular carcinoma cells when compared to non-tumoral liver cells (Wong et al, 2008; Lee et al, 2008). In contrast, our study showed that miR-31 was significantly down-regulated in LF and HF groups when compared to the LFR group. Therefore, the lower occurrence of liver inflammation (***Section 5.3.4***) in the LF and HF compared to LFR groups may be reflected in, or be due to, the down-regulation of miR-31.

MiR-466f has been found to regulate the expression of collagen genes in development, with predicted targets namely, COL1A1, COL19A1, COL1A2, COL4A1, COL4A5 and COL3A1 with the latter isoform being the main target (Sterling 2011). However, it is difficult to interpret the aforementioned observations in relation to the study for this thesis as collagen was not measured. MiR-466f was also found to decrease significantly in diabetic mice (Chen et al, 2011). In this study for the thesis, HF groups showed a down-regulation of miR-466f in comparison to the LFR group. Interestingly, the HF hypercaloric mice showed a significant decrease in miR-466f when compared to the LF group mice. However, the serum insulin and glucose from this study did not show signs of diabetes in both LF and HF groups (***Section 5.3.3***). This merits further investigation.

MiR-324-3p and miR-345-3p were significantly down-regulated in the HF group when compared with the LFR group. For the comparison between LFR vs LF groups, there was a down-regulation in miR-345-3p. Currently, there are no studies on both these selected miRNAs in relation to hepatic steatosis in response to different types of

hypercaloric diets. Thus, they may be suggested as novel miRNAs that respond to hypercaloric diets.

Our RT-qPCR study in general confirmed the array data. Thus, an in-depth analysis of the arrayed material of the 25 miRNAs expressed in the comparison of LFR vs LF and LFR vs HF should ideally be carried out, but time did not allow this. However, one needs to consider that some of the aforementioned discussion is speculative and further work needs to be carried out to determine the significance of these observations. In other words, the present observations are preliminary. Future studies could involve miRNA inhibitors and mimics. In general, an up-regulation of a specific miRNA should theoretically show a down-regulation in a particular mRNA expression, and *vice versa*. Such a simple relationship has potential to be used therapeutically in the treatment of dietary-related liver disease including the wide spectrum of fatty liver disorders.

8.4.4 Influence of EPA and DHA on miRNA expressions

There was no statistically significant change comparing both HF vs HFDHA and HF vs HFEPA using data derived from RT-qPCR. Thus it is difficult to further elaborate on mechanisms that may be responsible for the changes described in previous sections of the thesis where both DHA and EPA affected the liver lipid and histological profiles (***Chapter 5***). Ideally one needs to do pathway analysis on the collective miRNAs expressed in both the comparisons. To this date, there is only 1 paper on the effects of miRNA expression in relation to DHA. This shows miRNA profiling in the induction of apoptosis in glioma cells and the effects of DHA (Farago et al, 2011). In this aforementioned study, down-regulation of miRNAs such as miR-22 and 145 resulted in the up-regulation of sirtuin 1 and insulin receptor substrate 1, respectively. In the presence of DHA, Farago et al, (2011) showed that these changes in miRNAs were ameliorated. However, results in glioma cells are difficult to place within the context of the present studies of the thesis which focused almost exclusively on the liver. On the other hand, there are no papers published on miRNAs in relation to the effects of EPA.

8.4.5 Conclusion

In conclusion, hypercaloric feeding of mice with either low or high fat diets resulted in the changes in miRNA expression revealing an interesting approach to further investigate the regulation of steatosis.

Chapter 9:
Final discussion

9.1 General discussion and future studies

The aim of this thesis was to examine the role of dietary fat in the development of fatty liver and its progression to non-alcoholic steatohepatitis (NASH) and to try to identify novel biomarkers using "omics" approaches. Since the term NASH was coined by Ludwig et al, (1980), its prevalence has increased and the severity of its effects has become apparent, contributing to liver cancer and type 2 diabetes. The prevalence in the USA is estimated to be 30% of fatty liver disease cases, which parallels the frequency of insulin resistance (Jimba et al, 2005) and obesity (Caldwell et al, 2004).

Previous studies using mice to study NASH suggested that the accumulation and distribution of fat in the liver is promoted by high fat feeding, high cholesterol and/or methionine choline-deficient diet (Raubenheimer et al, 2006; Rinella et al, 2008; Stanton et al, 2011). More recently, attention has also been drawn to carbohydrates particularly fructose as a contributor (Samuel 2011). Some of the experimental models used are nutritionally imbalanced (e.g. choline deficient) and not very relevant to human dietary intake. For example, Stanton *et al*. (2011) induced severe inflammation and steatohepatitis in mice fed a high fat (45% energy) plus a high cholesterol intake (0.12% diet or about 300 mg/1000 kcal) whereas human diets in countries where NASH is prevalent provide closer to 35% energy and cholesterol intakes are in the range of 100-150 mg/1000 kcal. Cholesterol was not included in the diet in this thesis because the primary aim was to look at the effect of dietary fats on the liver. Furthermore, in the present study care was taken to ensure that the diets were nutritionally balanced.

The animal model used in this thesis involved feeding a high fat pelleted diet in conjunction with *ad libitum* access to condensed milk. Previous studies refer to such a diet as a high fat obesogenic diet (West *et al.* 1992; Eberhard *et al.* 1994; Samuelsson *et al*. 2008). Panchal *et al.* (2011) showed that feeding 8-9 weeks old rats on a similar diet increased liver weight, inflammation and fibrosis with elevated liver enzymes. The work in this thesis, however, shows that this dietary regimen is not particularly high in fat because the animals chose to derive more food energy from the condensed milk than from the pelleted diet. However, condensed milk with a low fat content resulted in a slightly low energy intake than condensed milk with a higher fat content because of differences in energy density. This diet should therefore not be referred to a high fat feeding regime.

The studies reported here in this thesis showed that fasting might exacerbate damage to the liver due to rapid mobilization of fat from adipose tissue to the liver. This

was also highlighted by Postic & Girard (2008). An improvement to the study design might be only to withdraw food from the animals 3-4 hours before sacrifice so as to avoid any acute mobilization of fat. A limitation of the present study is the relative short duration (6 weeks). While this is adequate to result in fatty liver, a longer period of dietary exposure may be needed to observe major inflammatory changes in the liver (Pachikian et al, 2011). A second limitation is that the results in the study are based mainly on finding in male animals and there may be difference between gender that are worthy of future study.

This thesis reports some novel finding with regards to the effects of DHA and EPA. Both DHA and EPA decreased the amount of cholesteryl oleate and total cholesteryl esters in the liver. These findings are in agreement with a report by Du et al, (2003). DHA, however, appeared to decrease the amount of fat accumulating in the liver. Although hepatic phospholipids showed a greater decrease in DHA fed mice, further work is needed to see whether there were changes in the classes of phospholipids species. Leflis et al, (2010) reported that mice fed a DHA rich diet for 16 days resulted in a significant increase in DHA incorporated in phosphatidylethanolamine and phosphatidylcholine in the liver (Leflis et al, 2010). These phospholipid species have been suggested as biomarkers of advanced liver disease in both murine and human liver tissues (Gorden et al, 2011). An interesting observation was that the synthesis of long-chain n-3 polyunsaturated fatty acids appeared to be enhanced with this overfeeding model. The mechanism for this is uncertain but it is possible that this might be promoted by higher levels of insulin that would accompany the overfeeding on condensed milk especially as insulin tends to promote the conversion of the parent essential fatty acids to their long-chain derivatives. High blood glucose levels, as observed in the animals fed the obesogenic diet, would also have the effect of suppressing fatty acid oxidation.

This thesis provides novel data on the effects of triacylglycerol structure of fats on liver lipids. The fats used in this study were the same as those used by Sanders et al. (2011) in a human study which showed difference in the extent of postprandial lipaemia between native palm olein and lard. The data provided in this thesis suggest that the metabolic fate on palmitic acid in the sn-2 position is different from that in the sn-1 and sn-3 position: notably an effect on hepatic cholesteryl ester concentrations and the conversion of linolenic acid to long-chain n-3 polyunsaturated fatty acids. These findings need to be independently verified.

The proteomics work reported here used 2D-DIGE which has the ability to investigate differential protein expression. Kendrick et al, (2011) showed that high fat feeding led to the down-regulation of sirtuins 3 which led to liver damage, mitochondrial fatty acid oxidative and gluconeogenesis. In this thesis, differential expression of the following proteins was found: isoform 1 of epoxide hydrolase 2, catalase, ATP synthase subunit-alpha mitochondrial, ornithine carbamoyltransferase-mitochondrial (OCT), regucalcin and carbonic anhydrase 3. Only carbonic anhydrase 3 was down-regulated when comparing the high fat hypercaloric with the low fat reference group.

The proteins that were identified to change in response to the high fat diet were involved in pathways of nitrogen metabolism, the urea cycle, aspartate and asparagines metabolism, arginine and hydroxyeicosatetraenoic acids (HETE) biosynthesis. No differences were noted in protein expression between EPA or DHA or with altered TAG structure. In addition to issues concerning the sensitivity and specificity of proteomics, there are statistical issues because of the number of comparisons being made means that some arise by play of chance. The complexity of liver proteomes also implies that the functional proteins in the liver related to lipid metabolism are difficult to map with DIGE. Studies have reported that the same type of proteins was identified in proteomes regardless of species or tissue samples used in DIGE and mass spectrometry (Wilkins et al, 1998). The low abundance and hydrophobic proteins were always undetected (Wilkins et al, 1998). These adversities are reflected in the current studies whereby high-throughput analysis based on proteomics still lack accurate sensitive tests toward the identification of novel biomarkers to assess NASH (Ariz et al, 2010). The results presented here do not suggest that proteomics is likely to yield information regarding biomarkers of NASH.

The findings with regard to miRNAs were more promising. It has been proposed that miRNAs regulate the metabolic pathways related to liver inflammation and hepatic fatty acid accumulation (Hand et al, 2009). The significant role of miRNAs in binding to complementary site of target messenger RNA causing either transcript degradation or translational repression (Wiklund et al, 2010) has been proposed to be useful as a potential diagnostic tool in the pathogenesis of non-alcoholic fatty liver disease (Jin et al, 2009). For instance, down-regulated miR-122 led to increased hepatic fatty-acid oxidation and decrease fatty acid synthesis rates in the liver (Esau et al, 2006). Therefore, this implies that miR-122 is a key regulator of lipid metabolism which may

act as a therapeutic target. In addition, the inhibition of miR-122 led to the activation of 5' AMP-activated protein kinase which stimulated hepatic fatty acid oxidation (Esau et al, 2006). The present study used microarrays and then confirmed candidate miRNAs of interest with RT-qPCR.

The RT-qPCR results showed that miR-199a-5p, miR-200b, miR-324-3p, miR-21*, miR-31* and miR-451 were down regulated in the animals fed a hypercaloric diet low in fat when compared to the animals fed a eucaloric diet. Animals overfed a high fat diet showed down-regulation of miR-199a-5p, miR-200b, miR-324-3p, miR-21*, miR-31*, miR-345-3p, miR-451 and miR-466f compared to the mice fed a eucaloric diet. Interestingly, there was a significant difference in miRNA expression between high fat and low fat hypercaloric feeding with miR-21* and miR-466f having lower values following the high fat regimen. However, none of these miRNAs were altered in response to either dietary EPA or DHA in comparison to HF diet.

There is limited information published on miRNAs, for example, there is only one study on miR-466f by Chen et al, (2011) who reported an increase in miR-466f expression in diabetic induced mice. This aforementioned study showed that there were 8 other miRNAs which were up-regulated such as miR-34a, 744 and 1937b. One needs to be aware that by comparing an individual miRNA with other studies, one may not obtain the true reflection on the pathological changes. In other words, miRNAs should be analysed collectively, for instance in this study, the miR-483, 501-3p, 466f-5p and 149 which were altered when comparing between both HF vs HFDHA and HF vs HFEPA may give an indication of true effects of EPA and/or DHA in relation to miRNA expression.

The selected miRNAs were not associated with the protein networks identified in this study for the thesis. In future work, a different approach may be taken by selecting miRNAs of interest before investigating protein expression. For example, Li et al, (2011) examined liver in ageing mice and identified that miR-34a and 93 increased. They then used 3 data mining tools namely *miRBase, Targetscan* and *RNA22*. These bioinformatic techniques indentified putative target mRNAs, namely those encoding the proteins Sirt1 and Mgst1. Both these protein are hepatoprotective (Li et al, 2011). The aforementioned authors then confirmed their findings by quantifying Sirt1 and Mgst1 by immunoassay and indeed the levels of these proteins were markedly reduced in livers of ageing mice. The role of miR-34a and 93 in suppressing their target proteins Sirt1 and Mgst1were subsequently confirmed by transfection studies (Li et al, 2011).

Although elegant in approach, it was not possible to carry out similar studies for this thesis due to time constraints.

9.2 Final remarks and conclusions

The work in this thesis indicates that overfeeding results in fatty liver and that this is not specifically made worse by a high fat diet. In the case of DHA, it appears to have favourable effects on fatty liver. However, further work on miRNAs is warranted. The increased prevalence of NASH globally is strongly related to the obesity epidemic and the increased prevalence of type 2 diabetes. Obesity results from an imbalance between energy intake and energy expenditure and there is a lack of consistent evidence to show that diets with different ratios of fat/carbohydrate differ in their respect to cause obesity. Restriction of energy intake is essential in order to prevent obesity and NASH. Increased physical activity may help maintain energy balance but is not an effective means of promoting weight loss. However, it is uncertain whether increased physical activity reduces liver fat and this would be worth of future study. In the meantime, the prevention of NASH will continue to depend on controlling the body mass index of the general population within a healthy range (20-25 kg/m^2).

REFERENCES

Abdelmalek MF & Diehl AM (2007) Nonalcoholic fatty liver disease as a complication of insulin resistance. *Med Clin North Am* **91**, 1125-1149, ix.

Abdelmegeed MA, Moon KH, Chen C, Gonzalez FJ & Song BJ (2010) Role of cytochrome P450 2E1 in protein nitration and ubiquitin-mediated degradation during acetaminophen toxicity. *Biochem Pharmacol* **79**, 57-66.

Abruzzo LV, Lee KY, Fuller A, Silverman A, Keating MJ, Medeiros LJ & Coombes KR (2005) Validation of oligonucleotide microarray data using microfluidic low-density arrays: a new statistical method to normalize real-time RT-PCR data. *Biotechniques* **38**, 785-792.

Ach RA, Wang H & Curry B (2008) Measuring microRNAs: comparisons of microarray and quantitative PCR measurements, and of different total RNA prep methods. *BMC Biotechnol* **8**, 69.

Ahn J, Lee H, Chung CH & Ha T (2011) High fat diet induced downregulation of microRNA-467b increased lipoprotein lipase in hepatic steatosis. *Biochem Biophys Res Commun* **414**, 664-669.

Alban A, David SO, Bjorkesten L, Andersson C, Sloge E, Lewis S & Currie I (2003) A novel experimental design for comparative two-dimensional gel analysis: Two-dimensional difference gel electrophoresis incorporating a pooled internal standard. *Proteomics* **3**, 36-44.

Alisi A, Da Sacco L, Bruscalupi G, Piemonte F, Panera N, De Vito R, Leoni S, Bottazzo GF, Masotti A & Nobili V (2011) Mirnome analysis reveals novel molecular determinants in the pathogenesis of diet-induced nonalcoholic fatty liver disease. *Lab Invest* **91**, 283-293.

Alvarez-Garcia I & Miska EA (2005) MicroRNA functions in animal development and human disease. *Development* **132**, 4653-4662.

Amarapurkar D, Kamani P, Patel N, Gupte P, Kumar P, Agal S, Baijal R, Lala S, Chaudhary D & Deshpande A (2007) Prevalence of non-alcoholic fatty liver disease: population based study. *Ann Hepatol* **6**, 161-163.

Ambros V (2004) The functions of animal microRNAs. *Nature* **431**, 350-355.

Angulo P (2002) Nonalcoholic fatty liver disease. *N Engl J Med* **346**, 1221-1231.

Angulo P (2007) Obesity and nonalcoholic fatty liver disease. *Nutr Rev* **65**, S57-63.

Ariz U, Mato JM, Lu SC & Martinez Chantar ML (2010) Nonalcoholic steatohepatitis, animal models, and biomarkers: what is new? *Methods Mol Biol* **593**, 109-136.

Arnold C, Konkel A, Fischer R & Schunck WH (2010) Cytochrome P450-dependent metabolism of omega-6 and omega-3 long-chain polyunsaturated fatty acids. *Pharmacol Rep* **62**, 536-547.

Bailey MA & Brunt EM (2002) Hepatocellular carcinoma: predisposing conditions and precursor lesions. *Gastroenterol Clin North Am* **31**, 641-662.

Bala S, Marcos M & Szabo G (2009) Emerging role of microRNAs in liver diseases. *World J Gastroenterol* **15**, 5633-5640.

Baranova A, Schlauch K, Elariny H, Jarrar M, Bennett C, Nugent C, Gowder SJ, Younoszai Z, Collantes R, Chandhoke V & Younossi ZM (2007) Gene expression patterns in hepatic tissue and visceral adipose tissue of patients with non-alcoholic fatty liver disease. *Obes Surg* **17**, 1111-1118.

Barboriak JJ, Krehl WA & Cowgill GR (1957) Pantothenic acid requirement of the growing and adult rat. *J Nutr* **61**, 13-21.

Barrows BR & Parks EJ (2006) Contributions of different fatty acid sources to very low-density lipoprotein-triacylglycerol in the fasted and fed states. *J Clin Endocrinol Metab* **91**, 1446-1452.

Bartel DP (2004) MicroRNAs: genomics, biogenesis, mechanism, and function. *Cell* **116**, 281-297.

Beharry S, Ackerley C, Corey M, Kent G, Heng YM, Christensen H, Luk C, Yantiss RK, Nasser IA, Zaman M, Freedman SD & Durie PR (2007) Long-term docosahexaenoic acid therapy in a congenic murine model of cystic fibrosis. *Am J Physiol Gastrointest Liver Physiol* **292**, G839-848.

Berry SE (2009) Triacylglycerol structure and interesterification of palmitic and stearic acid-rich fats: an overview and implications for cardiovascular disease. *Nutr Res Rev* **22**, 3-17.

Berry SE, Woodward R, Yeoh C, Miller GJ & Sanders TA (2007) Effect of interesterification of palmitic acid-rich triacylglycerol on postprandial lipid and factor VII response. *Lipids* **42**, 315-323.

Bhusari S, Hearne LB, Spiers DE, Lamberson WR & Antoniou E (2006) Effect of fescue toxicosis on hepatic gene expression in mice. *J Anim Sci* **84**, 1600-1612.

Bijland S, Pieterman EJ, Maas AC, van der Hoorn JW, van Erk MJ, van Klinken JB, Havekes LM, van Dijk KW, Princen HM & Rensen PC (2010) Fenofibrate increases very low density lipoprotein triglyceride production despite reducing plasma triglyceride levels in APOE*3-Leiden.CETP mice. *J Biol Chem* **285**, 25168-25175.

Bjorkegren J, Beigneux A, Bergo MO, Maher JJ & Young SG (2002) Blocking the secretion of hepatic very low density lipoproteins renders the liver more susceptible to toxin-induced injury. *J Biol Chem* **277**, 5476-5483.

Bolstad BM, Irizarry RA, Astrand M & Speed TP (2003) A comparison of normalization methods for high density oligonucleotide array data based on variance and bias. *Bioinformatics* **19**, 185-193.

Bonanome A, Bennett M & Grundy SM (1992) Metabolic effects of dietary stearic acid in mice: changes in the fatty acid composition of triglycerides and phospholipids in various tissues. *Atherosclerosis* **94**, 119-127.

Boquillon M, Paris R & Clement J (1977) The effect of various dietary factors on the size distribution of lymph fat particles in rat. *Lipids* **12**, 500-504.

Braconi C, Henry JC, Kogure T, Schmittgen T & Patel T (2011) The Role of MicroRNAs in Human Liver Cancers. *Semin Oncol* **38**, 752-763.

Bradbury MW & Berk PD (2004) Lipid metabolism in hepatic steatosis. *Clin Liver Dis* **8**, 639-671, xi.

Bradstreet RB (1965) The Kjeldahl method for organic nitrogen. 239.

Brown AM, Baker PW & Gibbons GF (1997) Changes in fatty acid metabolism in rat hepatocytes in response to dietary n-3 fatty acids are associated with changes in the intracellular metabolism and secretion of apolipoprotein B-48. *J Lipid Res* **38**, 469-481.

Browning JD, Szczepaniak LS, Dobbins R, Nuremberg P, Horton JD, Cohen JC, Grundy SM & Hobbs HH (2004) Prevalence of hepatic steatosis in an urban population in the United States: impact of ethnicity. *Hepatology* **40**, 1387-1395.

Brunt EM (2001) Nonalcoholic steatohepatitis: definition and pathology. *Semin Liver Dis* **21**, 3-16.

Brunt EM (2005) Nonalcoholic steatohepatitis: pathologic features and differential diagnosis. *Semin Diagn Pathol* **22**, 330-338.

Brunt EM (2005) Pathology of nonalcoholic steatohepatitis. *Hepatol Res* **33**, 68-71.

Brunt EM (2009) Histopathology of non-alcoholic fatty liver disease. *Clin Liver Dis* **13**, 533-544.

Brunt EM, Janney CG, Di Bisceglie AM, Neuschwander-Tetri BA & Bacon BR (1999) Nonalcoholic steatohepatitis: a proposal for grading and staging the histological lesions. *Am J Gastroenterol* **94**, 2467-2474.

Brunt EM, Neuschwander-Tetri BA, Oliver D, Wehmeier KR & Bacon BR (2004) Nonalcoholic steatohepatitis: histologic features and clinical correlations with 30 blinded biopsy specimens. *Hum Pathol* **35**, 1070-1082.

Brunt EM & Tiniakos DG (2010) Histopathology of nonalcoholic fatty liver disease. *World J Gastroenterol* **16**, 5286-5296.

Brusilow SW & Maestri NE (1996) Urea cycle disorders: diagnosis, pathophysiology, and therapy. *Adv Pediatr* **43**, 127-170.

Bugianesi E, Leone N, Vanni E, Marchesini G, Brunello F, Carucci P, Musso A, De Paolis P, Capussotti L, Salizzoni M & Rizzetto M (2002) Expanding the natural history of nonalcoholic steatohepatitis: from cryptogenic cirrhosis to hepatocellular carcinoma. *Gastroenterology* **123**, 134-140.

Bujanda L, Hijona E, Larzabal M, Beraza M, Aldazabal P, Garcia-Urkia N, Sarasqueta C, Cosme A, Irastorza B, Gonzalez A & Arenas JI, Jr. (2008) Resveratrol inhibits nonalcoholic fatty liver disease in rats. *BMC Gastroenterol* **8**, 40.

Burlamaqui IM, Dornelas CA, Valenca JT, Jr., Mesquita FJ, Veras LB & Rodrigues LV (2011) Hepatic and biochemical repercussions of a polyunsaturated fat-rich hypercaloric and hyperlipidic diet in Wistar rats. *Arq Gastroenterol* **48**, 153-158.

Caldwell SH, Crespo DM, Kang HS & Al-Osaimi AM (2004) Obesity and hepatocellular carcinoma. *Gastroenterology* **127**, S97-103.

Calin GA, Dumitru CD, Shimizu M, Bichi R, Zupo S, Noch E, Aldler H, Rattan S, Keating M, Rai K, Rassenti L, Kipps T, Negrini M, Bullrich F & Croce CM (2002) Frequent deletions and down-regulation of micro- RNA genes miR15 and miR16 at 13q14 in chronic lymphocytic leukemia. *Proc Natl Acad Sci U S A* **99**, 15524-15529.

Calin GA, Liu CG, Sevignani C, Ferracin M, Felli N, Dumitru CD, Shimizu M, Cimmino A, Zupo S, Dono M, Dell'Aquila ML, Alder H, Rassenti L, Kipps TJ, Bullrich F, Negrini M & Croce CM (2004) MicroRNA profiling reveals distinct signatures in B cell chronic lymphocytic leukemias. *Proc Natl Acad Sci U S A* **101**, 11755-11760.

Carmiel-Haggai M, Cederbaum AI & Nieto N (2005) A high-fat diet leads to the progression of non-alcoholic fatty liver disease in obese rats. *FASEB J* **19**, 136-138.

Charlton M (2007) Noninvasive indices of fibrosis in NAFLD: starting to think about a three-hit (at least) phenomenon. *Am J Gastroenterol* **102**, 409-411.

Chen CJ & Lee MH (2011) Early Diagnosis of Hepatocellular Carcinoma by Multiple microRNAs: Validity, Efficacy, and Cost-Effectiveness. *J Clin Oncol*.

Chen T, Li Z, Yan J, Yang X & Salminen W (2011) MicroRNA expression profiles distinguish the carcinogenic effects of riddelliine in rat liver. *Mutagenesis*.

Chen Z, Newberry EP, Norris JY, Xie Y, Luo J, Kennedy SM & Davidson NO (2008) ApoB100 is required for increased VLDL-triglyceride secretion by microsomal triglyceride transfer protein in ob/ob mice. *J Lipid Res* **49**, 2013-2022.

Cheng AM, Byrom MW, Shelton J & Ford LP (2005) Antisense inhibition of human miRNAs and indications for an involvement of miRNA in cell growth and apoptosis. *Nucleic Acids Res* **33**, 1290-1297.

Cheung O, Puri P, Eicken C, Contos MJ, Mirshahi F, Maher JW, Kellum JM, Min H, Luketic VA & Sanyal AJ (2008) Nonalcoholic steatohepatitis is associated with altered hepatic MicroRNA expression. *Hepatology* **48**, 1810-1820.

Chitturi S, Farrell GC, Hashimoto E, Saibara T, Lau GK & Sollano JD (2007) Non-alcoholic fatty liver disease in the Asia-Pacific region: definitions and overview of proposed guidelines. *J Gastroenterol Hepatol* **22**, 778-787.

Chow WC, Tai ES, Lian SC, Tan CK, Sng I & Ng HS (2007) Significant non-alcoholic fatty liver disease is found in non-diabetic, pre-obese Chinese in Singapore. *Singapore Med J* **48**, 752-757.

Christensen MM, Lund SP, Simonsen L, Hass U, Simonsen SE & Hoy CE (1998) Dietary structured triacylglycerols containing docosahexaenoic acid given from birth affect visual and auditory performance and tissue fatty acid profiles of rats. *J Nutr* **128**, 1011-1017.

Coleman DL (1982) Diabetes-obesity syndromes in mice. *Diabetes* **31**, 1-6.

Cong WN, Tao RY, Tian JY, Liu GT & Ye F (2008) The establishment of a novel non-alcoholic steatohepatitis model accompanied with obesity and insulin resistance in mice. *Life Sci* **82**, 983-990.

Cooper AD (1997) Hepatic uptake of chylomicron remnants. *J Lipid Res* **38**, 2173-2192.

Czaja MJ (2004) Liver injury in the setting of steatosis: crosstalk between adipokine and cytokine. *Hepatology* **40**, 19-22.

Dallinga-Thie GM, Franssen R, Mooij HL, Visser ME, Hassing HC, Peelman F, Kastelein JJ, Peterfy M & Nieuwdorp M (2010) The metabolism of triglyceride-rich lipoproteins revisited: new players, new insight. *Atherosclerosis* **211**, 1-8.

Day CP & James OF (1998) Steatohepatitis: a tale of two "hits"? *Gastroenterology* **114**, 842-845.

De Craemer D, Pauwels M & Van den Branden C (1996) Dietary docosahexaenoic acid has little effect on peroxisomes in healthy mice. *Lipids* **31**, 1157-1161.

De Craemer D, Vamecq J, Roels F, Vallee L, Pauwels M & Van den Branden C (1994) Peroxisomes in liver, heart, and kidney of mice fed a commercial fish oil preparation: original data and review on peroxisomal changes induced by high-fat diets. *J Lipid Res* **35**, 1241-1250.

de Roos B, Rungapamestry V, Ross K, Rucklidge G, Reid M, Duncan G, Horgan G, Toomey S, Browne J, Loscher CE, Mills KH & Roche HM (2009) Attenuation of inflammation and cellular stress-related pathways maintains insulin sensitivity in obese type I interleukin-1 receptor knockout mice on a high-fat diet. *Proteomics* **9**, 3244-3256.

Deckelbaum RJ, Worgall TS & Seo T (2006) n-3 fatty acids and gene expression. *Am J Clin Nutr* **83**, 1520S-1525S.

Demoz A, Willumsen N & Berge RK (1992) Eicosapentaenoic acid at hypotriglyceridemic dose enhances the hepatic antioxidant defense in mice. *Lipids* **27**, 968-971.

den Boer M, Voshol PJ, Kuipers F, Havekes LM & Romijn JA (2004) Hepatic steatosis: a mediator of the metabolic syndrome. Lessons from animal models. *Arterioscler Thromb Vasc Biol* **24**, 644-649.

Deng QG, She H, Cheng JH, French SW, Koop DR, Xiong S & Tsukamoto H (2005) Steatohepatitis induced by intragastric overfeeding in mice. *Hepatology* **42**, 905-914.

Di Liegro CM, Bellafiore M, Izquierdo JM, Rantanen A & Cuezva JM (2000) 3'-untranslated regions of oxidative phosphorylation mRNAs function in vivo as enhancers of translation. *Biochem J* **352 Pt 1**, 109-115.

DiBello PM, Dayal S, Kaveti S, Zhang D, Kinter M, Lentz SR & Jacobsen DW (2010) The nutrigenetics of hyperhomocysteinemia: quantitative proteomics reveals differences in the methionine cycle enzymes of gene-induced versus diet-induced hyperhomocysteinemia. *Mol Cell Proteomics* **9**, 471-485.

Do GM, Oh HY, Kwon EY, Cho YY, Shin SK, Park HJ, Jeon SM, Kim E, Hur CG, Park TS, Sung MK, McGregor RA & Choi MS (2011) Long-term adaptation of global transcription and metabolism in the liver of high-fat diet-fed C57BL/6J mice. *Mol Nutr Food Res* **55 Suppl 2**, S173-185.

Dolganiuc A, Petrasek J, Kodys K, Catalano D, Mandrekar P, Velayudham A & Szabo G (2009) MicroRNA expression profile in Lieber-DeCarli diet-induced alcoholic and methionine choline deficient diet-induced nonalcoholic steatohepatitis models in mice. *Alcohol Clin Exp Res* **33**, 1704-1710.

Donnelly KL, Margosian MR, Sheth SS, Lusis AJ & Parks EJ (2004) Increased lipogenesis and fatty acid reesterification contribute to hepatic triacylglycerol stores in hyperlipidemic Txnip-/- mice. *J Nutr* **134**, 1475-1480.

Donnelly KL, Smith CI, Schwarzenberg SJ, Jessurun J, Boldt MD & Parks EJ (2005) Sources of fatty acids stored in liver and secreted via lipoproteins in patients with nonalcoholic fatty liver disease. *J Clin Invest* **115**, 1343-1351.

Douette P, Navet R, Gerkens P, de Pauw E, Leprince P, Sluse-Goffart C & Sluse FE (2005) Steatosis-induced proteomic changes in liver mitochondria evidenced by two-dimensional differential in-gel electrophoresis. *J Proteome Res* **4**, 2024-2031.

Du C, Sato A, Watanabe S, Wu CZ, Ikemoto A, Ando K, Kikugawa K, Fujii Y & Okuyama H (2003) Cholesterol synthesis in mice is suppressed but lipofuscin formation is not affected by long-term feeding of n-3 fatty acid-enriched oils compared with lard and n-6 fatty acid-enriched oils. *Biol Pharm Bull* **26**, 766-770.

Eberhart GP, West DB, Boozer CN & Atkinson RL (1994) Insulin sensitivity of adipocytes from inbred mouse strains resistant or sensitive to diet-induced obesity. *Am J Physiol* **266**, R1423-1428.

Eberle D, Hegarty B, Bossard P, Ferre P & Foufelle F (2004) SREBP transcription factors: master regulators of lipid homeostasis. *Biochimie* **86**, 839-848.

Eccleston HB, Andringa KK, Betancourt AM, King AL, Mantena SK, Swain TM, Tinsley HN, Nolte RN, Nagy TR, Abrams GA & Bailey SM (2011) Chronic exposure to a high-fat diet induces hepatic steatosis, impairs nitric oxide

bioavailability, and modifies the mitochondrial proteome in mice. *Antioxid Redox Signal* **15**, 447-459.

Edvardsson U, von Lowenhielm HB, Panfilov O, Nystrom AC, Nilsson F & Dahllof B (2003) Hepatic protein expression of lean mice and obese diabetic mice treated with peroxisome proliferator-activated receptor activators. *Proteomics* **3**, 468-478.

Elchuri S, Naeemuddin M, Sharpe O, Robinson WH & Huang TT (2007) Identification of biomarkers associated with the development of hepatocellular carcinoma in CuZn superoxide dismutase deficient mice. *Proteomics* **7**, 2121-2129.

El-Mowafy AM, Abdel-Dayem MA, Abdel-Aziz A, El-Azab MF & Said SA (2011) Eicosapentaenoic acid ablates valproate-induced liver oxidative stress and cellular derangement without altering its clearance rate: dynamic synergy and therapeutic utility. *Biochim Biophys Acta* **1811**, 460-467.

Emanuele S, D'Anneo A, Bellavia G, Vassallo B, Lauricella M, De Blasio A, Vento R & Tesoriere G (2004) Sodium butyrate induces apoptosis in human hepatoma cells by a mitochondria/caspase pathway, associated with degradation of beta-catenin, pRb and Bcl-XL. *Eur J Cancer* **40**, 1441-1452.

Emken EA, Adlof RO, Duval SM & Nelson GJ (1999) Effect of dietary docosahexaenoic acid on desaturation and uptake in vivo of isotope-labeled oleic, linoleic, and linolenic acids by male subjects. *Lipids* **34**, 785-791.

Emken EA, Adlof RO, Rohwedder WK & Gulley RM (1993) Influence of linoleic acid on desaturation and uptake of deuterium-labeled palmitic and stearic acids in humans. *Biochim Biophys Acta* **1170**, 173-181.

Esau C, Davis S, Murray SF, Yu XX, Pandey SK, Pear M, Watts L, Booten SL, Graham M, McKay R, Subramaniam A, Propp S, Lollo BA, Freier S, Bennett CF, Bhanot S & Monia BP (2006) miR-122 regulation of lipid metabolism revealed by in vivo antisense targeting. *Cell Metab* **3**, 87-98.

Estep M, Armistead D, Hossain N, Elarainy H, Goodman Z, Baranova A, Chandhoke V & Younossi ZM (2010) Differential expression of miRNAs in the visceral adipose tissue of patients with non-alcoholic fatty liver disease. *Aliment Pharmacol Ther* **32**, 487-497.

Fabbrini E, Mohammed BS, Magkos F, Korenblat KM, Patterson BW & Klein S (2008) Alterations in adipose tissue and hepatic lipid kinetics in obese men and women with nonalcoholic fatty liver disease. *Gastroenterology* **134**, 424-431.

Farago N, Feher LZ, Kitajka K, Das UN & Puskas LG (2011) MicroRNA profile of polyunsaturated fatty acid treated glioma cells reveal apoptosis-specific expression changes. *Lipids Health Dis* **10**, 173.

Farrell GC & Larter CZ (2006) Nonalcoholic fatty liver disease: from steatosis to cirrhosis. *Hepatology* **43**, S99-S112.

Fernandes CL, Dong JH, Roebuck BD, Chisari FV, Montali JA, Schmidt DE, Jr. & Prochaska HJ (1996) Elevations of hepatic quinone reductase, glutathione, and alpha- and mu-class glutathione S-transferase isoforms in mice with chronic hepatitis: a compensatory response to injury. *Arch Biochem Biophys* **331**, 104-116.

Fernandes MT, Ferraro AA, de Azevedo RA & Fagundes Neto U (2010) Metabolic differences between male and female adolescents with non-alcoholic fatty liver disease, as detected by ultrasound. *Acta Paediatr* **99**, 1218-1223.

Fernandez JR, Redden DT, Pietrobelli A & Allison DB (2004) Waist circumference percentiles in nationally representative samples of African-American, European-American, and Mexican-American children and adolescents. *J Pediatr* **145**, 439-444.

Ferre P & Foufelle F (2010) Hepatic steatosis: a role for de novo lipogenesis and the transcription factor SREBP-1c. *Diabetes Obes Metab* **12 Suppl 2**, 83-92.

Ferreira DM, Castro RE, Machado MV, Evangelista T, Silvestre A, Costa A, Coutinho J, Carepa F, Cortez-Pinto H & Rodrigues CM (2011) Apoptosis and insulin resistance in liver and peripheral tissues of morbidly obese patients is associated with different stages of non-alcoholic fatty liver disease. *Diabetologia* **54**, 1788-1798.

Fiorentino L, Vivanti A, Cavalera M, Marzano V, Ronci M, Fabrizi M, Menini S, Pugliese G, Menghini R, Khokha R, Lauro R, Urbani A & Federici M (2010) Increased tumor necrosis factor alpha-converting enzyme activity induces insulin resistance and hepatosteatosis in mice. *Hepatology* **51**, 103-110.

Folch J, Lees M & Sloane Stanley GH (1957) A simple method for the isolation and purification of total lipides from animal tissues. *J Biol Chem* **226**, 497-509.

Folch J, Lees M & Stanley GHS (1957) A simple method for the isolation and purificaion of total lipids from animal tissues *Journal of Biological Chemistry* **226**, 497-509.

Forestell CA & LoLordo VM (2003) Palatability shifts in taste and flavour preference conditioning. *Q J Exp Psychol B* **56**, 140-160.

Fracanzani AL, Valenti L, Bugianesi E, Vanni E, Grieco A, Miele L, Consonni D, Fatta E, Lombardi R, Marchesini G & Fargion S (2011) Risk of nonalcoholic steatohepatitis and fibrosis in patients with nonalcoholic fatty liver disease and low visceral adiposity. *J Hepatol* **54**, 1244-1249.

Fraser A, Longnecker MP & Lawlor DA (2007) Prevalence of elevated alanine aminotransferase among US adolescents and associated factors: NHANES 1999-2004. *Gastroenterology* **133**, 1814-1820.

Frith J, Day CP, Henderson E, Burt AD & Newton JL (2009) Non-alcoholic fatty liver disease in older people. *Gerontology* **55**, 607-613.

Gaemers IC, Stallen JM, Kunne C, Wallner C, van Werven J, Nederveen A & Lamers WH (2011) Lipotoxicity and steatohepatitis in an overfed mouse model for non-alcoholic fatty liver disease. *Biochim Biophys Acta* **1812**, 447-458.

Gharahdaghi F, Weinberg CR, Meagher DA, Imai BS & Mische SM (1999) Mass spectrometric identification of proteins from silver-stained polyacrylamide gel: A method for the removal of silver ions to enhance sensitivity. *Electrophoresis* **20**, 601-605.

Gholam PM, Flancbaum L, Machan JT, Charney DA & Kotler DP (2007) Nonalcoholic fatty liver disease in severely obese subjects. *Am J Gastroenterol* **102**, 399-408.

Glatzle J, Wang Y, Adelson DW, Kalogeris TJ, Zittel TT, Tso P, Wei JY & Raybould HE (2003) Chylomicron components activate duodenal vagal afferents via a cholecystokinin A receptor-mediated pathway to inhibit gastric motor function in the rat. *J Physiol* **550**, 657-664.

Goldberg IJ & Ginsberg HN (2006) Ins and outs modulating hepatic triglyceride and development of nonalcoholic fatty liver disease. *Gastroenterology* **130**, 1343-1346.

Gonzalez-Periz A, Planaguma A, Gronert K, Miquel R, Lopez-Parra M, Titos E, Horrillo R, Ferre N, Deulofeu R, Arroyo V, Rodes J & Claria J (2006) Docosahexaenoic acid (DHA) blunts liver injury by conversion to protective lipid mediators: protectin D1 and 17S-hydroxy-DHA. *FASEB J* **20**, 2537-2539.

Gorden DL, Ivanova PT, Myers DS, McIntyre JO, VanSaun MN, Wright JK, Matrisian LM & Brown HA (2011) Increased diacylglycerols characterize hepatic lipid changes in progression of human nonalcoholic fatty liver disease; comparison to a murine model. *PLoS One* **6**, e22775.

Gorg A, Weiss W & Dunn MJ (2004) Current two-dimensional electrophoresis technology for proteomics. *Proteomics* **4**, 3665-3685.

Gorjao R, Azevedo-Martins AK, Rodrigues HG, Abdulkader F, Arcisio-Miranda M, Procopio J & Curi R (2009) Comparative effects of DHA and EPA on cell function. *Pharmacol Ther* **122**, 56-64.

Goth L (2008) Catalase deficiency and type 2 diabetes. *Diabetes Care* **31**, e93.

Gotoh N, Nagao K, Onoda S, Shirouchi B, Furuya K, Nagai T, Mizobe H, Ichioka K, Watanabe H, Yanagita T & Wada S (2009) Effects of three different highly purified n-3 series highly unsaturated fatty acids on lipid metabolism in C57BL/KsJ-db/db mice. *J Agric Food Chem* **57**, 11047-11054.

Grau T & Bonet A (2009) Caloric intake and liver dysfunction in critically ill patients. *Curr Opin Clin Nutr Metab Care* **12**, 175-179.

Green MH, Massaro ER & Green JB (1984) Multicompartmental analysis of the effects of dietary fat saturation and cholesterol on absorptive lipoprotein metabolism in the rat. *Am J Clin Nutr* **40**, 82-94.

Greenspan MD, Schroeder EA & Yudkovitz JB (1982) Studies on the in vivo synthesis of triacylglycerol in mouse liver. *Biochim Biophys Acta* **710**, 15-22.

Gregg SQ, Gutierrez V, Robinson AR, Woodell T, Nakao A, Ross MA, Michalopoulos GK, Rigatti L, Rothermel CE, Kamileri I, Garinis GA, Stolz DB & Niedernhofer LJ (2012) A mouse model of accelerated liver aging caused by a defect in DNA repair. *Hepatology* **55**, 609-621.

Griffiths-Jones S, Saini HK, van Dongen S & Enright AJ (2008) miRBase: tools for microRNA genomics. *Nucleic Acids Res* **36**, D154-158.

Guo H, Ingolia NT, Weissman JS & Bartel DP (2010) Mammalian microRNAs predominantly act to decrease target mRNA levels. *Nature* **466**, 835-840.

Hanbauer I, Rivero-Covelo I, Maloku E, Baca A, Hu Q, Hibbeln JR & Davis JM (2009) The Decrease of n-3 Fatty Acid Energy Percentage in an Equicaloric Diet Fed to B6C3Fe Mice for Three Generations Elicits Obesity. *Cardiovasc Psychiatry Neurol* **2009**, 867041.

Hand NJ, Master ZR, Le Lay J & Friedman JR (2009) Hepatic function is preserved in the absence of mature microRNAs. *Hepatology* **49**, 618-626.

Haque JA, McMahan RS, Campbell JS, Shimizu-Albergine M, Wilson AM, Botta D, Bammler TK, Beyer RP, Montine TJ, Yeh MM, Kavanagh TJ & Fausto N (2010) Attenuated progression of diet-induced steatohepatitis in glutathione-deficient mice. *Lab Invest* **90**, 1704-1717.

Harmon RC, Tiniakos DG & Argo CK (2011) Inflammation in nonalcoholic steatohepatitis. *Expert Rev Gastroenterol Hepatol* **5**, 189-200.

He H, Jazdzewski K, Li W, Liyanarachchi S, Nagy R, Volinia S, Calin GA, Liu CG, Franssila K, Suster S, Kloos RT, Croce CM & de la Chapelle A (2005) The role of microRNA genes in papillary thyroid carcinoma. *Proc Natl Acad Sci U S A* **102**, 19075-19080.

Heijboer AC, Donga E, Voshol PJ, Dang ZC, Havekes LM, Romijn JA & Corssmit EP (2005) Sixteen hours of fasting differentially affects hepatic and muscle insulin sensitivity in mice. *J Lipid Res* **46**, 582-588.

Henkel C, Roderfeld M, Weiskirchen R, Berres ML, Hillebrandt S, Lammert F, Meyer HE, Stuhler K, Graf J & Roeb E (2006) Changes of the hepatic proteome in murine models for toxically induced fibrogenesis and sclerosing cholangitis. *Proteomics* **6**, 6538-6548.

Herbert JD & Coulson RA (1984) A role for carbonic anhydrase in de novo fatty acid synthesis in liver. *Ann N Y Acad Sci* **429**, 525-527.

Heukeshoven J & Dernick R (1985) Characterization of a solvent system for separation of water-insoluble poliovirus proteins by reversed-phase high-performance liquid chromatography. *J Chromatogr.* **326**, 91-101.

Hirako S, Kim H, Arai T, Chiba H & Matsumoto A (2010) Effect of concomitantly used fish oil and cholesterol on lipid metabolism. *J Nutr Biochem* **21**, 573-579.

Holden PR & Tugwood JD (1999) Peroxisome proliferator-activated receptor alpha: role in rodent liver cancer and species differences. *J Mol Endocrinol* **22**, 1-8.

Hostetler HA, Kier AB & Schroeder F (2006) Very-long-chain and branched-chain fatty acyl-CoAs are high affinity ligands for the peroxisome proliferator-activated receptor alpha (PPARalpha). *Biochemistry* **45**, 7669-7681.

Hou J, Lin L, Zhou W, Wang Z, Ding G, Dong Q, Qin L, Wu X, Zheng Y, Yang Y, Tian W, Zhang Q, Wang C, Zhuang SM, Zheng L, Liang A, Tao W & Cao X (2011) Identification of miRNomes in human liver and hepatocellular carcinoma reveals miR-199a/b-3p as therapeutic target for hepatocellular carcinoma. *Cancer Cell* **19**, 232-243.

Huang J, Jia Y, Fu T, Viswakarma N, Bai L, Rao MS, Zhu Y, Borensztajn J & Reddy JK (2011) Sustained activation of PPAR{alpha} by endogenous ligands increases hepatic fatty acid oxidation and prevents obesity in ob/ob mice. *FASEB J*.

Huang ZP, Zhou H, He HL, Chen CL, Liang D & Qu LH (2005) Genome-wide analyses of two families of snoRNA genes from Drosophila melanogaster, demonstrating the extensive utilization of introns for coding of snoRNAs. *RNA* **11**, 1303-1316.

Hussain MM (2000) A proposed model for the assembly of chylomicrons. *Atherosclerosis* **148**, 1-15.

Hussein O, Grosovski M, Lasri E, Svalb S, Ravid U & Assy N (2007) Monounsaturated fat decreases hepatic lipid content in non-alcoholic fatty liver disease in rats. *World J Gastroenterol* **13**, 361-368.

Imlay JA (2003) Pathways of oxidative damage. *Annu Rev Microbiol* **57**, 395-418.

Infante JP, Tschanz CL, Shaw N, Michaud AL, Lawrence P & Brenna JT (2002) Straight-chain acyl-CoA oxidase knockout mouse accumulates extremely long chain fatty acids from alpha-linolenic acid: evidence for runaway carousel-type enzyme kinetics in peroxisomal beta-oxidation diseases. *Mol Genet Metab* **75**, 108-119.

Ioshikhes I, Roy S & Sen CK (2007) Algorithms for mapping of mRNA targets for microRNA. *DNA Cell Biol* **26**, 265-272.

Ishii H, Horie Y, Ohshima S, Anezaki Y, Kinoshita N, Dohmen T, Kataoka E, Sato W, Goto T, Sasaki J, Sasaki T, Watanabe S, Suzuki A & Ohnishi H (2009) Eicosapentaenoic acid ameliorates steatohepatitis and hepatocellular carcinoma in hepatocyte-specific Pten-deficient mice. *J Hepatol* **50**, 562-571.

Ishii Y, Blundell JE, Halford JC & Rodgers RJ (2003) Palatability, food intake and the behavioural satiety sequence in male rats. *Physiol Behav* **80**, 37-47.

Issemann I & Green S (1990) Activation of a member of the steroid hormone receptor superfamily by peroxisome proliferators. *Nature* **347**, 645-650.

Ito M, Suzuki J, Sasaki M, Watanabe K, Tsujioka S, Takahashi Y, Gomori A, Hirose H, Ishihara A, Iwaasa H & Kanatani A (2006) Development of nonalcoholic

steatohepatitis model through combination of high-fat diet and tetracycline with morbid obesity in mice. *Hepatol Res* **34**, 92-98.

Ito Y, Sorensen KK, Bethea NW, Svistounov D, McCuskey MK, Smedsrod BH & McCuskey RS (2007) Age-related changes in the hepatic microcirculation in mice. *Exp Gerontol* **42**, 789-797.

Jacobs RL, Zhao Y, Koonen DP, Sletten T, Su B, Lingrell S, Cao G, Peake DA, Kuo MS, Proctor SD, Kennedy BP, Dyck JR & Vance DE (2010) Impaired de novo choline synthesis explains why phosphatidylethanolamine N-methyltransferase-deficient mice are protected from diet-induced obesity. *J Biol Chem* **285**, 22403-22413.

Jiang L, Wang Q, Yu Y, Zhao F, Huang P, Zeng R, Qi RZ, Li W & Liu Y (2009) Leptin contributes to the adaptive responses of mice to high-fat diet intake through suppressing the lipogenic pathway. *PLoS One* **4**, e6884.

Jimba S, Nakagami T, Takahashi M, Wakamatsu T, Hirota Y, Iwamoto Y & Wasada T (2005) Prevalence of non-alcoholic fatty liver disease and its association with impaired glucose metabolism in Japanese adults. *Diabet Med* **22**, 1141-1145.

Jin X, Ye YF, Chen SH, Yu CH, Liu J & Li YM (2009) MicroRNA expression pattern in different stages of nonalcoholic fatty liver disease. *Dig Liver Dis* **41**, 289-297.

Jung K, Fechner C & Egger E (1976) Influence of auxiliary enzymes on the spectrophotometric measurement of alanine aminotransferase and aspartate aminotransferase activities. *J Clin Chem Clin Biochem* **14**, 53-57.

Kadohisa M, Rolls ET & Verhagen JV (2005) Neuronal representations of stimuli in the mouth: the primate insular taste cortex, orbitofrontal cortex and amygdala. *Chem Senses* **30**, 401-419.

Kagansky N, Levy S, Keter D, Rimon E, Taiba Z, Fridman Z, Berger D, Knobler H & Malnick S (2004) Non-alcoholic fatty liver disease--a common and benign finding in octogenarian patients. *Liver Int* **24**, 588-594.

Kajikawa S, Harada T, Kawashima A, Imada K & Mizuguchi K (2009) Highly purified eicosapentaenoic acid prevents the progression of hepatic steatosis by repressing monounsaturated fatty acid synthesis in high-fat/high-sucrose diet-fed mice. *Prostaglandins Leukot Essent Fatty Acids* **80**, 229-238.

Kajikawa S, Harada T, Kawashima A, Imada K & Mizuguchi K (2010) Highly purified eicosapentaenoic acid ethyl ester prevents development of steatosis and hepatic fibrosis in rats. *Dig Dis Sci* **55**, 631-641.

Kalupahana NS, Claycombe K, Newman SJ, Stewart T, Siriwardhana N, Matthan N, Lichtenstein AH & Moustaid-Moussa N (2010) Eicosapentaenoic acid prevents and reverses insulin resistance in high-fat diet-induced obese mice via modulation of adipose tissue inflammation. *J Nutr* **140**, 1915-1922.

Kaluzny MA, Duncan LA, Merritt MV & Epps DE (1985) Rapid separation of lipid classes in high yield and purity using bonded phase columns. *J Lipid Res* **26**, 135-140.

Kanda T, Ishibashi O, Kawahigashi Y, Mishima T, Kosuge T, Mizuguchi Y, Shimizu T, Arima Y, Yokomuro S, Yoshida H, Tajiri T, Uchida E & Takizawa T (2010) Identification of obstructive jaundice-related microRNAs in mouse liver. *Hepatogastroenterology* **57**, 1013-1023.

Karmen A, Wroblewski F & Ladue JS (1955) Transaminase activity in human blood. *J Clin Invest* **34**, 126-131.

Kayden HJ, Senior JR & Mattson FH (1967) The monoglyceride pathway of fat absorption in man. *J Clin Invest* **46**, 1695-1703.

Kendrick AA, Choudhury M, Rahman SM, McCurdy CE, Friederich M, Van Hove JL, Watson PA, Birdsey N, Bao J, Gius D, Sack MN, Jing E, Kahn CR, Friedman JE & Jonscher KR (2011) Fatty liver is associated with reduced SIRT3 activity and mitochondrial protein hyperacetylation. *Biochem J* **433**, 505-514.

Kim G, Lee TH, Wetzel P, Geers C, Robinson MA, Myers TG, Owens JW, Wehr NB, Eckhaus MW, Gros G, Wynshaw-Boris A & Levine RL (2004) Carbonic anhydrase III is not required in the mouse for normal growth, development, and life span. *Mol Cell Biol* **24**, 9942-9947.

Kim S, Hwang do W & Lee DS (2009) A study of microRNAs in silico and in vivo: bioimaging of microRNA biogenesis and regulation. *FEBS J* **276**, 2165-2174.

Kirfel J, Magin TM & Reichelt J (2003) Keratins: a structural scaffold with emerging functions. *Cell Mol Life Sci* **60**, 56-71.

Kirpich IA, Gobejishvili LN, Bon Homme M, Waigel S, Cave M, Arteel G, Barve SS, McClain CJ & Deaciuc IV (2011) Integrated hepatic transcriptome and proteome analysis of mice with high-fat diet-induced nonalcoholic fatty liver disease. *J Nutr Biochem* **22**, 38-45.

Kiss T (2002) Small nucleolar RNAs: an abundant group of noncoding RNAs with diverse cellular functions. *Cell* **109**, 145-148.

Klein CJ, Stanek GS & Wiles CE, 3rd (1998) Overfeeding macronutrients to critically ill adults: metabolic complications. *J Am Diet Assoc* **98**, 795-806.

Koba K, Rozee LA, Horrobin DF & Huang YS (1994) Effects of dietary protein and cholesterol on phosphatidylcholine and phosphatidylethanolamine molecular species in mouse liver. *Lipids* **29**, 33-39.

Kohout M, Kohoutova B & Heimberg M (1971) The regulation of hepatic triglyceride metabolism by free fatty acids. *J Biol Chem* **246**, 5067-5074.

Kojima S, Gatfield D, Esau CC & Green CB (2010) MicroRNA-122 modulates the rhythmic expression profile of the circadian deadenylase Nocturnin in mouse liver. *PLoS One* **5**, e11264.

Kuo WH, Chiang WL, Yang SF, Yeh KT, Yeh CM, Hsieh YS & Chu SC (2003) The differential expression of cytosolic carbonic anhydrase in human hepatocellular carcinoma. *Life Sci* **73**, 2211-2223.

Lambert MS, Avella MA, Botham KM & Mayes PA (2000) The type of dietary fat alters the hepatic uptake and biliary excretion of cholesterol from chylomicron remnants. *Br J Nutr* **83**, 431-438.

Larter CZ & Farrell GC (2006) Insulin resistance, adiponectin, cytokines in NASH: Which is the best target to treat? *J Hepatol* **44**, 253-261.

Larter CZ & Yeh MM (2008) Animal models of NASH: getting both pathology and metabolic context right. *J Gastroenterol Hepatol* **23**, 1635-1648.

Larter CZ, Yeh MM, Haigh WG, Williams J, Brown S, Bell-Anderson KS, Lee SP & Farrell GC (2008) Hepatic free fatty acids accumulate in experimental steatohepatitis: role of adaptive pathways. *J Hepatol* **48**, 638-647.

Larter CZ, Yeh MM, Van Rooyen DM, Teoh NC, Brooling J, Hou JY, Williams J, Clyne M, Nolan CJ & Farrell GC (2009) Roles of adipose restriction and metabolic factors in progression of steatosis to steatohepatitis in obese, diabetic mice. *J Gastroenterol Hepatol* **24**, 1658-1668.

Le Couteur DG, Warren A, Cogger VC, Smedsrod B, Sorensen KK, De Cabo R, Fraser R & McCuskey RS (2008) Old age and the hepatic sinusoid. *Anat Rec (Hoboken)* **291**, 672-683.

Leavens KF & Birnbaum MJ (2011) Insulin signaling to hepatic lipid metabolism in health and disease. *Crit Rev Biochem Mol Biol* **46**, 200-215.

Lee EJ, Baek M, Gusev Y, Brackett DJ, Nuovo GJ & Schmittgen TD (2008) Systematic evaluation of microRNA processing patterns in tissues, cell lines, and tumors. *RNA* **14**, 35-42.

Lee JH, Felipe P, Yang YH, Kim MY, Kwon OY, Sok DE, Kim HC & Kim MR (2009) Effects of dietary supplementation with red-pigmented leafy lettuce (Lactuca sativa) on lipid profiles and antioxidant status in C57BL/6J mice fed a high-fat high-cholesterol diet. *Br J Nutr* **101**, 1246-1254.

Lee JH, Garboczi DN, Thomas PJ & Pedersen PL (1990) Mitochondrial ATP synthase. cDNA cloning, amino acid sequence, overexpression, and properties of the rat liver alpha subunit. *J Biol Chem* **265**, 4664-4669.

Lee JY, Moon JH, Park JS, Lee BW, Kang ES, Ahn CW, Lee HC & Cha BS (2011) Dietary oleate has beneficial effects on every step of non-alcoholic Fatty liver disease progression in a methionine- and choline-deficient diet-fed animal model. *Diabetes Metab J* **35**, 489-496.

Lee PL, Halloran C, Cross AR & Beutler E (2000) NADH-ferric reductase activity associated with dihydropteridine reductase. *Biochem Biophys Res Commun* **271**, 788-795.

Lee SS, Chan WY, Lo CK, Wan DC, Tsang DS & Cheung WT (2004) Requirement of PPARalpha in maintaining phospholipid and triacylglycerol homeostasis during energy deprivation. *J Lipid Res* **45**, 2025-2037.

Lee YH, Boelsterli UA, Lin Q & Chung MC (2008) Proteomics profiling of hepatic mitochondria in heterozygous Sod2+/- mice, an animal model of discreet mitochondrial oxidative stress. *Proteomics* **8**, 555-568.

Lefils J, Geloen A, Vidal H, Lagarde M & Bernoud-Hubac N (2010) Dietary DHA: time course of tissue uptake and effects on cytokine secretion in mice. *Br J Nutr* **104**, 1304-1312.

Leite NC, Salles GF, Araujo AL, Villela-Nogueira CA & Cardoso CR (2009) Prevalence and associated factors of non-alcoholic fatty liver disease in patients with type-2 diabetes mellitus. *Liver Int* **29**, 113-119.

Lepage G & Roy CC (1986) Direct transesterification of all classes of lipids in a one-step reaction. *J Lipid Res* **27**, 114-120.

Lewis AP & Jopling CL (2010) Regulation and biological function of the liver-specific miR-122. *Biochem Soc Trans* **38**, 1553-1557.

Leyton J, Drury PJ & Crawford MA (1987) Differential oxidation of saturated and unsaturated fatty acids in vivo in the rat. *Br J Nutr* **57**, 383-393.

Li M, Fu W & Li XA (2010) Differential fatty acid profile in adipose and non-adipose tissues in obese mice. *Int J Clin Exp Med* **3**, 303-307.

Li N, Muthusamy S, Liang R, Sarojini H & Wang E (2011) Increased expression of miR-34a and miR-93 in rat liver during aging, and their impact on the expression of Mgst1 and Sirt1. *Mech Ageing Dev* **132**, 75-85.

Li Z, Agellon LB, Allen TM, Umeda M, Jewell L, Mason A & Vance DE (2006) The ratio of phosphatidylcholine to phosphatidylethanolamine influences membrane integrity and steatohepatitis. *Cell Metab* **3**, 321-331.

Li Z, Soloski MJ & Diehl AM (2005) Dietary factors alter hepatic innate immune system in mice with nonalcoholic fatty liver disease. *Hepatology* **42**, 880-885.

Lieber CS, DeCarli LM, Leo MA, Mak KM, Ponomarenko A, Ren C & Wang X (2008) Beneficial effects versus toxicity of medium-chain triacylglycerols in rats with NASH. *J Hepatol* **48**, 318-326.

Lieber CS, Leo MA, Mak KM, Xu Y, Cao Q, Ren C, Ponomarenko A & DeCarli LM (2004) Model of nonalcoholic steatohepatitis. *Am J Clin Nutr* **79**, 502-509.

Lin X, Yue P, Chen Z & Schonfeld G (2005) Hepatic triglyceride contents are genetically determined in mice: results of a strain survey. *Am J Physiol Gastrointest Liver Physiol* **288**, G1179-1189.

Liu HY & Chen J (2011) Polymorphisms in miRNA binding site: new insight into small cell lung cancer susceptibility. *Acta Pharmacol Sin* **32**, 1191-1192.

Lo CM, Nordskog BK, Nauli AM, Zheng S, Vonlehmden SB, Yang Q, Lee D, Swift LL, Davidson NO & Tso P (2008) Why does the gut choose apolipoprotein B48 but not B100 for chylomicron formation? *Am J Physiol Gastrointest Liver Physiol* **294**, G344-352.

Lof C, Cohen M, Vermeulen LP, van Roermund CW, Wanders RJ & Meijer AJ (1983) Properties of carbamoyl-phosphate synthetase (ammonia) in rat-liver mitochondria made permeable with toluene. *Eur J Biochem* **135**, 251-258.

Lorente-Cebrian S, Bustos M, Marti A, Martinez JA & Moreno-Aliaga MJ (2009) Eicosapentaenoic acid stimulates AMP-activated protein kinase and increases visfatin secretion in cultured murine adipocytes. *Clin Sci (Lond)* **117**, 243-249.

Lu S & Archer MC (2007) Celecoxib decreases fatty acid synthase expression via down-regulation of c-Jun N-terminal kinase-1. *Exp Biol Med (Maywood)* **232**, 643-653.

Ludwig J, Viggiano TR, McGill DB & Oh BJ (1980) Nonalcoholic steatohepatitis: Mayo Clinic experiences with a hitherto unnamed disease. *Mayo Clin Proc* **55**, 434-438.

Ludwig J, Viggiano TR, McGill DB & Oh BJ (1980) Nonalcoholic steatohepatitis: Mayo Clinic experiences with a hitherto unnamed disease. *Mayo Clin Proc* **55**, 434-438.

Lynch CJ, Fox H, Hazen SA, Stanley BA, Dodgson S & Lanoue KF (1995) Role of hepatic carbonic anhydrase in de novo lipogenesis. *Biochem J* **310 (Pt 1)**, 197-202.

Magdeldin S, Elewa Y, Ikeda T, Ikei J, Zhang Y, Xu B, Nameta M, Fujinaka H, Yoshida Y, Yaoita E & Yamamoto T (2009) Dietary supplementation with arachidonic acid but not eicosapentaenoic or docosahexaenoic acids alter lipids metabolism in C57BL/6J mice. *Gen Physiol Biophys* **28**, 266-275.

Marchesini G, Brizi M, Bianchi G, Tomassetti S, Bugianesi E, Lenzi M, McCullough AJ, Natale S, Forlani G & Melchionda N (2001) Nonalcoholic fatty liver disease: a feature of the metabolic syndrome. *Diabetes* **50**, 1844-1850.

Marchesini G, Brizi M, Morselli-Labate AM, Bianchi G, Bugianesi E, McCullough AJ, Forlani G & Melchionda N (1999) Association of nonalcoholic fatty liver disease with insulin resistance. *Am J Med* **107**, 450-455.

Marchesini G & Marzocchi R (2007) Metabolic syndrome and NASH. *Clin Liver Dis* **11**, 105-117, ix.

Markham R (1942) A steam distillation apparatus suitable for micro-Kjeldahl analysis. *Biohcem J* **36**, 790-791.

Marouga R, David S & Hawkins E (2005) The development of the DIGE system: 2D fluorescence difference gel analysis technology. *Anal Bioanal Chem* **382**, 669-678.

Marquez RT, Wendlandt E, Galle CS, Keck K & McCaffrey AP (2010) MicroRNA-21 is upregulated during the proliferative phase of liver regeneration, targets Pellino-1, and inhibits NF-kappaB signaling. *Am J Physiol Gastrointest Liver Physiol* **298**, G535-541.

Mathiesen UL, Franzen LE, Fryden A, Foberg U & Bodemar G (1999) The clinical significance of slightly to moderately increased liver transaminase values in asymptomatic patients. *Scand J Gastroenterol* **34**, 85-91.

Mavrommatis Y, Ross K, Rucklidge G, Reid M, Duncan G, Gordon MJ, Thies F, Sneddon A & de Roos B (2010) Intervention with fish oil, but not with docosahexaenoic acid, results in lower levels of hepatic soluble epoxide hydrolase with time in apoE knockout mice. *Br J Nutr* **103**, 16-24.

Mayes PA & Felts JM (1967) Regulation of fat metabolism of the liver. *Nature* **215**, 716-718.

Menahan LA & Sobocinski KA (1983) Comparison of carbohydrate and lipid metabolism in mice and rats during fasting. *Comp Biochem Physiol B* **74**, 859-864.

Meng F, Henson R, Wehbe-Janek H, Ghoshal K, Jacob ST & Patel T (2007) MicroRNA-21 regulates expression of the PTEN tumor suppressor gene in human hepatocellular cancer. *Gastroenterology* **133**, 647-658.

Merat S, Aduli M, Kazemi R, Sotoudeh M, Sedighi N, Sohrabi M & Malekzadeh R (2008) Liver histology changes in nonalcoholic steatohepatitis after one year of treatment with probucol. *Dig Dis Sci* **53**, 2246-2250.

Mestdagh P, Van Vlierberghe P, De Weer A, Muth D, Westermann F, Speleman F & Vandesompele J (2009) A novel and universal method for microRNA RT-qPCR data normalization. *Genome Biol* **10**, R64.

Meyer SU, Pfaffl MW & Ulbrich SE (2010) Normalization strategies for microRNA profiling experiments: a 'normal' way to a hidden layer of complexity? *Biotechnol Lett* **32**, 1777-1788.

Miller DS & Payne PR (1959) A ballistic bomb calorimeter. *British Journal of Nutrition*, pp 501-508.

Minehira K, Young SG, Villanueva CJ, Yetukuri L, Oresic M, Hellerstein MK, Farese RV, Jr., Horton JD, Preitner F, Thorens B & Tappy L (2008) Blocking VLDL secretion causes hepatic steatosis but does not affect peripheral lipid stores or insulin sensitivity in mice. *J Lipid Res* **49**, 2038-2044.

Mittendorfer B, Patterson BW & Klein S (2003) Effect of sex and obesity on basal VLDL-triacylglycerol kinetics. *Am J Clin Nutr* **77**, 573-579.

Mofrad P, Contos MJ, Haque M, Sargeant C, Fisher RA, Luketic VA, Sterling RK, Shiffman ML, Stravitz RT & Sanyal AJ (2003) Clinical and histologic spectrum of nonalcoholic fatty liver disease associated with normal ALT values. *Hepatology* **37**, 1286-1292.

Moll R & Franke WW (1982) Intermediate filaments and their interaction with membranes. The desmosome-cytokeratin filament complex and epithelial differentiation. *Pathol Res Pract* **175**, 146-161.

Moore JB (2010) Non-alcoholic fatty liver disease: the hepatic consequence of obesity and the metabolic syndrome. *Proc Nutr Soc* **69**, 211-220.

Moran-Salvador E, Lopez-Parra M, Garcia-Alonso V, Titos E, Martinez-Clemente M, Gonzalez-Periz A, Lopez-Vicario C, Barak Y, Arroyo V & Claria J (2011) Role for PPARgamma in obesity-induced hepatic steatosis as determined by hepatocyte- and macrophage-specific conditional knockouts. *FASEB J* **25**, 2538-2550.

Morizono H, Listrom CD, Rajagopal BS, Aoyagi M, McCann MT, Allewell NM & Tuchman M (1997) 'Late onset' ornithine transcarbamylase deficiency: function of three purified recombinant mutant enzymes. *Hum Mol Genet* **6**, 963-968.

Morlando M, Ballarino M, Gromak N, Pagano F, Bozzoni I & Proudfoot NJ (2008) Primary microRNA transcripts are processed co-transcriptionally. *Nat Struct Mol Biol* **15**, 902-909.

Murakami Y, Toyoda H, Tanaka M, Kuroda M, Harada Y, Matsuda F, Tajima A, Kosaka N, Ochiya T & Shimotohno K (2011) The progression of liver fibrosis is related with overexpression of the miR-199 and 200 families. *PLoS One* **6**, e16081.

Murase T, Misawa K, Minegishi Y, Aoki M, Ominami H, Suzuki Y, Shibuya Y & Hase T (2011) Coffee polyphenols suppress diet-induced body fat accumulation by downregulating SREBP-1c and related molecules in C57BL/6J mice. *Am J Physiol Endocrinol Metab* **300**, E122-133.

Murata T & Yamaguchi M (1997) Molecular cloning of the cDNA coding for regucalcin and its mRNA expression in mouse liver: the expression is stimulated by calcium administration. *Mol Cell Biochem* **173**, 127-133.

Myers RP (2008) Noninvasive markers of liver fibrosis: playing the probabilities. *Liver Int* **28**, 1328-1331.

Nakashima C & Yamaguchi M (2006) Overexpression of regucalcin enhances glucose utilization and lipid production in cloned rat hepatoma H4-II-E cells: Involvement of insulin resistance. *J Cell Biochem* **99**, 1582-1592.

Nanji AA (2004) Animal models of nonalcoholic fatty liver disease and steatohepatitis. *Clin Liver Dis* **8**, 559-574, ix.

Neat CE, Thomassen MS & Osmundsen H (1980) Induction of peroxisomal beta-oxidation in rat liver by high-fat diets. *Biochem J* **186**, 369-371.

Nelson GJ, Kelley DS, Schmidt PC & Serrato CM (1987) The effects of fat-free, saturated and polyunsaturated fat diets on rat liver and plasma lipids. *Lipids* **22**, 88-94.

Nemoto N, Suzuki S, Kikuchi H, Okabe H, Sassa S & Sakamoto S (2009) Ethyl-eicosapentaenoic acid reduces liver lipids and lowers plasma levels of lipids in mice fed a high-fat diet. *In Vivo* **23**, 685-689.

Neuhoff V, Arold N, Taube D & Ehrhardt W (1988) Improved staining of proteins in polyacrylamide gels including isoelectric focusing gels with clear background at nanogram sensitivity using Coomassie Brilliant Blue G-250 and R-250. *Electrophoresis.* **9**, 255-262.

Neuschwander-Tetri BA (2005) Nonalcoholic steatohepatitis and the metabolic syndrome. *Am J Med Sci* **330**, 326-335.

Neuschwander-Tetri BA & Caldwell SH (2003) Nonalcoholic steatohepatitis: summary of an AASLD Single Topic Conference. *Hepatology* **37**, 1202-1219.

Nikolsky Y, Kirillov E, Zuev R, Rakhmatulin E & Nikolskaya T (2009) Functional analysis of OMICs data and small molecule compounds in an integrated "knowledge-based" platform. *Methods Mol Biol* **563**, 177-196.

Nilsen TW (2007) Mechanisms of microRNA-mediated gene regulation in animal cells. *Trends Genet* **23**, 243-249.

Ning J, Hong T, Yang X, Mei S, Liu Z, Liu HY & Cao W (2011) Insulin and insulin signaling play a critical role in fat induction of insulin resistance in mouse. *Am J Physiol Endocrinol Metab* **301**, E391-401.

Nishikawa S, Yasoshima A, Doi K, Nakayama H & Uetsuka K (2007) Involvement of sex, strain and age factors in high fat diet-induced obesity in C57BL/6J and BALB/cA mice. *Exp Anim* **56**, 263-272.

Noga AA & Vance DE (2003) A gender-specific role for phosphatidylethanolamine N-methyltransferase-derived phosphatidylcholine in the regulation of plasma high density and very low density lipoproteins in mice. *J Biol Chem* **278**, 21851-21859.

Nosadini R, Avogaro A, Mollo F, Marescotti C, Tiengo A, Duner E, Merkel C, Gatta A, Zuin R, de Kreutzenberg S & et al. (1984) Carbohydrate and lipid metabolism in cirrhosis. Evidence that hepatic uptake of gluconeogenic precursors and of free fatty acids depends on effective hepatic flow. *J Clin Endocrinol Metab* **58**, 1125-1132.

Okabe H, Uji Y, Nagashima K & Noma A (1980) Enzymic determination of free fatty acids in serum. *Clin Chem* **26**, 1540-1543.

Olson P, Lu J, Zhang H, Shai A, Chun MG, Wang Y, Libutti SK, Nakakura EK, Golub TR & Hanahan D (2009) MicroRNA dynamics in the stages of tumorigenesis correlate with hallmark capabilities of cancer. *Genes Dev* **23**, 2152-2165.

Olsson IA & Dahlborn K (2002) Improving housing conditions for laboratory mice: a review of "environmental enrichment". *Lab Anim* **36**, 243-270.

Ono H, Shimano H, Katagiri H, Yahagi N, Sakoda H, Onishi Y, Anai M, Ogihara T, Fujishiro M, Viana AY, Fukushima Y, Abe M, Shojima N, Kikuchi M, Yamada

N, Oka Y & Asano T (2003) Hepatic Akt activation induces marked hypoglycemia, hepatomegaly, and hypertriglyceridemia with sterol regulatory element binding protein involvement. *Diabetes* **52**, 2905-2913.

Pachikian BD, Essaghir A, Demoulin JB, Neyrinck AM, Catry E, De Backer FC, Dejeans N, Dewulf EM, Sohet FM, Portois L, Deldicque L, Molendi-Coste O, Leclercq IA, Francaux M, Carpentier YA, Foufelle F, Muccioli GG, Cani PD & Delzenne NM (2011) Hepatic n-3 polyunsaturated fatty acid depletion promotes steatosis and insulin resistance in mice: genomic analysis of cellular targets. *PLoS One* **6**, e23365.

Padgett KA, Lan RY, Leung PC, Lleo A, Dawson K, Pfeiff J, Mao TK, Coppel RL, Ansari AA & Gershwin ME (2009) Primary biliary cirrhosis is associated with altered hepatic microRNA expression. *J Autoimmun* **32**, 246-253.

Pais R, Pascale A, Fedchuck L, Charlotte F, Poynard T & Ratziu V (2010) Progression from isolated steatosis to steatohepatitis and fibrosis in nonalcoholic fatty liver disease. *Gastroenterol Clin Biol*.

Pan M, Cederbaum AI, Zhang YL, Ginsberg HN, Williams KJ & Fisher EA (2004) Lipid peroxidation and oxidant stress regulate hepatic apolipoprotein B degradation and VLDL production. *J Clin Invest* **113**, 1277-1287.

Panchal SK, Poudyal H, Iyer A, Nazer R, Alam MA, Diwan V, Kauter K, Sernia C, Campbell F, Ward L, Gobe G, Fenning A & Brown L (2011) High-carbohydrate, high-fat diet-induced metabolic syndrome and cardiovascular remodeling in rats. *J Cardiovasc Pharmacol* **57**, 611-624.

Park HJ, DiNatale DA, Chung MY, Park YK, Lee JY, Koo SI, O'Connor M, Manautou JE & Bruno RS (2011) Green tea extract attenuates hepatic steatosis by decreasing adipose lipogenesis and enhancing hepatic antioxidant defenses in ob/ob mice. *J Nutr Biochem* **22**, 393-400.

Pascale A, Pais R & Ratziu V (2010) An overview of nonalcoholic steatohepatitis: past, present and future directions. *J Gastrointestin Liver Dis* **19**, 415-423.

Pawlicki JM & Steitz JA (2008) Primary microRNA transcript retention at sites of transcription leads to enhanced microRNA production. *J Cell Biol* **182**, 61-76.

Perl AK, Wilgenbus P, Dahl U, Semb H & Christofori G (1998) A causal role for E-cadherin in the transition from adenoma to carcinoma. *Nature* **392**, 190-193.

Pfeffer S, Zavolan M, Grasser FA, Chien M, Russo JJ, Ju J, John B, Enright AJ, Marks D, Sander C & Tuschl T (2004) Identification of virus-encoded microRNAs. *Science* **304**, 734-736.

Phinney DG, Keiper CL, Francis MK & Ryder K (1994) Quantitative analysis of the contribution made by 5'-flanking and 3'-flanking sequences to the transcriptional regulation of junB by growth factors. *Oncogene* **9**, 2353-2362.

Pickens MK, Ogata H, Soon RK, Grenert JP & Maher JJ (2010) Dietary fructose exacerbates hepatocellular injury when incorporated into a methionine-choline-deficient diet. *Liver Int* **30**, 1229-1239.

Polozova A, Gionfriddo E & Salem N, Jr. (2006) Effect of docosahexaenoic acid on tissue targeting and metabolism of plasma lipoproteins. *Prostaglandins Leukot Essent Fatty Acids* **75**, 183-190.

Polozova A & Salem N, Jr. (2007) Role of liver and plasma lipoproteins in selective transport of n-3 fatty acids to tissues: a comparative study of 14C-DHA and 3H-oleic acid tracers. *J Mol Neurosci* **33**, 56-66.

Postic C & Girard J (2008) The role of the lipogenic pathway in the development of hepatic steatosis. *Diabetes Metab* **34**, 643-648.

Priego T, Sanchez J, Pico C & Palou A (2008) Sex-differential expression of metabolism-related genes in response to a high-fat diet. *Obesity (Silver Spring)* **16**, 819-826.

Qin W, Sundaram M, Wang Y, Zhou H, Zhong S, Chang CC, Manhas S, Yao EF, Parks RJ, McFie PJ, Stone SJ, Jiang ZG, Wang C, Figeys D, Jia W & Yao Z (2011) Missense mutation in APOC3 within the C-terminal lipid binding domain of human ApoC-III results in impaired assembly and secretion of triacylglycerol-rich very low density lipoproteins: evidence that ApoC-III plays a major role in the formation of lipid precursors within the microsomal lumen. *J Biol Chem* **286**, 27769-27780.

Qureshi K & Abrams GA (2007) Metabolic liver disease of obesity and role of adipose tissue in the pathogenesis of nonalcoholic fatty liver disease. *World J Gastroenterol* **13**, 3540-3553.

Radonjic M, van Erk MJ, Pasman WJ, Wortelboer HM, Hendriks HF & van Ommen B (2009) Effect of body fat distribution on the transcription response to dietary fat interventions. *Genes Nutr* **4**, 143-149.

Raisanen SR, Lehenkari P, Tasanen M, Rahkila P, Harkonen PL & Vaananen HK (1999) Carbonic anhydrase III protects cells from hydrogen peroxide-induced apoptosis. *FASEB J* **13**, 513-522.

Rand TA, Petersen S, Du F & Wang X (2005) Argonaute2 cleaves the anti-guide strand of siRNA during RISC activation. *Cell* **123**, 621-629.

Ratziu V, Bellentani S, Cortez-Pinto H, Day C & Marchesini G (2010) A position statement on NAFLD/NASH based on the EASL 2009 special conference. *J Hepatol* **53**, 372-384.

Raubenheimer PJ, Nyirenda MJ & Walker BR (2006) A choline-deficient diet exacerbates fatty liver but attenuates insulin resistance and glucose intolerance in mice fed a high-fat diet. *Diabetes* **55**, 2015-2020.

Redgrave TG (1970) Formation of cholesteryl ester-rich particulate lipid during metabolism of chylomicrons. *J Clin Invest* **49**, 465-471.

Reid BN, Ables GP, Otlivanchik OA, Schoiswohl G, Zechner R, Blaner WS, Goldberg IJ, Schwabe RF, Chua SC, Jr. & Huang LS (2008) Hepatic overexpression of hormone-sensitive lipase and adipose triglyceride lipase promotes fatty acid oxidation, stimulates direct release of free fatty acids, and ameliorates steatosis. *J Biol Chem* **283**, 13087-13099.

Remily-Wood ER, Liu RZ, Xiang Y, Chen Y, Thomas CE, Rajyaguru N, Kaufman LM, Ochoa JE, Hazlehurst L, Pinilla-Ibarz J, Lancet J, Zhang G, Haura E, Shibata D, Yeatman T, Smalley KS, Dalton WS, Huang E, Scott E, Bloom GC, Eschrich SA & Koomen JM (2011) A database of reaction monitoring mass spectrometry assays for elucidating therapeutic response in cancer. *Proteomics Clin Appl* **5**, 383-396.

Rinella ME, Elias MS, Smolak RR, Fu T, Borensztajn J & Green RM (2008) Mechanisms of hepatic steatosis in mice fed a lipogenic methionine choline-deficient diet. *J Lipid Res* **49**, 1068-1076.

Robins SJ, Fasulo JM, Robins VF & Patton GM (1991) Utilization of different fatty acids for hepatic and biliary phosphatidylcholine formation and the effect of changes in phosphatidylcholine molecular species on biliary lipid secretion. *J Lipid Res* **32**, 985-992.

Rodriguez A, Griffiths-Jones S, Ashurst JL & Bradley A (2004) Identification of mammalian microRNA host genes and transcription units. *Genome Res* **14**, 1902-1910.

Rodriguez E, Ribot J, Rodriguez AM & Palou A (2004) PPAR-gamma2 expression in response to cafeteria diet: gender- and depot-specific effects. *Obes Res* **12**, 1455-1463.

Rodriguez-Suarez E, Duce AM, Caballeria J, Martinez Arrieta F, Fernandez E, Gomara C, Alkorta N, Ariz U, Martinez-Chantar ML, Lu SC, Elortza F & Mato JM (2010) Non-alcoholic fatty liver disease proteomics. *Proteomics Clin Appl* **4**, 362-371.

Romestaing C, Piquet MA, Letexier D, Rey B, Mourier A, Servais S, Belouze M, Rouleau V, Dautresme M, Ollivier I, Favier R, Rigoulet M, Duchamp C & Sibille B (2008) Mitochondrial adaptations to steatohepatitis induced by a methionine- and choline-deficient diet. *Am J Physiol Endocrinol Metab* **294**, E110-119.

Ronchi VP, Conde RD, Guillemot JC & Sanllorenti PM (2004) The mouse liver content of carbonic anhydrase III and glutathione S-tranferases A3 and P1 depend on dietary supply of methionine and cysteine. *Int J Biochem Cell Biol* **36**, 1993-2004.

Rubio-Aliaga I, Roos B, Sailer M, McLoughlin GA, Boekschoten MV, van Erk M, Bachmair EM, van Schothorst EM, Keijer J, Coort SL, Evelo C, Gibney MJ, Daniel H, Muller M, Kleemann R & Brennan L (2011) Alterations in hepatic one-carbon metabolism and related pathways following a high-fat dietary intervention. *Physiol Genomics* **43**, 408-416.

Salter AM, Mangiapane EH, Bennett AJ, Bruce JS, Billett MA, Anderton KL, Marenah CB, Lawson N & White DA (1998) The effect of different dietary fatty acids on lipoprotein metabolism: concentration-dependent effects of diets enriched in oleic, myristic, palmitic and stearic acids. *Br J Nutr* **79**, 195-202.

Samuel VT (2011) Fructose induced lipogenesis: from sugar to fat to insulin resistance. *Trends Endocrinol Metab* **22**, 60-65.

Samuelsson AM, Matthews PA, Argenton M, Christie MR, McConnell JM, Jansen EH, Piersma AH, Ozanne SE, Twinn DF, Remacle C, Rowlerson A, Poston L & Taylor PD (2008) Diet-induced obesity in female mice leads to offspring hyperphagia, adiposity, hypertension, and insulin resistance: a novel murine model of developmental programming. *Hypertension* **51**, 383-392.

Sanchez JC, Chiappe D, Converset V, Hoogland C, Binz PA, Paesano S, Appel RD, Wang S, Sennitt M, Nolan A, Cawthorne MA & Hochstrasser DF (2001) The mouse SWISS-2D PAGE database: a tool for proteomics study of diabetes and obesity. *Proteomics* **1**, 136-163.

Sanders TA, de Grassi T, Miller GJ & Morrissey JH (2000) Influence of fatty acid chain length and cis/trans isomerization on postprandial lipemia and factor VII in healthy subjects (postprandial lipids and factor VII). *Atherosclerosis* **149**, 413-420.

Sanders TA, Filippou A, Berry SE, Baumgartner S & Mensink RP (2011) Palmitic acid in the sn-2 position of triacylglycerols acutely influences postprandial lipid metabolism. *Am J Clin Nutr* **94**, 1433-1441.

Sanyal AJ (2011) NASH: A global health problem. *Hepatol Res* **41**, 670-674.

Sanyal G (1984) The carbon dioxide hydration activity of the sulfonamide-resistant carbonic anhydrase from the liver of male rat: pH independence of the steady-state kinetics. *Arch Biochem Biophys* **234**, 576-579.

Sato N (2007) Central role of mitochondria in metabolic regulation of liver pathophysiology. *J Gastroenterol Hepatol* **22 Suppl 1**, S1-6.

Satyanarayana A, Klarmann KD, Gavrilova O & Keller JR (2011) Ablation of the transcriptional regulator Id1 enhances energy expenditure, increases insulin sensitivity, and protects against age and diet induced insulin resistance, and hepatosteatosis. *FASEB J*.

Schmid GM, Converset V, Walter N, Sennitt MV, Leung KY, Byers H, Ward M, Hochstrasser DF, Cawthorne MA & Sanchez JC (2004) Effect of high-fat diet on the expression of proteins in muscle, adipose tissues, and liver of C57BL/6 mice. *Proteomics* **4**, 2270-2282.

Schmid PC, Spimrova I & Schmid HH (1997) Generation and remodeling of highly polyunsaturated molecular species of rat hepatocyte phospholipids. *Lipids* **32**, 1181-1187.

Schmitz G & Ecker J (2008) The opposing effects of n-3 and n-6 fatty acids. *Prog Lipid Res* **47**, 147-155.

Schoonjans K, Staels B & Auwerx J (1996) The peroxisome proliferator activated receptors (PPARS) and their effects on lipid metabolism and adipocyte differentiation. *Biochim Biophys Acta* **1302**, 93-109.

Seidner DL, Mascioli EA, Istfan NW, Porter KA, Selleck K, Blackburn GL & Bistrian BR (1989) Effects of long-chain triglyceride emulsions on reticuloendothelial system function in humans. *JPEN J Parenter Enteral Nutr* **13**, 614-619.

Seo T, Blaner WS & Deckelbaum RJ (2005) Omega-3 fatty acids: molecular approaches to optimal biological outcomes. *Curr Opin Lipidol* **16**, 11-18.

Seppala-Lindroos A, Vehkavaara S, Hakkinen AM, Goto T, Westerbacka J, Sovijarvi A, Halavaara J & Yki-Jarvinen H (2002) Fat accumulation in the liver is associated with defects in insulin suppression of glucose production and serum free fatty acids independent of obesity in normal men. *J Clin Endocrinol Metab* **87**, 3023-3028.

Serviddio G, Giudetti AM, Bellanti F, Priore P, Rollo T, Tamborra R, Siculella L, Vendemiale G, Altomare E & Gnoni GV (2011) Oxidation of hepatic carnitine palmitoyl transferase-I (CPT-I) impairs fatty acid beta-oxidation in rats fed a methionine-choline deficient diet. *PLoS One* **6**, e24084.

Shaw DI, Hall WL, Jeffs NR & Williams CM (2007) Comparative effects of fatty acids on endothelial inflammatory gene expression. *Eur J Nutr* **46**, 321-328.

Shen Q, Cicinnati VR, Zhang X, Iacob S, Weber F, Sotiropoulos GC, Radtke A, Lu M, Paul A, Gerken G & Beckebaum S (2010) Role of microRNA-199a-5p and discoidin domain receptor 1 in human hepatocellular carcinoma invasion. *Mol Cancer* **9**, 227.

Sheng X, Wang M, Lu M, Xi B, Sheng H & Zang YQ (2011) Rhein ameliorates fatty liver disease through negative energy balance, hepatic lipogenic regulation, and immunomodulation in diet-induced obese mice. *Am J Physiol Endocrinol Metab* **300**, E886-893.

Sinclair AJ & Crawford MA (1972) The incorporation of linolenic aid and docosahexaenoic acid into liver and brain lipids of developing rats. *FEBS Lett* **26**, 127-129.

Small DM (1991) The effects of glyceride structure on absorption and metabolism. *Annu. Rev. Nutr* **11**, 413-434.

Snider NT, Weerasinghe SV, Iniguez-Lluhi JA, Herrmann H & Omary MB (2011) Keratin hypersumoylation alters filament dynamics and is a marker for human liver disease and keratin mutation. *J Biol Chem* **286**, 2273-2284.

Sniderman KW (1998) Hepatocellular carcinoma with portal vein tumor thrombus. *Radiology* **207**, 552-553.

Song B, Wang C, Liu J, Wang X, Lv L, Wei L, Xie L, Zheng Y & Song X (2010) MicroRNA-21 regulates breast cancer invasion partly by targeting tissue inhibitor of metalloproteinase 3 expression. *J Exp Clin Cancer Res* **29**, 29.

Song G, Sharma AD, Roll GR, Ng R, Lee AY, Blelloch RH, Frandsen NM & Willenbring H (2010) MicroRNAs control hepatocyte proliferation during liver regeneration. *Hepatology* **51**, 1735-1743.

Song JH, Fujimoto K & Miyazawa T (2000) Polyunsaturated (n-3) fatty acids susceptible to peroxidation are increased in plasma and tissue lipids of rats fed docosahexaenoic acid-containing oils. *J Nutr* **130**, 3028-3033.

Sorrentino P, Tarantino G, Conca P, Perrella A, Terracciano ML, Vecchione R, Gargiulo G, Gennarelli N & Lobello R (2004) Silent non-alcoholic fatty liver disease-a clinical-histological study. *J Hepatol* **41**, 751-757.

Spadaro L, Magliocco O, Spampinato D, Piro S, Oliveri C, Alagona C, Papa G, Rabuazzo AM & Purrello F (2008) Effects of n-3 polyunsaturated fatty acids in subjects with nonalcoholic fatty liver disease. *Dig Liver Dis* **40**, 194-199.

Spector AA (1984) Plasma lipid transport. *Clin Physiol Biochem* **2**, 123-134.

Sprecher H (2000) Metabolism of highly unsaturated n-3 and n-6 fatty acids. *Biochim Biophys Acta* **1486**, 219-231.

Srivastava AR, Kumar S, Agarwal GG & Ranjan P (2007) Blunt abdominal injury: serum ALT-A marker of liver injury and a guide to assessment of its severity. *Injury* **38**, 1069-1074.

Srivastava S & Chan C (2007) Hydrogen peroxide and hydroxyl radicals mediate palmitate-induced cytotoxicity to hepatoma cells: relation to mitochondrial permeability transition. *Free Radic Res* **41**, 38-49.

Stanton MC, Chen SC, Jackson JV, Rojas-Triana A, Kinsley D, Cui L, Fine JS, Greenfeder S, Bober LA & Jenh CH (2011) Inflammatory Signals shift from adipose to liver during high fat feeding and influence the development of steatohepatitis in mice. *J Inflamm (Lond)* **8**, 8.

Stewart M (1990) Intermediate filaments: structure, assembly and molecular interactions. *Curr Opin Cell Biol* **2**, 91-100.

Stratford-Perricaudet LD, Levrero M, Chasse JF, Perricaudet M & Briand P (1990) Evaluation of the transfer and expression in mice of an enzyme-encoding gene using a human adenovirus vector. *Hum Gene Ther* **1**, 241-256.

Su WL, Kleinhanz RR & Schadt EE (2011) Characterizing the role of miRNAs within gene regulatory networks using integrative genomics techniques. *Mol Syst Biol* **7**, 490.

Sugden MC, Bulmer K, Gibbons GF, Knight BL & Holness MJ (2002) Peroxisome-proliferator-activated receptor-alpha (PPARalpha) deficiency leads to dysregulation of hepatic lipid and carbohydrate metabolism by fatty acids and insulin. *Biochem J* **364**, 361-368.

Sugiyama E, Ishikawa Y, Li Y, Kagai T, Nobayashi M, Tanaka N, Kamijo Y, Yokoyama S, Hara A & Aoyama T (2008) Eicosapentaenoic acid lowers plasma and liver cholesterol levels in the presence of peroxisome proliferators-activated receptor alpha. *Life Sci* **83**, 19-28.

Sun C, Wei ZW & Li Y (2011) DHA regulates lipogenesis and lipolysis genes in mice adipose and liver. *Mol Biol Rep* **38**, 731-737.

Sundram K, Karupaiah T & Hayes KC (2007) Stearic acid-rich interesterified fat and trans-rich fat raise the LDL/HDL ratio and plasma glucose relative to palm olein in humans. *Nutr Metab (Lond)* **4**, 3.

Takahashi M, Tsuboyama-Kasaoka N, Nakatani T, Ishii M, Tsutsumi S, Aburatani H & Ezaki O (2002) Fish oil feeding alters liver gene expressions to defend against PPARalpha activation and ROS production. *Am J Physiol Gastrointest Liver Physiol* **282**, G338-348.

Takahashi Y, Kushiro M, Shinohara K & Ide T (2003) Activity and mRNA levels of enzymes involved in hepatic fatty acid synthesis and oxidation in mice fed conjugated linoleic acid. *Biochim Biophys Acta* **1631**, 265-273.

Takeda M, Imaizumi M, Sawano S, Manabe Y & Fushiki T (2001) Long-term optional ingestion of corn oil induces excessive caloric intake and obesity in mice. *Nutrition* **17**, 117-120.

Takeuchi H, Kato T, Ikegami H & Imai H (1999) Regulation of plasma and liver total cholesterol levels by dietary oleic acid in rats fed a high-cholesterol diet. *J Nutr Sci Vitaminol (Tokyo)* **45**, 63-77.

Tanaka N, Sano K, Horiuchi A, Tanaka E, Kiyosawa K & Aoyama T (2008) Highly purified eicosapentaenoic acid treatment improves nonalcoholic steatohepatitis. *J Clin Gastroenterol* **42**, 413-418.

Tanaka N, Zhang X, Sugiyama E, Kono H, Horiuchi A, Nakajima T, Kanbe H, Tanaka E, Gonzalez FJ & Aoyama T (2010) Eicosapentaenoic acid improves hepatic steatosis independent of PPARalpha activation through inhibition of SREBP-1 maturation in mice. *Biochem Pharmacol* **80**, 1601-1612.

Tappenden DM, Lynn SG, Crawford RB, Lee K, Vengellur A, Kaminski NE, Thomas RS & LaPres JJ (2011) The aryl hydrocarbon receptor interacts with ATP5alpha1, a subunit of the ATP synthase complex, and modulates mitochondrial function. *Toxicol Appl Pharmacol* **254**, 299-310.

Tietz NW, Burtis CA, Duncan P, Ervin K, Petitclerc CJ, Rinker AD, Shuey D & Zygowicz ER (1983) A reference method for measurement of alkaline phosphatase activity in human serum. *Clin Chem* **29**, 751-761.

Tijsterman M & Plasterk RH (2004) Dicers at RISC; the mechanism of RNAi. *Cell* **117**, 1-3.

Tiniakos DG, Vos MB & Brunt EM (2010) Nonalcoholic fatty liver disease: pathology and pathogenesis. *Annu Rev Pathol* **5**, 145-171.

Tonge R, Shaw J, Middleton B, Rowlinson R, Rayner S, Young J, Pognan F, Hawkins E, Currie I & Davison M (2001) Validation and development of fluorescence two-dimensional differential gel electrophoresis proteomics technology. *Proteomics* **1**, 377-396.

Turner SM, Murphy EJ, Neese RA, Antelo F, Thomas T, Agarwal A, Go C & Hellerstein MK (2003) Measurement of TG synthesis and turnover in vivo by 2H2O incorporation into the glycerol moiety and application of MIDA. *Am J Physiol Endocrinol Metab* **285**, E790-803.

Tweedie S & Edwards Y (1989) Mouse carbonic anhydrase III: nucleotide sequence and expression studies. *Biochem Genet* **27**, 17-30.

Tzur G, Israel A, Levy A, Benjamin H, Meiri E, Shufaro Y, Meir K, Khvalevsky E, Spector Y, Rojansky N, Bentwich Z, Reubinoff BE & Galun E (2009) Comprehensive gene and microRNA expression profiling reveals a role for microRNAs in human liver development. *PLoS One* **4**, e7511.

Uwakwe (2004) CyDye DIGE Fluor saturation dyes for labelling and detection of scarce protein samples using Ettan DIGE system:Application of the pooled internal standard to the investigation of a model system. *Innovations Forum: CyDye DIGE Fluor saturation dyes*.

Valencak TG & Ruf T (2011) Feeding into old age: long-term effects of dietary fatty acid supplementation on tissue composition and life span in mice. *J Comp Physiol B* **181**, 289-298.

Valencia-Sanchez MA, Liu J, Hannon GJ & Parker R (2006) Control of translation and mRNA degradation by miRNAs and siRNAs. *Genes Dev* **20**, 515-524.

Vallim T & Salter AM (2010) Regulation of hepatic gene expression by saturated fatty acids. *Prostaglandins Leukot Essent Fatty Acids* **82**, 211-218.

Van de Weerd HA, Van Loo PL, Van Zutphen LF, Koolhaas JM & Baumans V (1997) Preferences for nesting material as environmental enrichment for laboratory mice. *Lab Anim* **31**, 133-143.

van Roermund CW, Hettema EH, Kal AJ, van den Berg M, Tabak HF & Wanders RJ (1998) Peroxisomal beta-oxidation of polyunsaturated fatty acids in Saccharomyces cerevisiae: isocitrate dehydrogenase provides NADPH for reduction of double bonds at even positions. *EMBO J* **17**, 677-687.

Vemuri M, Kelley DS, Mackey BE, Rasooly R & Bartolini G (2007) Docosahexaenoic Acid (DHA) But Not Eicosapentaenoic Acid (EPA) Prevents Trans-10, Cis-12 Conjugated Linoleic Acid (CLA)-Induced Insulin Resistance in Mice. *Metab Syndr Relat Disord* **5**, 315-322.

Vermunt SH, Mensink RP, Simonis MM & Hornstra G (2000) Effects of dietary alpha-linolenic acid on the conversion and oxidation of 13C-alpha-linolenic acid. *Lipids* **35**, 137-142.

Wang B, Majumder S, Nuovo G, Kutay H, Volinia S, Patel T, Schmittgen TD, Croce C, Ghoshal K & Jacob ST (2009) Role of microRNA-155 at early stages of hepatocarcinogenesis induced by choline-deficient and amino acid-defined diet in C57BL/6 mice. *Hepatology* **50**, 1152-1161.

Wang P, Bouwman FG & Mariman EC (2009) Generally detected proteins in comparative proteomics--a matter of cellular stress response? *Proteomics* **9**, 2955-2966.

Warren A, Bertolino P, Cogger VC, McLean AJ, Fraser R & Le Couteur DG (2005) Hepatic pseudocapillarization in aged mice. *Exp Gerontol* **40**, 807-812.

Wasinger VC, Cordwell SJ, Cerpa-Poljak A, Yan JX, Gooley AA, Wilkins MR, Duncan MW, Harris R, Williams KL & Humphery-Smith I (1995) Progress with gene-product mapping of the Mollicutes: Mycoplasma genitalium. *Electrophoresis* **16**, 1090-1094.

West DB, Boozer CN, Moody DL & Atkinson RL (1992) Dietary obesity in nine inbred mouse strains. *Am J Physiol* **262**, R1025-1032.

Weston SR, Leyden W, Murphy R, Bass NM, Bell BP, Manos MM & Terrault NA (2005) Racial and ethnic distribution of nonalcoholic fatty liver in persons with newly diagnosed chronic liver disease. *Hepatology* **41**, 372-379.

Wiklund ED, Kjems J & Clark SJ (2010) Epigenetic architecture and miRNA: reciprocal regulators. *Epigenomics* **2**, 823-840.

Wilkins MR, Gasteiger E, Sanchez JC, Bairoch A & Hochstrasser DF (1998) Two-dimensional gel electrophoresis for proteome projects: the effects of protein hydrophobicity and copy number. *Electrophoresis* **19**, 1501-1505.

Winkler C, Denker K, Wortelkamp S & Sickmann A (2007) Silver- and Coomassie-staining protocols: detection limits and compatibility with ESI MS. *Electrophoresis* **28**, 2095-2099.

Wolfensohn S & Lloyd M (2003) Handbook of laboratory animal management and welfare.

Wong QW, Lung RW, Law PT, Lai PB, Chan KY, To KF & Wong N (2008) MicroRNA-223 is commonly repressed in hepatocellular carcinoma and potentiates expression of Stathmin1. *Gastroenterology* **135**, 257-269.

Wree A, Kahraman A, Gerken G & Canbay A (2011) Obesity affects the liver - the link between adipocytes and hepatocytes. *Digestion* **83**, 124-133.

Wu MK & Cohen DE (2005) Phosphatidylcholine transfer protein regulates size and hepatic uptake of high-density lipoproteins. *Am J Physiol Gastrointest Liver Physiol* **289**, G1067-1074.

Xu J, Wu C, Che X, Wang L, Yu D, Zhang T, Huang L, Li H, Tan W, Wang C & Lin D (2010) Circulating MicroRNAs, miR-21, miR-122, and miR-223, in patients with hepatocellular carcinoma or chronic hepatitis. *Mol Carcinog*.

Yamaguchi K, Yang L, McCall S, Huang J, Yu XX, Pandey SK, Bhanot S, Monia BP, Li YX & Diehl AM (2007) Inhibiting triglyceride synthesis improves hepatic steatosis but exacerbates liver damage and fibrosis in obese mice with nonalcoholic steatohepatitis. *Hepatology* **45**, 1366-1374.

Yamaguchi K, Yang L, McCall S, Huang J, Yu XX, Pandey SK, Bhanot S, Monia BP, Li YX & Diehl AM (2008) Diacylglycerol acyltranferase 1 anti-sense oligonucleotides reduce hepatic fibrosis in mice with nonalcoholic steatohepatitis. *Hepatology* **47**, 625-635.

Yamaguchi M (2000) The role of regucalcin in nuclear regulation of regenerating liver. *Biochem Biophys Res Commun* **276**, 1-6.

Yamaguchi M & Oishi K (1995) 17 beta-Estradiol stimulates the expression of hepatic calcium-binding protein regucalcin mRNA in rats. *Mol Cell Biochem* **143**, 137-141.

Yamaguchi M, Oishi K & Isogai M (1995) Expression of hepatic calcium-binding protein regucalcin mRNA is elevated by refeeding of fasted rats: involvement of glucose, insulin and calcium as stimulating factors. *Mol Cell Biochem* **142**, 35-41.

Yamasaki T, Takahashi A, Pan J, Yamaguchi N & Yokoyama KK (2009) Phosphorylation of Activation Transcription Factor-2 at Serine 121 by Protein Kinase C Controls c-Jun-mediated Activation of Transcription. *J Biol Chem* **284**, 8567-8581.

Yan JX, Wait R, Berkelman T, Harry RA, Westbrook JA, Wheeler CH & Dunn MJ (2000) A modified silver staining protocol for visualization of proteins compatible with matrix-assisted laser desorption/ionization and electrospray ionization-mass spectrometry. *Electrophoresis* **21**, 3666-3672.

Yang L, Zhang Y, Wang L, Fan F, Zhu L, Li Z, Ruan X, Huang H, Wang Z, Huang Z, Huang Y, Yan X & Chen Y (2010) Amelioration of high fat diet induced liver lipogenesis and hepatic steatosis by interleukin-22. *J Hepatol* **53**, 339-347.

Yasunaga K, Saito S, Zhang YL, Hernandez-Ono A & Ginsberg HN (2007) Effects of triacylglycerol and diacylglycerol oils on blood clearance, tissue uptake, and hepatic apolipoprotein B secretion in mice. *J Lipid Res* **48**, 1108-1121.

Yeligar S, Tsukamoto H & Kalra VK (2009) Ethanol-induced expression of ET-1 and ET-BR in liver sinusoidal endothelial cells and human endothelial cells involves hypoxia-inducible factor-1alpha and microrNA-199. *J Immunol* **183**, 5232-5243.

Yimin, Furumaki H, Matsuoka S, Sakurai T, Kohanawa M, Zhao S, Kuge Y, Tamaki N & Chiba H (2011) A novel murine model for non-alcoholic steatohepatitis developed by combination of a high-fat diet and oxidized low-density lipoprotein. *Lab Invest*.

Young DD, Connelly CM, Grohmann C & Deiters A (2010) Small molecule modifiers of microRNA miR-122 function for the treatment of hepatitis C virus infection and hepatocellular carcinoma. *J Am Chem Soc* **132**, 7976-7981.

Yusufi AN, Cheng J, Thompson MA, Walker HJ, Gray CE, Warner GM & Grande JP (2003) Differential effects of low-dose docosahexaenoic acid and eicosapentaenoic acid on the regulation of mitogenic signaling pathways in mesangial cells. *J Lab Clin Med* **141**, 318-329.

Zatloukal K, Stumptner C, Fuchsbichler A, Fickert P, Lackner C, Trauner M & Denk H (2004) The keratin cytoskeleton in liver diseases. *J Pathol* **204**, 367-376.

Zhang T, Wang Q, Zhao D, Cui Y, Cao B, Guo L & Lu SH (2011) The oncogenetic role of microRNA-31 as a potential biomarker in oesophageal squamous cell carcinoma. *Clin Sci (Lond)* **121**, 437-447.

Zhang Y, Liu Y, Wang J, Zhang R, Jing H, Yu X, Xu Q, Zhang J, Zheng Z, Nosaka N, Arai C, Kasai M, Aoyama T, Wu J & Xue C (2010) Medium- and long-chain triacylglycerols reduce body fat and blood triacylglycerols in hypertriacylglycerolemic, overweight but not obese, Chinese individuals. *Lipids* **45**, 501-510.

Zheng L, Lv GC, Sheng J & Yang YD (2010) Effect of miRNA-10b in regulating cellular steatosis level by targeting PPAR-alpha expression, a novel mechanism for the pathogenesis of NAFLD. *J Gastroenterol Hepatol* **25**, 156-163.

Zheng X, Rivabene R, Cavallari C, Napolitano M, Avella M, Bravo E & Botham KM (2002) The effects of chylomicron remnants enriched in n-3 or n-6 polyunsaturated fatty acids on the transcription of genes regulating their uptake and metabolism by the liver: influence of cellular oxidative state. *Free Radic Biol Med* **32**, 1123-1131.

Zhou S, Bailey MJ, Dunn MJ, Preedy VR & Emery PW (2005) A quantitative investigation into the losses of proteins at different stages of a two-dimensional gel electrophoresis procedure. *Proteomics* **5**, 2739-2747.

Zhu Y, Yu X, Fu H, Wang H, Wang P, Zheng X & Wang Y (2010) MicroRNA-21 is involved in ionizing radiation-promoted liver carcinogenesis. *Int J Clin Exp Med* **3**, 211-222.

Zimmermann A (2004) Regulation of liver regeneration. *Nephrol Dial Transplant* **19 Suppl 4**, iv6-10.

APPENDICES

Appendix 2.1: Cycle threshold (Ct) values and relative quantification (RQ) of the selected miRNAs in response to low fat hypercaloric diet (LF group) and HF hypercaloric diet (HF group) to the controls (LFR group)

Sample	mmu-miR-199a-5p			mmu-miR-200b			mmu-miR-324-3p		
	ΔCt	ΔΔCt	RQ	Δ Ct	ΔΔCt	RQ	Δ Ct	ΔΔCt	RQ
A2	3.38	-0.71	1.64	1.06	-1.20	2.30	5.21	0.19	0.88
A3	3.61	-0.49	1.40	1.13	-1.13	2.19	5.34	0.31	0.80
A5	4.56	0.46	0.73	1.25	-1.01	2.02	4.12	-0.90	1.87
A6	5.38	1.29	0.41	4.46	2.20	0.22	5.32	0.29	0.82
A7	2.44	-1.66	3.16	1.00	-1.26	2.39	4.4	-0.62	1.53
A8	5.21	1.11	0.46	4.67	2.41	0.19	5.74	0.72	0.61
Average	4.10		1.3±0.42	2.26		1.55±0.43	5.02		1.08±0.20
B10	5.22	1.13	0.46	4.01	1.75	0.30	5.22	0.19	0.87
B12	5.39	1.29	0.41	4.58	2.32	0.20	5.50	0.48	0.72
B13	4.98	0.89	0.54	3.09	0.83	0.56	5.87	0.84	0.56
B14	4.93	0.84	0.56	3.75	1.49	0.36	5.32	0.29	0.82
B16	5.43	1.34	0.40	3.28	1.02	0.49	5.89	0.87	0.55
B9	5.82	1.72	0.30	4.07	1.81	0.28	5.73	0.71	0.61
Average			0.44±0.04			0.37±0.06			0.69±0.06
C17	8.11	4.02	0.06	5.32	3.06	0.12	6.47	1.45	0.37
C20	6.61	2.52	0.17	6.05	3.79	0.07	6.46	1.44	0.37
C21	7.58	3.48	0.09	5.06	2.80	0.14	6.12	1.10	0.47
C22	6.93	2.83	0.14	3.72	1.46	0.36	5.59	0.57	0.67
C23	5.20	1.10	0.47	3.33	1.07	0.48	5.05	0.02	0.98
C24	7.11	3.01	0.12	4.95	2.69	0.15	6.81	1.79	0.29
Average			0.18±0.06			0.22±0.07			0.53±0.11

ΔCt = normalized Ct values = (Ct miRNA – Ct of endogenous control). Ct values for selected miRNA and endogenous control are in Appendices XX. ΔΔ Ct = (ΔCt – Average of ΔCt of control group). Relative quantification (RQ) = 2^-ΔΔCt. Average of RQ values are expressed in Mean ± SEM

Appendix 2.2: Continuation of Appendix 2.1. Cycle threshold (Ct) values and relative quantification (RQ) of the selected miRNAs in response to low fat diet (LF group) and obesogenic diets (HF group) to the controls (LFR group) generated from real time RT-qPCR run

Sample	mmu-miR-21*			mmu-miR-31*			mmu-miR-345-3p			mmu-miR-451			mmu-miR-466f		
	Δ Ct	ΔΔCt	RQ	Δ Ct	ΔΔCt	RQ	Δ Ct	ΔΔCt	RQ	Δ Ct	ΔΔCt	RQ	Δ Ct	ΔΔCt	RQ
A2	3.66	-0.48	1.40	2.62	0.15	0.90	4.94	-0.38	1.30	0.83	-0.21	1.16	4.64	-0.26	1.19
A3	4.76	0.61	0.65	2.46	0.00	1.00	5.66	0.34	0.79	2.35	1.30	0.40	5.71	0.82	0.57
A5	3.72	-0.42	1.34	1.82	-0.65	1.56	4.71	-0.61	1.53	-0.71	-1.76	3.38	4.87	-0.03	1.02
A6	3.73	-0.41	1.33	2.76	0.29	0.82	5.37	0.04	0.97	1.02	-0.02	1.02	4.44	-0.46	1.38
A7	4.04	-0.10	1.07	1.60	-0.86	1.82	5.23	-0.09	1.06	2.10	1.06	0.48	4.53	-0.37	1.29
A8	4.95	0.80	0.57	3.52	1.06	0.48	6.03	0.70	0.61	0.68	-0.37	1.29	5.19	0.29	0.82
Average	4.15		1.06±0.15	2.46		1.1±0.20	5.32		1.05±0.14	1.04		1.29±0.44	4.90		1.04±0.13
B10	4.76	0.62	0.65	3.46	1.00	0.50	5.98	0.65	0.64	-0.07	-1.11	2.16	4.89	-0.01	1.01
B12	4.66	0.51	0.70	4.58	2.12	0.23	6.17	0.85	0.56	1.20	0.15	0.90	4.52	-0.38	1.30
B13	4.86	0.71	0.61	3.97	1.51	0.35	5.78	0.46	0.73	1.25	0.21	0.87	5.51	0.62	0.65
B14	3.84	-0.31	1.24	3.90	-0.14	1.10	5.86	0.54	0.69	1.15	0.11	0.93	-	-	-
B16	6.02	1.87	0.27	3.98	1.52	0.35	6.91	1.58	0.33	1.11	0.06	0.96	-	-	-
B9	4.49	0.34	0.79	4.32	1.86	0.28	6.18	0.86	0.55	0.80	-0.25	1.19	5.81	0.91	0.53
Average			0.71±0.13			0.47±0.13			0.58±0.06			1.17±0.20			0.87±0.18
C17	6.77	2.62	0.16	5.22	2.76	0.15	7.66	2.33	0.20	2.30	1.26	0.42	6.58	1.69	0.31
C20	6.12	1.98	0.25	5.30	2.83	0.14	7.20	1.88	0.27	2.10	1.06	0.48	6.22	1.32	0.40
C21	7.95	3.80	0.07	4.71	2.24	0.21	7.19	1.87	0.27	1.80	0.76	0.59	6.11	1.22	0.43
C22	5.97	1.83	0.28	4.02	1.55	0.34	7.93	2.61	0.16	1.95	0.91	0.53	5.59	0.69	0.62
C23	4.76	0.62	0.65	3.29	0.83	0.56	6.16	0.84	0.56	1.11	0.07	0.95	6.25	1.36	0.39
C24	8.25	4.11	0.06	4.94	2.48	0.18	7.15	1.83	0.28	1.84	0.79	0.58	7.16	2.27	0.21
Average			0.25±0.09			0.26±0.07			0.29±0.06			0.59±0.08			0.39±0.06

ΔCt = normalized Ct values = (Ct miRNA – Ct of endogenous control). Ct values for selected miRNA and endogenous control are in Appendices XX. ΔΔ Ct = (ΔCt – Average of ΔCt of control group). Relative quantification (RQ) = 2^-ΔΔCt. Average of RQ values are expressed in Mean ± SE.

Appendix 2.3: Cycle threshold (Ct) values and relative quantification (RQ) of intensities of the selected miRNAs in response to DHA (HFDHA group) and EPA (HFEPA group) to the controls (HF group) generated from RT-qPCR run

		mmu-miR-21*			mmu-miR-31*			mmu-miR-345-3p			mmu-miR-451			mmu-miR-466f-5p		
		ΔCt	ΔΔCt	RQ	Δ Ct	ΔΔCt	RQ	Δ Ct	ΔΔCt	RQ	Δ Ct	ΔΔCt	RQ	ΔCt	ΔΔCt	RQ
HF	C17	6.77	0.13	0.91	5.22	0.65	0.64	7.66	0.44	0.74	2.30	0.45	0.73	6.58	0.26	0.83
	C20	6.12	-0.51	1.43	5.30	0.72	0.61	7.20	-0.01	1.01	2.10	0.25	0.84	6.22	-0.10	1.07
	C21	7.95	1.31	0.40	4.71	0.13	0.92	7.19	-0.03	1.02	1.80	-0.05	1.03	6.11	-0.21	1.15
	C22	5.97	-0.66	1.58	4.02	-0.56	1.48	7.93	0.72	0.61	1.95	0.10	0.93	5.59	-0.73	1.66
	C23	4.76	-1.88	3.67	3.29	-1.29	2.44	6.16	-1.06	2.08	1.11	-0.74	1.67	6.25	-0.07	1.05
	C24	8.25	1.61	0.33	4.94	0.36	0.78	7.15	-0.06	1.05	1.84	-0.02	1.01	7.16	0.84	0.56
	Average	6.64		1.39±0.50	4.58		1.14±0.29	7.21		1.08±0.21	1.85		1.04±0.13	6.32		1.05±0.15
HFDHA	D26	6.84	0.20	0.87	4.84	0.26	0.84	8.48	1.27	0.42	2.95	1.10	0.47	7.15	0.83	0.56
	D27	5.48	-1.16	2.23	4.53	-0.05	1.04	7.71	0.49	0.71	3.18	1.32	0.40	6.45	0.13	0.91
	D28	6.06	-0.58	1.50	4.51	-0.07	1.05	6.80	-0.42	1.34	1.74	-0.11	1.08	6.66	0.34	0.79
	D30	8.65	2.01	0.25	6.83	2.26	0.21	9.76	2.55	0.17	4.83	2.97	0.13	7.88	1.56	0.34
	D31	7.40	0.77	0.59	5.51	0.93	0.52	7.62	0.40	0.76	3.57	1.71	0.30	7.96	1.64	0.32
	D32	6.54	-0.10	1.07	4.48	-0.10	1.07	7.37	0.16	0.90	1.66	-0.19	1.14	5.69	-0.63	1.55
	Average			1.09±0.29			0.79±0.14			0.71±0.16			0.59±0.17			0.75±0.19
HFEPA	E33	4.68	-1.95	3.88	4.21	-0.37	1.29	6.25	-0.96	1.95	0.64	-1.21	2.31	-	-	-
	E34	7.04	0.40	0.76	4.69	0.11	0.93	7.41	0.19	0.88	1.59	-0.26	1.20	5.28	-1.04	2.06
	E35	6.35	-0.29	1.22	5.23	0.65	0.64	7.19	-0.03	1.02	1.43	-0.42	1.34	7.01	0.69	0.62
	E37	7.08	0.44	0.74	6.11	1.53	0.35	7.98	0.76	0.59	2.10	0.25	0.84	7.21	0.89	0.54
	E38	7.94	1.30	0.41	5.99	1.41	0.38	8.80	1.59	0.33	3.53	1.68	0.31	6.85	0.53	0.69
	E40	10.99	4.35	0.05	4.91	0.33	0.79	8.12	0.90	0.53	2.34	0.49	0.71	6.67	0.35	0.78
	Average			1.17±0.48			0.73±0.30			0.88±0.36			1.12±0.46			0.94±0.42

Legend for Table XX: ΔCt = normalized Ct values = (Ct miRNA – Ct of endogenous control). Ct values for selected miRNA and endogenous control are in Appendices XX. ΔΔ Ct = (ΔCt – Average of ΔCt of control group). Relative quantification (RQ) = 2^-ΔΔCt. Average of RQ values are expressed in Mean ± SE.

Appendix 2.4: Continuation of Appendix 2.5. Cycle threshold (Ct) values and relative quantification (RQ) of intensities of the selected miRNAs in response to DHA (HFDHA group) and EPA (HFEPA group) to the controls (HF group) generated from RT-qPCR run

	mmu-miR-199a-5p			mmu-miR-200b			mmu-miR-324-3p		
	Δ Ct	ΔΔCt	RQ	ΔCt	ΔΔCt	RQ	ΔCt	ΔΔCt	RQ
C17	8.11	1.19	0.44	5.32	0.58	0.67	6.47	0.39	0.76
C20	6.61	-0.31	1.24	6.05	1.31	0.40	6.46	0.38	0.77
C21	7.58	0.65	0.64	5.06	0.32	0.80	6.12	0.04	0.97
C22	6.93	0.00	1.00	3.72	-1.02	2.02	5.59	-0.49	1.41
C23	5.20	-1.72	3.30	3.33	-1.41	2.65	5.05	-1.04	2.05
C24	7.11	0.18	0.88	4.95	0.22	0.86	6.81	0.73	0.60
Average	6.92		1.25±0.43	4.74		1.23±0.36	6.28		1.10±0.22
D26	8.55	1.63	0.32	5.31	0.57	0.67	7.09	1.01	0.50
D27	6.59	-0.33	1.25	5.45	0.71	0.61	7.15	1.06	0.48
D28	6.06	-0.86	1.82	4.29	-0.45	1.36	6.01	-0.08	1.06
D30	9.29	2.36	0.19	6.59	1.85	0.28	8.34	2.26	0.21
D31	7.24	0.32	0.80	5.85	1.12	0.46	8.07	1.99	0.25
D32	6.26	-0.66	1.59	3.86	-0.87	1.83	5.55	-0.54	1.45
Average			1.00±0.27			0.87±0.24			0.66±0.20
E33	5.99	-0.93	1.91	4.25	-0.49	1.40	5.97	-0.11	1.08
E34	6.95	0.03	0.98	4.80	0.06	0.96	7.08	1.00	0.50
E35	6.79	-0.14	1.10	4.64	-0.10	1.07	7.51	1.42	0.37

E37	11.34	4.42	0.05	5.24	0.50	0.70	6.75	0.66	0.63
E38	8.74	1.81	0.28	5.14	0.40	0.76	7.24	1.16	0.45
E40	7.30	0.38	0.77	4.85	0.11	0.93	6.66	0.58	0.67
Average			0.85±0.35			0.97±0.40			0.62±0.25

Appendix 5.1: Total energy intake (kcal/week) from the consumption of all sources during run-in and over 6 weeks of feeding period in mice fed either low fat reference (LFR), low fat (LF), high fat (HF), high fat DHA (HFDHA) or high fat EPA (HFEPA) diets

	LFR	LF	HF	HFDHA	HFEPA	P Anova
Week 1	58 [a] (52,63)	62 [a,b] (53,71)	63 [a,b] (56,70)	71 [b] (69,74)	68 [b] (64,73)	P=0.005
Week 2	85 [a] (82,89)	95 [a,b] (86,105)	103 [a,b] (97,109)	111 [b] (91,131)	96 [a,b] (90,102)	P=0.005
Week 3	71 [a] (65,77)	90 [b] (84,96)	100 [b] (92,108)	99 [b] (92,106)	100 [b] (94,106)	P<0.001
Week 4	78 [a] (73,84)	90 [a,b] (84,96)	99 [b] (88,111)	102 [b] (95,108)	103 [b] (95,110)	P<0.001
Week 5	79 [a] (74,85)	93 [a,b] (85,100)	104 [b] (92,115)	106 [b] (94,118)	106 [b] (98,114)	P<0.001
Week 6	82 [a] (76,87)	96 [b] (89,102)	111 [c] (103,119)	114 [c] (103,126)	111 [c] (105,117)	P<0.001
Week 7	84 [a] (79,89)	96 [a] (87,104)	113 [b] (100,126)	120 [b] (107,133)	118 [b] (110,125)	P<0.001

Values are expressed as mean with 95% CI. One way analysis of variance (ANOVA) and Tukey's multiple range test was used for data from run-in to week 6. Repeated measure was used to analyse energy intake of mice from Week 1 to 6. Values with different superscripts indicate significant differences between treatments.

Appendix 5.2: Energy intake (kcal/week) from solid food intake during run-in and over 6 weeks of feeding period in mice fed either low fat reference (LFR), low fat (LF), high fat (HF), high fat DHA (HFDHA) or high fat EPA (HFEPA) diets

	LFR	LF	HF	HFDHA	HFEPA	P Anova
Week 1	58 [a] (52,63)	62 [a,b] (53,71)	63 [a,b] (56,70)	71 [b] (69,74)	69 [b] (64,73)	P<0.001
Week 2	85 [a,b] (82,89)	7 [c] (4,10)	6 [a] (4,8)	7 [a,b] (2,11)	14 [b] (7,21)	P<0.001
Week 3	71 [a] (65,77)	4 [b] (3,6)	6 [b] (2,9)	6 [b] (2,10)	8 [b] (2,17)	P<0.001
Week 4	78 [a] (73,84)	5 [b] (0,9)	7 [b] (3,11)	7 [b] (4,9)	6 [b] (0,11)	P<0.001
Week 5	79 [c] (74,85)	4 [a] (2,7)	13 [b] (6,20)	4 [a] (1,7)	6 [a,b] (2,10)	P<0.001
Week 6	82 [a] (76,87)	7 [b] (3,11)	10 [b] (6,14)	6 [b] (2,10)	6 [b] (1,11)	P<0.001
Week 7	84 [a] (79,89)	8 [b] (4,12)	8 [b] (4,13)	7 [b] (3,12)	6 [b] (0,11)	P<0.001

Values are expressed as mean with 95% CI. One way analysis of variance (ANOVA) and Tukey's multiple range test was used for data from run-in to week 6. Repeated measure was used to analyse solid food intake of mice from Week 1 to 6. Values with different superscripts indicate significant differences between treatments.

Appendix 5.3: Energy intake (kcal/week) from milk intakes over 6 weeks of feeding period in mice fed either low fat reference (LFR), low fat (LF), high fat (HF), high fat DHA (HFDHA) or high fat EPA (HFEPA) diets. No milk was administered to mice from low fat reference group

	LFR	LF	HF	HFDHA	HFEPA	P Anova
Week 2	0 [a] (0,0)	88 [b,c] (78,99)	97 [b,c] (92,102)	105 [c] (84,125)	82 [b] (72,92)	P<0.001
Week 3	0 [a] (0,0)	86 [b] (80,92)	94 [b] (87,101)	93 [b] (85,101)	92 [b] (83,101)	P<0.001
Week 4	0 [a] (0,0)	85 [b] (77,94)	93 [b] (79,106)	95 [b] (87,104)	97 [b] (90,105)	P<0.001
Week 5	0 [a] (0,0)	88 [b] (79,97)	91 [b] (79,104)	102 [b] (87,117)	100 [b] (93,108)	P<0.001
Week 6	0 [a] (0,0)	89 [b] (80,98)	101 [b,c] (93,108)	108 [c] (94,123)	105 [c] (99,111)	P<0.001
Week 7	0 [a] (0,0)	88 [b] (78,99)	105 [b,c] (90,120)	112 [c] (96,128)	112 [c] (106,118)	P<0.001

Values are expressed as mean with 95% CI and Student's independent t-test was used for data from run-in to week 6.

Appendix 5.4: Body weights (g) during run-in and over 6 weeks of feeding period in low fat reference (LFR), low fat (LF), high fat (HF), high fat DHA (HFDHA) and high fat EPA (HFEPA) groups

	LFR	LF	HF	HFDHA	HFEPA	P Anova
Run-in	15.8[a,b] (14.5,17.0)	15.3[a] (14.6,16.1)	17.3[b] (16.5,18.2)	16.7[a,b] (15.4,18.0)	16.8[a,b] (15.5,18.1)	P=0.031
Week 1	17.4[a] (16.2,18.6)	18.0[a,b] (16.8,19.3)	19.9[b] (18.6,21.2)	19.8[b] (18.7,20.9)	19.4[a,b] (18.0,20.8)	P=0.004
Week 2	17.6[a] (16.3,19.0)	20.6[b] (19.6,21.6)	21.8[b] (20.3,23.3)	22.2[b] (20.8,23.5)	21.8[b] (20.3,23.3)	P<0.001
Week 3	17.7[a] (15.9,19.4)	22.2[b] (21.5,22.8)	23.4[b] (21.7,25.1)	23.8[b] (22.3,25.4)	23.6[b] (21.8,25.3)	P<0.001
Week 4	18.5[a] (16.7,20.3)	23.4[b] (22.9,23.8)	24.7[b] (22.7,26.7)	25.3[b] (23.5,27.2)	25.4[b] (23.3,27.5)	P<0.001
Week 5	19.5[a] (17.9,21.1)	24.2[b] (23.5,24.8)	26.4[b] (24.0,28.9)	26.9[b] (24.7,29.0)	26.8[b] (24.6,29.1)	P<0.001
Week 6	20.1[a] (18.5,21.7)	24.9[b] (24.1,25.8)	27.7[b] (24.9,30.4)	28.4[b] (25.9,30.9)	28.6[b] (26.3,30.9)	P<0.001

Values are expressed as mean with 95% CI. One way analysis of variance (ANOVA) and Tukey's multiple range test was used. Values with different superscripts indicate significant differences between treatments.

Appendix 5.5: Weight gain (g) of mice before and after fasting

	LFR	LF	HF	HFDHA	HFEPA	P Anova
Before fasting	20.6 [a] (19.0,22.2)	25.1 [b] (24.1,26.1)	28.9 [b,c] (25.9,31.8)	29.9 [c] (27.1,32.8)	29.9 [c] (27.5,32.3)	P<0.001
After fasting	17.9(16.4,19.4)	22.8(21.8,23.8)	26.6(23.6,29.5)	27.7(25.0,30.5)	27.4(25.0,29.7)	P<0.001
Weight gain after fasting	5.21 [a] (3.50,6.92)	10.34 [b] (9.20,11.48)	11.96 [b,c] (9.70,14.23)	13.85 [c] (11.86,15.84)	13.83 [c] (12.23,15.42)	P<0.001

Values are expressed as mean with 95% CI. One way analysis of variance (ANOVA) and Tukey's multiple range test was used. Values with different superscripts indicate significant differences between treatments.

Appendix 5.6: Fatty acids composition (weight %) derived from adipose tissue of C57BL/6J mice fed either low fat reference (LFR), low fat (LF), high fat (HF), high fat DHA (HFDHA) or high fat EPA (HFEPA) diets

	LFR group			LF group			HF group			HFDHA group			HFEPA group			P Anova
	Diet	Adipose FA	SD	Diet	Adipose FA	SD	Diet	Adipose FA	SD	Diet	Adipose FA	SD	Diet	Adipose FA	SD	
16:0	11.3	24.8	1.3	11.3	22.2	2.9	40.3	25.1	1.2	33.7	33.8	1.5	33.6	32.7	1.6	P=0.914
16:1	0.0	10.9	2.6	0.0	13.1	6.6	0.2	7.9	2.0	0.2	6.0	1.0	0.2	7.7	3.4	P=0.728
18:0	1.7	4.5	1.0	1.7	1.9	0.4	4.4	1.9	0.5	3.8	2.8	0.2	3.7	2.6	0.5	P=0.474
18:1n-9	28.7	45.8	1.7	28.7	47.3	8.5	42.7	54.7	2.3	36.1	39.1	1.3	35.8	42.3	1.0	P=0.978
18:2n-6	56.8	13.1	2.9	56.8	14.9	1.6	11.3	9.7	0.2	9.7	9.7	0.8	9.9	10.8	1.7	P=0.907
18:3n-3	1.2	0.1	0.0	1.2	0.1	0.0	0.0	0.1	0.0	0.1	0.1	0.0	0.3	0.1	0.1	P=0.581
20:3n-6	0.0	0.1	0.0	0.0	0.2	0.1	0.0	0.1	0.0	0.0	0.1	0.0	0.0	0.1	0.0	P=0.715
20:4n-6	0.0	0.5	0.7	0.0	0.2	0.2	0.0	0.2	0.0	0.7	0.6	0.1	0.7	0.4	0.3	P=0.718
20:5n-3	**0.0**	**0.1** [a,b]	**0.0**	**0.0**	**0.1** [a]	**0.0**	**0.0**	**0.1** [a,b]	**0.0**	**2.5**	**0.2** [a,b]	**0.0**	**12.2**	**0.4** [b]	**0.1**	**P=0.033**
22:4n-6	0.2	0.1	0.0	0.2	0.0	0.0	0.0	0.0	0.0	0.1	0.1	0.0	0.3	0.0	0.0	P=0.367
22:5n-6	**0.0**	**0.2** [a,b]	**0.1**	**0.0**	**0.1** [a,b]	**0.1**	**0.0**	**0.0** [a]	**0.0**	**0.6**	**0.3** [b]	**0.0**	**0.1**	**0.1** [a,b]	**0.0**	**P=0.053**
22:5n-3	**0.0**	**0.0** [a]	**0.0**	**0.0**	**0.0** [a]	**0.0**	**0.0**	**0.1** [a]	**0.0**	**0.6**	**0.5** [a,b]	**0.1**	**0.4**	**1.1** [b]	**0.3**	**P=0.004**
22:6n-3	**0.0**	**0.1** [a]	**0.1**	**0.0**	**0.0** [a]	**0.0**	**0.0**	**0.2** [a]	**0.1**	**10.9**	**6.8** [b]	**0.2**	**1.9**	**1.7** [a]	**0.4**	**P=0.001**

Values of fatty acids in adipose tissue are expressed as mean ± standard deviation. One way analysis of variance (ANOVA) and Tukey's multiple range test was used. Values with different superscripts indicate significant differences between treatments.

Appendix 6.1: Energy intake (kcal/week) from consumption of all sources over 6 weeks of feeding period in mice fed either a high fat high oleic sunflower oil (HFHOSO), HF palm oil (HFPO), HF interesterified palm (HFIPO) or HF lard (HFL) diet

Period	Diets	N	Mean	95% Confidence interval Bounds		P Anova
				Lower	Upper	
Week 1	High fat HOSO	8	107[a]	101	114	P=0.013
	High fat PO	7	125 [b]	115	134	
	High fat IPO	8	112 [a,b]	102	123	
	High fat Lard	8	110 [a]	103	117	
Week 2	High fat HOSO	8	112 [a,b]	106	120	P=0.001
	High fat PO	7	103 [a]	94	112	
	High fat IPO	8	112 [a,b]	107	116	
	High fat Lard	8	120 [b]	115	126	
Week 3	High fat HOSO	8	101 [a]	96	106	P=0.002
	High fat PO	7	111 [b]	104	118	
	High fat IPO	8	112 [b]	106	117	
	High fat Lard	8	101 [a]	96	106	
Week 4	High fat HOSO	8	98 [a]	91	105	P=0.050
	High fat PO	7	101 [a.b]	92	111	
	High fat IPO	8	110 [b]	105	115	
	High fat Lard	8	104 [a,b]	98	111	
Week 5	High fat HOSO	8	98 [a]	90	108	P=0.028
	High fat PO	7	107 [a,b]	99	114	
	High fat IPO	8	116 [b]	109	124	
	High fat Lard	8	109 [a,b]	97	121	
Week 6	High fat HOSO	8	102	92	113	P=0.204
	High fat PO	7	107	99	115	
	High fat IPO	8	114	105	122	
	High fat Lard	8	108	101	115	
Week 1-6	High fat HOSO	8	104	98	109	P=0.067
	High fat PO	7	109	102	116	
	High fat IPO	8	113	108	117	
	High fat Lard	8	109	104	113	

Values are expressed as mean ± SD with 95% CI. One way analysis of variance (ANOVA) and Tukey's multiple range test was used for data week 1to 6. Repeated measure was used to analyse energy intake of mice from Week 1 to 6. Values with different superscripts indicate significant differences between treatments

Appendix 6.2: Energy intake (kcal/week) from solid food intake over 6 weeks of feeding period in mice fed either a high fat high oleic sunflower oil (HFHOSO), HF palm oil (HFPO), HF interesterified palm (HFIPO) or HF lard (HFL) diet

Period	Diets	n	Mean	95% Confidence Interval Bounds		P Anova
				Lower	Upper	
Week 1	High fat HOSO	8	40 [b]	28	53	P=0.399
	High fat PO	7	47 [a]	37	56	
	High fat IPO	8	53 [a]	39	66	
	High fat Lard	8	55 [a]	32	77	
Week 2	High fat HOSO	8	36 [b]	21	51	P<0.001
	High fat PO	7	14 [a]	2	26	
	High fat IPO	8	47 [b]	34	60	
	High fat Lard	8	53 [b]	40	66	
Week 3	High fat HOSO	8	16 [c]	2	30	P=0.105
	High fat PO	7	9 [a]	3	15	
	High fat IPO	8	28 [b]	14	43	
	High fat Lard	8	20 [a,b]	7	33	
Week 4	High fat HOSO	8	19 [c]	6	31	P=0.041
	High fat PO	7	8 [a]	5	10	
	High fat IPO	8	29 [b]	15	42	
	High fat Lard	8	29 [b]	12	45	
Week 5	High fat HOSO	8	18 [a]	7	28	P=0.200
	High fat PO	7	12 [b]	8	16	
	High fat IPO	8	29 [b]	13	46	
	High fat Lard	8	22 [b]	6	38	
Week 6	High fat HOSO	8	20 [a,b]	11	29	P=0.005
	High fat PO	7	11 [a]	8	15	
	High fat IPO	8	28 [b]	17	40	
	High fat Lard	8	13 [a]	9	18	
Week 1-6	High fat HOSO	8	24	16	32	P=0.317
	High fat PO	7	11	2	20	
	High fat IPO	8	31	23	40	
	High fat Lard	8	26	17	34	

Values are expressed as mean ± SD with 95% CI. One way analysis of variance (ANOVA) and Tukey's multiple range test was used for data week 1to 6. Repeated measure was used to analyse energy intake of mice from Week 1 to 6. Values with different superscripts indicate significant differences between treatments

Appendix 6.3: Energy intake (kcal/week) from condensed milk intake over 6 weeks of feeding period in mice fed either a high fat high oleic sunflower oil (HFHOSO), HF palm oil (HFPO), HF interesterified palm (HFIPO) or HF lard (HFL) diet

Period	Diets	n	Mean	95% Confidence interval Bounds		P Value
				Lower	Upper	
Week 1	High fat HOSO	8	67 [a,b]	58	76	P=0.019
	High fat PO	7	78 [b]	65	91	
	High fat IPO	8	60 [a,b]	52	67	
	High fat Lard	8	55 [a]	39	71	
Week 2	High fat HOSO	8	77 [a,b]	64	91	P=0.032
	High fat PO	7	89 [b]	72	106	
	High fat IPO	8	64 [a]	54	75	
	High fat Lard	8	67 [a,b]	51	83	
Week 3	High fat HOSO	8	85	68	101	P=0.058
	High fat PO	7	102	96	108	
	High fat IPO	8	83	71	95	
	High fat Lard	8	81	66	96	
Week 4	High fat HOSO	8	80	66	93	P=0.188
	High fat PO	7	94	85	102	
	High fat IPO	8	81	68	95	
	High fat Lard	8	76	59	92	
Week 5	High fat HOSO	8	81	67	96	P=0.423
	High fat PO	7	94	90	99	
	High fat IPO	8	87	71	103	
	High fat Lard	8	87	77	98	
Week 6	High fat HOSO	8	82	69	95	P=0.150
	High fat PO	7	96	87	105	
	High fat IPO	8	85	71	99	
	High fat Lard	8	94	86	102	
Week 1-6	High fat HOSO	8	80	71	89	P=0.067
	High fat PO	7	91	80	102	
	High fat IPO	8	82	72	91	
	High fat Lard	8	84	74	94	

Values are expressed as mean ± SD with 95% CI. One way analysis of variance (ANOVA) and Tukey's multiple range test was used for data week 1to 6. Repeated measure was used to analyse energy intake of mice from Week 1 to 6. Values with different superscripts indicate significant differences between treatments

Appendix 6.4: Body weights (g) over 6 weeks of feeding period in mice fed either a high fat high oleic sunflower oil (HFHOSO), HF palm oil (HFPO), HF interesterified palm (HFIPO) or HF lard (HFL) diet

Period	Diets	n	Mean	95% Confidence Interval Bounds		P Anova
				Lower	Upper	
Week 1	High fat HOSO	8	16.1	15.2	17.0	P=0.126
	High fat PO	7	16.6	15.6	17.5	
	High fat IPO	8	16.6	15.8	17.4	
	High fat Lard	8	15.5	14.6	16.3	
Week 2	High fat HOSO	8	17.9 [a,b]	16.7	19.0	P=0.011
	High fat PO	7	18.9 [a,b]	17.7	20.1	
	High fat IPO	8	19.3 [b]	18.4	20.3	
	High fat Lard	8	17.5 [a]	17.0	18.0	
Week 3	High fat HOSO	8	19.3 [a,b]	18.1	20.5	P=0.012
	High fat PO	7	20.7 [a,b]	19.6	21.9	
	High fat IPO	8	20.9 [b]	19.7	22.0	
	High fat Lard	8	19.1 [a]	18.5	19.7	
Week 4	High fat HOSO	8	20.4 [a,b]	19.1	21.7	P=0.028
	High fat PO	7	21.2 [a,b]	19.7	22.7	
	High fat IPO	8	22.2 [b]	20.9	23.6	
	High fat Lard	8	20.1 [a]	19.2	20.9	
Week 5	High fat HOSO	8	21.2	19.7	22.7	P=0.075
	High fat PO	7	22.1	20.4	23.9	
	High fat IPO	8	23.2	21.3	25.0	
	High fat Lard	8	20.9	19.9	21.9	
Week 6	High fat HOSO	8	21.9	20.3	23.6	P=0.086
	High fat PO	7	22.8	20.8	24.7	
	High fat IPO	8	24.4	22.3	26.6	
	High fat Lard	8	22.1	20.9	23.3	
Weight gain from Week 1-6	High fat HOSO	8	10.1	8.0	12.1	P=0.161
	High fat PO	7	11.0	8.5	13.4	
	High fat IPO	8	12.8	10.4	15.1	
	High fat Lard	8	10.8	9.6	12.1	

Values are expressed as mean ± SD with 95% CI. One way analysis of variance (ANOVA) and Tukey's multiple range test was used for data week 1to 6. Repeated measure was used to analyse milk intake of mice from Week 1 to 6. Values with different superscripts indicate significant differences between treatments

Appendix 6.5: Mean weight loss before and after fasting in mice fed either a high fat high oleic sunflower oil (HFHOSO), HF palm oil (HFPO), HF interesterified palm (HFIPO) or HF lard (HFL) diet

Period	Diets	n	Mean	95% Confidence Interval Bounds		P Anova
				Lower	Upper	
Body weight before fasting	High fat HOSO	8	21.9±2.0	20.3	23.6	P=0.086
	High fat PO	7	22.8±2.1	20.8	24.7	
	High fat IPO	8	24.4±2.6	22.3	26.6	
	High fat lard	8	22.1±1.4	20.9	23.3	
Body weight after fasting	High fat HOSO	8	19.6±2.0	17.9	21.3	P=0.262
	High fat PO	7	20.2±2.4	18.0	22.4	
	High fat IPO	8	21.8±3.1	19.2	24.4	
	High fat lard	8	19.8±1.8	18.3	21.3	
Weight loss	High fat HOSO	8	2.3±0.5	1.9	2.8	P=0.630
	High fat PO	7	2.6±0.4	2.2	2.9	
	High fat IPO	8	2.6±0.8	1.9	3.3	
	High fat lard	8	2.3±0.5	1.9	2.7	

Values are expressed as mean ± SD with 95% CI. One way analysis of variance (ANOVA) and Tukey's multiple range test was used. Values with different superscripts indicate significant differences between treatments.

Appendix 6.6: Fatty acids composition (weight %) derived from adipose tissue of C57BL/6J male mice fed either a high fat high oleic sunflower oil (HFHOSO), HF palm oil (HFPO), HF interesterified palm (HFIPO) or HF lard (HFL) diet

Fatty acids	Fatty acid composition in HOSO (%)	High fat HOSO (n=8)	Fatty acid composition in PO (%)	High fat PO (n=7)	Fatty acid composition in IPO (%)	High fat IPO (n=8)	Fatty acid composition in Lard (%)	High fat Lard (n=8)	P Anova
16:0	4.0	11.6 ^{a} ± 1.1	40.3	23.8 ^{b} ± 0.7	40.5	27.3 ^{c} ± 1.0	27.8	24.6 ^{b} ± 1.0	P<0.001
16:1	0.1	3.0 ^{a} ± .9	0.2	7.5 ^{b} ± 1.3	0.2	9.3 ^{b} ± 1.1	2.5	8.0 ^{b} ± 1.3	P<0.001
18:0	2.9	1.6 ^{b} ± 0.3	4.4	2.2 ^{a} ± 0.4	4.4	2.0 ^{a} ± 0.1	17.9	3.6 ^{a} ± 0.9	P<0.001
18:1n-9	81.7	74.1 ^{b} ± 2.9	42.7	55.6 ^{a} ± 1.8	42.5	53.1 ^{a} ± 1.9	39.7	54.8 ^{a} ± 1.8	P<0.001
18:2n-6	10.7	8.9 ^{a,b} ± 1.1	11.3	9.9 ^{b} ± 0.9	11.0	7.9 ^{a} ± 1.0	9.3	8.3 ^{a} ± 0.9	P=0.003
18:3n-3	-	0.1 ± 0.1	-	0.0 ± 0.0	-	0.1 ± 0.0	-	0.1 ± 0.1	P=0.085
20:3n-6	-	0.1 ± 0.0	-	0.1 ± 0.0	-	0.1 ± 0.0	-	0.1 ± 0.0	P=0.548
20:4n-6	-	0.2 ± 0.1	-	0.3 ± 0.1	-	0.2 ± 0.1	-	0.2 ± 0.1	P=0.453
20:5n-3	-	0.0 ^{a} ± 0.0	-	0.1 ^{b} ± 0.0	-	0.1 ^{a} ± 0.1	-	0.1 ^{a} ± 0.1	P<0.001
22:4n-6	-	0.0 ± 0.1	-	0.0 ± 0.0	-	0.0 ± 0.0	-	0.0 ± 0.0	P=0.354
22:5n-6	-	0.0 ± 0.1	-	0.0 ± 0.0	-	0.0 ± 0.0	-	0.0 ± 0.0	P=0.652
22:5n-3	-	0.0 ^{a} ± 0.0	-	0.1 ^{b} ± 0.0	-	0.0 ^{a} ± 0.0	-	0.0 ^{a} ± 0.0	P<0.001
22:6n-3	-	0.0 ^{a} ± 0.0	-	0.3 ^{b} ± 0.1	-	0.0 ^{a} ± 0.1	-	0.1 ^{a} ± 0.1	P<0.001

Values are expressed as mean with 95% CI. One way analysis of variance (ANOVA) and Tukey's multiple range test was used. Values with different superscripts indicate significant differences between treatments.

Appendix 8.1: Snapshot of the amplification plot of miR-200b generated from real time RT-qPCR

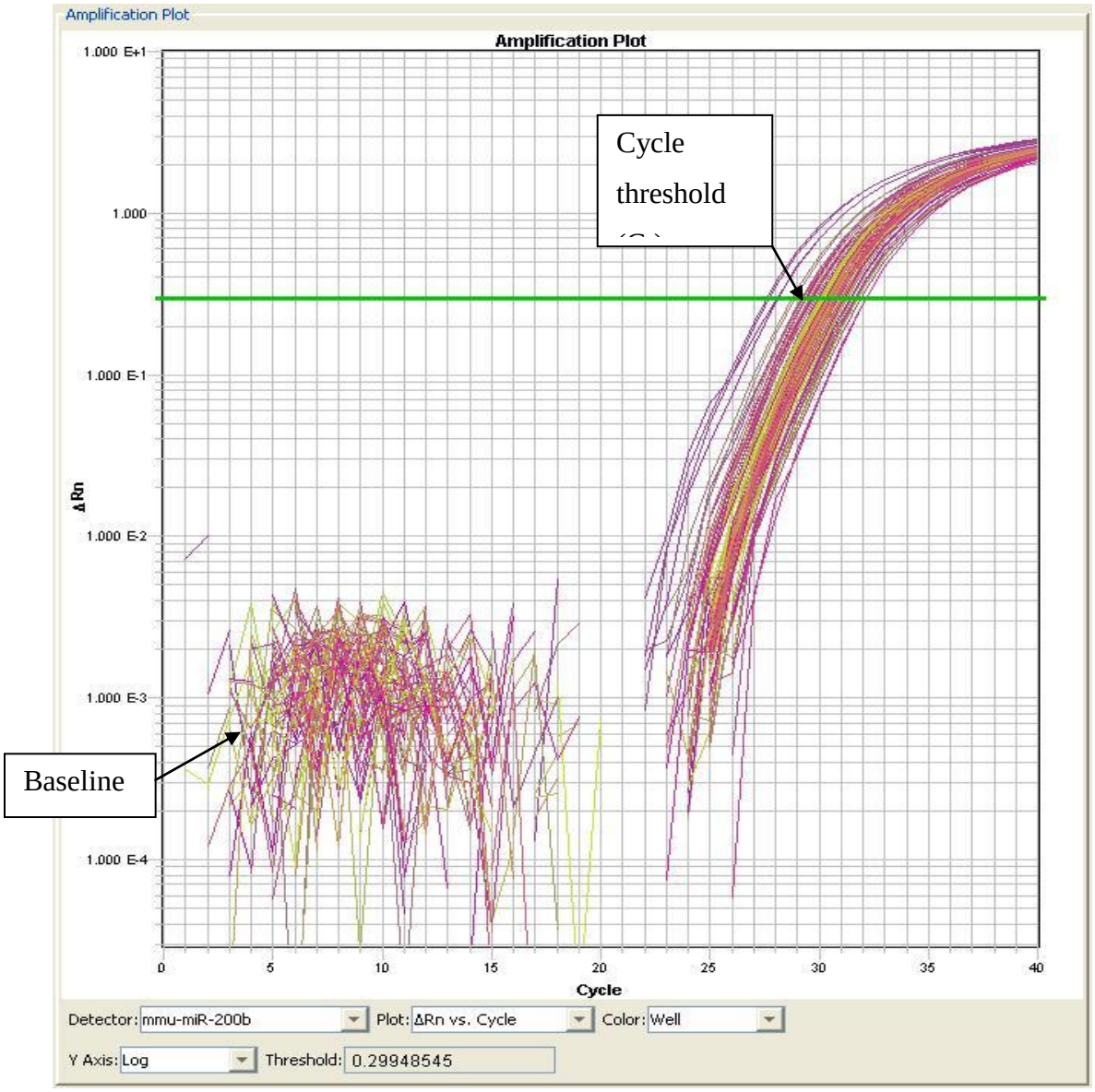

The amplification plot shows the fluorescence signal (in log scale) against cycle number. Baseline of graph shows there's little change in fluorescence in initial cycles of PCR. The fixed threshold is represented by green line parallel to x-axis. Ct values are determined at the exponential phase of the curve whereby the fluorescence signal reaches threshold level.

Appendix 8.2: Changes in miRNAs in LF and HF groups compared to the LFR group using either microarrays or RT-qPCR.

	Changes from Microarray		Changes from RT- qPCR	
	% change in LF	% change in HF	% change in LF	% change in HF
miR-199a-5p	-62%	-62%	-66%	-86%
miR-200b	-46%	-63%	-76%	-86%
miR-324-3p	+54%	+69%	-36%	-51%
miR-21*	-11%	-24%	-33%	-76%
miR-31*	-36%	-31%	-57%	-76%
miR-345-3p	-38%	-16%	0%	-72%
miR-451	0%	+5%	-9%	-54%
miR-466f	-49%	-6%	-44%	-62%

The % changes in miRNA expression of treated samples in comparison to LFR controls are tabulated according to data generated via the microarray (using pooled samples) or RT-qPCR (using individual samples). The table is compiled from data contained within the information sets in Tables 10.1 & 10.2 and Figure 10.6 & 10.7; -x% means down regulation in treated sample and vice versa.

Appendix 8.3: Changes in miRNAs in HFDHA and HFEPA groups compared to HF group using either microarrays or RT-qPCR

	Changes from microarray		Changes from RT-qPCR	
	% change in HFDHA	% change in HFEPA	% change in HFDHA	% change in HFEPA
miR-199a-5p	+3%	+4%	-20%	-32%
miR-200b	+35%	-27%	-30%	-21%
miR-324-3p	-39%	-45%	-40%	-43%
miR-21*	-29%	+62%	-22%	-15%
miR-31*	-15%	-51%	-31%	-36%
miR-345-3p	+12%	-63%	-34%	-18%
miR-451	-61%	-15%	-43%	+8%
mir-466f	-34%	-36%	-29%	-26%

Data were analysed using independent t-test; P-value < 0.05 indicates significant difference between groups. x% represents percentage difference in miRNA expression of treated samples in comparison to control; -x% means down regulation in treated sample and vice versa.